TECHNISCHE UNIVERSITÄT DARMSTADT

Data-Driven Modeling of Decarbonization Pathways for Worldwide Energy Systems Based on Archetypes and Spatial Clustering Methods

Vom Fachbereich Elektrotechnik und Informationstechnik der Technischen Universität Darmstadt zur Erlangung des akademischen Grades eines Doktoringenieurs (Dr.-Ing.) genehmigte Dissertation

von
Martin Küppers, M. Sc.
geboren in Grevenbroich, Deutschland

Referent: Prof. Dr.-Ing. Stefan Niessen, MBA

Korreferent: Prof. Dr. rer. nat. Florian Steinke

Tag der Einreichung: 29.06.2021, Tag der Prüfung: 20.10.2021

D 17
Darmstadt 2021

Abstract

Energy systems worldwide face transitions by the integration of renewable generation sources which are a major driver to reduce carbon emissions and fulfill decarbonization targets. To quantify mid- and long-term effects of these transitions, energy system optimization models are applied. These models can support the design of efficient policies and the development of suitable technologies. However, modeling each country individually requires computational power, sufficient data, and human processing time for the validation and result evaluation.

This thesis provides an efficient framework for the comparison of countries' decarbonization pathways. Instead of increasing the computational power with brute force, the key principal is a data-driven approach accelerating the preparation and evaluation of energy system models. For this purpose, clustering algorithms are applied in two hierarcical stages: the first stage summarizes countries in global energy system archetypes to assess transitions for a reduced number of prototypical countries. The second stage clusters spatially highly resolved data to generate suitable regions for a multi-region model considering the differing spatial potentials of renewable generation. Both approaches are validated by three exemplary use cases: 1) grid topology, 2) green hydrogen production, and 3) coal phase-out.

The developed approach is based on a global data basis combining socio-economic, geographic, and energy data including highly resolved geospatial data. This data basis is required for both clustering algorithms. The archetype clustering uses an extended k-Means algorithm. In the second stage, Ward's method is implemented to cluster the spatial data. To avoid the curse of dimensionality by the high spatio-temporal resolution of hourly renewable generation profiles, Dynamic Time Warping and Principal Component Analysis reduce the time dimension in the clustering. For the first and third use case, the framework processes OpenStreetMap data to synthesize the existing grid structure and identify coal mining areas. The hydrogen use case uses a break-even price approach.

The countries are classified in 15 archetypes, which is in a similar range as the definition of subregions by the United Nations. Compared to these regions, the classification in archetypes considers countries on different continents and thereby represents the energy system characteristics on average 30% better. Modeling an 80% decarbonization scenario between 2015 and 2045 for all archetypes shows the fundamental challenge that huge investments in currently less developed countries are needed. Furthermore, the modeling results confirm that the decarbonization pathway of countries is 10-30% closer to countries within the same archetype than to countries within the same geographic region.

The use cases apply the developed framework from archetype clustering to regional clustering. For all three use cases, the archetypes lead to a selection of countries with suitable characteristis. Regarding the grid, Denmark, representing a country of a high renewable share, foresees fewer changes in its grid topology than Morocco. Second, Saudi Arabia is highly attractive for green hydrogen production with a low break-even price of 1€/kg in the context of a decarbonized system. Last, coal-dominated regions in South Africa face significant challenges since a coal phase-out shifts the generation to other regions with good renewable conditions.

This thesis contributes to the worldwide application of energy system models which are important to determine cost-optimal decarbonized energy systems. The implementation of data-driven clustering methods simplifies and accelerates the modeling of each country globally. Thereby, modelers can use the data analysis as a first indication and focus on the model or its evaluation, policymakers can compare countries, or even regions within countries, and technology companies are able to quickly assess markets for their products.

Zusammenfassung

Weltweit verändern sich Energiesysteme durch die Integration von erneuerbaren Energien, die ein wesentlicher Treiber für die Reduzierung von CO_2-Emissionen und die Erfüllung von Dekarbonisierungszielen sind. Optimierungsmodelle ermöglichen es, diese mittel- und langfristigen Veränderungen in Energiesystemen zu quantifizieren. Die Ergebnisse können somit sowohl die Entwicklung effizienter politischer Strategien als auch innovativer Technologien unterstützen. Die Modellierung jedes einzelnen Landes erfordert jedoch eine hohe Rechenleistung, eine intensive Datenrecherche sowie Bearbeitungszeit für die Validierung und Auswertung.

Diese Arbeit verfolgt einen datengetriebenen Ansatz, um den Vergleich nationaler Dekarbonisierungspfade zu vereinfachen. Dazu werden die Vorbereitung und die Auswertung der Modelle durch die Anwendung von Clustering-Algorithmen in zwei Stufen beschleunigt: die erste Stufe ordnet Länder in globale Energiesystem-Archetypen ein, um Entwicklungen nur für eine reduzierte Anzahl prototypischer Länder bewerten zu müssen. In der zweiten Stufe werden örtlich aufgelöste Daten geclustert. Somit können Regionen für ein Ländermodell datenbasiert definiert werden, welches räumlich variable Potenziale erneuerbarer Erzeugungstechnologien berücksichtigen kann. Drei konkrete Anwendungsfälle unterstützen die Validierung der beiden Ansätze: 1) Analyse der Netztopologie, 2) grüne Wasserstoffproduktion und 3) Kohleausstieg.

Der Ansatz basiert auf einer globalen Datenbasis, die sozioökonomische, geografische und energiebezogene Daten, einschließlich hoch aufgelöster Geodaten, beinhaltet. Darauf aufbauend verwendet das Archetyp-Clustering einen erweiterten k-Means-Algorithmus und das räumliche Clustering Ward's Method. Ein Dynamic Time Warping Ansatz und eine Hauptkomponentenanalyse reduzieren die hohe räumliche und zeitliche Dimensionalität, um auch stündlich aufgelöste Erzeugungsprofile clustern zu können. Für den ersten und dritten Anwendungsfall werden OpenStreetMap-Daten verarbeitet, die das vorhandene Stromnetz und Kohleabbaugebiete identifizieren. Der Wasserstoff Anwendungsfall verwendet einen Break-Even-Preis-Ansatz.

Weltweit werden die Länder in 15 Archetypen eingeteilt. Diese Anzahl ist gut vergleichbar zu der Einteilung in Subregionen durch die Vereinten Nationen. Im Vergleich zu diesen Subregionen, sind die Archetypen über verschiedene Kontinente verteilt und repräsentieren die Länder-Energiesysteme im Durchschnitt 30 % besser als eine geopolitische Einteilung. Die Ergebnisse modellierter Dekarbonisierungspfade von 2015 bis 2045 heben insbesondere die Notwendigkeit hoher Investitionen in derzeit weniger entwickelten Ländern als Herausforderung hervor. Darüber hinaus belegen die Ergebnisse, dass die Transformationspfade von Ländern innerhalb des gleichen Archetyps 10 – 30 % ähnlicher sind als innerhalb ihrer geografischen Region.

Die Modellierung der drei definierten Anwendungsfälle unterstreicht den Mehrwert des entwickelten Verfahrens vom Archetyp-Clustering bis zum regionalen Clustering. In allen drei Fällen führt die Auswahl der Archetypen zu geeigneten Ländern. Im Hinblick auf das Stromnetz zeigt Dänemark, ein Land mit einem hohen Anteil an erneuerbaren Energien, weniger Veränderungen in seiner Netztopologie als Marokko. Außerdem ist Saudi-Arabien sehr attraktiv für die Produktion von grünem Wasserstoff mit einem niedrigen Break-Even-Preis von 1€/kg. Zuletzt führt ein Kohleausstieg in Südafrika zu großen Veränderungen für von Kohle geprägte Regionen, da die Erzeugung in andere Regionen mit guten Bedingungen für erneuerbare Energien verlagert wird.

Diese Arbeit trägt dazu bei, Energiesystemmodelle für die Berechnung von Dekarbonisierungspfaden weltweit anwenden zu können. Die entwickelten datengetriebenen Clustering-Methoden vereinfachen und beschleunigen die Auswertung einzelner Länder. Dadurch haben Modellierer*innen eine erste Indikation aus der Datenauswertung und können sich vor allem auf die Auswertung verschiedener Szenarien konzentrieren, politische Entscheidungsträger können Länder oder Regionen vergleichen und Technologieunternehmen sind in der Lage, Märkte für ihre Produkte schnell abzuschätzen.

Acknowledgments

The past 3.5 years, in which I have worked on this thesis, have been a marathon with many enthusiastic sprints but also some suffering phases. I want to use this opportunity to thank several people, coaches, fellow runners and spectators, who have supported me throughout this route and thereby boosted my physical and mental stamina.

First of all, I want to thank my supervisor Professor Stefan Niessen for many enriching discussions, challenging questions, and his rigorous feedback - all with a cooperative way of communication and collaboration. I was relieved by his willingness to take over the supervision from Professor Armin Schnettler, who I would like to thank for his support in finding the way to energy system modeling and shaping this topic in an early stage. I would also like to express my gratitude to Professor Florian Steinke for co-supervising this thesis, his very valuable feedback on the methodology, and especially on this manuscript.

The major part of this thesis was conducted in the Energy System Modeling team of Siemens Technology. I am extremely thankful for the great support I received in this team during my journey. First, I would like to mention the support of my supervisors, Michael and Matthias, who spent countless hours with me discussing methodological approaches, intermediate results, or publication opportunities. All these discussions were my constant compass to stay on track. Second, I want to highlight the support of Hans Jörg, who contributed in many right moments with concise input to keep the big picture in mind and left plenty of freedom for my personal development by his leadership style. Third, the support of the entire team. Dieter, Mathias, Paul, and Simon were always eager to bring in their expertise solving any kind of arising question or providing open feedback on ideas. And of course, I also want to include Dominik, Eva, and Till who not only provided support as colleagues but also an open platform for exchange on any topic. During all the time, I was delighted to (co-) supervise various great student projects that all directly or indirectly contributed to this thesis. A big thanks to Ben, Christian, Evelina, Martin, Matthias, Miltos, Nils, Pedro, Rim, Siang-Jie, and Stephany.

Next to my direct colleagues, many other colleagues in various departments within Siemens and externally, I would particularly like to mention the FfE e.V. here, have crossed my way and contributed to the presented results. Their interest and ingenious ideas in many discussions have always increased my motivation for this topic. In this context, I would also like to thank other doctoral students for various discussions on our topics, progress, and life. Thank you, Christoph, Fabian, Iris, Jan, Niklas, Oliver, Sebastian, Simon, and many other colleagues from the Siemens PhD Network.

To endure a marathon, external stimuli are essential. All this would have never been possible without the endless support of my family and friends. I would like to deeply thank my parents, Sabine and Stefan, for raising my curiosity in life, supporting me in every decision, giving and allowing me an incredible education, and helping me to find my interest in the energy sector. I would also like to thank my siblings, Christoph with Hannah and Jakob (a real bliss during the writing process), Johanna, and Paula, for the extraordinary cohesion and the joy of spending time together with both, discussions and distractions. The same applies to many friends, in Munich, Köln, and other cities, who accompanied my way. From the first semesters in Aachen to the last years and especially in the time of a global pandemic, they were a great support not to lose myself in numerous words and numbers but keeping up the stamina and happiness for a long-distance run. Thank you all, especially Ben, David, David, Hauke, Henrik, Kevin, Martin, Max, Mayte, Oliver, Rajib, and Steffen.

Ultimately, I want to express my deepest gratitude to Gabriela for her sincere encouragement, beneficial advices, serene patience, and joyful attitude, especially in the final phase of this thesis.

Thank you, merci, gracias und ein großes Danke!

Table of Contents

List of Figures

List of Tables

1. Introduction

Climate change is one of the significant global challenges in current times. In his speech at the U.N. Climate Change Summit 2014, Barack Obama highlighted the urgency thus encouraging imminent actions to prevent irreversible changes [1]. To better understand systematical changes and support political decisions leading to concrete actions, modeling scenarios that project future developments is an important method. By modeling future energy systems, this thesis contributes to better understand the decarbonization of the energy sector and support the definition of actions that lower the effect of climate change. The framework developed here improves the application of energy system models to each country worldwide. In the first chapter, the following sections present the relevance of this topic, its academic background, and the specific research questions.

1.1. Motivation

The past years have shown a significant increase in global temperatures. Just in the period from 2010 to 2018, the average temperature has increased by 0.95°C compared to the average temperature in the base period 1951-1980. Except for one month, September 1992, every month between 1981 and 2019 has globally been warmer than in the mentioned base period [2], [3]. These deviations in weather data quantify climate change, a major global challenge of the 21st century affecting all countries worldwide. It impacts physical systems, e.g., by melting glaciers or draughts of rivers, biological systems, e.g., by changing marine ecosystems or increasing wildfires, and even human and managed systems, e.g., by changing conditions for food productions. All these impacts can be found on every continent [4].

In the last decades, increasing greenhouse gas emissions have led to these rising temperatures and changes in natural systems. Next to gases such as methane or nitrogen oxides, carbon dioxide emissions (CO_2) amount to two-thirds of the total global greenhouse gas emissions [5]. The energy sector accounts for around 85-90% of these CO_2 emissions [6]. As depicted in Figure 1-1, the energy-related emissions rose from 1990 until 2019 by more than 60%.

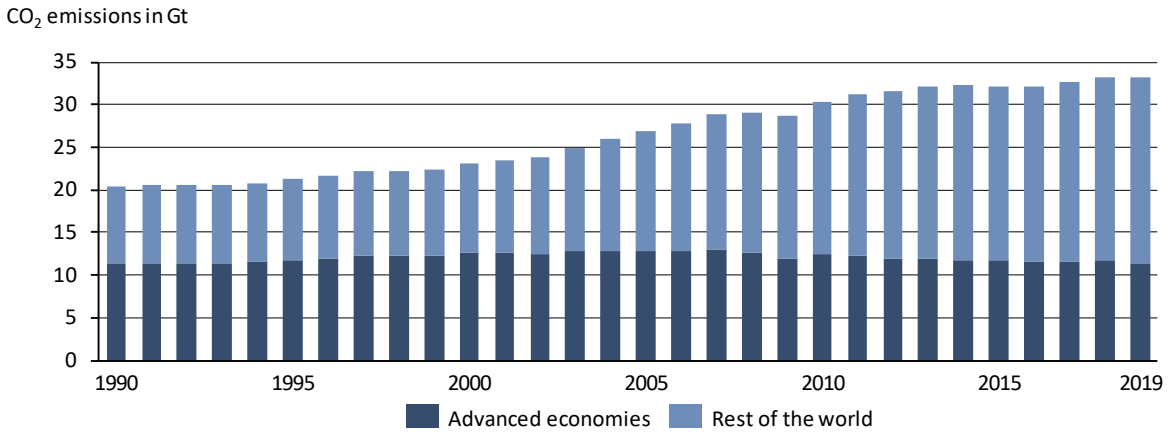

Figure 1-1. Energy-related CO_2 emissions 1990-2019, adapted from [7].

While "advanced economies"[1], which currently have a significantly higher emission level per capita, have started to decrease emissions slowly, the global increase is mainly due to the economic growth of emerging countries. For a global emission reduction, "advanced economies" need to continue the transformation process of lowering their high emission level by intensifying decarbonization measures.

[1] According to the *IEA*, advanced economies are Australia, Canada, Chile, European Union, Iceland, Israel, Japan, Korea, Mexico, Norway, New Zealand, Switzerland, Turkey, and United States.

By contrast, countries that currently face economic development need to decouple economic growth and increasing emissions.

Even though crises such as the financial crisis 2009 or the COVID-19 pandemic in 2020 resulted in a short-term drop, emissions usually have reached the pre-crisis level quickly and continued to increase [7], [8]. Therefore, long-term strategies are required to reduce the emissions sustainably by transforming the energy systems. The Paris Agreement, signed at the 21st Conference of the Parties (COP21), has addressed the global awareness and political urgency for such strategies. Therein, the countries have agreed to keep the temperature increase below 2°C and even try to limit it to 1.5° above pre-industrial level [9]. To prevent imbalances, the agreement includes a support mechanism for less developed countries. Even though some transnational unions have agreed on common strategies, e.g., the European Union (EU) with the Green Deal [10], each country still has the primary responsibility to realize these goals. Therefore, the countries need to define specific measures in National Determined Contributions (NDC) [9]. Despite this framework being implemented and agreed upon, the current NDC are by far not enough to meet the 2°C goal. A review report indicates that there is, e.g., a gap of 15 Gt CO_2 for the 2030 interim goal [11]. Similarly, the current World Energy Outlook 2020 confirms that much more political measures are required to reach the COP21 goals [8]. This lack of contributions underlines that the fight against climate change requires further measures to decarbonize the energy systems globally.

The efforts to reduce emissions and transform the energy system can be tracked by several indicators. The total carbon emissions are the main indicator among others such as the final energy carbon intensity, the energy intensity of the economy, or the electrification rate of the total energy [12]. Based on analyses of the *International Energy Agency* (*IEA*), Figure 1-2 visualizes the development of the primary indicator, the carbon emissions, between 2017 and 2018 by the effect of specific measures.

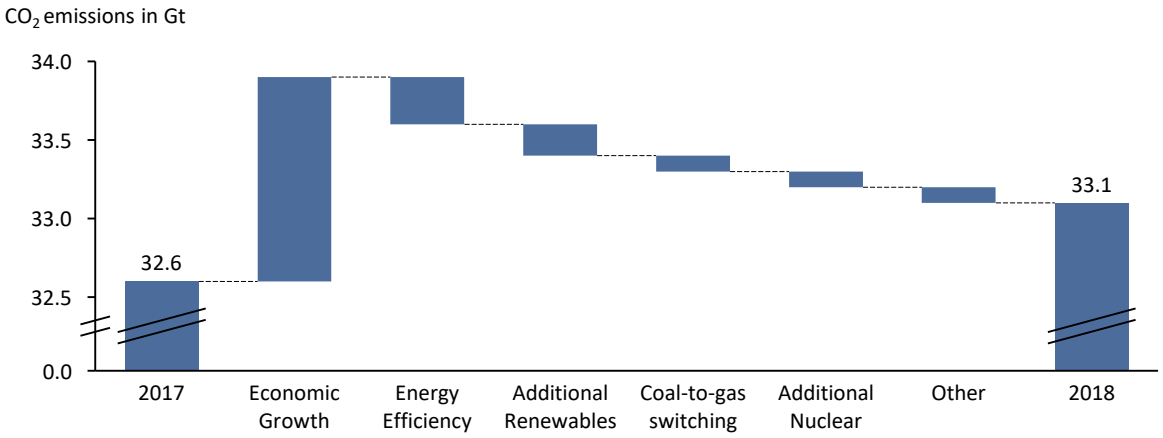

Figure 1-2. Change of global energy-related CO_2 emissions between 2017 and 2018, adapted from [13].

As explained in the context of global emissions in Figure 1-1, the increase in 2018 confirms economic growth as the primary driver of increasing emissions. By contrast, energy efficiency, the integration of renewables, coal-to-gas switching, and an increased generation of nuclear power plants are currently the most effective reduction measures. The last three measures as well as the mentioned indicator of the overall electrification rate underline the importance of the electricity sector. By electrifying other end-uses, such as road traffic by electric vehicles or heating by heat pumps, the overall energy efficiency can be improved through higher energy conversion efficiencies [14]. These approaches lead to a fundamental change of the energy system: different sectors are coupled by electrification.

The importance of the electricity sector is further underlined by an important driver to fulfill the rising electricity demand and decarbonize the current generation: emission-free renewable energy sources (RES). Their increasing expansion globally improves the economical attractiveness of RES, especially

of wind and photovoltaic (PV) generation [15]. Compared to conventional generation technologies, these sources, referred to as variable renewable energy sources (VRES), depend on the weather conditions. They are not necessarily available when electricity is needed. The resulting fluctuations require storage options, other flexible generation sources in the system, or a flexible adaptation of the demand to ensure energy security in times of reduced output of VRES. Next to this time challenge, the dependency on weather conditions induces a spatial challenge to the energy system. Compared to today, the spatial location of generation changes and requires, e.g., an expansion of the existing electrical grids [16].

Energy system models have been proven as a suitable solution to analyze the effects of these changes on the energy system [17]. A model is defined as *"a representation of something in words or numbers that can be used to tell what is likely to happen if particular facts are considered as true"* [18]. Transferring this definition to energy systems, models help better understanding the required assets and their operation in future energy systems, e.g., to analyze decarbonization scenarios with a high share of varying renewable energy sources or changing energy demands. Thereby, they support finding a technically reasonable and economically attractive mix of technologies to reach political targets [19]. Overall, such models address all three dimensions to plan and evaluate sustainable national energy systems, which the World Energy Council summarizes in the energy trilemma [20]: (1) energy security, a technologically feasible energy system, (2) energy equity, an economical energy system, (3) and energy sustainability, a low-carbon energy system representing goals from Paris Agreement.

Various institutions use energy system models with differing purposes [21]: research institutions that aim at improving the algorithms and elaborating the impact of new innovative technologies in the system, governmental agencies contributing with consultations to new policies, and technology companies such as utilities that want to project their business model or the impact of technological developments. All user groups require sufficient data to apply their models to different scenarios. Furthermore, a comprehensive data basis helps to accelerate the modeling time, generate reproducible results, and simplify the evaluation process.

In this thesis, the target is to apply an **energy system optimization model** to **as many countries as possible**. This application enables a **globally standardized evaluation of decarbonization pathways** for **national energy systems**. It provides the opportunity to identify future technology mixes for reaching the Paris Agreement goals. For this purpose, the described modeling approach considers only the electricity sector as it is currently most contributing to emission reductions and plays an important role in decarbonizing other sectors. Within the electricity sector, the framework developed here is applied to **three use cases** to demonstrate its benefits for modeling country energy systems. The definition of these use cases is inspired by the World Energy Outlook 2020. It identifies the massive expansion of RES, which leads to significant grid expansions, and a reduction of coal capacities as two key challenges. Concerning the coupling of RES and the electricity sector to other sectors, the integration of low-carbon fuels such as hydrogen is stated as an important measure [8]. By representing trends in future energy systems, the use cases are relevant for all described user groups of energy system models. They can be shortly described as follows:

1. **Grid topology**: To find cost-optimal solutions, the grid topology must be included in the expansion planning of the energy system and is therefore further examined in the first use case [19]. The increasing amount of VRES changes the spatial distribution of electricity generation, requiring grid expansion measures [8]. Consequently, the electricity grid structure might change fundamentally.
2. **Green hydrogen production**: this use case focuses on identifying suitable countries and regions for green hydrogen production in the macroeconomic context of a country's decarbonization process. Green hydrogen, produced by electrolyzers using electricity from RES, is a lever for decarbonization [8]. This hydrogen can either be burned in turbines to

generate electricity or substitute fuels in other sectors such as industrial processes or the transport sector. Additionally, it can be used to store VRES overproduction. In current systems, green hydrogen is costly compared to conventional technologies. However, an increasing penetration is expected in future systems improving the profitability. Its production costs also differ depending on the RES potentials of each country [22].

3. **Coal phase-out**: the third use case shows the effects of a coal phase-out in coal-dominated power systems from a global level to specific regions characterized by coal power plants or mining activities. Worldwide, an increasing number countries decide on phasing out their coal power plants [23]. The missing generation capacities can either be substituted directly by RES or by gas power plants in a transition phase. The latter ensures firm capacity while still decarbonizing the energy system [24]. This process is often referred to as a coal-to-gas shift. It has already been a lever to reduce emissions, according to Figure 1-2. The specific CO_2 emissions of natural gas plants (around 0.2 kg CO_2/kWh_{th}) are lower than emissions of coal and lignite power plants (0.34 - 0.41 kg CO_2/kWh_{th})[2] [25].

1.2. Literature Review

For evaluating upcoming challenges, such as the ones represented by the three use cases, energy system models provide the basis to analyze future energy systems. There is a considerable amount of literature reviewing these models. As a first step, different model characteristics can be deducted from various review studies. Figure 1-3 provides a simplified summary of these characteristics by comparing them in several categories. These categories include the model approaches, perspectives, purposes, methodologies, detail levels, and model types. The composed visualization is a simplification because models can have multiple properties across the classifications. However, the summary of review papers state the general difference between short-term, bottom-up, very detailed simulation models and long-term, top-down scenario models [14], [17], [26]-[31].

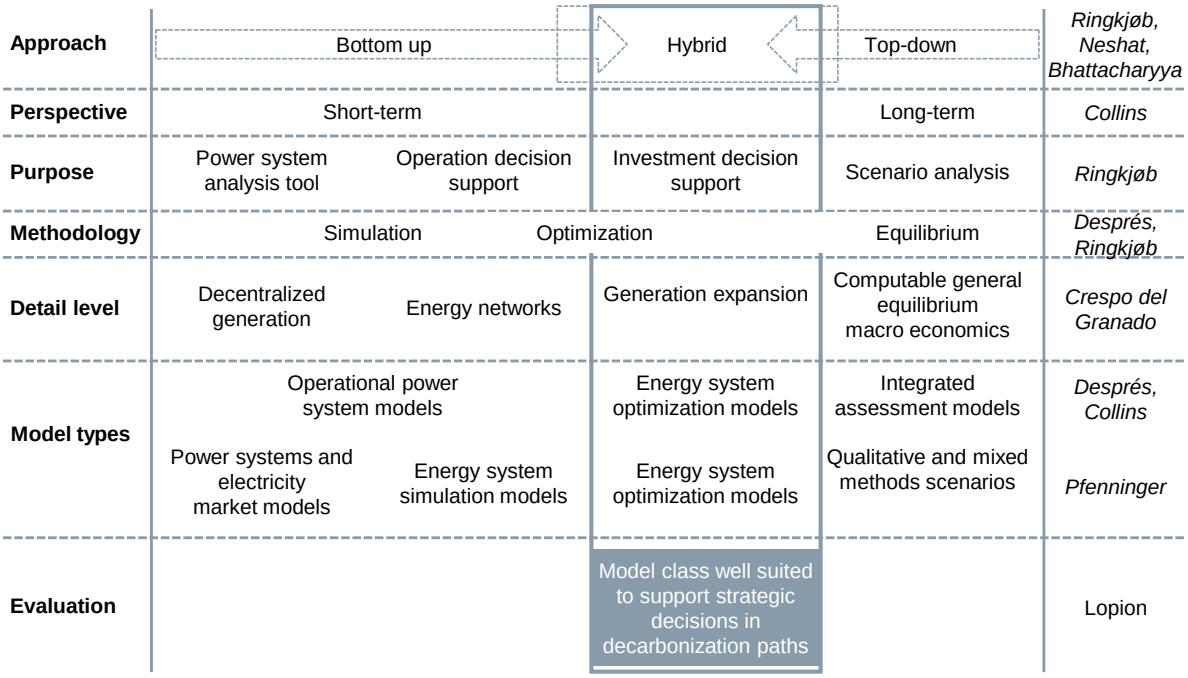

Figure 1-3. Classification of energy system model characteristics composed from the literature reviews referenced in the last column [14], [17], [26]-[31].

[2] Methane emissions during the exploration process of natural gas are not considered in this thesis.

The approaches range from bottom-up models on a technically detailed level to more general economic top-down models, including hybrid models combining both perspectives [26]. For short-term perspectives, the models calculate the energy system for one day or one year, while long-term perspectives aim at system projections for decades [27]. Methodologically, models apply simulations of technical characteristics and behaviors such as agent-based simulations, mathematical optimizations minimizing an objective function, e.g., the system costs, or computations of equilibriums balancing the system across different players [26].

For the scope of this thesis, the final evaluation in the last row summarizes that energy system optimization models are a well suited model type to project the decarbonization of the electricity sector. They are often applied to calculate an optimal mix of technologies and analyze decarbonization strategies on a country level. The main objective of these models is to find a cost-optimal solution for a mid- or long-term view under the boundary conditions of meeting emission targets and ensuring a technically reliable system. An exemplary model formulation with these functionalities is provided by *Mancarella et al.* [32]. Additionally, models of this type are mentioned as the optimal compromise *"to support governments with strategic decisions on the future of their countries' energy supply and to accomplish climate goals based on the Paris Agreement of 2015"* [31]. According to *Lopion et al.*, around 95% of the identified models, which are suitable to model climate goals, are bottom-up or hybrid optimization models [31]. The International Renewable Agency (*IRENA*) also highlights the importance of "generation expansion planning models" for an effective transition towards future energy systems, including a high share of RES [19]. Frequently mentioned examples for such optimization models, which will be discussed further below, are MARKAL/TIMES, MESSAGE, OSeMOSYS, BALMOREL.

For energy system optimization models, several challenges for further development and improvement have been identified by recent studies [17], [21], [26], [27], [31]-[34]. The two challenges of spatial resolution and a worldwide consistent data basis are the main focus of this thesis and therefore highlighted bold in the list below:

- Time resolution: finding a suitable resolution of time series to represent the variability of RES appropriately [17], [26], [27], [31]
- **Spatial resolution:** finding a suitable resolution of spatial details to represent different potentials of RES depending on geographic characteristics or the electrical grid appropriately [17], [27], [31], [32]
- **Data:** gathering all required data for a consistent model, generating a transparent data set, processing raw data, and enabling the transferable usage of data for different country models [26], [31]-[33]
- Open data and models: providing data and model source code in an open-source community to focus on the evaluation of the model results, increase transparency, and facilitate reproducibility of model results [21], [34]
- Impacts of other sectors on the electricity sector: including further sectors in the model to optimize the degree of electrification and optimize sector coupling technologies [26]
- Technical representation: finding a representation of considered technologies which reflects the technical characteristics appropriately for the model environment [27]
- Computational efforts: simplifying models to keep the computational complexity in a solvable range [31]

Many of the mentioned challenges, such as selecting a suitable time and spatial resolution, sector coupling, or the technical representation, are closely connected to the computational efforts. They all deal with the conflict of increasing the detail of modeling while keeping the model in a computationally solvable size. In this context, it is essential to focus on one of these challenges and finding approaches

to reduce complexity in one dimension [31]. Therefore, this thesis considers the challenge of the spatial resolution in models as it suits the goal of finding a model approach for all countries globally. In addition to the spatial details, the modeling of all countries requires a solid and well-defined data basis. This data basis must ensure to be transferable to all countries, should be consistent, and lead to reproducible results. Concerning the time resolution, several studies, for example, by *Teichgraeber and Brandt* [35] or *Kotzur et al.* [36], have already been carried out. The challenge of sector coupling is not elaborated in detail since the thesis' scope focuses on the electricity sector.

To analyze the state-of-the-art of these two challenges, energy system studies are classified into three general **types of studies**: world studies, country studies, and regional studies. These types can be further described by their **considered scope**, from a local scope to a global scope, and the **data** used, from aggregated data to detailed spatial data. Since this thesis focuses on evaluating the challenge of the spatial resolution in models, the **regional model resolution** of a country is the fourth classification level: a country can be modeled as a single region with a simplified profile or in a multi-region model by using spatially resolved data and considering electricity exchange between the regions [37]. Figure 1-4 provides a schematic overview of the four mentioned classification levels. Even though there might be deviations in distinct model approaches, most studies follow this scheme to keep the model in a solvable range.

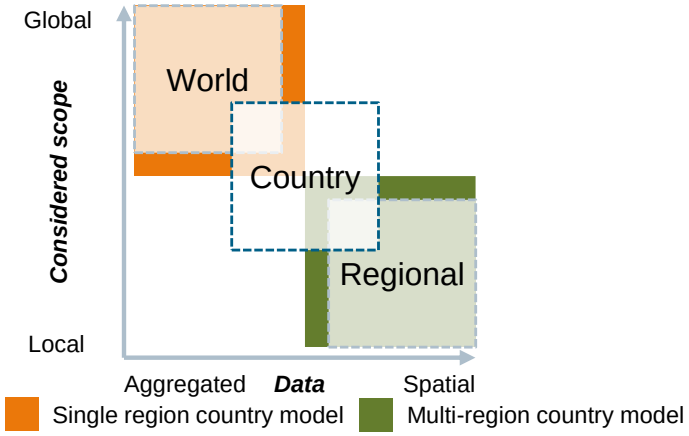

Figure 1-4. Classification of studies using energy system optimization models.

Studies concerning the entire world mostly aim to calculate the world energy mix in future decarbonized energy systems or estimate the reaction of global markets on certain trends [29]. Examples for such global studies are available for the three mentioned models: the global MESSAGE [38], GENeSYS-MOD for OSeMOSYS [39], and the World-TIMES for MARKAL/TIMES [40]. Another group of global studies has elaborated the possibility of a global grid connection by analyzing potential generation areas [41] or creating a global model with around 50 regions [42]. Researchers from the Lappeenranta University of Technology have created a global model that is even more detailed by using 150 regions [43], [44]. In these studies, detailed pathways towards 100% renewable future energy systems have been calculated. They analyze a global scope, use mostly aggregated data, and represent the countries mainly as a single region. Sometimes models are even applied using continents or sub-continents as one modeled region aggregating the countries therein. In the global study of *Ram et al.* [43], countries with a large area, such as the United States of America (USA) or Russia, have been split into regions. Other countries, for instance, in Africa, have been aggregated. An intermediate granularity level between world and country studies are evaluations of continents and subcontinents. These studies mainly consider each country as one region. Two examples for such studies are models of Europe [45] and South-East Asia [46].

The next level are specific country studies, which are available for many countries worldwide and various levels of detail. Most of these studies are primarily based on a dataset individually gathered

for the respective country and usually focus on a particularly relevant technology or trend. Referring to the dimensions mentioned in Figure 1-4, the scope of country systems is the country itself and potentially its neighboring countries. The data are generally aggregated, but some models also include spatially resolved data. Regarding the spatial resolution, some studies consider the countries as one region while others use multi-region models to represent the spatial differences. Examples for single region country studies are studies for decarbonized systems in Saudi Arabia [47], Denmark [48], or Ireland [49]. By contrast, the following exemplary studies analyze the green hydrogen production in Great Britain [50], a 100% renewable system in South Africa [51], and different decarbonization scenarios in China [52] by resolving the respective country in different regions.

The third type of studies introduced in Figure 1-4 contains regional models that consider a local scope with spatially detailed data. Those models are usually regionally resolved but might also consider just one region in the model. Examples for such studies are an evaluation of California as a region in the USA [53], a detailed geodata-based analysis of a region in India [54], or a regional analysis of the German federal state Bavaria [55].

The transfer of these existing studies to the elaborated focus on data and spatial resolution leads to two particular challenges: (1) country models need to be aggregated to a global scope without losing information on their energy system characteristics and (2) spatial data need to consider detailed regional characteristics in a country while still being solvable. These two challenges, which aim to reduce the complexity of modeling while still including detailed data, are further analyzed regarding their state-of-the-art in current literature.

Challenge 1: Global scope

As mentioned before, various studies have analyzed world energy systems or the overall impact of a transition towards decarbonized energy systems in a global scope. These studies have applied different energy system models, such as the World-Times [40], the global MESSAGE [38], or GENeSYS-MOD, a global application of OSeMOSYS [39]. In these models, countries are aggregated in geographic regions based on their continent or sub-continent. This classification leads to splitting the world into 10-15 modeled regions. Other studies have modeled the world in a much higher resolution, as it has already been described for 50 regions to calculate a globally connected electricity system [42] or 150 regions to evaluate global pathways to 100% renewable energy systems [43]. Another project has developed a detailed data basis to represent the current global energy system, e.g., by deriving technical details for power plants [56]. Even though data are available on such detailed levels and the models can solve this resolution, all studies summarize countries in a second step to facilitate a manageable evaluation of the results. The approach, which uses 50 regions, summarizes countries to compare the modeling results to other existing global studies [42]. The 150 countries are aggregated to 9 world regions for which the modeling data are available and the overall evaluations are described [43]. Comparably to these definitions of regions based on geographic criteria, the *United Nations* (*UN*) provide an official classification of six continents, including Antarctica, which will be neglected in the following evaluations. In a second level, the remaining five continents are split into 17 sub-continents which is closer to the number of regions used in most energy system studies [57].

In contrast to these purely geographical classifications, various approaches use data-driven classifications of countries. These approaches frequently apply clustering algorithms on a set of countries and data categories to summarize similar countries for a specific purpose. One example in the context of energy systems is the discussion paper of *Atallah and Bean*. Therein, they have classified 39 countries in three clusters by a K-means approach to determine their energy productivity [58]. In another example, *Csereklyei et al.* have focused on evaluating energy systems in the EU by clustering the energy mix development in a model-based approach. Precisely, seven clusters represent the shares of commodities in the primary energy mix based on historical developments [59]. *Stuckenberger et al.* have developed five so-called archetypes based on 40 countries in a top-down classification process to

describe their current state of the energy system and anticipate possible future developments [60]. A similar top-down classification has been used in [61] to choose eight countries that can serve as exemplary energy systems for the future, showing different decarbonization pathways depending on the conditions in these countries. Last, a global application of two cluster algorithms, K-means and Gaussian Mixture, has been compared for all countries and six data categories by *Zipperle and Orthofer* [62]. They identify data-driven clustering as a sound alternative methodology to a pure geographic classification. However, their selected data categories strongly focus on integrating renewable energies and do not represent the entire energy system, including currently installed power plants.

Overall, studies often aggregate countries to extend their scope to a global level. Therefore, most current energy system models split countries into geographic regions similar to the official *UN* sub-continents. However, this classification neglects the characteristics of country energy systems since it only considers the geographical location. Clustering approaches are a suitable alternative methodology for summarizing countries not based on their geographic region but driven by energy data. Even though some clustering approaches have already used energy-related data, there has not been a holistic global approach to consider a broad data basis and all countries worldwide in a joint clustering identified yet. Furthermore, the existing clustering approaches have not applied the results in an energy system optimization model to confirm the data-driven classification and project potential decarbonization paths into the future.

Challenge 2: Spatial data

Some country studies include spatially resolved data, mainly by using country-specific data sources. The data sources are even more specific when the scope is reduced to regional studies. Comparably to the challenge of a global scope, the approaches to tackle the challenge of spatial data can be divided into geographic classifications and data-driven approaches. This thesis does not consider a third alternative approach that tackles the spatial resolution directly in the optimization problem since it does not solve the challenge of data provision. This approach improves the solvability of the optimization problem and thereby increases the number of computable regions, e.g., by improving the decomposition of the mathematical problem [63].

Two dissertations have already developed a global and spatially highly resolved data basis applied directly to energy system models. These approaches especially contain profiles of wind and solar generation, which strongly depend on spatial characteristics. The first dissertation [64] applies this data basis to evaluate the average values for each continent. Besides, the data has been used to perform a more detailed evaluation of the European continent with one model region for each country. In this case, the determination of regions is based on geographic classifications and simple aggregation methods. Similarly, the second dissertation [65] has applied its data basis to a European model and a global grid using existing geographic or administrative regions. Even some of the mentioned global models contain spatially resolved data, e.g., the evaluation of a global electricity generation system [42]. However, as many multi-region country studies, these approaches aggregate their data by geographic calculations and are based on administrative boundaries [51], [52], or existing grid zones [50].

For the challenge of including spatially highly resolved data, geospatial clustering represents a data-driven approach. Various research studies have already used geospatial clustering methods for different applications, such as classifying districts in Sao Paulo [66] or analyzing votes in different counties for the US presidential election in 2004 [67]. Even for energy systems, several approaches have already been developed. One group of these studies aims explicitly at clustering regions to find a suitable split representing bottlenecks in the electrical grid. *Cao et al.* have applied a spectral clustering approach to evaluate the redispatch in Germany [68]. Similarly, *Hörsch and Brown* have developed a clustering method to calculate the required grid expansion in Europe for different numbers of regions [69]. The e-Highway project contains a combined approach: the European countries have first been

clustered in a pre-defined number of regions by criteria such as renewable conditions, population, and installed capacities. Based on these regions, a simplified grid model has been deducted [70]. In addition to these grid-focused applications, another clustering approach has used 59 data categories to cluster 11,131 municipalities in Germany using Ward's method [71]. As a result, ten clusters represent the typical energy systems of municipalities in Germany. However, compared to the other approaches, this study has clustered regions even if they are not directly connected. The municipalities belonging to the same clusters are distributed within Germany. *Siala and Mahfouz* have developed a methodology to determine tailored regions for energy system models by combining the K-means and the max-p algorithm. They cluster the electricity demand, PV full load hours, and wind full load hours separately within Europe [72]. As underlying layers, the approach has considered continuous spatial raster. Handling the complexity of this high resolution, the K-means algorithm pre-clusters the continuous layers to apply the max-p algorithm. A similar approach has been developed by *Fleischer* [73]. It uses the max-p algorithm to prepare regions for an energy system model and compare them to randomly generated regions and political boundaries. However, both approaches are mainly applied to Europe and do not include time series of VRES, which are essential for the future systems or existing conventional power plant data.

Summarizing the existing literature on the challenge of including spatial data, data-driven approaches can avoid a purely geographical or administrative classification of regions but rather consider energy system-related data. To address the decarbonization of all countries globally in a model, the literature review shows a lack of globally applicable approaches. The evaluated studies mainly focus on Europe or one aspect of the energy system, such as reducing the complexity of the electrical grid. Overall, a clustering approach based on a holistic global data basis, from existing power plants to time series of renewables, which is thereby applicable to all countries globally, has not been identified in the analysis.

Research gap

For both challenges, the global scope and spatial data, data-driven approaches that reduce the model complexity are suitable solutions. These approaches can handle an increasing complexity resulting from a higher number of countries or spatially higher data resolution. Figure 1-5 depicts the identified research gaps for both challenges, based on the introduced classification of energy system studies in Figure 1-4. Even though there are already research gaps for each of the two challenges, this thesis aims at combining them to facilitate global modeling of countries and still including spatially highly resolved data. In this context, addressing both challenges in one hierarchical framework by two steps simplifies and accelerates evaluations of country models. The two steps are a new country classification towards a global scope and a new classification of regions within a country for a multi-region spatial analysis.

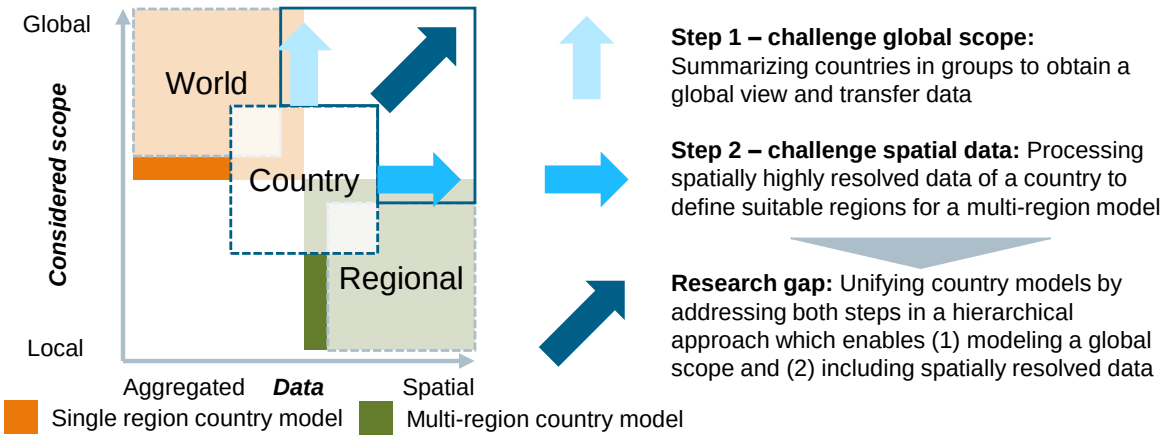

Figure 1-5. Research gap for country energy system modeling addressed by this thesis.

Specifically, the analysis of data-driven approaches to solve both challenges leads to the conclusion that clustering approaches are well-suited for alternative classifications. Cluster analysis is a technique that belongs to the field of unsupervised learning, also called *"learning without a teacher"* [74]. It aims at *"grouping or segmenting a collection of objects into subsets or 'clusters', such that those within each cluster are more closely related to one another than objects assigned to different clusters"* [74]. This definition matches well the idea of a purely data-driven classification of countries or spatial characteristics which is intended to be independent from administrative boundaries or political divisions. Thereby, clustering provides a possibility to solve the challenges of handling complexity for the global scope and the spatial data. It is able to group countries or regions based on their data characteristics, specifically focusing the characteristics of the energy system, without a direct user intervention.

Concluding the literature review, the goal of global applicability including spatial data leads to one further requirement: a transferable global data basis. This data basis is the core element for a unified model approach to the decarbonization of all countries globally and is required as an input to apply clustering approaches.

1.3. Objective, Central Research Questions, and Structure of this Thesis

This thesis aims to enable an energy system optimization model to evaluate decarbonization pathways in the electricity sector for all countries worldwide. The modeling is performed in a globally transferable approach while still considering spatially resolved data. Instead of increasing the computing power drastically, data-driven clustering approaches based on a global data basis are combined in a hierarchical framework. They summarize countries for considering a global scope and simultaneously use spatially highly resolved data to define regions within countries. Following the trends of an increased RES integration in future energy systems and the overall decarbonization, three use cases demonstrate the application of the developed framework. These use cases are the future grid topology, production of green hydrogen, and a coal phase-out.

This described objective leads to the **central research question,** which is answered in this thesis:

- How can clustering techniques be applied to allow for a **global coverage** of energy system studies with low efforts while still including **spatially highly resolved data** in a hierarchical framework?

This general research question is split into three sub-questions:

- **Research question 1:** How can a **unified** and **globally transferable model input** for country energy systems be defined?
- **Research question 2:** Which **clustering techniques** are suitable for summarizing countries in a global scope and summarizing spatially resolved data in regions? How can **metrics** validate the plausibility of the generated clusters?
- **Research question 3:** How can the **three selected use cases** be modeled in a globally applicable energy system model? How can they underline the benefits of a hierarchical approach considering a global scope and spatially resolved data?

Answers to these questions have several benefits for the three mentioned user groups of energy system models: policymakers, technology providers, and the research community. It provides fast and standardized evaluations for policymakers in which the decarbonization progress and its regional impact can be compared between different countries. This comparison is even scalable to specific regions within a country or regions in different countries. Technology providers can use this framework to identify market potentials in different countries or the regional potentials within a country. Furthermore, they can analyze the potential usage patterns of new and innovative technologies in a worldwide, transferable model environment. Third, the approach simplifies the

general setup of energy system models for the modeling community. Saving time for the collection and preparation of input data leaves more resources for detailed evaluation and interpretation of results. Furthermore, the transferable character of the model helps to compare different countries by their decarbonization pathways and use these results to identify critical input parameters for energy system models. The clustering approach also provides evaluations of energy systems even before calculating the decarbonization pathway by highlighting similar country energy systems or regional characteristics. By comparing cluster characteristics to modeling results, the cluster analysis can support the interpretation of the calculated decarbonization paths.

The following chapters develop the answers to the defined research questions. Figure 1-6 visualizes their sequence and a brief description of each chapter. After this introduction, which includes the relevance of the topic, the precise scope, a literature analysis, and the central research questions, chapter 2 contains a more detailed analysis of the research questions. The fundamental principles of energy system modeling, clustering and the use cases to solve the defined questions are explained and the requirements for the framework are derived. The basic structure of the framework, which is designed to fulfill the derived requirements and answer the research questions, is described in chapter 3. Chapter 4 further elaborates on the abstract framework definition by describing the methodological developments and their implementation. These developments are assessed and applied in an energy system optimization model in chapter 5, the results chapter. Therein, the selected clustering techniques are evaluated, global modeling results are presented, and the overall framework is applied to the three selected use cases. Last, the benefits of the framework and the modeling results are summarized and discussed in chapter 6, including potential subsequent research topics.

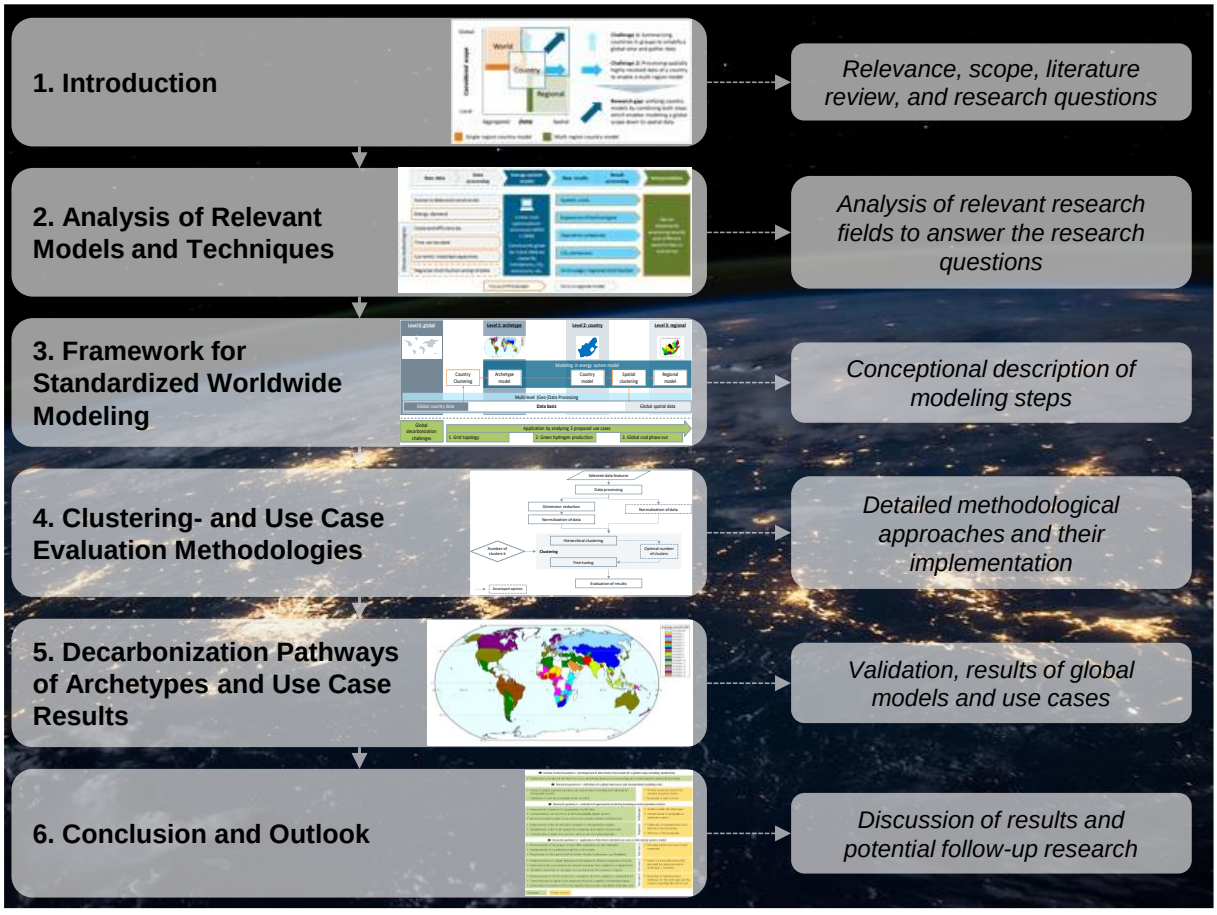

Figure 1-6. Structure of this thesis.

2. Analysis of Relevant Models and Techniques

Following the defined research questions, their context is analyzed in the following chapter to define requirements for the developed framework. Therefore, the identified challenges are quantified, requirements for a transferable energy system model are defined, different clustering techniques and their evaluation metrics are explained, and current modeling approaches for the three defined use cases are examined.

2.1. Quantification of Country Modeling Challenges

The literature review has identified two challenges as a research gap for modeling country energy systems: first, including countries in a global scope and second, including spatial details. To confirm these two challenges, this chapter performs a quantitative analysis of both cases. This quantification is the result of applying the selected energy system optimization model and the developed standardized modeling rules, presented below in chapter 3.3.

Concerning the global applicability of the models, an important aspect is the required time for the modeling process. An evaluation of all countries in the world would sum up to 193 processes. Therein, only the general model setup and the result evaluation can be generalized, while country-specific data, such as installed capacities, still need to be collected individually. Although only linearly increasing, the required time to collect data, calculate the model, and effectively analyze the results is enormous. Even with automated data preparation and result evaluation developed in this thesis, one country model requires around 20 minutes. This time accumulates to more than 60 hours for all countries worldwide. When computing more scenarios or sensitivities, this time is needed for each scenario, making it difficult to quickly evaluate certain developments' impacts. The quantified efforts confirm the need for an aggregation by a data-driven global clustering to evaluate effects easily and quickly.

The spatial challenge is analyzed by varying the regional resolution of a multi-region country energy system. South Africa is a good exemplary case illustrating this. The regional resolution covers three different administrative levels from nine provinces (Level 1) to 234 counties (Level 3) according to the global classification of administrative areas [75]. The model calculates the future system spatially disaggregated by these three levels for different temporal resolutions. These calculations provide the basis to analyze the effect of the spatial and temporal resolution on the modeling results, the runtime of the model, and the general solvability. Figure 2-1 compares these results.

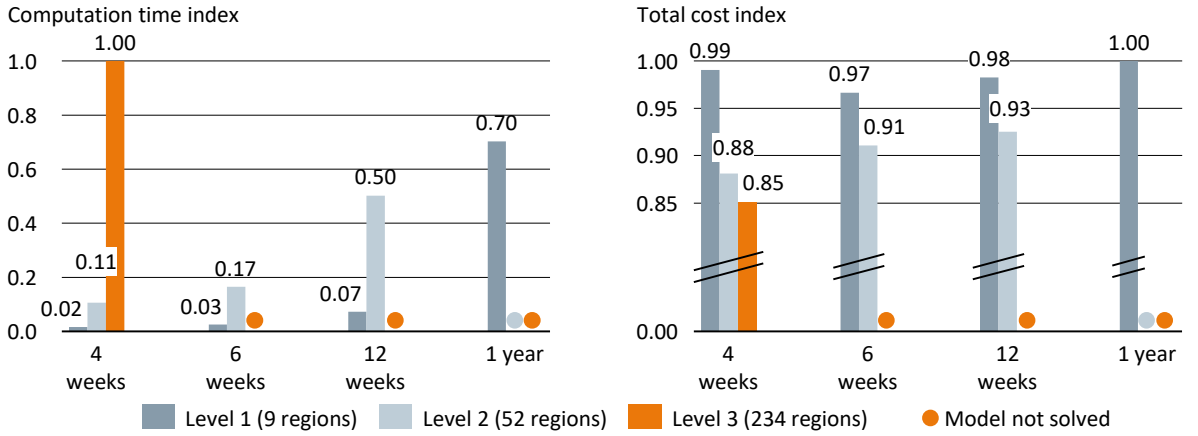

Figure 2-1. Relative computation time (left) and computed total system costs (right) compared to the most detailed (left) and the less detailed model solution (right) for the three simulated levels and four different time step selections.

These exemplary computations, that consider every third hour, show several effects. First, the highly resolved model is only solvable with the available computational infrastructure[3] for a short time horizon of 4 weeks, while the model on level 2 with 50 regions is not solvable for 1 year. Second, the computation time increases strongly when including more spatial details in the model. For the time horizon 4 weeks, it increases more than the number of regions which shows a non-linear dependency. Last, the comparison of costs shows that a higher number of regions leads to lower total system costs. Spatially higher resolved models represent better the individual RES potentials of each region and better use the best regions. By contrast, the aggregation in a lower number of regions leads to an underestimation of the potential.

The conflicting priorities, an increase of computational runtime using more regions which lead to more precise results, are also confirmed by other analyses varying the regional resolution of energy system optimization models. *Zipperle and Orthofer* illustrate the increasing computational complexity [76], while *Siala and Mahfouz* [72] and *Fleischer* [73] confirm the improvement of results using a higher regional resolution. The latter two studies also show that determining a regional grouping not based on states shapes but driven by data leads to improved result quality. For the number of regions, the quantification in Figure 2-1 indicates the range between Level 1 and Level 2 as a suitable resolution for this framework.

2.2. Energy System Modeling Process

The energy system model is central for this thesis since it computes the cost-optimized and decarbonized future energy systems. For the first research sub-question, a globally transferable model setup, the setup process of such models is analyzed with a focus on the input and output data.

2.2.1. Setup Process of Energy System Models

According to *Pfenninger et al.*, the setup process of energy system models consists of four major phases: (1) input data preparation, (2) implementation and computation of the model, (3) result evaluation, and (4) interpretation of results [21]. These phases are visualized in Figure 2-2. Next to the general steps, the schematic overview also contains details for each step from various literature sources [32], [26], [42], [77]. The input data preparation of a model can be split into collecting raw data and processing this raw data. Similarly, this data processing also needs to be executed for the results.

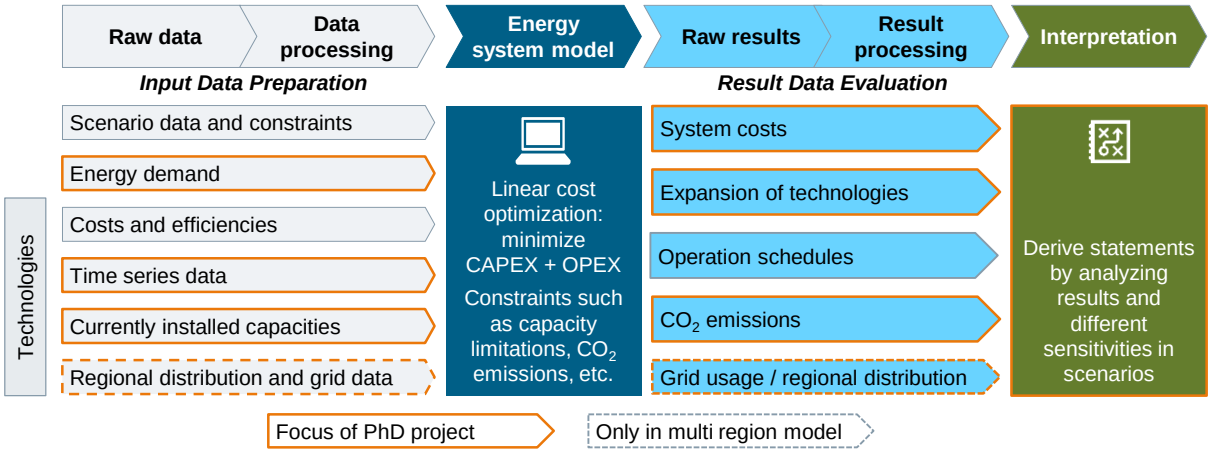

Figure 2-2. Setup process of energy system models partially adapted from [21].

The relevant input data categories are scenario data, the energy demand, and data for the modeled technologies. Multi-region models require further input data reflecting the regional distribution of

[3] The compute server has the following characteristics: Intel Xeon E5-2620, 2x2x6 cores, 115 GB memory.

technologies and the connecting grid. The second step is the model itself, which optimizes the total costs (TOTEX) by considering capital expenditures (CAPEX) and operational expenditures (OPEX). It includes boundary constraints such as emission targets. Several reviews of energy system models show that many different models exist, of which some are even available as open-source models [34] [78]. Therefore, developing a suitable model is not part of the methodological developments in this thesis. Reflecting the model formulation, result data are the system costs and CO_2 emissions. Furthermore, the selected technologies can be evaluated by their expanded capacities and hourly operation schedules. Additional results of the multi-region models are the future distribution of technologies, the grid usage, and its expansion. To conclude from the results for policy implications or statements about specific technologies, the result interpretation signifies the last step. A frequently applied approach is the comparison of sensitivities by different scenarios.

Addressing the first research sub-question, the input data is essential in the modeling process. To ensure a globally applicable and transferable model setup, the input data must be prepared in a standardized way and available for all countries worldwide. The standardized evaluation of modeling results and the definition of key result indicators are further requirements. Therefore, the following chapters, 2.2.2 and 2.2.3, address these two steps. The interpretation process is essential for the overall questions, how energy systems worldwide can reach the goals of the Paris Agreement.

2.2.2. Input Data Preparation

The six input categories mentioned in Figure 2-2 are analyzed to define requirements for a standardized model. Therein, data is classified between being relevant for global assumptions or for each country individually. The detailed integration of this analysis in the modeling framework is described in chapter 3.3.2.

Scenario data and constraints

The scenario data and constraints describe general assumptions and boundary conditions of the energy system, i.e., financial assumptions, CO_2 prices, decarbonization targets, and the time horizon. Since these assumptions strongly depend on political decisions or regulatory aspects, they are handled globally for all countries to keep the scenarios comparable.

In the context of financial assumptions of energy system models, the weighted average cost of capital (WACC) is an essential factor. It represents the overall costs of capital expected for investments by the ratio between equity and debts [79]. In general, the WACC differs between different countries as there are different financing conditions such as interest rates and there are already approaches that identify country-specific WACC [80]. However, it is challenging to find updated publicly available data for this calculation and a uniform approach to estimate the future cost of capital globally [81]. Therefore, the WACC is kept constant at a value of 7% for all countries, which is comparable to global agencies such as *IRENA* and the *IEA* or other global modeling approaches [81].

The decarbonization target reflects the goals of the Paris Agreement. For example, the EU member states have agreed to reduce 80-95% of their emissions by 2050 [82]. Other studies evaluate 100% renewable energy systems for the target year 2050 [44], [83]. To validate the starting point, the model starts with the historical year 2015. Based on this validation step, the global scenario in this thesis contains a linear reduction of emissions by 80% until 2045, with an intermediate step in 2030. Thereby, a 100% reduction until 2050 is still reachable and the calculations fulfill the targets of the Paris Agreement. An alternative way to force decarbonization is the incorporation of a CO_2 price. For this thesis, the CO_2 cap is defined in the base assumptions since there is no global framework for such a price.

Energy demand

The energy demand is an essential input for an energy system model. It determines the demand which must be provided by the optimized generation capacities [32]. Since the model in this thesis focuses on the electricity sector, included by an exogenous demand, it requires an electricity demand projection. The electrification of other sectors like heating/cooling is included in this demand. In a global approach, the demand needs to be projected for each country since it varies depending on its structure, population size, or economic situation. Therefore, economic and population growth are input data for the projection. For long-term projections, regression models are mainly used [84]. However, these regression models usually aim to forecast the demand for specific countries. For a global scope, *Toktarova et al.* have developed a formula that projects the annual demand depending on the country's characteristics, including its hourly profile [85]. Since this approach meets the requirements of a globally applicable approach best, it is implemented in this thesis tailored to the modeling framework. Two further aspects supplement the electricity demand: the grid losses and electricity imports or exports. As both vary between countries, these categories are required for each country individually and kept constant. Particularly the electricity trade might change in future decarbonized energy systems since countries with good renewable conditions could increase electricity exports. However, this requires modeling all neighboring countries directly, which is not in the scope of this thesis.

The second aspect of energy demand in the power system is the demand for resources that are needed to generate electricity. The most relevant resources are gas, coal, and oil, either directly explored by the countries or imported. Since the prices differ, the model requires information on whether a country explores or imports these resources. However, distinguishing market and exploration prices for each country individually is difficult as they depend on other influences such as the accessibility of resources [86] or geographical markets [87]. Therefore, each resource gets a standard global price for exploration and import.

Technologies

The third important input category of the model describes the technologies which generate the consumed electricity. In general, the spectrum of technologies consists of conventional and renewable technologies as well as storage options, as depicted in Figure 2-3.

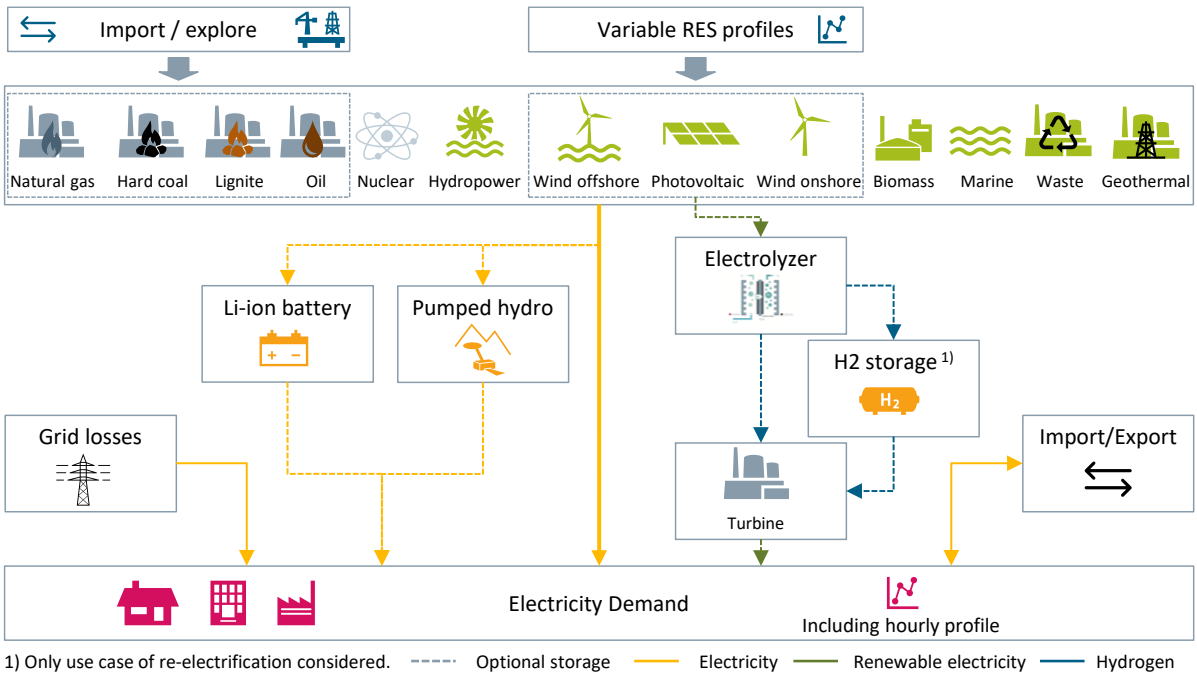

Figure 2-3. Overview of modeled technologies.

Each technology is modeled with the same efficiency and cost assumptions worldwide. Even though efficiencies or costs can vary between countries due to different climatic conditions or market environments, the same assumptions ensure a similar model setup. Most global studies use this approach [42], [43]. In detail, these assumptions include the power plant efficiency, the technical lifetime, specific investment costs, and specific operational costs.

The hourly available wind and solar irradiation are further vital input factors since these VRES technologies are decisive for the transition towards decarbonized energy systems. To account for their variability, the hourly resolution is required. These time series are ideally included for the same year as the demand profile since weather effects are better represented. Even though historical time series do not exactly project the hourly system in the long-term future, using the same years for generation and demand is a profound basis for the general role of VRES. Their conditions vary between the countries and even between regions within a country. Therefore, the profile must be integrated for each country and ideally for each model region individually.

Next to the renewable profiles, the existing system also influences the decarbonization pathway. The currently installed capacities are integrated for each country individually to allow for a realistic starting point. This starting point, which calculates the dispatch of the existing power plants, is compared to historical energy statistics and therefore used to calibrate and validate the model.

In contrast to single region models, multi-region models require the regional distribution and grid data as another input. Based on the previous analysis, the spatial distribution of the electricity demand, the regional profiles of variable RES, the installed generation technologies, and the existing grid are essential input data.

Analyzing the displayed technologies in Figure 2-3, some require simplifications for a global model setup:

- Conventional power plants: in many countries, the co-generation of electricity and heat, especially for industrial applications, plays an essential role in dispatching thermal power plants. Since the approach in this thesis does not model the heat demand explicitly, setting minimum operating hours for the power plants includes this dependency. Additionally, ramping constraints and minimum power of the power plants are not considered because they convert the optimization problem to a mixed-integer linear programming (MILP) approach. A MILP problem increases the complexity of the model, which is critical, especially for multi-region models. Furthermore, linear programming is widespread for long-term planning [31]. The model aggregates the capacities for each generation technology and calculates the operation, preventing using plant-specific ramping characteristics [26].
- Nuclear power plants: some studies consider nuclear power plants an alternative decarbonization technology since they generate electricity reliably without directly emitting CO_2. However, new plant construction projects in several countries such as Finland, France, or the USA have delayed and increased costs [88]. Since the technology shows high cost escalations by overruns in projects [89] and strongly depends on the countries' political agendas, the expansion of nuclear power plants is not part of this model. It is limited to the currently installed capacities. However, the framework provides the possibility to evaluate the role of nuclear power plants in further calculations.
- Hydropower plants: besides pumped hydro storage, hydropower plants can be split into run-of-river plants and reservoirs. Their generation capacity depends on various factors, e.g., precipitation, melting of snow, or minimal/maximal levels of rivers and reservoirs. While run-of-river plants often have a more constant flow and only small storage capacities, reservoirs are usually more flexible [90]. To account for these characteristics without increasing the runtime by linking a particular hydropower model, the hydropower generation

is divided into a constant and a flexible part. Since the flexibility of hydropower plants not only depends on the type but also on the conditions, e.g., cascades of turbines or touristic uses, both parts are assumed equal. Additionally, hydropower plants can be retrofitted for lower costs since certain investments, e.g., the construction costs for a barrage, are not required again after the end of a turbine's lifetime [91].

- Further (innovative) decarbonization technologies: the development of a globally applicable and standardized approach complicates integrating technologies that strongly depend on local regulatory aspects. Examples of such technologies are carbon capture utilization and storage (CCUS) or demand response.

2.2.3. Result Data Evaluation

Comparing output data in different scales, such as energy systems of countries around the world with different sizes, requires the normalization of data [92]. Based on an analysis of significant outputs, indicators are defined to ensure comparable results between countries.

The TOTEX are the primary output of the energy system model resulting directly from the objective function. Since the costs vary strongly depending on the system size, they must be normalized to compare different countries and assess the costs of decarbonization. For the developed standardized modeling, the $Specific\ 30-year\ decarbonization\ costs$ are defined. They consider the total system costs of the pathway C^{TOTEX} normalized by the sum of the demand D_y in the three modeled year steps y. Each of these demand values is weighted by the factor 10 to approximate the total demand within the 30 modeled years by the three modeled steps

$$Specific\ 30-year\ decarbonization\ costs = \frac{C^{TOTEX}}{\sum_y D_y * \frac{2045-2015}{3}}. \tag{2.1}$$

This defined index provides costs in the same unit as the levelized cost of electricity (LCOE), which are frequently used to compare the costs of energy systems. The LCOE calculates the fixed investment costs and variable operation and maintenance costs per generated unit electricity [93] over the financial lifetime.

Next to the costs, the expansion and operation of technologies is an important output to evaluate which technologies are built and used for decarbonized energy systems. Two criteria show the expanded technologies: the installed capacities and the generated electricity. Since the latter also includes information about operational aspects, it is further used here. Like the costs, the generated electricity must also be normalized to compare certain technologies in countries with different electricity demands. Therefore, the annual generation $E_{y,te}$ of a technology te is normalized by the generation of all technologies TE. This approach is frequently used, e.g., in reports or statistics of the *IEA* [94]. For storage technologies, the output electricity $E_{y,st}$ is normalized by the demand D_y. The evaluation factors, energy mix $EM_{y,te}$ and storage mix $EM_{y,st}$, can be summarized by the following two equations:

$$EM_{y,te} = \frac{E_{y,te}}{\sum_{te} E_{y,te}}, \tag{2.2}$$

$$EM_{y,st} = \frac{E_{y,st}}{D_y}. \tag{2.3}$$

A separate index considers the development of RES with an emission factor EF equal to zero representing significant technologies for the decarbonization process. For this purpose, it evaluates the difference of the respective energy mixes from today until the target year 2045. This newly defined

index signifies the gap which needs to be covered for the 80% decarbonization and is called $RE\ Gap$. It exempts hydropower and nuclear generation as they are widespread technologies in today's systems:

$$RE\ Gap = \sum_{te} EM_{2045,\mathrm{te}} - \sum_{te} EM_{2015,\mathrm{te}}, \forall\ te: EF_t = 0, te \neq hydro, nuclear. \tag{2.4}$$

As mentioned in the input analysis, demand is an important input parameter of the energy system model. Since it develops differently in countries depending on their economic situation, it must be considered when analyzing the modeling results. Therefore, the following equation defines the $30 - year - Demand\ Growth$ as follows:

$$30 - year - Demand\ Growth = \frac{D_{2045}}{D_{2015}}. \tag{2.5}$$

Its significance is confirmed by comparing cost indices of an exemplary archetype for different $30 - year - Demand\ Growth$ factors in Figure 2-4.

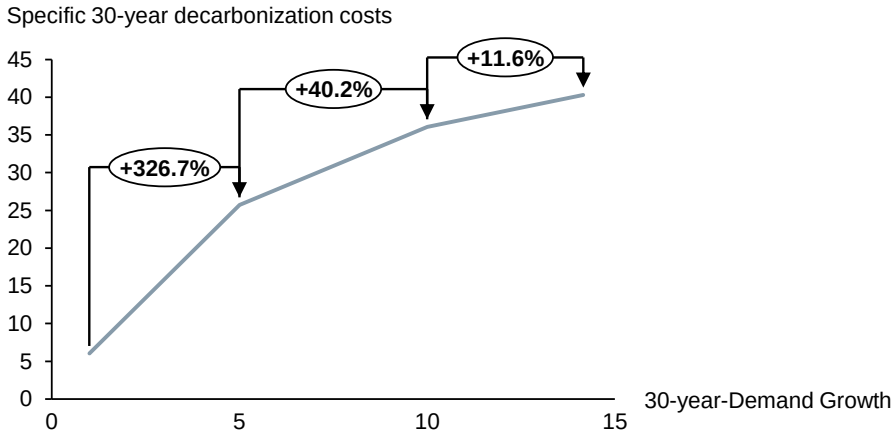

Figure 2-4. *Specific* $30 - year\ decarbonization\ costs$ for different values of $30 - year - Demand\ Growth$ in an exemplary model (Archetype 2).

The costs increase strongly, especially for a $30 - year - Demand\ Growth$ between 1 and 5. Around values between 10 and 15, the growth is reduced to only 11.6% but still observable. The correlation underlines that demand growth is vital for evaluating the decarbonization processes by influencing the transformation costs.

Besides the generation and demand, the electricity sector emissions are a major indicator to assess the decarbonization pathway, especially regarding the targets of the Paris Agreement [12]. The emissions can be analyzed in two ways: first, a $Decarbonization\ Index$ can represent their development from 2015 to a particular year. Second, the specific emissions in a country are evaluated by normalizing the total emissions Em_y by the demand. This $Emission\ Index$ provides the possibility to compare the CO_2 intensity of different countries. The *IEA* also uses this metric to compare the development of various OECD countries [95]. The two corresponding metrics are defined as follows:

$$Decarbonization\ Index_y = \frac{Em_y}{Em_{2015}}, \tag{2.6}$$

$$Emission\ Index_y = \frac{Em_y}{D_y}. \tag{2.7}$$

Last, the evaluation of multi-region energy systems must be analyzed. To compare the role of different regions, the total values of each region are evaluated. They describe how much each region is contributing to the national energy system. The comparison of absolute values is possible here since the different regions are all computed in the same country system. Next to the installed capacities and distribution of technologies, the evaluation of the grid is the second additional output. The evaluation of the grid delivers two supplementary information expressed by absolute values: the utilization of the lines described by the transported amount of electricity and the required grid expansion described by the exchange capacity [37], [96].

2.3. Clustering

In the introduction, clustering is identified as a suitable unsupervised learning approach to group data. Applied to energy system modeling, it reduces the complexity of handling many countries globally and including spatially highly resolved data [74]. The most common clustering techniques are analyzed to identify applicable clustering algorithms, including their ability to consider spatial data. Additionally, the analysis introduces indicators and metrics to evaluate clustering results. This sub-chapter prepares to answer the second research question concerning suitable cluster techniques and their evaluation metrics.

In general, clustering aims at partitioning a set of input data $X = \{x_1, .., x_j, \dots, x_N\}$, where each subset x_j contains features of different data categories $x_j = (x_{j1}, x_{j2}, \dots, x_{jd})$, into clusters $C = \{C_1, .., C_k, \dots, C_K\}, (K \leq N)$ that represent similar categories or groups [97]. The mathematical computation of assigning the input sets to the clusters varies between different clustering techniques.

2.3.1. Clustering Techniques

Out of the various clustering techniques, Table 2-1 presents the most common and frequently mentioned methods [67], [97]-[103], including a brief description, advantages, and disadvantages.

Table 2-1. Overview of clustering methods and their characteristics based on [67], [97]-[103].

Exemplary approach	K-means	Agglomerative hierarchical clustering	DBSCAN	CLIQUE / STING
Description	In iterations, computing *K* Centroids and assigning objects to the nearest centroid; the number of centroids is always *K*	Starting with each object as one cluster and linking the closest objects based on a proximity matrix, update proximity matrix and link next objects until only one cluster is left	Assigning at least *Minpts* objects to *core objects* in an ε neighborhood	Defining dense data cells and assigning objects to these cells; computing density and eliminating cells whose density is below a threshold, forming clusters from contiguous dense cells
Advantages	• Best researched, most popular clustering algorithm • Limited complexity, efficient algorithm	• Good structure of clustered data and hierarchy of similarity between objects • Very popular and frequently applied	• Well scalable • Computed clusters have arbitrary shapes	• Well scalable and computation very efficient • Easy to run parallelized
Disadvantages	• Convergence and initial partition: no global optimum and solution depending on initial partition • Number of clusters	• High computational complexity • Once assigned to a cluster, not considered again • Sensitive to outliers	• Two decisive inputs, ε and *Minpts*, not trivial to choose • Different data could require a different parametrization	• Using summarized information leads to lower accuracy for high dimensions • Threshold as an input parameter
Further approaches	Expectation maximization, Gaussian mixture models	Divisive hierarchical clustering	OPTICS (Ordering Points To Identify the Clustering Structure)	WaveCluster, Fractal Clustering
Applicability to spatial data	No explicit spatial contiguity constraint	Spatial contiguity can be integrated by adaption of method	Applicable but decisive impact of the two parameters	Applicable, but user input required for threshold

The two most common methods are partitioning and hierarchical clustering methods. The literature analysis in chapter 1.2 shows that these two methods have been applied most for energy data. However, density-based and grid-based clustering are also mentioned as widespread techniques [97], [103]. The major disadvantage of the latter two methods is the dependency on threshold parameters involving the user in the parameterization of the algorithm. On the other side, partitioning and hierarchical methods do not determine an optimal clustering solution and face the challenge of defining a suitable number of clusters [104]. Additionally, hierarchical methods compute a hierarchy in which objects remain in the same cluster. This approach neglects that objects might be closer to newly merged clusters than the one they are assigned to. Overall, these characteristics represent the basis for choosing applicable clustering algorithms for the implementation in the presented framework.

2.3.2. Spatial Clustering

Clustering spatial data, as required to find regions for multi-region energy systems, leads to additional requirements for the clustering algorithm. In this context, spatial contiguity is the most critical aspect. It aims at only clustering points which are located directly next to each other [100]. When preparing an energy system model, this spatial contiguity is essential, e.g., to consider the grid between regions. A second challenge is the combination of spatial data with temporal data required in the energy system model to represent the time series of VRES generations in different locations. The analysis of available spatial clustering approaches shows a gap for a spatio-temporal clustering in combination with energy system models [69], [72], [73].

Table 2-1 already includes the general spatial applicability of the described clustering methods. Especially hierarchical clustering can be adapted to include the spatial contiguity constraint, which even accelerates the process by reducing the number of potential combinations [67]. Density-based and grid-based methods are also well suited for this constraint. By contrast, in the K-means algorithm it is more difficult to directly implement spatial contiguity. It can be included by using the geographic position in the clustering process or post-processing the clustered regions [100].

For the specific challenge of spatial clustering, *Duque et al.* have developed the max-p clustering approach based on a MILP optimization problem [105]. It aims at finding a suitable number of regions p that are as homogenous as possible by considering the characteristics of attributes with threshold values. Thereby, the optimal number of clusters is part of the optimization problem and does not have to be found by other indicators. However, the MILP problem leads to high computational complexity, especially for many regions and the threshold values require the user's input [105].

Considering a temporal component in addition to the spatial dimension extends the complexity of the clustering algorithm. In spatio-temporal clustering, the use case of a time series, e.g., a VRES generation time series, with a defined position is referred to as a "geo-referenced time series" by *Kisilevich et al.* [106]. However, including the temporal dimension builds up a high dimensional dataset which can lead to the curse of dimensionality [107]. The latter describes the effect that more dimensions increase the sparseness of the data which complicates finding characteristic clusters. A suitable approach to reduce the dimensions uses correlation metrics between the different dimensions [106]. Since the spatial dimension is identified as a relevant research field in this thesis, the dimension reduction needs to be applied to the temporal dimension. Thus, the framework must include practical approaches to summarize time series.

2.3.3. Clustering Validity Indicators and Performance Metrics

Next to selecting and parametrizing a suitable clustering algorithm, suitable metrics need to evaluate the results. Therefore, two types of metrics are introduced: clustering validity indicators (CVI) which directly evaluate the clustering results and general performance metrics, eligible for accuracy calculations apart from the direct evaluation of the clustering.

Clustering validity indicators

Several indicators are available to compare different cluster algorithms, different parametrizations, or determine a suitable number of clusters. This evaluation can either be performed based on a visual approach or by calculated indices [97]. The most common approaches are presented below based on an extensive study of validity indicators by *Arbelaitz et al.* [108]. This study characterizes the following indices as the best-performing ones:

- Elbow criterion (EBC): the EBC is a graphical approach to determine the validity of clustering by displaying the cluster variances as a function of the number of clusters. It shows the most significant reduction of the clusters' variances, which is often used to find a suitable number of clusters. This part of the curve looks like an elbow in the usually monotonously decreasing function [104].
- Silhouette Index (SI): the SI combines two characteristics that describe the calculated clusters. It includes the compactness of each cluster $a(i)$ as well as the separation between the different clusters $b(i)$. For each clustered observation, it analyzes the similarity to the calculated cluster and the separation from other clusters. The SI is defined in the interval [-1,1], while a higher value SI signifies a better clustering result [109]. The equation to calculate the $si(i)$ is defined by

$$si(i) = \frac{b(i) - a(i)}{\max\{a(i), b(i)\}}. \tag{2.8}$$

  In this equation, $a(i)$ is calculated as the average distance of a point to the other points in the same cluster while $b(i)$ signifies the average of the shortest distance of each point to another point in a different cluster.
- Davies-Bouldin Index (DBI): Like the SI, the DBI combines intra-cluster and inter-cluster characteristics to calculate an index for the clustering evaluation. The clustering performs best for lower DBI, optimally close to zero [110]. The index is defined as follows:

$$dbi = \frac{1}{K}\sum_{i=1}^{K} \max_{i \neq j}\left(\frac{e_i + e_j}{M_{ij}}\right). \tag{2.9}$$

  The distance M_{ij} defines the distance between two clusters i and j. By contrast, e_i and e_j calculate the compactness of these two clusters.
- Calinski-Harabasz Index (CHI): the third index includes the inter-cluster and intra-cluster evaluation differently. It uses their traces $WGSS$ (within-group sum of squares) and $BGSS$ (between-group sum of squares) to calculate the index depending on the number of clusters K and the number of objects N. In this case, a higher index corresponds to a better classification [111]. The CHI is defined by:

$$chi = \frac{BGSS}{K-1} \Big/ \frac{WGSS}{N-K}. \tag{2.10}$$

- S_Dbw: the S_Dbw classification uses a set of formulas to calculate the inter-cluster density $Densbw(K)$ and the intra-cluster variance $Scat(K)$. The density is based on the density within the cluster compared to the data points around it. The variance defines an average scattering of the cluster variance itself compared to the variance of the entire dataset. A lower S_Dbw index shows a better clustering. The index calculation can be summarized as follows while a detailed description of the calculations is provided by *Halkidi and Vazirgiannis* [112]:

$$S_{Dbw} = Scat(K) + Densbw(K). \tag{2.11}$$

When choosing a suitable validity indicator, e.g., to determine the optimal number of clusters or compare different clustering techniques, the selection of a suitable indicator varies with the characteristics of the input data. Therefore, the indicators need to be compared. Additionally, the objective and the context domain of the desired clustering are relevant decision factors [99]. Furthermore, many studies compare the performance of different indicators and thereby evaluate the most suitable one for their requirements.

Performance metrics

Next to the direct evaluation of the clustering, the performance of data-driven approaches, such as data mining or machine learning, is usually evaluated by performance metrics. Therefore, a prediction, e.g., the results of a model, is compared to actual values that can be observed or measured [113]. In a global review, *Botchkarev* has developed a formula that describes most of the available performance metrics, including their functionality and preferred application [113]:

$$error_{metric} = G^Z_{n=1,N}\{N^Z[D^Z(A_n, P_n)]\}. \tag{2.12}$$

The three parameters G^Z, N^Z, and D^Z represent the selected method for the aggregation, normalization, and distance calculation. The superscript Z signifies the index of the respective method in this review study. A_n and P_n are the actual and predicted values for the dataset with the size N. As an example, the frequently used mean average percentage error (MAPE) can be described by G^1, N^2, and D^2. This combination signifies, according to the presented method, a mean aggregation, a normalization by actual values, and an absolute distance calculation.

The analyzed study also evaluates the top three applied performance metrics. Next to the already mentioned MAPE, the mean absolute error (MAE) and the mean or root mean square error (MSE/RMSE) are mostly used according to four cited review studies [113]. From the latter two, only the RMSE is considered since it transfers the squared distance back to the original unit. These three errors are defined as follows:

$$MAE = \frac{1}{N}\sum_{n=1}^{N}|A_n - P_n|, G^1, N^1, and\ D^2, \tag{2.13}$$

$$MAPE = \frac{100}{N}\sum_{n=1}^{N}\frac{|A_n - P_n|}{|A_n|}, G^1, N^2, and\ D^2, \tag{2.14}$$

$$RMSE = \sqrt{\frac{\sum_{n=1}^{N}(A_n - P_n)^2}{N}}, G^1, N^1, and\ D^3. \tag{2.15}$$

The generic approach of the metric calculation allows for a very step-by-step approach to select a suitable performance metric.

2.4. Use Cases

Addressing the third research sub-question, the three selected use cases are analyzed to derive requirements for their consideration in a global model. Furthermore, characteristics of countries are defined for which the use cases are particularly relevant. These countries are then analyzed in the result chapter. For the model evaluation, this sub-chapter derives specific key result indicators. Figure 2-5 summarizes the general results of the following analysis for each use case.

	Use case 1: Grid topology	Use case 2: Green hydrogen production	Use case 3: Coal phase out
Description	Analyzing the effect of increasing generation from RES on the regional grid topology	Analyzing suitable areas for green H2 production while decarbonizing the energy system	Analyzing the effect of a coal phase-out by decarbonizing coal-dominated systems
Focus countries	Large increase of RES generation between 2015 and 2045	Good conditions for green hydrogen production	Currently strongly relying on electricity production from coal
Framework requirements	• Standardized capacity model based on OSM data • Focus on transmission grid	• Price-driven model approach • Infrastructure and transportation analysis	• Global analysis of drivers • Analyzing infrastructure with special regard to coal regions
Evaluation indicators	• Change of grid patterns • Required grid expansion	• Price for green hydrogen production • Required infrastructure	• Delta in generation capacity • Contribution to national energy mix

Figure 2-5. Results of analyzing the selected use cases, including requirements for their integration into the model framework.

2.4.1. Grid Topology

The general idea of the first use case, analyzing the grid topology of countries in the decarbonization process, follows the spatial transformation by an increasing VRES integration. Since the location of generation units changes, it also affects the grid. It might face fundamental changes in its topology, e.g. by required grid expansion measures [19]. In this context, this use case is especially relevant for countries with a significant increase of RES generation, neglecting hydroelectricity which is already for the current electricity system in many countries. Thereby, the VRES wind and PV are focused. They also primarily affect the spatial topology with their variable character depending on geographic or climatic characteristics [19].

There are different ways to combine the grid infrastructure with a projection of the energy system model. Two exemplary studies consider the grid in the decarbonization process by soft-linking a generation expansion model with a grid simulation model [28], [114]. This approach allows for a detailed computation of the grid utilization and physically overloaded lines. Since the proposed use case aims at analyzing the immediate impact of changes in generation technologies on the overall grid topology of the country, it is essential to consider generation capacities, storage technologies, and the grid in a joint optimization problem.

For this integrated approach, there are three possibilities: (1) a capacity-based, (2) a direct current (DC) power flow, and (3) an alternating current (AC) power flow representation in the model [26]. The capacity-based model only calculates exchange capacities between regions. By contrast, the DC power flow considers a simplified physical representation of the lines by calculating active power. The AC power flow includes a detailed physical representation by reflecting active and reactive power. These three different detail levels require a trade-off between detail and complexity: more physical details improve the model accuracy by approximating the actual physical effects better. However, each level requires more detailed data and increases the computational complexity [115].

To keep the optimization model solvable and linear, most energy system planning models, e.g. [45], [69], [68], or [43], use either the capacity-based or the DC power flow model approach. Since data availability is an important factor for the global approach in this thesis, the capacity-based grid model, which requires less data input, is sufficient for the global modeling approach [26], [96]. Overall, detailed grid models with geospatial references are rarely available. As an alternative, OpenStreetMap (OSM) [116] is frequently used to build up grid models [117]. For a globally transferable modeling approach, it is today the only viable platform to provide grid data. However, being an open-source platform and relying on users' data, the data quality of OSM data is often discussed and not sufficient for a detailed technical representation [115]. The capacity-based model also suits the overall model

objective. It rather aims at analyzing general topological developments from the current grid to a future grid than detailed grid simulations with an impact on operations.

Next to the grid representation, the detail of grid modeling also needs to be analyzed. In general, the transmission grid ensures the transport of electricity for long distances on high voltage levels and the distribution grid for short distances on lower voltage levels to reduce losses. A planning model for the overall grid topology only considers the transmission grid since the integration of the distribution grid would drastically increase the complexity by numerous data points. Furthermore, the data quality on this level does not allow for a good representation. To evaluate the impact on the distribution grid, simulations with exemplary grids must be performed, as, e.g., executed by *Raths et al.* [118]. Therefore, the grid topology only includes voltages higher than 100 kV, which is comparable to the classification in the European Transmission System provided by *ENTSO-E* [119].

Summarizing the analysis, the essential requirements for the globally applicable framework are accessing grid data globally from OSM, preparing the data for a capacity-based model, and building up a model of the existing transmission grid considering lines with voltages of 100 kV and higher. The primary evaluation indicators are the absolute values of transported electricity between regions, the direction of flows, and the required expansion of additional transmission lines.

2.4.2. Green Hydrogen Production

Green hydrogen, produced without emitting additional CO_2, provides an opportunity to decarbonize energy systems. To analyze the requirements for integrating hydrogen in the global modeling approach, its production, its value-chain, and existing modeling approaches are evaluated.

Hydrogen production

Overall, there are four possibilities to produce hydrogen [22]:

- Hydrogen from natural gas: natural gas is currently the source of most globally produced hydrogen due to the lowest production costs. Specifically, Steam Methane Reforming (SMR) is the widespread method to generate hydrogen. CCUS is an option to lower the CO_2 emissions of SMR.
- Hydrogen from coal: the process of producing hydrogen from coal is mainly applied in China. In comparison to gas, the production from coal leads to higher costs and higher emissions. Similarly, CCUS can be applied to reduce emissions.
- Hydrogen from electricity and water: electrolysis produces hydrogen from electricity and water. There are currently three leading technologies available for this process: Alkaline electrolysis, Polymer Electrolyte Membrane (PEM) electrolysis, and Solid Oxide Electrolyzer Cells (SOEC).
- Hydrogen from biomass: hydrogen can also be produced from biomass. Due to the complex process, high costs and a high amount of required biomass, this technology is rarely used and mostly applied in smaller scales.

Hydrogen storage, transportation, and end-use

In general, hydrogen (H_2) can be stored, transported, and used in different forms: as a compressed gas (GH2), liquefied (LH2), or chemically by using liquid organic compounds as Liquid Organic Hydrogen Carrier (LOHC). The different forms lead to different storage types divided into geological storage and storage tanks [22]. While geological storage is well suited for large-scale applications, tanks are more flexible and provide a faster charging and discharging process [22].

Hydrogen can be transported by pipelines, trucks, trains, or via ship [120]. Currently, the most common transportation methods are pipelines and trucks, while ships represent an option for long-

distance transport routes in international hydrogen trading [121]. The most suitable transportation method depends on the existing infrastructure, geography, scale, and the distance [22].

The hydrogen demand can be classified into four applications. For industrial applications, the petroleum, iron and steel, and fertilizer industry are the principal users of hydrogen, e.g., to refine fuels or produce ammonia [122]. Furthermore, it can serve as an alternative fuel in the transport sector for road transport such as passenger cars or public buses but also for ships and airplanes. In buildings, hydrogen can substitute natural gas or oil for heating. Last, turbines or fuel cells can use hydrogen to generate electricity [22].

Hydrogen in energy system models

Various studies analyze the impact of hydrogen in future energy systems. These studies differ in their model type and hydrogen modeling approach: the model types differentiate between optimization models and techno-economical assessments. The hydrogen modeling approach is either driven by a defined demand or a specific price. These two classifications are visualized in Figure 2-6.

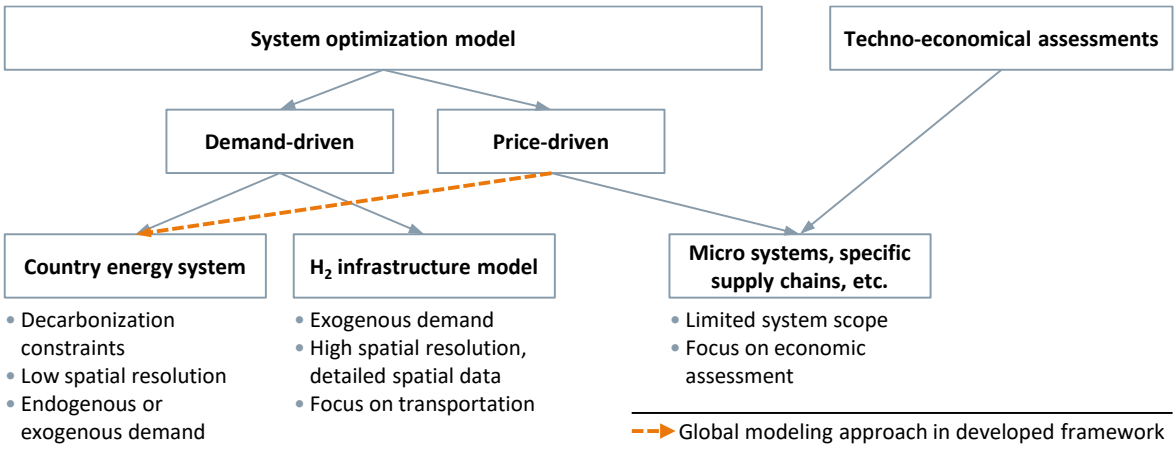

Figure 2-6. Approaches to consider hydrogen in energy system models.

The different mentioned approaches are defined as follows:

- Demand-driven optimization models: As described in chapter 1.2, optimization models are often used to model medium- and long-term developments in energy systems. For hydrogen modeling, most of these models use an exogenous hydrogen demand to calculate the required scale of production, storage, and transportation technologies. In this context, some studies emphasize the general development of a country's energy system, e.g., in a decarbonization context, while other studies perform a detailed evaluation of the hydrogen infrastructure. The scope of high-level country energy system studies with hydrogen focus is often limited to the European Union, the US, or Japan [123]-[125]. Infrastructure models use more detailed data to consider spatial aspects, especially for the transportation infrastructure to integrate hydrogen in an energy system [120], [126].
- Price-driven optimization models: price-driven optimization models evaluate the price for which hydrogen can be sold. There have been a few examples in literature applying this approach to particular technical configurations and a limited regional scope [127]-[129].
- Techno-economic assessment models: Apart from system optimization, techno-economic assessment models usually calculate the operation of hydrogen systems. They evaluate specific technologies by analyzing their costs and efficiencies without a detailed optimization of the energy system. Examples for such models range from spreadsheet models [130] over cost evaluations of specific trading routes [121] to the evaluation of stand-alone systems [131], [132].

Requirements for the global modeling approach

Combining all described aspects of hydrogen modeling with the application in a globally transferable modeling approach leads to the definition of the following requirements. In the context of a decarbonization scenario supporting the goals of the Paris Agreement, hydrogen production should not emit further CO_2 emissions. Therefore, only hydrogen production by electrolysis based on wind and solar electricity generation is considered. The other production technologies, SMR and coal, lead to emissions. These emissions could partially be captured by CCUS, which is not in the scope of this thesis. A production from biomass is not suitable for large-scale production. Analyzing the different electrolyzer types, PEM electrolyzers signify the widespread technology in recent years [22].

As a storage technology, the model considers cavern storage. It is suitable for large-scale applications, which is vital to integrate hydrogen into a country's energy system. These caverns are assumed to be available in the respective countries. Transportation is not directly included in the model since it extends the complexity of the model by many data points, such as existing infrastructure of harbors, highways, gas stations, or pipelines. The analysis of modeling approaches shows that many models focus only on transporting hydrogen, which confirms this decision. However, hydrogen transportation can influence the suitability of hydrogen production, especially in spatially resolved models. Therefore, it needs to be considered in a post-processing analysis. Regarding the end-uses, the power generation is already addressed in the energy system model setup (see chapter 2.2.2). Similar to the modeling of hydrogen transportation, the other end uses of hydrogen, e.g., industrial hydrogen demand, require detailed data that is currently not available on a global scale. Furthermore, explicit modeling of the demand would require a standardized projection for each country. To account for these challenges in a global context, price-driven modeling approach is required which is demand-independent.

According to the review of analyzed literature, such a price-driven approach has not been applied yet to analyze the green hydrogen potential of worldwide country energy systems. It enables the modeling of green hydrogen production from a global to a spatial level by representing the value chain through using PEM electrolyzers and cavern storages, executing a post-processing infrastructure analysis, and considering prices instead of explicit demands. Different scenarios can represent a range of potential prices which need to be generated by a global benchmark analysis. Overall, these requirements lead to a model being capable to identify prices for which the production of green hydrogen is economical in each country or region next to the decarbonization of the energy system. A second evaluation criterion apart from these break-even prices is the required infrastructure in a spatial analysis.

2.4.3. Coal Phase-Out

The third use case, an evaluation of a coal phase-out, addresses the fact that coal is the fuel with the highest specific emissions [25] and responsible for almost half of all energy-related CO_2 emissions [13]. A report published by *Climate Analytics* states that a coal phase-out must be executed until 2040 to reach the goals of the Paris Agreement [133]. Similarly, *McKinsey*'s global study of electricity generation foresees a decrease in coal generation until 2050 due to the integration of renewables and a switch to gas power plants despite an increased demand [134]. Even economically, coal power plants face challenges in electricity markets due to lower full load hours caused by the integration of cheaper RES, emission pricing, less operational flexibility compared to gas power plants, and a lower gas price [135]. Influenced by these trends, first countries, such as France, Germany, the United Kingdom, and Canada, have already decided on a political coal phase-out [23]. In a global context, these plans are still not enough for the COP 21 goals which shows the need for further actions [133]. Therefore, this use case is especially relevant for countries and regions, which currently depend on coal for their power generation or have coal mines exporting to the world market.

In energy system modeling, coal phase-outs are analyzed on different levels. Global evaluations have defined required measures for an effective coal phase-out or have evaluated the general share of power

generation from coal in future energy systems [133], [134]. In contrast to these more generic global statements, several studies have calculated coal phase-outs on a national or continental level. For example, the recently decided German coal phase-out has been analyzed in two studies to assess its effect on the European electricity system and market [136], [137]. Another study has focused on its technical consequences for the electrical grid [138]. For Portugal, which currently has a share of around 20% of power generation from coal, a study has quantified the effect of a coal phase-out. The integration of photovoltaic generation has been identified as a lever to substitute coal power plants [139]. A similar study has been conducted for China. It determines required developments to reach the Paris Agreement's targets. In detail, the regional effects of lower electricity generation in currently coal-dominated regions have been compared between a "Limited effort", a "Paris Agreement, and an "Ambitious" scenario [140]. Highlighting regional aspects of a coal phase-out, *Harris et al.* have interviewed stakeholders involved in Ontario's coal exit. They focus especially on the political and social process. Their study also aims to provide learnings for other regions [141]. The last example of an energy system evaluation has not examined a coal phase-out in a country but analyzed the effects of coal phase-outs on mining and exporting countries. For the specific case of Colombia, this study has raised a re-consideration of expanding coal mining activities and provides an evaluation of new business opportunities [142]. Concluding the mentioned studies, they have focused either on regional details or qualitative global statements. Furthermore, the studies have been performed specifically for one country or the effects on other linked systems. For example, the German coal phase-out studies have evaluated technical details such as grid congestion or stability analysis.

In this thesis, the third use case aims at providing a globally applicable approach to model a coal phase-out in all countries by including regional effects. For this reason, the evaluation of a coal exit requires to consider further aspects. On a global level, the objective is to identify drivers for a coal phase-out and the most affected countries. On a more detailed regional level, a country's infrastructure needs to be analyzed to identify regions that are currently important for the coal industry. Besides the distribution of installed power plant capacities, an analysis of mining activities is also relevant in this context. Similar to the evaluation of the grid, OSM provides a globally available and comparable data basis for this analysis.

The results of this use case aim primarily at evaluating the transformation of regions within country energy systems caused by a coal phase-out. Therefore, key indicators are the contribution of each region to the overall country electricity generation and the change of generation capacity within each region. Furthermore, this use case can also use the developments of the first use case, the evaluation of future grid topologies, to assess the impact of a coal phase-out on the grid topology.

2.5. Summary Framework Requirements

The analysis of relevant aspects to develop a data-driven modeling framework evaluating the decarbonization pathway of countries by three exemplary use cases leads to various requirements that need to be considered in the design of this framework. The following enumeration summarizes all derived requirements.

1. Requirements for the two challenges concerning the general framework definition:
    - Global scope: modeling all countries in a global scope strongly increases data and evaluation efforts. These efforts are even more significant when comparing different sensitivities. Therefore, the framework needs to reduce the number of considered countries to a feasible number while still including the overall energy system characteristics of a country. The development of a clustering approach can solve this challenge and addresses the central research question.
    - Spatial data: a model resolved in the smallest regions of a country and considering each hour of the year is for most computation servers not solvable. Additionally, the result evaluation of many regions requires another aggregation step to be observable

and manageable. Therefore, the number of model regions needs to be selected to generate a solvable model that can still include a representative number of time steps in the representative years. For this purpose, the definition of regions is aimed to be data-driven based on energy characteristics by a spatial clustering approach.

2. Requirements for the energy system model:
    - Global data basis: in general, the data input of a model can be divided in globally valid and country-specific data. All data categories need to be sorted in these two categories by either describing the overall scenario or the country-specific energy system.
    - Energy demand: the projection of the electricity demand depends on the projected development of the economy and population within a country. Therefore, these data categories need to be available for countries. Furthermore, the availability of resources such as coal, gas, or oil in a country needs to be considered since it affects the price.
    - Technologies: time profiles for variable RES need to be included in the country models as well as the currently installed fleet of power plants. For multi-region models, these data need to be available spatially resolved to consider regional differences. Equally, the electricity demand needs to be available spatially resolved.
3. Requirements for the clustering techniques:
    - General clustering: the selected clustering technique needs to consider the broad data set thoroughly. Furthermore, finding a suitable number of clusters and an approach to ensure optimality are challenges for implementing a suitable approach.
    - Spatial clustering: including spatial data in the clustering leads especially to the requirement that the selected technique ensures spatial contiguity. Additional requirements are keeping the algorithm in a solvable range and handling the curse of dimensionality when extending the clustering from the spatial to the spatio-temporal dimension.
    - Validity indices and performance metrics: to confirm the accuracy of the clustering and validate it, Clustering Validity Indices and performance metrics are used. Out of the most frequently used methods, the choice of these metrics needs to consider the domain of the clustering application and the selected clustering techniques.
4. Requirements for the three selected use cases summarized in Figure 2-5:
    - Grid topology: a simplified capacity grid model needs to be synthesized for all countries using OSM data. This model only needs to consider the transmission grid.
    - Green hydrogen production: a price-driven approach shows advantages to compare the production of green hydrogen in decarbonization pathways globally since no exogenous demand is required. Additionally, a post-processing step needs to evaluate the infrastructure and transportation of the hydrogen.
    - Coal phase-out: on a global level, trends need to be analyzed that drive and follow a phase-out of electricity generation from coal. In coal-dominated countries, the regional effects need to be modeled by focusing on coal dominated regions and elaborate their role in future decarbonized energy systems.

3. Framework for Standardized Worldwide Modeling

Based on the analyzed requirements, a framework is developed which enables modeling all countries globally down to their spatial level with the same data basis. In this framework, the described use cases can be analyzed to evaluate the impacts of decarbonization in different countries. The following chapter provides a general overview of the framework and detailed explanations about the data basis, the applied energy system optimization model, and the clustering process.

3.1. General Overview

Figure 3-1 depicts the overall framework, including the data layer, the data processing by clustering, the modeling, and the application of the use cases. Derived from the requirements, it needs to reduce the complexity of analyzing all countries globally and including spatially highly resolved data. For both challenges, it incorporates clustering methods.

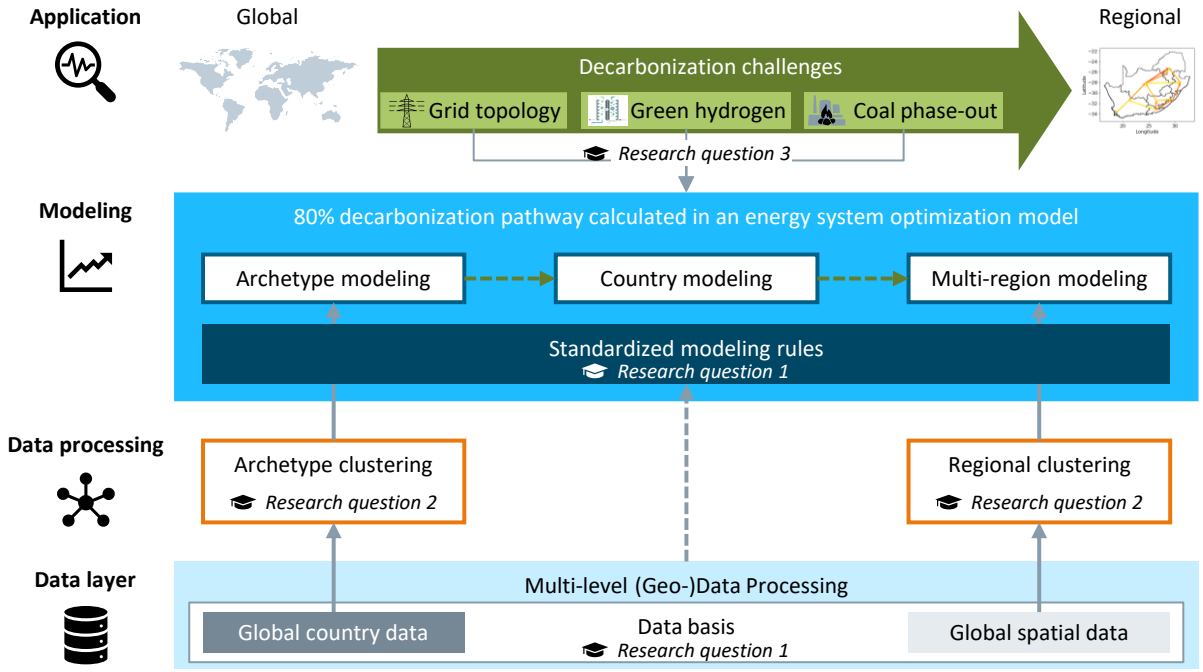

Figure 3-1. Model framework from a global to a regional level including each step's reference to the three research sub-questions, defined in chapter 1.3.

Four layers are defined from the base data to the applications to answer all three defined research questions. Overall, this framework addresses the central research question to use clustering techniques which simplify the application of an energy system model to countries worldwide including geospatial data. For the first research question, a worldwide, transferable model, the data basis must be defined, including country data and geospatial data. This data basis is used to derive standardized modeling rules allowing for a globally transferable model approach.

The central connection between the data and the energy system model are the two implemented clustering algorithms answering the second research sub-question. They perform the data processing along the modeling process on two levels (see Figure 2-2). First, all countries are clustered in energy system archetypes. These archetypes are synthetic representatives for the energy system characteristics [143]. Next to the efficiency gain of being able to model the world by a few archetypes instead of modeling each country individually, the archetypes provide three other advantages: (1) they can be used by technology companies to evaluate the effect of specific technologies in different energy systems, (2) they provide an overview for policymakers which countries face similar challenges, and (3) they can help modelers to find data by showing similarly structured energy systems. The second

clustering approach processes the geospatial data. It aims at generating regions for a multi-region model based on energy data instead of political boundaries. This clustering step provides the advantage of highlighting spatial energy system characteristics within a country before the model application. In the model, it amplifies effects in the decarbonization pathway since the regions differ more by their characteristics. Political classifications might not represent the energy system characteristics well, which are the main regionalization criterion of the data-driven clustering approach. Last, the number of regions is flexible. It can either be set to the optimal number indicated by clustering validity indicators or manually defined to be suitable for the computational infrastructure.

For the application of the energy system model, the three selected use cases are implemented. This highest layer addresses the third research sub-question to integrate the use cases in the energy system model. The use cases show the strength of considering the range from a global scope to regional characteristics by data-driven approaches. They are first applied on the archetype level, which provides a selection of interesting countries for each use case. The second step is then the country modeling. Based on these modeling results, the most relevant countries can be chosen and modeled in a spatially resolved multi-region model. By modeling all three steps from the clustered archetypes over the countries to the clustered regions, this approach integrates spatially highly resolved details and chooses relevant countries on a global level. The modeling process requires a globally standardized approach that addresses the first research sub-question.

For all three layers, data process, modeling and the application, a profound global data basis is essential. It is the input for the clustering algorithms and enables a comparable model setup. Chapter 3.2. includes a detailed description of the considered country and spatial data. The energy system model uses these data to optimize the decarbonization pathway, including standardized modeling rules described in chapter 3.3. Last, chapter 3.4 defines the process to select, benchmark, and validate the two clustering approaches.

3.2. Global Data Basis

The global data basis needs to consider the input parameters of the energy system model and the characteristics of the clustering methods. The included data and data sources must fulfill specific criteria to build up a comparable and consistent dataset. First, each selected source must cover the respective data category for as many countries as possible to avoid inconsistencies from several sources for the same data category. Second, for the same reason, the number of different sources should be kept small to collect data categories from the same source. Third, for the archetype clustering and models, the data must be on a country level [143]. By contrast, the spatial clustering and the regional model require spatially resolved data, including a geo-reference for each data point in the data basis.

Considering the purposes of the models on both levels, the data requirements for the clustering and the following model differ. The archetype model is a high-level model to evaluate trends of different energy systems worldwide. Therefore, the archetypes are generated based on a broad data basis, including socio-economic and geographic/climatic data besides energy data [143]. The exact setup of the global country data basis is described in chapter 3.2.1. For spatial clustering, spatially resolved data is not globally easily accessible and publicly available. Consequently, the clustering on this level is limited to the essential model input parameters according to the model setup explained in Figure 2-2 [144]. Furthermore, this reduction is suitable since the regional model is the final modeling level in the described framework (see Figure 3-1). Chapter 3.2.2 contains the definition of a global spatially resolved data basis.

3.2.1. Global Country Data

Global country data is the basis to cluster countries and summarize similar worldwide energy systems. For this purpose, energy data are collected on a very detailed level. Besides, the data basis includes socio-economic and climatic-geographic data since the energy system is also affected by these two aspects [61], [62]. In a first step, this results in 321 data categories for 193 *UN* member states[4] concerning the three criteria described above: a broad coverage of sources, a low total number of different sources, and data on country level.

The initial dataset includes 56 categories of socio-economic data, i.e., economics, population, infrastructure, regulatory, and development data. Twenty-four categories are collected for the category climatic-geographic data, including climate data, geographic locations, and renewable full load hours. The third category, energy data, represents with 75% the most significant part. Examples for energy data are electricity, primary energy, emission, petroleum, coal, natural gas, hydrocarbon gas liquids, and biofuel data. Electricity data, the focus of this thesis, accumulate to more than half of these 241 categories, including detailed data about the installed capacities and the energy mix from different sources. The comparison of different sources validates the data and supports the identification of a comprehensive dataset. Additionally, further external sources extend the validation process, e.g., the *IEA* energy statistics [94]. Next to data validation, the generation of a unified and comparable dataset is required. Therefore, different data formats from various sources must be unified. Also, units need to be converted to one base unit. In this case, Watt W or Watthours Wh are the selected base units since they are primarily used in the context of electricity generation and consumption.

The clustering algorithm requires precise criteria to select the final dataset since its results strongly depend on the selected input data features. The selection of these criteria must fit the desired application of the data since there is no general approach [99]. In the context of global energy system archetypes, relevant selection criteria are defined as follows:

- Features must not be double or similar: the same or redundant data categories amplify the impact of single features on the clustering result.
- Features must be comparable: selected data categories need to be in a comparable dimension or on a comparable level. For example, comparing hard coal with sub-products of lignite increases the number of criteria for the more detailed category and thereby emphasizes these data categories more.
- Features must be available for at least 85% of the considered countries: data categories with low coverage of countries lead to excluding many countries from the clustering methodology. A threshold of 85% leads to a stable list of countries.
- Features must be relative or comparative: absolute numbers impact the clustering significantly. As an example, the total installed capacity of PV generation in China is high in the global context, while its share of the total installed generation is lower than in countries such as Germany or Denmark. Therefore, data categories are normalized by the installed capacity, the consumption, the total population, or the area.
- Features must cover the data required for the energy system model: the final goal of the clustered archetypes is to be modeled in an energy system model (see Figure 3-1). The input data required for the model setup defined in Figure 2-3 needs to be covered by the clustered features.

The selected criteria lead to the following list, Table 3-1, of finally considered data features (*DF*):

[4] Andorra, Liechtenstein, Marshall Islands, Monaco, Palau, and San Marino are not considered due to the lack of available data.

Table 3-1. Selected data categories considered for country clustering.

Major topic	Data categories	Source
Socio-economic (14)	GDP per capita, GDP growth	[145]
	Human Development Index	[146]
	GDP distribution: agriculture, industry; political stability index, population density, urban population, urban population growth, access to electricity, rural access to electricity, time required to get electricity	[147]
	Electric vehicles per capita	[148]
	Population growth	[149]
Climatic / geographic (11)	Hydropower capacity factor	[150]
	Agricultural area, forest area	[145]
	Coast / area ratio	[151]
	Latitude absolute	[152]
	Average temperature, average precipitation	[153]
	Heating degree days, cooling degree days	[154]
	Solar capacity factor, wind capacity factor	[155]
Energy-related (37)	Primary Energy intensity: consumption per capita, economic intensity, consumption fossil fuels, consumption renewables; Electricity: consumption per capita, share consumption / installed capacity, share net imports, distribution losses; Shares installed capacity: fossil fuels, nuclear, renewables, hydropower, solar, geothermal, tidal and wave, hydroelectricity pumped storage; CO_2 economic intensity; Shares resources production/consumption: petroleum, hard coal, lignite, natural gas	[145]
	Shares installed capacity: wind onshore, wind offshore, biomass, waste	[145],[150]
	Shares installed capacity: oil, hard coal, lignite, natural gas	[145],[156]
	Total natural resource rents, CO_2 emissions per capita	[147]
	Emissions change from 1990	[6]
	Shares installed capacity storage: total, electrochemical, electromechanical, thermal, hydrogen	[157]

The selected features reduce the number of considered countries (*CO*) from 193 to 141 due to the lack of data for specific categories. However, all included data categories are publicly available, which ensures reproducibility and regular updates. Considering all features, 2015 is chosen as a base year, even if more recent data are available. There are two reasons for this choice: first, it provides the broadest coverage and makes the data comparable since there can be significant changes between several years, e.g., the expansion of RES. Second, the modeled transformation path starts with a historical year for which actual data is available to validate the input parameters and the overall model setup. The distribution of features regarding the three major topics represents the objective of the archetypes: while energy-related data is most important with around 60% of all features, socio-economic and climatic/geographic features represent around 20% each.

3.2.2. Global Spatial Data

In contrast to energy data on the country level, spatially highly resolved data is less accessible for all countries globally. There are already several projects which offer, e.g., renewable generation profiles [64], [158], [159] or a global database for PLEXOS [56]. However, there is no public database available with all required data categories for a multi-region energy system model of each country. For this reason, several data sources must be combined to a global data basis covering the most critical input categories of the energy system model as features for the clustering algorithm. According to the model setup, these categories are electricity demand data, the current distribution of installed capacities for each technology, spatially resolved renewable profiles, and the usable areas for renewable expansion. Furthermore, grid data and further infrastructure data such as harbors, e.g., for the evaluation of hydrogen infrastructure, are collected to model the use cases. Besides, a global

classification of administrative areas is required to define the smallest regions for the clustering algorithm. The setup of this data basis for each data category, which has been partially part of projects between Siemens AG, Technology and "Forschungsstelle für Energiewirtschaft e.V.", is described in the following sections. The categories have mainly been verified by comparing them to available public data, e.g., the electricity demand of cities.

Electricity demand

Based on available sources with a globally high spatial resolution, the electricity demand data differs between private household (PHH) and commercial, trade, service, and industrial (CTSI) demand [160]. These two categories allow for distinguishing between both demands in the energy system model, e.g., with different time series, by identifying areas that are more residential or more industrial.

For the PHH demand, the global human settlement layer is used [161]. The population density distributes the overall household demand of each country [162] in a resolution of a 250 m x 250 m raster. To ensure a correct number of total population correlated to the total demand, the population for each pixel within a country is corrected by the total country population [147]. For the CTSI demand, the overall country demand is disaggregated based on areas indicated as *commercial*, *industrial*, or *retail* in OSM [116]. Its resolution is also 250 m x 250 m. Figure 3-2 visualizes the worldwide distribution of both categories.

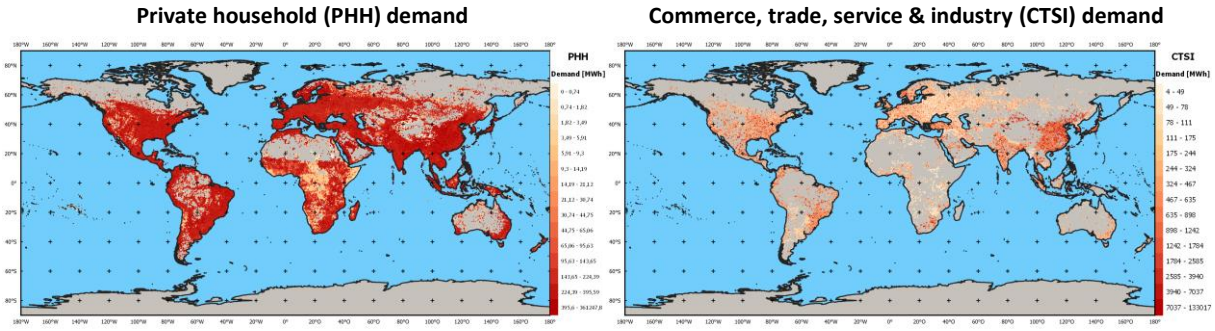

Figure 3-2. Global PHH and CTSI demand based on [160].

The PHH demand visualizes the distribution of settlements. Some countries in Africa, South America, Central Asia, or regions in Australia have a lower population density. By contrast, in Europe, there are no differences between countries identifiable on the world map. The CTSI demand highlights industrial centers in the countries. Depending on the country, these centers can either be cities with relevant industrial activities or rural areas where extensive industrial activities occur, e.g., mining.

Electricity generation

The *World Resource Institute* provides a global, publicly available, and spatially resolved data basis of generation units [156]. It specifies the geo-position, the primary fuel technology, and the installed power for each entry. Especially for conventional power plants, the accuracy is good, with a coverage of 80-100% [163]. By contrast, it only includes 20-50% of renewable units, so that especially wind and PV generation units are underrepresented [163]. Since both technologies are not vital in many countries yet and are still included in the database by their profiles and local potentials, this low accuracy is still acceptable. Figure 3-3 depicts the worldwide distribution of all technologies. It identifies, for example, hydropower plants in South America, North America, Northern Europe, or South-East Asia, coal power plants in Europe, India, China, Australia, or South Africa, and oil and gas power plants in North Africa or the Middle East region.

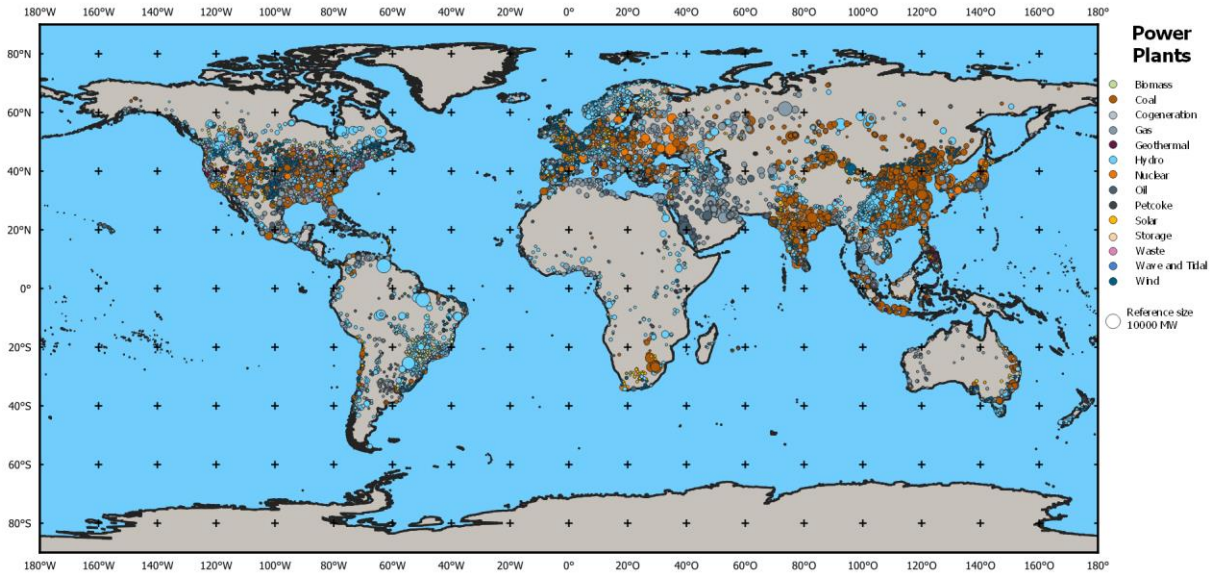

Figure 3-3. Global power plants provided by the World Resource Institute [156].

Renewable profiles

The third data categories are hourly and spatially resolved profiles of the VRES technologies wind and PV. To generate the data, publicly available weather data is required combined with the technical details of the respective technologies. MERRA-2 constitutes the primary source for this database with a suitable coverage of weather data [164]-[168]. The raw weather data products are processed to reflect technical characteristics of different wind turbines or different orientations and angles of PV units as developed by *Albrecht* [169]. According to the MERRA-2 data, the resolution of the renewable profiles is 0.625° x 0.5°. For the described data basis, the weather year 2015 is chosen since it corresponds to the data of the archetype clustering. Wind profiles are calculated for five different turbine types. To find a unified rule for wind locations, the turbine type with the highest annual full load hours is always selected. For PV generation, two variables influence the normalized power output. The North-South orientation varies in 22.5° steps and the module angle is available in 5 steps between 0 and 45°. The best combination of both variables is chosen for each location. Figure 3-4 shows the visualization of this data basis for both technologies, global PV and wind potential, sorted by the annual full load hours. The PV potential increases towards the equator but decreases in tropic zones. The highest wind potential is between Patagonia and Antarctica. On landmasses, North America, Northern Europe, North Africa, and Australia show good potentials.

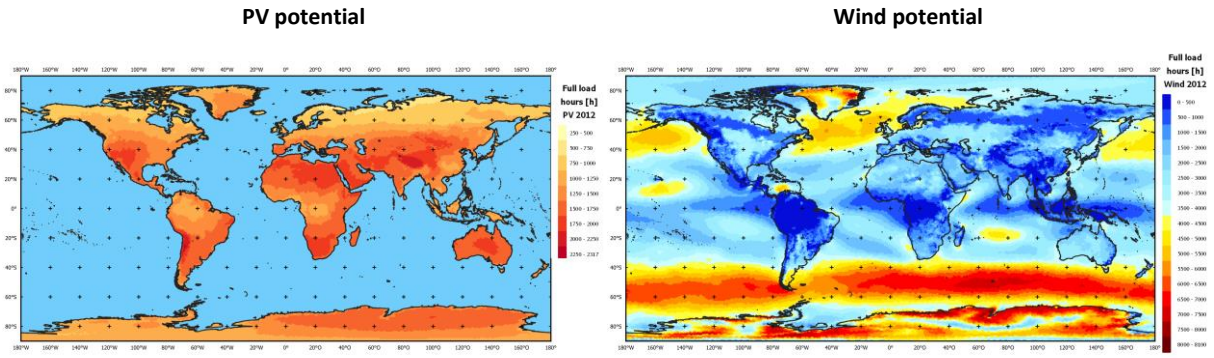

Figure 3-4. Global PV and wind potential derived from [164]-[168].

Land use restrictions

Completing a geospatial data basis for the future renewable potential, another category are the usable areas for renewable expansion. Many countries do not allow to install VRES close to settlements or in protected areas. To identify potential expansion areas, a global raster combines different exclusion criteria: natural reserves, which are only included in Europe [170], [171], residential areas with a buffer of 1000 m [116], terrain with more than 10% slope based on an altitude raster [172], and lakes and rivers worldwide [116]. Like the electricity demand raster, this raster has a resolution of 250 m x 250 m. In Figure 3-5, the restricted areas are visualized. Next to the densely populated areas in Europe, mountain ranges are visible such as the Rocky Mountains, the Andes, or the Himalayas. It also identifies the large inland waters in East Africa around Kenia, Uganda, and Tanzania. By including the distances to settlements, this map also correlates to the PHH demand map.

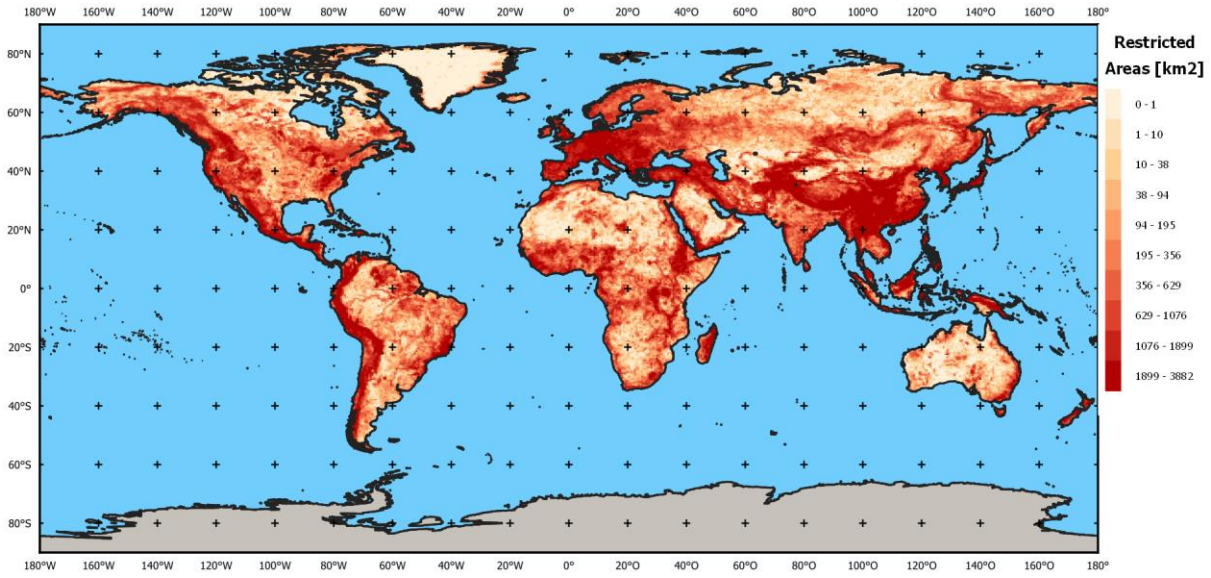

Figure 3-5. Globally restricted areas for RES expansion by distance to settlements [116], natural reserves [170], [171], inland waters [116], and altitude profiles [172] in km² for comparable raster.

Grid and infrastructure data

The three use cases require additional data: grid data for the first, infrastructure data such as harbors or pipelines for the second, and data of coal mining activities for the third use case. OSM provides an opportunity to evaluate all these categories globally [116]. Being a community-driven dataset, the data quality varies between different countries and for grids between the different voltage levels. However, OSM is the only publicly available global dataset that can serve detailed, geo-referenced data. The respective sections describing the methodology for each use case specify the usage of data and tags. To underline the global OSM coverage, Figure 3-6 shows the grid data globally.

Administrative areas

The political boundaries of all countries are the last required data category for the spatial data basis. A dataset providing administrative areas on different levels is required to develop a spatial clustering approach for energy system models based on the smallest administrative areas such as cities or counties. The GADM dataset fulfills this requirement by providing four administrative levels from country-level to city/council level [75]. The different levels of regions are presented in Figure 3-7. The map shows how countries are separated differently. Some countries, e.g., Australia, Argentina, or

Namibia, have only lower levels available and are characterized by areas with a low population density. By contrast, regions that are densely populated, such as India, the coastline of Brazil, the East Coast of the US, or Germany, show tiny regions on administrative level 3. The classification in the US illustrates how regions can be different on the same level. The regions on level two are relatively small in the East, while the regions are much larger in the Midwest. These different sizes of areas need to be considered when using the data.

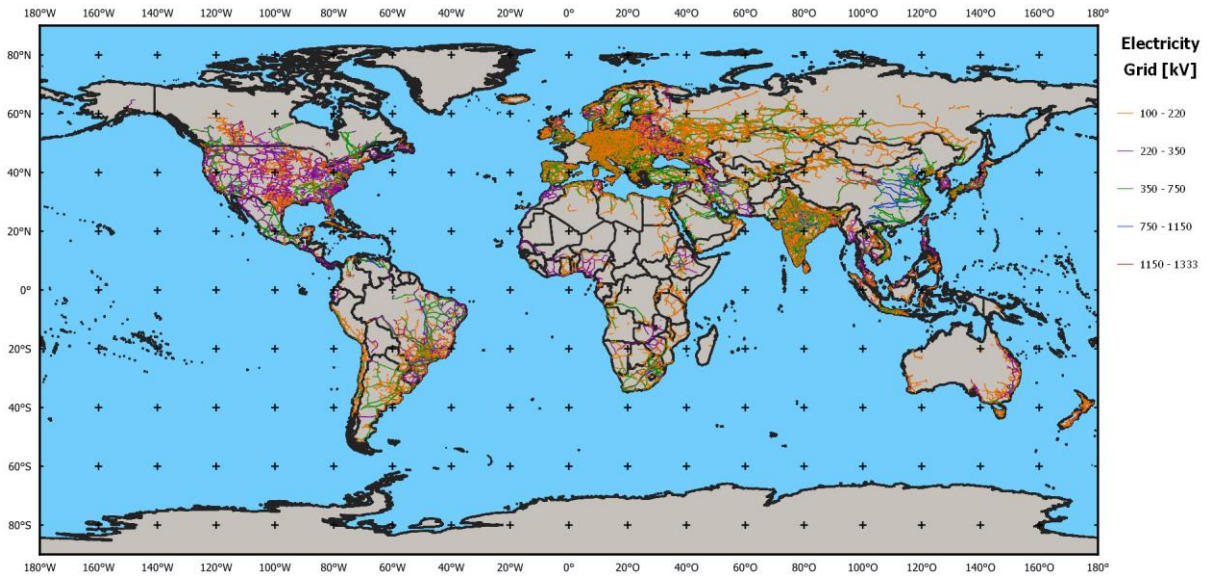

Figure 3-6. Global electricity grid data based on OSM [116].

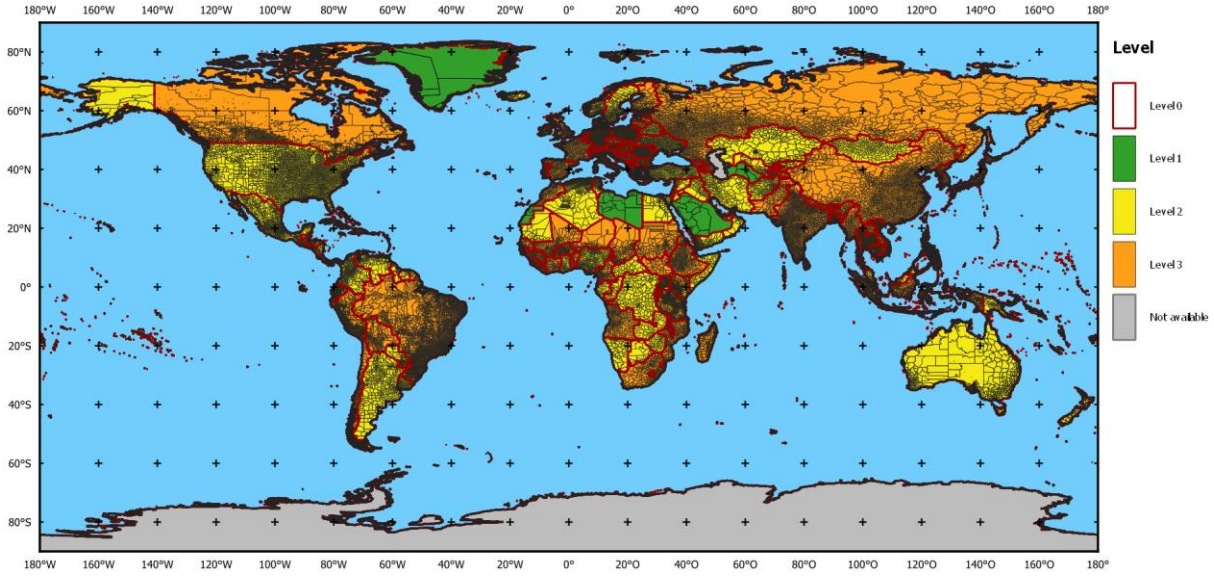

Figure 3-7. The administrative levels according to the classification from Level 0 (country) to Level 3 (municipalities) by [75].

3.3. Applied Energy System Model

Based on the literature review and the analysis, energy system optimization models can determine a cost-optimized transformation towards future energy systems to show pathways how countries can reach their climate targets. This thesis focuses primarily on the model input and output by preparing data-driven models and evaluating these approaches in a standardized way. Thereby, models can be enabled to analyze all countries globally in a standardized and efficient way. Since there are already various models available, this approach uses an existing model. It must fulfill the general requirements defined in chapter 2.2 and the specific requirements for the three use cases. Furthermore, the first research question requires standardized rules to enable a comparable projection of the modeled technologies for all countries.

3.3.1. Description and Adequacy of Applied Model

The applied energy system model is the Energy System Development Plan (ESDP). The ESDP can be classified as an energy system optimization model with a typical model formulation [32]. A detailed model description is provided in Appendix A.

In general, the model distinguishes between technology data and volume data. Volume data are particularly spatial, temporal, and spatio-temporal data series depending on the model resolution. Technologies are modeled by commodities and conversion processes. Commodities represent energy vectors such as electricity, natural gas as input for gas power plants, or hydrogen for the second use case. Conversion processes represent the conversion from one commodity to another, e.g., gas power plants converting natural gas to electricity, heat, and emissions. The techno-economical characteristics such as efficiency, costs, lifetime, or technical limitations describe each conversion process [114]. Figure 2-3 provides a visualization of the modeled conversion processes and commodities.

Fulfilling the requirements of the overall framework, the research questions, and the three modeled use cases, the ESDP is a suitable model due to the following reasons:

- Its objective function optimizes the total costs, which is typical for medium- / long-term planning energy system optimization models [114]. Therefore, it minimizes the C^{CAPEX} and C^{OPEX} of all technologies during the considered period by

$$\min C^{CAPEX} + C^{OPEX}. \tag{3.1}$$

  The calculation of CAPEX and OPEX is described in equation (A.2) and (A.3).
- In addition to the objective function, boundary conditions extend the optimization problem. For the analyzed research question, a critical boundary condition is the limitation of CO_2 emissions. The applied model provides three possibilities for this purpose: fixing an upper limit of emissions, a total emission budget, or including a CO_2 price per emitted ton in the operational costs [114]. Considering the modeling target of an 80% emission reduction, the upper limit is selected, similar to detailed country studies evaluating their pathway to meet Paris Agreement goals [173]. In the model, the emissions Em_y are calculated by the emission factor $EF_{y,cp}$ and the energy output$E_{y,cp}$ of each conversion process cp and each year y and must respect the upper limit EL_y as a boundary:

$$Em_y = \sum_{cp} \left(E_{y,cp} * EF_{y,cp}\right), \tag{3.2}$$

$$Em_y \leq EL_y. \tag{3.3}$$

Regarding the CO_2 price, there is no regulatory basis for a worldwide comparable and unified price. However, it can provide a suitable comparison to the modeling results and guidance for policymakers on which price is effective for a successful decarbonization process. Next to energy equity, represented in the objective function, this boundary condition covers energy sustainability from the energy trilemma [20].

- A second critical boundary condition, which the model setup fulfills, is the hourly match of supply and demand. Especially for energy system dominated by VRES, an hourly resolved optimization is essential to find a system which is still reliable in the worst hour. The model considers this requirement by matching the input P^{In} and output P^{Out} power for each modeled time step t including the exchange $Trp^{tot}_{y,com,reg,t}$ between different regions reg. To prevent infeasibilities, this equation contains a slack variable P^{slack}, which, e.g., can be used for curtailing variable RES by

$$\sum_{cp} P^{in}_{y,cp,reg,t} + P^{in,slack}_{y,com,reg,t} + Trp^{tot}_{y,com,reg,t} = \sum_{cp} P^{out}_{y,cp,reg,t} + P^{out,slack}_{y,com,reg,t}. \tag{3.4}$$

The balancing equation ensures the third aspect of the energy trilemma: energy security even with fluctuating energy sources [20]. Furthermore, the hourly consideration can model storage technologies and their state of charge (SOC), described by equation (A.14).

- Another relevant aspect to model decarbonization pathways is evaluating this process along the entire pathway, starting with the current system. The model includes several year steps in the modeling process. The installed capacity in a specific year $Ca_{cp,y}$ includes newly built $Ca^{new}_{cp,y}$, retired existing $Ca^{early\ retired}_{cp,y}$, and residual capacities $Ca^{residual}_{cp}$ [114]:

$$Ca_{y,cp,reg} = Ca^{residual}_{y,cp} - Ca^{early\ retired}_{y,cp} + Ca^{new}_{y,cp}. \tag{3.5}$$

- To consider the spatio-temporal differences within an energy system, the applied model needs to be capable of such a resolution. The regional clustering and all three use cases require a multi-region model. The ESDP also meets this requirement [114]. It can model the grid between regions by a capacity-based approach [114], [144], [174] which has been identified as a suitable methodology to keep the optimization problem in a solvable range, especially for the first use case. The output power $P^{out,trans}_{y,com,reg1,reg2,t}$ of a line for a commodity com, e.g. electricity, is modeled by its input $P^{in,trans}_{y,com,reg1,reg2,t}$, the line length LE, the specific line losses $LL_{y,com}$, and the maximum transferable capacity $Trp_{y,com,reg1,reg2}$ as follows:

$$P^{out,trans}_{y,com,reg1,reg2,t} = P^{in,trans}_{y,com,reg1,reg2,t} * (1 - LE * LL_{y,com}), \quad P^{in,trans}_{y,com,reg1,reg2,t} \leq Trp_{y,com,reg1,reg2}. \tag{3.6}$$

- The second use case, modeling green hydrogen production, requires a very flexible model formulation for an implementation of a tailored modeling approach. As explained in the general model description, the ESDP can include all different kinds of energy carriers and technologies by applying the concept of commodities and conversion processes [114]. Thereby, it provides high flexibility to model each use case.

Several projects have proven the application of the ESDP as a long-term planning energy system model for the described requirements. It has been used to calculate a pathway for Germany to reach its Paris Agreement goals in a cross-sectoral model [173] which has been extended by a detailed

European market and grid simulation [114]. Similarly, it is applied in the publicly funded European Horizon2020 project "plan4res" to calculate the optimal technologies in an integrated European model with a high spatial resolution [175]. In the German research project "InnoSys", the model's spatio-temporal capabilities and grid representation are demonstrated. In this context, the impact of flexibility technologies to contribute to a modified transmission grid operation is determined [174] .

3.3.2. Standardized Modeling Rules

Based on the described input of the energy system model in chapter 2.2.2, standardized modeling rules are a requirement to guarantee a transferable model setup for all countries. These rules connect the clustering results of the presented categories in Table 3-1 to the input of the energy system model, depicted in Figure 2-3. The first rule defines the modeled scenario conditions by calculating the maximum CO_2 emissions for the final year of consideration Em_{2045} based on the calculated emissions in 2015 Em_{2015}. The decarbonization of the base scenario is set to 80% which is reflected in the calculation of the emission limit:

$$Em_{2045} \leq Em_{2015} * 0.2 = EL_{2045}. \tag{3.7}$$

In addition to this scenario definition, five categories divide all further defined rules: scaling the archetype models, preparing the time series, calculating the electricity demand and resource availability, determining limits for the technology expansion, and setting up a multi-region model. These five categories address the derived requirements for the standardized modeling rules. Figure 3-8 visualizes the detailed connection between the data basis, the rules, and the model input.

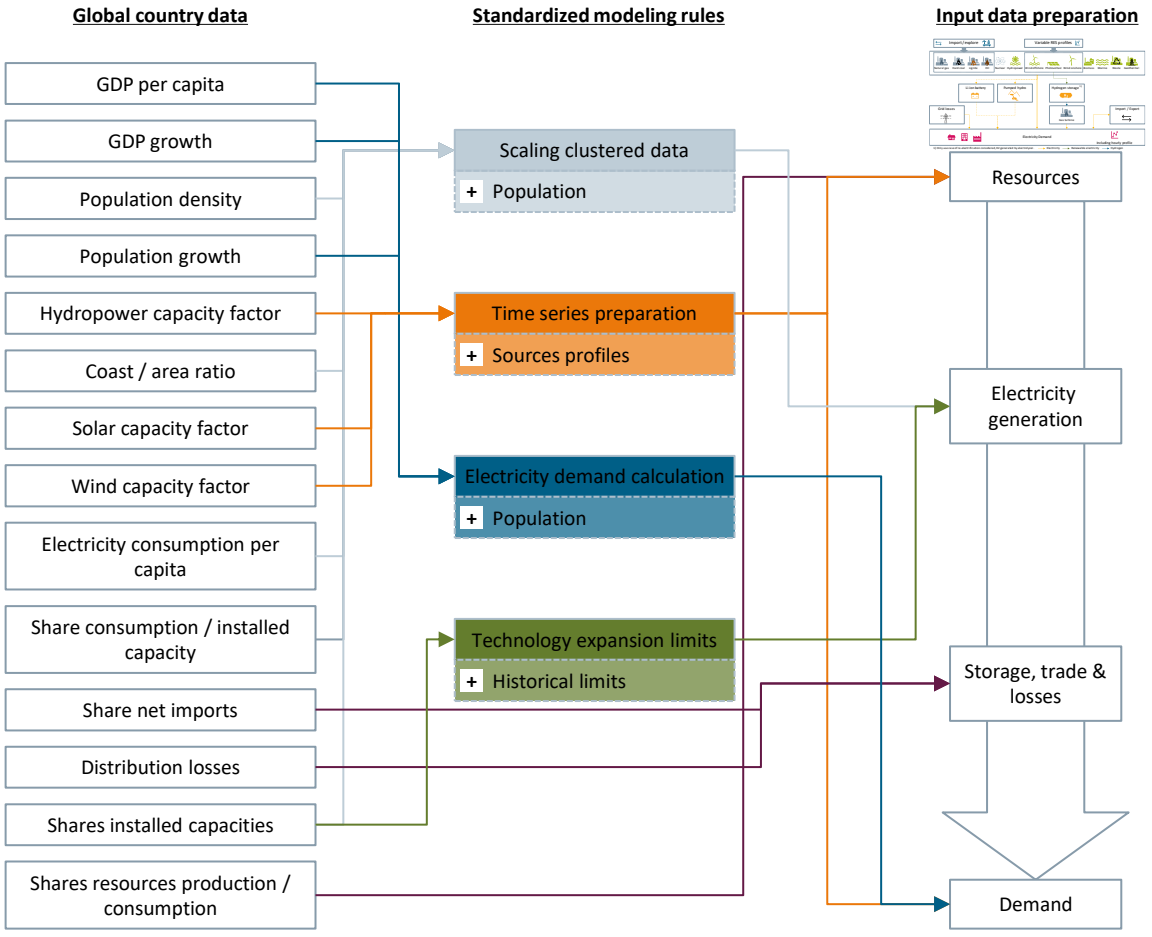

Figure 3-8. Integration of standardized modeling rules processing global country data (Table 3-1) for the input data preparation (Figure 2-3), including additionally required information (+).

All described rules are developed based on data research, comparisons to other model approaches, or iterative tests. While only the archetype model requires the scaling, the other three rules are valid for all three model levels. Only the renewable profiles of PV and wind generation are updated based on the spatial database for the regional model level. Two publications provide a more detailed description and validation of these rules [176], [177].

Scaling clustered data

The data in the global country dataset are normalized by the four categories: installed capacity, consumption, population, and area. To simplify scaling the normalized clustering results to a computable model, the model only considers the population. This approach also facilitates modeling countries for which the archetype is known but little energy-related data is available. To have all information available, the data category *Share consumption/installed capacity* is included in the clustering. It defines the ratio between the installed power capacity and the electricity consumption.

Since an analysis of this ratio shows a linear relationship for most countries globally [176], it is used for the approximation. The following formulas are then applied to define the archetype model based on the global country data used for the clustering in Table 3-1. The only additionally required data category is the average population size $"Population"_{2015,at}$ of all countries within the modeled archetype at.

$$D_{2015,at} = "Electricity\ consumption\ per\ capita"_{2015,at} * "Population"_{2015,at}, \tag{3.8}$$

$$Ca_{2015,at} = D_{2015,at} * "Share\ consumption/installed\ capacity"_{2015,at}. \tag{3.9}$$

The total installed capacity is used to determine the installed capacities of each technology te in the base year 2015:

$$Ca_{te,2015,at} = Ca_{2015,at} * "Share\ installed\ capacities"_{te,2015,at}. \tag{3.10}$$

The last category used for scaling is the area. Since the archetypes represent prototypical countries, an approximated area is computed by using the population and the population density:

$$Area_{at} = \frac{"Population"_{2015,at}}{"Population\ Density"_{2015,at}}. \tag{3.11}$$

Consequently, the area is applied to calculate the coastline length as follows:

$$Coastline_{at} = Area_{at} * "Coast/area\ ratio"_{at}. \tag{3.12}$$

This rescaling allows for parameterizing the model in 2015. Additionally, it is the basis to define further rules for a global setup preparing the computation of the decarbonization path.

Time series preparation

According to Figure 2-3, VRES generation and the electricity demand require hourly resolved time series. The electricity demand profiles are researched globally for as many countries as possible. Examples for data sources are the *ENTSO-E* for Europe, national data platforms, or even data on a state basis [178]-[180]. Assuming similar characteristics of their energy systems, including similar climatic characteristics, at least one demand profile per archetype is required. For countries without publicly available profiles, synthesized profiles generated by *Toktarova et al.* are included [85]. All model levels use the same demand profiles. For each archetype, the profile of the country closest to the cluster center is used. Even in a multi-region model, one profile is considered for the entire country since the spatial data basis does not provide hourly resolved demands.

For PV and wind generation, profiles are generated based on five points within each country's shape. Based on data from *Renewables.ninja* [155], the hourly profiles of each point are synthesized to a country profile by weighting them according to their annual generation potential [176]. The resulting profile is a first suitable approximation and can directly be used on the country level. On the archetype level, the hourly profiles are based on the same country providing the demand profile. They are scaled by the average full load hours of the archetype. The multi-region models on the most detailed level use the spatial profile based on the data basis described in chapter 3.2.2. For hydropower, the model includes the country or archetype capacity factor to approximate the water availability.

Electricity demand and resource availability calculation

Some conversions are required to combine the global country data basis with the identified approach to calculate future electricity demand. Instead of using a simplified linear regression, the formula to calculate the electricity demand per capita $D_{2045,cap}$ by this approach is defined as follows [85]:

$$D_{2045,cap} = a * \left(e^{(b*GDP_{2045,cap})} - e^{(c*GDP_{2045,cap})}\right)$$
$$with\ a = 7.721 * 10^4\ [kWh], b = -1.95 * 10^{-6} \frac{1}{\left[\frac{€}{capita}\right]}, c = -5.655 * 10^{-6}\ \frac{1}{\left[\frac{€}{capita}\right]}. \quad (3.13)$$

The GDP per capita for the final year 2045 is projected by using the current GDP growth and the period Δy:

$$GDP_{2045,Cap} = GDP\ per\ capita * (1 + GDP\ growth * \Delta y). \quad (3.14)$$

Next to the GDP, the population also must be projected to scale the demand per capita to the total demand:

$$Population_{2045} = Population_{2015} * (1 + Population\ growth * \Delta y). \quad (3.15)$$

Based on these parameters, the total electricity demand D_{2045} can be determined by

$$D_{2045} = D_{2045,Cap} * Population_{2045}. \quad (3.16)$$

These formulas combine the demand projection with the socio-economic development of countries. Especially less developed countries expect a high electricity demand increase until 2045 mainly due to their economic progress. Additionally, the formula considers the population growth in this period. It can be applied to the archetype level using the average archetype values or a specific country using its values from the country data basis.

Next to the electricity demand, the demand for resources also plays a role in the model. As depicted in the overview of modeled technologies in Figure 2-3, the model distinguishes between the domestic exploration and import of resources each at different costs. By this differentiation, countries might favor resources that they explore in their country for power generation instead of importing other resources. To reflect this in the model, the clustering feature *"Shares resources production/consumption"* ($SRPC_{c,co}$) of each modeled commodity com and modeled country co is considered for the calculation of costs $C_{com,co}$. The global exploration and import prices $C_{com,explore}$ and $C_{com,import}$ are used in this context:

$$C_{com,co} = SRPC_{com,co} * C_{com,explore} + \left(1 - SRPC_{c,co}\right) * C_{com,import} \quad (3.17)$$

Technology expansion limits

The last set of rules defines the allowed expansion of technologies. Limiting the expansion is mainly required due to geographic restrictions. Technologies, such as hydropower or geothermal electricity production, are not available in every country and cannot be expanded unlimitedly. Even wind and photovoltaic generation have limited potential due to the area of a country.

Especially for wind, the available area is an essential factor. For example, in Germany, the wind expansion is slowed down to only around one GW per year due to the increasing area and distance restrictions [181]. To account for these difficulties, a limiting factor is calculated based on historical expansion values of countries with the currently highest share of wind generation. The average wind density can then determine the maximal expandable wind capacity in MW per km² by the calculated and rescaled country/archetype area. The wind offshore potential follows a similar calculation, but it uses the coastline length instead of the area. By contrast, the potential PV expansion is determined by the total electricity demand and the capacity factor of PV [176]. This difference reflects that many countries limit the expansion of onshore wind to reduce the aesthetic impact [182].

Hydropower and pumped hydro storage expansions are limited to global annual growth shares and only allowed in countries with existing hydropower installations. In the regional model, the expansion is even limited to the respective regions with the installed base. A similar global average annual growth approach is applied to the other modeled RES technologies biomass, geothermal, waste, and marine [176]. All expansion limits are used in the model to represent the potential availability of generation technologies in the evaluated energy system, include their technical and geographic potential, and avoid overcapacities for just one technology because the linear optimization algorithm favors it.

For the existing fleet of power plants, a linear ramp-down until the end of their technical lifetime LT_{te} is assumed. In this approach, a second conversion process per conventional technology, e.g., *"Gas PP new"*, represents the newly built power plants. Nuclear power is the only exception without any expansion due to the project execution complexity. The decommissioning of technologies, which contributes to the residual capacity $Ca_{y,cp,reg}^{residual}$ in equation (A.4), is expressed by defining the installed capacity $Ca_{y1,te}$ in a year y_1 as follows:

$$Ca_{y1,te} = Ca_{y0,te} - \frac{Ca_{y0}}{LT_{te}} * (y_1 - y_0). \tag{3.18}$$

Next to the decommissioning at the end of the lifetime, the model also allows for early retirements of power plants if their operation is not economical.

Multi-region model

The regional model setup is based on applying the same rules described above to the respective country but includes some additional information based on the global spatial data basis. The integration of this regional data basis is visualized in Figure 3-9.

Except for the wind and PV time series, which are entirely independent of the country model, the spatial data distribute the total country data for demand and existing generation technologies to the determined regions. To model this distribution, the distribution factor $\mathrm{RD}_{cp,reg}^{Ca}$, described in equation (A.5), is used. Additionally, the availability factor $\mathrm{RA}_{cp,reg}$ in equation (A.6) limits technologies in regions such as hydropower or wind offshore according to the technology expansion limits. By this process, the models are kept comparable to the other modeling levels.

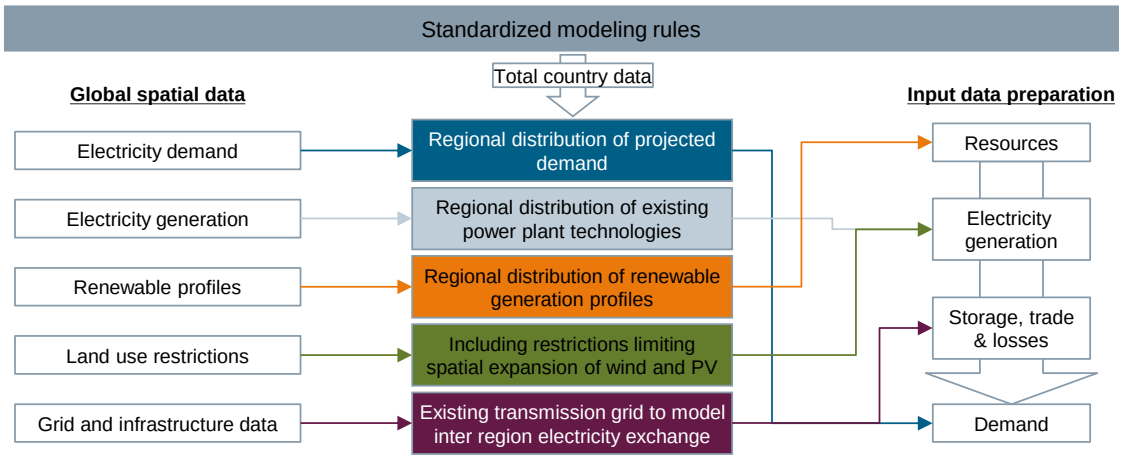

Figure 3-9. Combination of standardized modeling rules with the global spatial data basis to set up multi-region models.

In detail, matching the global spatial data and the country model requires minor adjustments. For the electricity demand, the split of the total country demand into PHH and CTSI demand reflects the ratio in the global spatial data basis. Since the development depends on complex socio-economic developments, this ratio is assumed to be constant until 2045 and both demand categories follow the same hourly profile. The spatial distribution of electricity generation technologies focuses on the existing technologies in the base year 2015. Thereby, it represents the spatial characteristics of the current system. For the future modeled years, technologies can be built in any region to find a spatially optimized solution.

In contrast to the previously described regional distributions, which only extend the existing model setup, the integration of land-use restrictions requires a model extension. These restrictions are helpful for a more realistic representation of the available area to avoid that, e.g., all wind units are built in a large agglomeration. The implementation of the restriction introduces the area as another model dimension. This area is linked to the processes of wind and PV according to equation (A.12) and (A.13) based on the following steps:

1. The available area in square kilometers is calculated for the model regions applying all exclusion criteria mentioned in chapter 3.2.2 with a distance rule of 1 km.
2. For both technologies, factors are defined, which represent the density of their expansion. PV is assumed with a density of 0.03 MW/km² [183] and wind with 3 MW/km² [184]. These factors represent the parameter $TLINK$.
3. During the optimization process, the available area in each region can be used either for wind or PV expansion. Thereby, each region can only expand renewable generation units based on its area availability.

Last, the multi-region model requires the grid capacity between the regions to calculate their energy exchange. Chapter 4.3.1 contains the precise implementation of a grid model.

3.4. Clustering and Validation Process

The two clustering applications constitute a significant part of the developed framework. They answer the second research sub-question, which aims at implementing and validating suitable clustering techniques. These available techniques must address the requirements for the archetype and the spatial clustering. For their implementation, there is a general procedure of identification, implementation, validation, and interpretation, defined by *Xu and Wunsch* [97]. The procedure precisely names four steps: (1) feature selection or extraction, (2) clustering algorithm design or selection, (3) cluster validation, and (4) result interpretation.

These four steps are applied to the two clustering algorithms by including requirements resulting from the analysis in chapter 2.3 and their role in the context of the overall framework (see Figure 3-1). Therein, archetype clustering is applied as a first filter to reduce the complexity of all global countries. The regional clustering prepares the highest detail of modeling. This differentiation, which is also considered in the different data bases, leads to different requirements – as summarized in Figure 3-10. The following subchapters deduce the consequences of these requirements for the definition of each clustering approach. The detailed implementations of both clustering algorithms are then described in chapters 4.1 and 4.2.

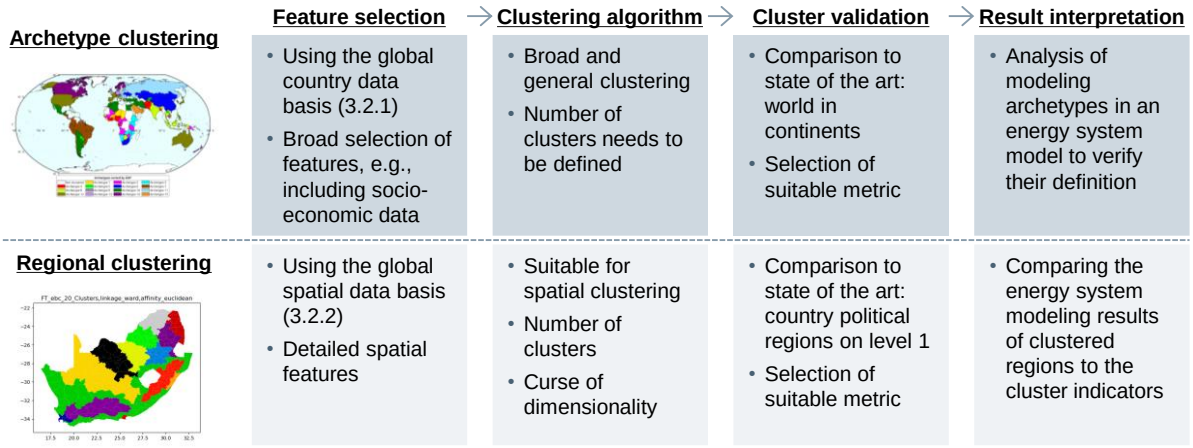

Figure 3-10. Structure of the clustering process on the archetype and regional level based on the four steps defined in [97].

3.4.1. Archetype Clustering

The generation of archetypes, for example in sustainability research, is evaluated systematically by *Eisenack et al.* [185]. Therein, archetypes are defined as *"a comparative approach that seeks to identify recurrent patterns among cases in which general regularities that apply to all cases cannot be expected"*. This definition fits the idea of energy system archetypes very well: the energy systems of countries worldwide differ in their details, but archetypes can characterize similar patterns. Therefore, the archetypes consider a broad data basis with various features. This approach sets them as a first filter to distinguish between different prototypical countries and identify countries for a more detailed evaluation.

Following the mentioned evaluation, certain aspects need to be considered when defining archetypes. It is essential to specify the domain in which it is valid and ensure the consistency between the input features, the theoretical approach, and the validation [185]. Specifying the theoretical approach, clustering is mentioned as being frequently used and suitable to define archetypes. Combining the four basic steps of clustering with the requirements for archetypes emphasizes the steps of validation and result evaluation. In this thesis, the defined archetypes are valid as a data analysis of the global country data basis. However, the goal is to prove that the archetypes also support the analysis of future energy systems by modeling them in a decarbonization scenario. Therefore, the archetypes are validated a second time in the step of result evaluation by systematically comparing the modeling results.

Feature selection

The archetype clustering developed here includes 62 features for 141 countries. The detailed features, their selection criteria, and the country selection are explained in chapter 3.2.1. By including not only direct input data of the energy system model but also other features, the clustering considers various impacts on energy systems and leads to broader archetypes.

Clustering algorithm

Derived from the application of a broad representation, the clustering algorithm needs to consider all features bottom-up. It should generate a direct assignment of countries to archetypes instead of providing probabilities or percentages. Furthermore, it should be easily interpretable and directly connect data input and clustering results. Applying these requirements to the analyzed clustering techniques, the K-means clustering is identified as the most suitable technique. It includes the features equally bottom-up and does not require a particular parametrization or threshold values. Furthermore, it is well established [99] and has also already been used for similar problems [58], [62]. For the implementation of the K-means algorithm, its two disadvantages have to be considered: the dependency on the initial solution without guaranteeing a global optimum in the final solution and the difficulty to find a suitable number of clusters.

Addressing the first problem, the framework includes stabilization approaches in the implementation of the algorithm. These approaches are the K-means++ method and iterations of the algorithm [99], [186]. K-means++ aims to overcome the dependency on the initial solution by finding an initial solution that is already data-driven and not arbitrary [187]. Iterating the algorithm is frequently used to improve the final results by finding different solutions and choosing the best one with the lowest variance of the iterations. Both extensions of the K-means algorithm ensure that each application of the algorithm to the same dataset leads to the same results and, thereby, the same archetypes.

Second, the number of clusters is always critical to find. A standard method is the EBC, as defined in chapter 2.3.3. Analyzing the variance curve for the applied dataset in Figure 3-11, there is no characteristic elbow recognizable. This phenomenon is known for the K-means algorithm and complicates the selection of cluster numbers [104]. However, the curve shows significant improvements in the interval between 2 and around 25 clusters.

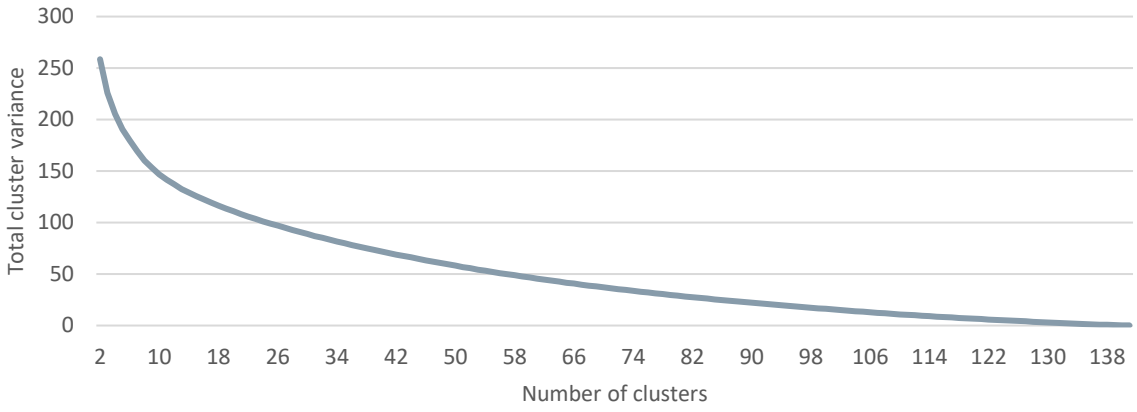

Figure 3-11. Variance for the different number of clusters.

Since the elbow method does not lead to a clear result, the number of clusters is chosen based on a comparison to other classifications. This approach simplifies also the validation since the clustering results are directly comparable to an official classification. In this context, the official sub-continental classification of the United Nations is used [57]. For the countries in the final clustering dataset, 15 regions remain. Only the regions of Melanesia and Polynesia are summarized because the countries in these regions are comparably small. Transferring this classification to the clustering, the number of clusters is set to 15, which equals an average number of fewer than ten countries per archetype. From the application side, this average number provides a good mix between summarizing countries and reducing the complexity based on explainable indicators but still different between the clusters.

Cluster validation

The validation process aims at calculating the accuracy of the clustering results directly. It requires a suitable validity metric and covers two aspects. First, the archetypes are analyzed by their characteristics to determine whether they show similar features. This analysis primarily describes the archetypes. Second, the archetypes are compared to current approaches of summarizing countries: the classification in geographical zones. This comparison refers to the studies with a global scope mentioned in chapter 1.2., including the *UN* subcontinental classification, which influences the selected number of clusters. To compare the clustering and the geographic classification, all clustered countries co and selected features df are considered. The applied K-means clustering and the EBC use the Euclidean distance to calculate the shortest distances. Therefore, the validation also calculates the Euclidean distance to identify the variance Var_{cl} by the distance between each country and the cluster center:

$$Var_{cl} = \sqrt{\sum_{df,co} \left(x_{df,co} - x_{df,cl}\right)^2}, \forall co \in cl \tag{3.19}$$

The total variance Var_K for a defined number of clusters K is then determined by summing up the variances of each cluster Var_{cl}:

$$Var_K = \sum_{cl} Var_{cl}. \tag{3.20}$$

Transferring this process to the geographic classification, the average $\overline{x_{df,co}}$ of each clustered feature df is calculated for each geographic zone defining the values $x_{df,geo}$. For each zone, only the relevant countries co are included:

$$x_{df,geo} = \overline{x_{df,co}}, \forall co \in geo. \tag{3.21}$$

Finally, the sum of all Euclidean distances Var_{GEO} between the feature centers of the zones and their countries is calculated. The result represents the same dimension as the sum of the clustering results Var_k defined in equation (3.20) and is defined by:

$$Var_{GEO} = \sum_{geo} \sqrt{\sum_{df,co \in geo} \left(x_{df,co} - x_{df,geo}\right)^2}. \tag{3.22}$$

For the final evaluation, each study is compared to the clustering results in which the number of zones is equal to the number of clusters K. For the difference, the $Benchmark\ Index_K$ is defined, which calculates the difference between the geographic variance Var_{GEO} and the respective clustering variance $Var_{K=GEO}$:

$$Benchmark\ Index_K = 1 - \frac{Var_{K=GEO}}{Var_{GEO}}. \tag{3.23}$$

Result interpretation

Interpreting the archetype results can also be split into a qualitative and quantitative step. For the qualitative interpretation, the description of important characteristics is the basis to discuss them with domain experts. This is an important validation for the application in energy system models since the clustering and archetype methodologies highlight that the results strongly depend on the application [99], [185]. As an additional performance indicator, the geographical distribution of archetypes is analyzed, comparing them to geographic zones.

The quantitative interpretation of the archetypes uses the energy system optimization model. In general, the archetypes follow the hypothesis to summarize energy systems of countries better than in a geographic classification. After evaluating this hypothesis for the direct clustering output by applying the benchmark analysis, it needs to be validated for the model results. This step is required to apply the framework in which global use cases are modeled from a global to a regional level, depicted in Figure 3-1.

For this purpose, the standardized modeling rules, defined in chapter 3.3.2, are applied to all 141 clustered countries. After applying the model, the result evaluation of each country differs between the archetype classification and the classification of the 15 *UN* subregions. Figure 3-12 visualizes the overall approach. For measuring the accuracy, the two introduced error measures, MAE and RMSE, are used since they are commonly applied [188]. Comparing both, the RMSE highlights outliers more, but a combination of performance metrics is often helpful to evaluate the performance. The third often applied error, MAPE, is in this case equal to the MAE [113]. Since the error is calculated based on the energy mix, which is according to equation (2.2) a percentage to ensure comparability across countries, the MAE provides a percentage error.

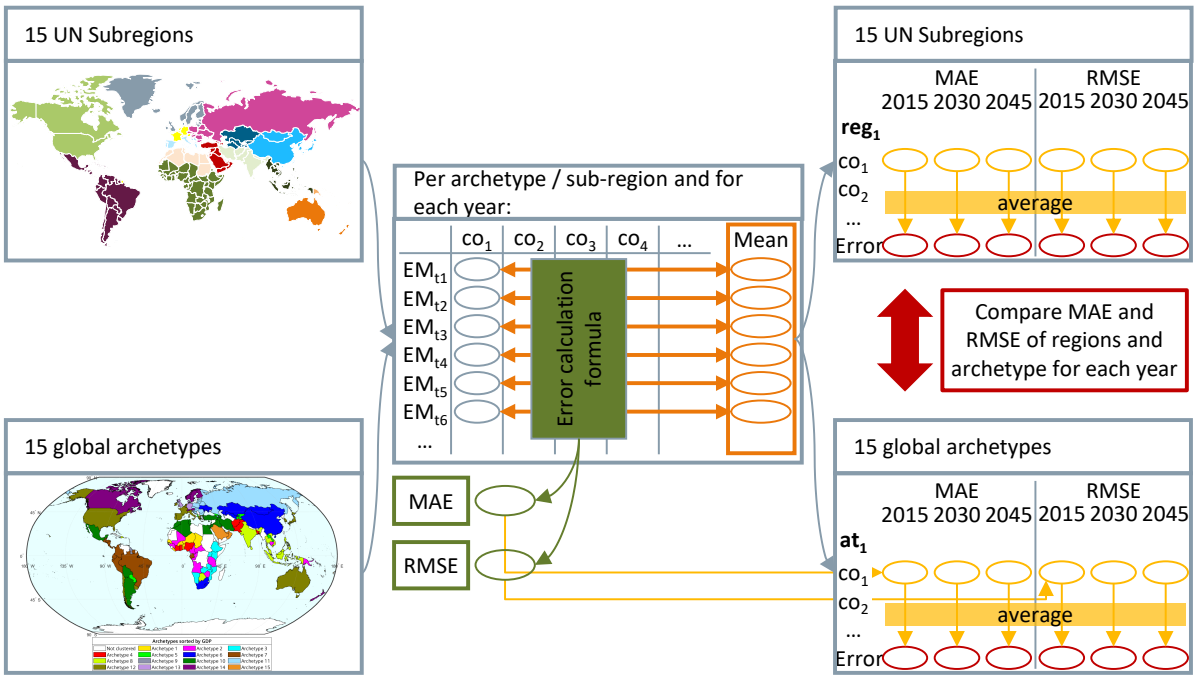

Figure 3-12. Validation approach of the 15 energy system archetypes in the energy system optimization model.

The following equations define the application of the performance calculation to the model results. As a first evaluation step, the contribution to the energy mix EM of all generation technologies te and storage technologies st is calculated for all countries and modeled years according to equations (2.2) and (2.3). For all countries co within an archetype at or a geographic zone geo, the average energy $EM_{y,te}$ and storage $EM_{y,st}$ mix is then calculated by the following four equations:

$$EM_{y,te,at} = \overline{EM_{y,te,co}}, \forall co \in at, \tag{3.24}$$

$$EM_{y,st,at} = \overline{EM_{y,st,co}}, \forall co \in at, \tag{3.25}$$

$$EM_{y,te,geo} = \overline{EM_{y,te,co}}, \forall co \in geo, \tag{3.26}$$

$$EM_{y,st,geo} = \overline{EM_{y,st,co}}, \forall co \in geo. \tag{3.27}$$

Based on these mean energy mixes, the MAE and the $RMSE$ error are determined for each country co considering its archetype at or geographic region geo. For these performance calculations, the archetype or geographic region represents the prediction P_n and the country result the actual value A_n as follows:

$$MAE_{y,co}^{at} = \frac{\sum_{te}\left|EM_{y,te,co} - EM_{y,te,at}\right| + \sum_{st}\left|EM_{y,st,co} - EM_{y,st,at}\right|}{TE + ST}, \forall co \in at, \tag{3.28}$$

$$RMSE_{y,co}^{at} = \sqrt{\frac{\sum_{te}\left(EM_{y,te,co} - EM_{y,te,at}\right)^2 + \sum_{st}\left(EM_{y,st,co} - EM_{y,st,at}\right)^2}{TE + ST}}, \tag{3.29}$$

$$MAE_{y,co}^{geo} = \frac{\sum_{te}\left|EM_{y,te,co} - EM_{y,te,geo}\right| + \sum_{st}\left|EM_{y,st,co} - EM_{y,st,geo}\right|}{TE + ST}, \tag{3.30}$$

$$RMSE_{y,co}^{geo} = \sqrt{\frac{\sum_{te}\left(EM_{y,te,co} - EM_{y,te,geo}\right)^2 + \sum_{st}\left(EM_{y,st,co} - EM_{y,st,geo}\right)^2}{TE + ST}}. \tag{3.31}$$

Summarizing these country errors for all archetypes and geographic zones provides the possibility to calculate the overall error for the archetype and geographic zone approach for each year:

$$MAE_{y}^{AT} = \frac{\sum_{co} MAE_{y,co}^{at}}{CO}, \tag{3.32}$$

$$RMSE_{y}^{AT} = \frac{\sum_{co} RMSE_{y,co}^{at}}{CO}, \tag{3.33}$$

$$MAE_{y}^{GEO} = \frac{\sum_{co} MAE_{y,co}^{geo}}{CO}, \tag{3.34}$$

$$RMSE_{y}^{GEO} = \frac{\sum_{co} RMSE_{y,co}^{geo}}{CO}. \tag{3.35}$$

Finally, these errors can be compared for each year to compare the classification of countries in archetypes and geographic zones. The development of the errors between the years indicates how the general similarity of energy systems develops and how increasing decarbonization influences the difference between the two compared approaches.

3.4.2. Regional Clustering

Compared to the archetype clustering, which is applied on a first level to better understand global challenges by simplified archetypal models, the regional clustering aims to prepare detailed country models. For this purpose, the spatial clustering algorithm generates a set of regions representing the structure of the energy system. This detailed clustering requires the consideration of direct data input of the energy system model. The following sections describe the precise approach according to the four introduced steps: feature selection, clustering algorithm, validation, and result interpretation.

Feature selection

The regional clustering considers the regional distribution of the critical input parameters to set up the energy system model. Based on Figure 2-2, the regional distribution of the installed capacities, the time series of variable inputs, and the electricity demand are the most critical parameters for the regional structure of a country's energy system. Based on these requirements, the definition of a global spatial data basis is described in chapter 3.2.2.

The selected features do not include the electrical grid since there are many regions without any connection to the transmission grid based on the smallest administrative areas. Furthermore, the objective of the evaluations, especially for the first use case, is not a detailed grid model but rather understanding general patterns of electricity flows. Therefore, the regions are first clustered without grid information and the grid between the regions is then calculated in a second step. Similarly, land use restrictions are calculated after the clustering for each region in the model and not directly considered in the clustering. They provide further boundaries for future energy systems, especially with a high share of variable RES, but do not essentially characterize them.

Clustering algorithm

The main requirement for the spatial clustering preparing a multi-region energy system model is the spatial contiguity of regions. For this requirement, the developed framework in this thesis applies a hierarchical clustering algorithm. Based on the analysis in chapter 2.3.2, hierarchical clustering has been applied successfully in many spatial clustering approaches and the spatial contiguity even improves the efficiency of the algorithm. Concerning the other presented clustering techniques, the spatial contiguity excludes the K-means algorithm since it does not include this requirement directly. The density-based and grid-based methods are susceptible to user threshold definitions. Since the goal is to find a clustering algorithm that is globally applicable and ideally extendable to other features, this dependency on user input excludes both approaches. Last, exact optimization models, such as the max-p regions algorithm, consider spatial contiguity directly. However, they face the challenge of computational complexity with a high number of regions [100]. Considering the application based on the smallest administrative areas, this computational complexity is critical. Germany, for example, consists of 4680 smallest administrative areas. *Siala and Mahfouz* solve this problem by first applying a K-means clustering [72].

For the implementation of the selected hierarchical clustering, its disadvantage not to find a globally optimal solution, needs to be considered. In general, hierarchical clustering algorithms mainly differ in their linkage criterion, which defines the merging process of two clusters cl_A and cl_B to one cluster. The most common linkage criteria are [97]:

- Single linkage: the single-linkage criterion defines the distance between two clusters by their distance to their two closest clusters. It can be described by evaluating the nearest neighbors.
- Complete linkage: contrary to the single linkage, the complete linkage uses the two farthest clusters instead of the closest clusters.
- Average linkage: the average linkage defines the distance by the average distance of all data points. They can be either weighted equally (group average linkage) or weighted by the number of data points (weighted average linkage).
- Centroid linkage: the centroid linkage uses the centroid of each cluster to calculate the distance and decide which clusters are merged.
- Median linkage: compared to the centroid linkage, the distance calculation for the median linkage is similar but weights all clusters equally and not by their distance.
- Ward's method: Ward's method aims at minimizing the increase of the squared errors of the sums within a cluster. It is computed for both clusters cl_A and cl_B as well as for the cluster combining both.

For the application of clustering regions within a country energy system, Ward's method is chosen. Ward's method is frequently applied for hierarchical clustering, it is the method that uses squared errors, and the approach is not sensitive to outliers [71], [97]. The other linkage approaches have disadvantages concerning their shapes or clustering results, such as single linkage tending to form chains or average linkage clustering points into wrong clusters as a trade-off. Furthermore, a comparison of the approaches has shown the best clustering results for Ward's method.

Similar to K-means clustering, hierarchical clustering also faces the challenge of determining the optimal number of clusters. For the regional clustering, the number of clusters needs to be determined in a comparable way for each country. Therefore, two options are provided: either the user can directly select it, or the algorithm can calculate the number of clusters. The use cases in this thesis apply a fixed selected number to compare the clustering results to the equivalent results on the first administrative level, e.g., states or provinces. Additionally, the SI score is selected to determine the optimal number of clusters. The advantage of the silhouette coefficient is that it considers simultaneously the intra-cluster and inter-cluster distances, leading to well summarized and well-separated clusters. Furthermore, the SI finds reliable values for the identified interval of regions in a quantitative comparison to the other CVI (see Figure D-4). To determine an optimal and computable number of regions, the highest SI score in this interval between five and 50 clustered regions is selected as the optimal number of clusters.

The regional clustering faces another challenge: by including hourly profiles of wind and solar generation, the dimension of the input features increases drastically. The direct clustering of both time series contains 17,520 data features. This high number of features leads to a sparse dataset which complicates the calculation of suitable clusters. To reduce this complexity, a frequently successfully applied approach is implemented: Dynamic Time Warping (DTW) [189]. It is combined with a principal component analysis (PCA) to summarize the effects of the time series analysis [107]. Chapter 4.2 deals with the detailed sequence of steps to solve the two challenges by preparing the data and implementing a suitable regional clustering approach.

Cluster validation

Similar to the validation of the archetypes, the regional clustering results are validated by comparing them to administrative regions on the highest level in the applied data set [75]. Level 1 includes a classification of states/regions/provinces for each country, which usually splits a country in the range of 5-50 regions (see Figure 3-7). Based on the literature analysis in chapter 1.2, multi-region models usually resolve countries in administrative regions on this level. Thereby, this level represents the state-of-the-art and a suitable benchmark for a regional classification.

The Euclidean distance is selected for the cluster validation. Since the objective of selected Ward's method is to calculate the squared sum of errors, it matches the calculation of Euclidean distance. Thereby, the clustering algorithm and the validation use similar mathematical principles. The Silhouette Index is a second validation metric since it performs best of all CVIs in the considered range. Both indicators compare all regionally clustered countries and two datasets: the full dataset including all time steps of the hourly PV and wind profiles and the data set with reduced time dimensions developed to improve the clustering performance. Thereby, the benchmarking is performed for the initial and the reduced data set.

For the Euclidean distance calculation of the regional clustering results, the applied formulas are comparable to the archetype clustering described in equations (3.19)-(3.22). The clusters are evaluated by calculating the distance of each smallest administrative area to the centroid of its assigned cluster. To evaluate the administrative classifications, their centroids must be calculated by determining the average values of the administrative regions on level 1 based on all smallest regions. These administrative centroids can then use the same Euclidean distance formula to compare both results. For the comparison of SI coefficients, the administrative classification is considered as an alternative set of clusters and thereby applies the same formula.

Result interpretation

The result interpretation differs for both clustering approaches. They both have in common that the results are applied in an energy system model to improve modeling capabilities. However, a holistic

global interpretation of regionally resolved models, such as performed for the archetype validation, would require a complex and time-consuming clustering and modeling process. This detailed validation is essential for the archetypes (see Figure 3-1) since their modeling results operate as a selection filter. Due to the complex evaluation and the last step in the framework, the regional modeling results are evaluated qualitatively.

For this qualitative approach, the modeling results of exemplary countries are compared to the characteristics of each clustered region. As a first evaluation step, the modeling results of the base year 2015 are expected to reflect the regional distribution of existing power plants. This distribution primarily considers conventional power plants and hydropower generation since the share of renewable generation technologies is comparably low in most energy systems in 2015. The conventional power plants are historically often located close to load centers. This combination includes the distribution of electricity demand within the country in the validation. Overall, this first interpretation step is suitable to validate the first modeled year and the clustering of existing generation and demand technologies.

Evaluating the other two years, 2030 and 2045, in the multi-region modeling requires to consider more modeling results and clustering features. First, the distribution of wind and PV generation in the model is expected to match the characteristics of the clusters regarding their annual capacity factors. Nonetheless, the expansion of these technologies is not only influenced by the direct ranking of the capacity factors. The remaining spatial data categories introduced in chapter 3.2.2, the electrical demand, land-use restrictions, and the electrical grid, also influence the regional allocation of new generation technologies. The model might favor some regions with a lower potential of wind or PV generation since they are closer to load centers, better connected to the existing electrical grid, or have enough area available to cover the expansion. These effects can also be analyzed by evaluating the clusters' characteristics and comparing them to the model results. Last, the variance of capacity factors between the minimum and maximum value plays a significant role. For some countries, such as countries with a large area, e.g., Russia or the USA, or widespread geography, e.g., Chile or Argentina, potentials for wind or PV differ strongly between the regions. By contrast, countries with a more geographical compact shape mostly show much fewer variations between the maximum and the minimum value so that the regional differences have a lower effect on the modeling results.

In this thesis, the regional models evaluate countries for three defined use cases. These use cases imply hypotheses, which define the result interpretation process. First, these hypotheses are stated, representing the expected model results in a global context of the use case. Second, the clustering results are analyzed regarding the regional characteristics and a particular focus on the defined hypotheses. Last, the modeling results are evaluated based on the clustering results by the described qualitative interpretation steps. This evaluation process finally confirms or corrects the first hypotheses and, in the meantime, interprets the clustering results.

4. Clustering and Use Case Evaluation Methodologies

The described framework requires the implementation of several algorithms and methodologies to evaluate worldwide energy systems. This chapter provides an overview of their detailed implementations. Based on the model descriptions in chapter 3.4, the first two sub-chapters include the implementation of the archetype and regional clustering algorithms. These descriptions are followed by specifically developed methodologies and implementations for the three use cases.

4.1. Archetype Clustering Algorithm

The archetype clustering algorithm is applied to the selected data features and the countries for which these features are available. A general overview of the following steps to cluster this dataset, which formally consists of the two dimensions $CO \times DF$, is provided by Figure 4-1. For the formal definition of the clustering algorithm, the 141 countries represent the set of observations X and the 62 selected data categories represent variables. This subchapter describes all steps which lead from this dataset to the energy system archetypes.

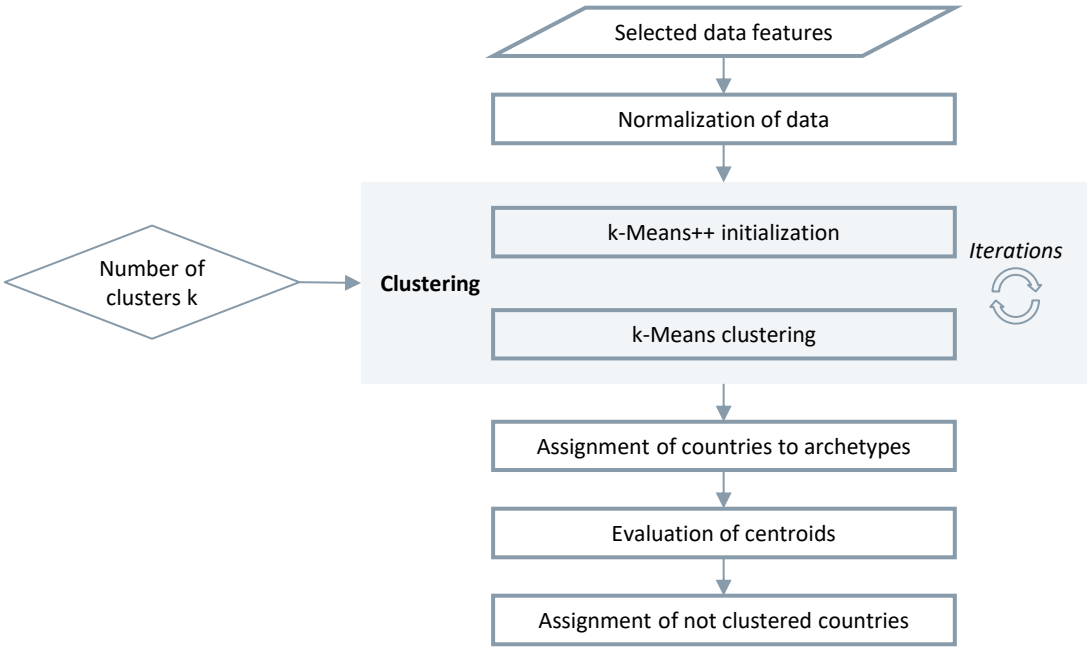

Figure 4-1. Process steps of the archetype clustering algorithm.

The clustering algorithm is programmed in MATLAB. In addition to the standard functions, the "Statistics and Machine Learning Toolbox" is used to implement clustering algorithms [190].

Normalization of data

In general, the data must be relative to be comparable between countries and different data categories. This comparability ensures an equal weighting in the clustering. For this purpose, clustering algorithms frequently use normalization as a pre-processing step. The normalization of all data features prevents more extensive features from being overvalued compared to features with lower values or data features with different units. Therefore, all data features are normalized by the minimum and maximum values. In comparison to normalizing by the standard deviation, this approach maintains the same scale. The normalization of all data points $x^*_{df,co}$ to the clustering input $x_{df,co}$ can formally be described by the following equation:

$$x_{df,co} = \frac{x^*_{df,co} - \min x^*_{df,CO}}{\max x^*_{df,CO} - \min x^*_{df,CO}}. \tag{4.1}$$

Thereby, the final dataset consists of values in the interval [0,1] ensuring an equal weighting and dimension of all data features.

Clustering

The normalized data set is the input of the clustering algorithm. In general, the K-means algorithm aims at minimizing the squared error between cluster centroids $x_{df,cl}$ and the objects of the data set $x_{df,co}$. Its primary function calculates the total distance J by the following equation:

$$J = \sum_{k \in K} \sum_{x_{df,co} \in cl_k} \left(x_{df,co} - x_{df,cl}\right)^2. \tag{4.2}$$

This equation requires a given number of clusters K to find the minimal distance. If K is equal to the number of observations, the countries co, the centroids are equal to the actual values and the variance is 0. As discussed before, K is set to 15 clusters for the archetypes. To implement the objective of reducing the distance between values and centroids, the algorithm generally follows three steps [99]:

1. The algorithm starts with a random partition of all objects to initial clusters.
2. All objects are assigned to the cluster centroid, which is closest to their characteristics using Euclidean distances.
3. The cluster centroids are re-calculated based on all assigned values.

The algorithm repeats the second and the third step until it has identified a stable solution and cluster memberships of observations do not change anymore. The two extensions to stabilize the results influence the first step, the random partition, and the repetition of all three steps.

To improve the random partition, the algorithm is extended by K-means++ [187]. It aims at choosing the initial partition based on data characteristics instead of a purely random selection to accelerate the runtime and avoid the algorithm to identify local minima as the final solution. This pre-processing includes the following three steps [187]:

1. It starts by picking one random value out of the initial random partition described in the steps of the K-means algorithm.
2. In the next step, the following initial center is determined by calculating a probability function for all objects in the dataset. This probability function reflects the distance of each data point to the first randomly selected cluster centroid over the sum of all distances. Subsequently, the value with the highest probability is assigned as the next centroid.
3. The second step is repeated for the pre-defined number of clusters K. The distance calculation includes all already defined initial cluster centers.

The second extension, iterating the three steps of the K-means algorithm $ITER$ times, increases the probability to find a global minimum for the distance J instead of a local minimum. Out of all computed solutions, it finally selects the clustering result with the minimal distance:

$$J_{final} = \min_{ITER} J_{iter}. \tag{4.3}$$

The number of iterations depends on the size and complexity of the dataset. Therefore, it is set relatively high to 100,000 iterations. An experimental approach defines this number since it always leads to the same clustering result for the same dataset compared to lower numbers. Thereby, the results are reproducible for each time the clustering is updated and repeated.

Assignments of countries to archetypes

The result of the iterated clustering algorithm is not only the final variance J_{final} but also the corresponding clusters and centroids. Equation (4.2) contains the cluster centroids $x_{df,cl}$ for each data feature df and the assignment of all countries co to the cluster cl with the closest distance. The initial data set with the dimensions $CO \times DF$ is thereby reduced to the dimensions $CL \times DF$.

At this point, the clusters CL are renamed to archetypes AT to proceed with the evaluation and interpretation of the results. The countries are listed in a table to summarize the assignment of each country to the archetype. Furthermore, the 15 archetypes are sorted by the data feature $GDP\ per\ capita$. This sortation simplifies the classification and interpretation of the archetypes by the economic development, which is easily interpretable.

Evaluation of centroids

Next to the assignment of countries to their archetypes, the archetypes themselves are evaluated and compared. Therefore, the centroids $x_{df,cl}$ are further processed by scaling them back to their actual value. This process provides interpretable results in the same dimension as the initial data. It also prepares the setup of an energy system model for each archetype. For this purpose, the minima and maxima of each data feature, used in the normalization process described in equation (4.1), are applied again.

$$x^*_{df,at} = x_{df,at} * (\max x^*_{df,CO} - \min x^*_{df,CO}) + \min x^*_{df,CO}, \forall df \in DF \tag{4.4}$$

The rescaled clustering centroids can also be compared between the different archetypes. For each data feature, the highest and lowest archetype values are determined to simplify the interpretation of the archetypes and define their characteristics.

Assignments of non-clustered countries

The selection of data features leads to a reduction of clustered countries: out of 193 countries, only 141 are clustered since the required data categories are only available for these countries. However, the framework aims at finding an approach that also clusters countries without complete data. Therefore, a post-processing step uses all available data features to assign the non-clustered countries to the defined archetypes.

For this purpose, the Euclidean distance calculation of the K-means algorithm is applied to these countries. First, the distance of each non-clustered country to all archetypes is calculated by only considering the data features $DF_{\mathrm{co_{ncl}}}$ which are available for the respective country

$$J(at) = \sum_{x_{df,\mathrm{co_{ncl}}}} \left(x_{df,\mathrm{co_{ncl}}} - x_{df,at}\right)^2, \forall df \in DF_{\mathrm{co_{ncl}}}. \tag{4.5}$$

The country is then assigned to the archetype $at_{co_{ncl}}$ which is closest to the country:

$$at_{co_{ncl}} = \arg\min_{AT} J(at). \tag{4.6}$$

For the application in the energy system model, the assignment to an archetype facilitates to reconstruct missing data. Alternatively, the archetype can be modeled directly just scaled by the population to evaluate the decarbonization pathway of countries which are usually difficult to evaluate.

4.2. Regional Clustering Algorithm

The regional clustering algorithm generally uses the spatial data features SDF, included in the global spatial data basis. Furthermore, the observations are the regions of a considered country, broken down to the smallest available administrative classification available AR [75]. The consecutive formal description of the basic data set is $AR \times SDF$. Figure 4-2 visualizes the process of the following clustering algorithm processing this data set to regional clusters.

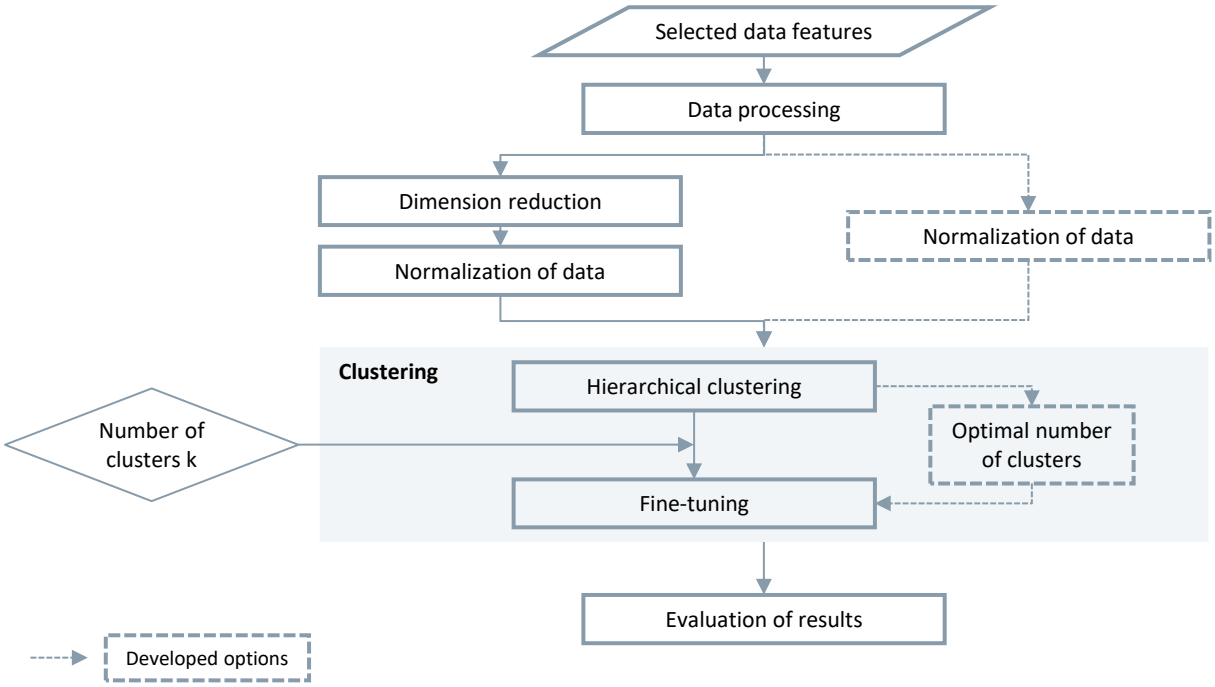

Figure 4-2. Process steps of the regional clustering algorithm.

Compared to the archetype clustering, the regional clustering process requires further steps, such as additional data processing and dimension reduction. Furthermore, there are some options included in the clustering process. The first option, the direct normalization of data, enables a clustering approach based on the entire dataset as it has been used for an exemplary study on South Africa [144]. The second option provides the opportunity to use an optimal number of clusters instead of a fixed number. As already described, the results of this thesis use a fixed number to compare the data to existing predefined regions. However, the algorithm to select the optimal number is included in this chapter to provide a complete description of the framework. In general, the spatial data are stored in a PostGIS 3.1 database [191] and the clustering algorithm is implemented in Python by mainly using the package "scikit-learn" [192]. The entire process is implemented in a Python graphical user interface (GUI). This GUI allows for an interactive clustering process. Therein, the user can change between a pre-parametrized process and an expert view. Furthermore, it visualizes intermediate results to ensure that the data input and all parameters are chosen accordingly to the application. The following sections explain each implemented step in detail.

Data processing

The usage of predefined administrative regions leads to several conflicts when preparing the data set for clustering. In this context, the processing primarily focuses on two cases: handling the smallest administrative regions that are, by their definition, spatially not contiguous and the handling of islands.

The first case occurs, for example, for non-contiguous cities, counties, or islands belonging to a mainland region. To ensure spatially contiguous clusters, these regions must be split. Therefore, the

algorithm checks all shapes of regions, identifies multi-polygon shapes, and splits them into contiguous polygons.

Second, islands have different impacts in countries around the world. Many countries with coastlines have small islands that are, for example, used for touristic purposes. By contrast, some countries have islands with essential importance for the country's economy and energy system, such as Tasmania in Australia or Sicily in Italy. The third group of countries predominantly consist of islands such as New Zealand, Indonesia, or the Philippines.

To cover all these three groups, three general rules for the handling of islands are developed:

1. Islands without any electric demand or generation are neglected since they do not influence the energy system model.
2. A threshold value is introduced to detect important islands within the country. Therefore, the algorithm calculates the area of all islands and compares it to the total area of the country. Islands represent essential islands for the country if the share is higher than the threshold. Otherwise, the islands are neglected. Based on experimental evaluations for several countries, the model proposes a default threshold of 1% which is adaptable by the user. During the parametrization process, the GUI visualizes which areas the threshold considers. If the visualization shows that the threshold neglects significant islands, the user can still adapt it.
3. Islands below the threshold but close to the mainland are linked to the closest region. The clustering does not consider islands with a distance longer than 50 km and below the defined threshold value since they might have a standalone system. The definition of 50km reflects the classification of territorial waters. Therein, it corresponds to the third level, "contiguous zone" [193].

The processing steps are applied to the standardized smallest administrative regions and lead to the final data set. They can increase the number of regions by splitting polygons, but also decrease it by neglecting islands without significance for the country's energy system. The data included in the global spatial data basis are then assigned to the final set of regions depending on their resolution. For the highly resolved features demand and generation, the points or raster within the polygon of the smallest regions are summed. For the VRES time series, the respective MERRA weather cell is used. If several cells overlap in a region, they are weighted based on their share of the total area.

Another processing step is the normalization of data for the two summed features, demand and generation. Since the algorithm uses predefined administrative shapes of regions, the size of a region's area influences the results of the clustering algorithm. Figure 3-7 visualizes this effect since the size of regions on the same administrative level in the same country can largely deviate. Examples of such deviations are, e.g., Australia, Canada, or Russia. Therefore, the two mentioned data categories are normalized by the area of each region. This normalization process is exemplarily defined for the demand density D_{ar} which is the input for the algorithm based on the calculated total demand D_{ar}^{*} in the region ar:

$$D_{ar} = \frac{D_{ar}^{*}}{Area_{ar}}. \tag{4.7}$$

Dimension reduction

After processing the administrative regions and normalizing the demand and generation data for the clustering, the third data feature must also be prepared. Due to the complexity increase by spatio-temporal data features of the VRES time series, the dimension of the final dataset requires a reduction. In the optional approach, the profiles are normalized and clustered directly [144]. However, such a large dataset leads to the curse of dimensionality and complicates applying a clustering algorithm.

Based on an analysis of several spatio-temporal clustering approaches, the Dynamic Time Warping (DTW) method is chosen to reduce the dimensionality of both technologies. DTW is an efficient approach to evaluate the similarity of time series and their shapes [194]. In the method, the two time series $ts_{te,ar1}$ and $ts_{te,ar2}$ of the VRES technology te in the two exemplary administrative regions $ar1$ and $ar2$ are compared:

$$ts_{te,ar1}(t) = ts_{te,ar1}(t_1), ts_{te,ar1}(t_2), ts_{te,ar1}(t_3), \dots, ts_{te,ar1}(t_T), \tag{4.8}$$

$$ts_{te,ar2}(t) = ts_{te,ar2}(t_1), ts_{te,ar2}(t_2), ts_{te,ar2}(t_3), \dots, ts_{te,ar2}(t_T). \tag{4.9}$$

For these two defined time series, a warping path $ts_{te,w(ar1,ar2)}(t)$ is defined based on the shortest distance between them:

$$ts_{te,w(ar1,ar2)}(t) = ts_{te,w(ar1,ar2)}(t_1), ts_{te,w(ar1,ar2)}(t_2), \dots, ts_{te,w(ar1,ar2)}(t_T), \tag{4.10}$$

$$DTW(ar1, ar2) = \min \sum_{t=t_1}^{t_T} \left(ts_{te,ar1}(t) - ts_{te,ar2}(t) \right)^2. \tag{4.11}$$

This warping path must fulfill two restrictions to reduce the complexity: monotonicity and continuity. Therefore, the time steps t need to be monotonically and be continuous. Besides, there are two further parameters derived from further restrictions which influence the DTW distance: first, the psi-relaxation, which changes the beginning $t_1 + \psi$ and the endpoint $t_T - \psi$ of the distance calculation to leave out these independent time steps. Second, the warping window allows to consider the period $t + \omega$, e.g., to reflect different time zones, but heavily influences the computation time. Based on experimental validations of several countries, the values are set to $\psi = 5$ and $\omega = 2$. The effect of these two parameters ψ and ω on the computation extends the definition of (4.11) by

$$DTW(ar1, ar2) = \min \sum_{t=t_1+\psi}^{t_T-\psi} \left(ts_{te,ar1}([t + \omega]) - ts_{te,ar2}([t]) \right)^2. \tag{4.12}$$

The example defines the distance calculation for the relation between two regions $ar1$ and $ar2$. To synthesize these individual distance calculations into a data set, which can be an input of a clustering methodology, they need to be discrete values. Therefore, the calculation of DTW features introduced by *Kate* is applied [189]. It aims to define the matrix of distances between all observations by referring the distances to specific training features ar_{tr}. In the case of this thesis, these training features are all administrative regions of the final data set.

$$DTW\ Feature(ar_{tr}) = DTW(ar_{tr}, [ar_1, \dots, ar_{AR}]), \forall ar_{tr} \in AR \tag{4.13}$$

The DTW features change the dimension of the dataset for an exemplary time series ts_t of one technology from $AR \times T$ to $AR \times AR$. The corresponding matrix of all features is defined as DTW_{AR} with the entries dt_1, dt_2, …, dt_{DT} for each region ar. However, the DTW features and thereby the reduction still depend on the number of smallest administrative regions. For example, in Germany, there are 4869 regions on the lowest administrative level [75], which would reduce dimensions by less than 50% compared to the 8760 time steps in the base data set. To ensure an effective reduction for all countries independent of their smallest administrative regions, a Principal Component Analysis (PCA) further reduces the DTW features. Compared to non-linear techniques for dimension reduction, PCA is still very effective and mostly outperforms other approaches [195].

Applying the general definition of PCA to the calculated DTW feature matrix leads to the objective of finding a vector that provides the maximum variance of linear constants to describe the base matrix

DTW_{AR}. Therefore, the covariance matrix of DTW_{AR} is determined [195]. The principal components are then defined by the eigenvectors and eigenvalues of this covariance matrix, solving the problem

$$cov(DTW_{AR})a = \lambda a. \tag{4.14}$$

This problem for the matrix DTW_{AR} has AR different eigenvalues λ and corresponding vectors a. To further reduce the number of vectors and thereby the dimensions to the principle components, only the number of PC most variant vectors are considered. Therefore, the $percentage\ of\ total\ variance$ is introduced and calculated [196]:

$$percentage\ of\ total\ variance = \frac{\sum_{j=1}^{PC} \lambda_j}{\sum_{j=1}^{AR} \lambda_j}. \tag{4.15}$$

To reduce the number of dimensions, the $percentage\ of\ total\ variance$ is set to 90%. This value is even higher than 70%, a frequently used benchmark [196]. Finally, the retransformation of the eigenvectors concludes the principal components pc of each administrative region ar in the final matrix with the dimensions $AR \times PC$. In comparison to the dimensionality of $AR \times TSP$ for each technology, these dimensions are in a manageable number while still reflecting the characteristics of each time series.

Normalization of data

After dimension reduction, the generated data set must be unified to ensure that all features are comparable, in the same range, and do not differ in units. However, in the case of spatial data, the data need to be weighted first. The three major data categories, electricity demand, generation technologies, and renewable profiles, contain data in different dimensions and different numbers of data features. For the latter two, these numbers are even different for all countries since the existing power plant technologies and the number of principal components depend on the characteristics of each country. The weighting process is depicted in Figure 4-3, including a visualization of the dimension reduction described in the section before.

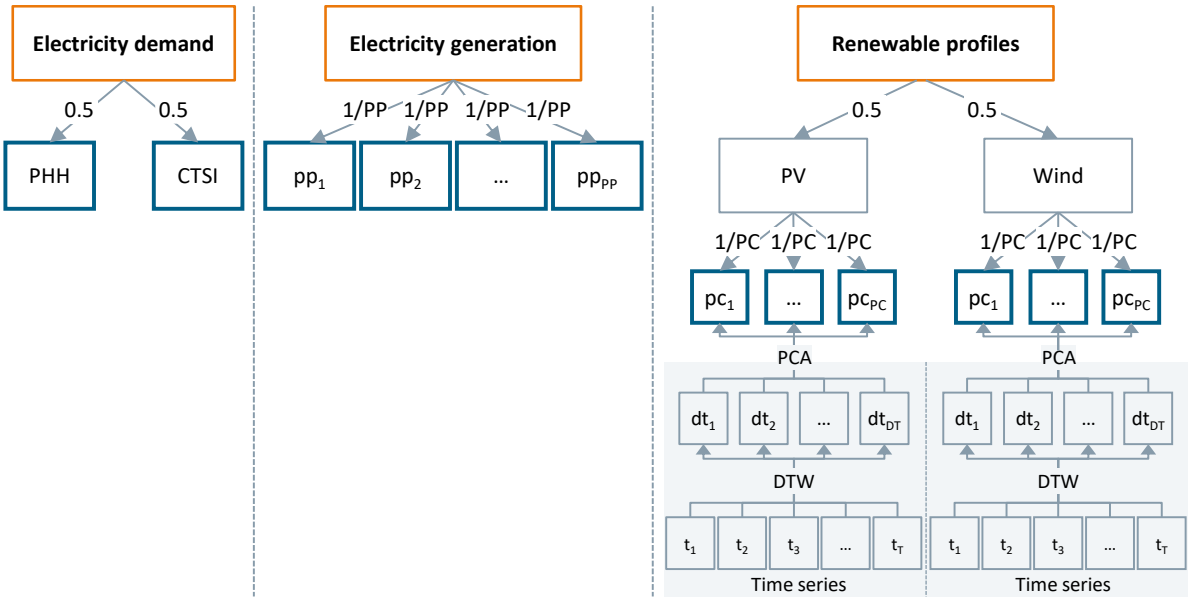

PP: number of electricity generation technologies pp in analyzed shape; T: number of timesteps (t); PC: number of principle components pc; DT: number of the DTW features dt (which is equal to administrative regions AR)

Figure 4-3. Normalization of data for the regional clustering algorithm showing the three major categories in orange, the final data for clustering in blue, and the process of dimension reduction in grey.

The three main categories, demand, generation and VRES profiles, have an equal weight. On the next level, the demand weighting is always split equally between the two categories PHH and CTSI. All power plant technologies are weighted by their number PP. By contrast, the weighting process of the renewable profiles is more complex. First, PV and wind are weighted both by 0.5. Consequently, the calculated principal components of each technology are weighted by their number PC.

The next step applies the normalization by the minimum and the maximum value, which is similar to the approach used for the archetype clustering described in equation (4.1). Therefore, each data feature highlighted by a blue frame in Figure 4-3 is scaled to the interval [0,1] and multiplied by the respective weight.

Clustering

In the applied version of the clustering algorithm, the number of provinces /states on the first administrative level defines the number of clusters. As visualized in Figure 4-2, this number is an input parameter for the clustering algorithm. The other input is the reduced, weighted, and normalized matrix of spatial data features and corrected regions on the smallest administrative areas $AR \times SDF$.

The hierarchical clustering is applied to this dataset by using Ward's method. It combines the regions with the lowest distance out of the entire distance metric in each step. The distance calculation uses the Euclidean distance:

$$J = \sum_{k} \sum_{x_{sdf,ar} \in cl_k} \left(x_{sdf,ar} - x_{sdf,cr}\right)^2 . \tag{4.16}$$

The process starts with each region as one cluster and then subsequently merges the regions with the shortest distances in clusters. The distance matrix is constantly updated to include the distances to the already merged regions [97]. This procedure stops if the number of clusters is equal to the defined number of regions K.

The characteristic of keeping regions in clusters that have been merged in a step before requires a post-processing approach to find a better solution. For this purpose, a "fine-tuning" algorithm is implemented after the clustering [197]. This algorithm performs a detailed evaluation of regions at the borders of contiguous clusters. For these side regions, the approach evaluates a shift to other clusters while keeping the criterion of spatial contiguity. If this shift improves the overall distance criterion, it is realized. Otherwise, the region is dropped from the list. This process stops when all regions have been checked and potentially moved. In the developments of the frameworks, the original algorithm has been extended by not only considering the changes evoked by shifting one single region but also of connected regions. Thereby it prevents, that a change of one region to another cluster improves the overall value but prevents the change of another single region [144].

Next to using the states as a defined number of clusters, the framework also includes an approach to determine the optimal number of clusters. This optimal number contains valuable information about the energy system. Its relation to the number of states indicates whether the country system is more distributed or centralized than the political regions. The analysis of runtime and solvability of multi-region models in chapter 2.1 identifies an interval for the optimal number between 5 and 50 regions. For the determination of an optimal number, the SI is most promising out of the described CVI. Based on the general formulation in equation (2.8), it is calculated for an interval of numbers of clusters k by the average index of all regions which are included in the clustering as follows

$$SI_k = \frac{1}{AR} \sum_{ar \in AR} \frac{b(x_{ar}) - a(x_{ar})}{\max\{a(x_{ar}), b(x_{ar})\}}. \tag{4.17}$$

Since a high SI represents a better result, the optimal number of clusters K is calculated for the defined interval by

$$K = \arg\max_{k \in [5;50]} SI_k. \tag{4.18}$$

If this option is applied, the results of the hierarchical clustering for the calculated K are the input of the fine-tuning algorithm and further processed for the result evaluation.

Assignment of results

In hierarchical clustering, the assignment of regions to clusters is directly included in the algorithm. The resulting clustered regions are numbered from 1 to K to use these names in the description and comparison of the results. For this comparison, the centroids of the clusters are used. For the demand and generation technologies, the total values are calculated by a sum of all administrative regions ar in a clustered region cr. Similarly, the time series evaluation consists of two steps: the time series as an input of the energy system model is calculated based on the profiles of the smallest regions within a clustered region. For the evaluation, each clustered region's average full load hours are calculated since it is easier to compare than an hourly time series.

4.3. Methodological Approaches for Use Cases

Next to the algorithms implemented for the clustering approaches, the three defined use cases require further specific implementations to be included in the framework and fulfill the derived requirements. The following three sections describe these implementations.

4.3.1. Use case 1: Grid Topology

The analysis of grid topologies in medium- and long-term optimization models identifies a capacity-based model as a good approximation. Also, the transmission grid is focused. The major challenge is to derive these capacities from the available data source OSM for the desired application to all countries. Therefore, standardized rules must be defined to synthesize the transmission grid. Even though this process is developed specifically for this use case, it is also suitable for other use cases, especially for the coal phase-out.

For accessing OSM data, the specific tags are used to filter energy data. On the first level, the primary feature *power* fits this purpose. Within the power feature, the two tags, *cable* and *line*, are selected to evaluate transmission lines since all other tags are linked to components on lower voltage levels, in substations, or power plants. Furthermore, the process neglects tags for other components along the lines since they increase the amount of data to be processed and the risk of incomplete data. Both selected tags, *cable* and *line*, are usually defined as ways between two nodes [198]. The available keys to specify further details are listed in Table 4-1 and Table 4-2.

Table 4-1. Available keys to describe the tag *cable* in OSM [198].

Key	Description
Voltage	The voltage level of the cable in V
Location	The precise location of the cable, e.g., underwater or indoor
Operator	The operating company of the cable section
Cables	The number of single cables representing the phases and by multiple of three the circuits
Circuits	The number of independent electrical circuits which should correspond to the number of cables
Frequency	The operating frequency in Hz
Name	The name of the cable section
Ref	A reference id for the specific cable section to specify the location, e.g., in industrial areas

Table 4-2. Available keys to describe the tag *line* in OSM [198].

Key	Description
Voltage	The voltage level of the cable in V
Cables	The number of single cables in this line section representing the phases and by multiple of three the circuits
Circuits	The number of independent electrical circuits which should correspond to the number of cables
Operator	The operating company of the line section
Wires	The bundling of cables in sub-conductors on the line (e.g., single, double, triple)
Frequency	The operating frequency in Hz
Name	The name of the line section
Ref	A reference id for the specific line section to specify the location, e.g., in industrial areas
Line	If the line is in a substation, this tag specifies it and differs between a busbar and a bay

For the calculation of transfer capacities, both tags are unified and hereafter referred to as connections since, in the end, the model only requires one transfer capacity between two regions. Based on the commonly available keys and neglecting text or specifier keys, the keys *voltage*, *cables*, *circuits*, and *frequency* are remaining. For these keys, several standardized rules are developed to calculate the capacity between two clustered regions cr_i and cr_j:

1. All connections within the examined area, e.g., a country, are extracted. Based on the results of the regional clustering, the connections with a starting and endpoint in two different clustered regions are stored for the following steps.
2. The key *frequency* is a filter to reduce the number of connections. First, all connections with a frequency of 50Hz or 60Hz are filtered since these two levels represent the frequencies used worldwide [199]. Connections with an empty value or the voltage 0 are either incomplete data or High Voltage Direct Current (HVDC) connections. For the latter, the name of the connection is checked whether it includes the term HVDC. Otherwise, the voltage is set to the most common voltage level in the extracted connections. Connections with other numeric values than 0, 50, or 60Hz are removed since they belong to independent systems such as the railway system. For example, in Germany, the railway operates its power grid with 16.67 Hz.
3. The number of *cables* Nca must be adjusted to be a multiple of 3 and be concordant to the number of *circuits*. Therefore, missing cables are added or exceeding cables are removed. The frequency and voltage of additional cables are set to the value of the existing cables. The number of circuits Nci_{cr_i,cr_j} is then set to

$$Nci_{cr_i,cr_j} = \frac{Nca_{adjusted,cr_i,cr_j}}{3}. \tag{4.19}$$

4. The fourth selected key is the *voltage*. First, the process only keeps connections with a voltage level higher than 100 kV as only the transmission grid is considered here. Second, connections without a voltage level are assumed to have the most frequent level of all lines. This approach leads to errors due to insufficient data but still considers the lines by assigning the most probable voltage. Based on literature values for typical currents on each voltage level vl [200], [201], a standard transmission capacity $TrCap_{vl}$ is calculated. Table 4-3 summarizes these standard capacities. For voltage levels in between these values, the transmission capacity is interpolated.

Table 4-3. Standard transmission capacities depending on voltage levels based on [200], [201].

vl [kV]	110	220	380	750	1150
$TrCap_{vl}$ [MW]	343	520	1790	5404	13750

5. Last, the model requires a security constraint to avoid using the total capacity and ensure an n-1 secure system. This margin is set to 70% based on the experience in the German grid development plan [202].

According to the described developments, the final maximum capacity between two regions $Trp_{2015,elec,cr_i,cr_j}$ is calculated by multiplying the number of circuits of each voltage level with the respective standard transmission capacities

$$Trp_{2015,elec,cr_i,cr_j} = 0.7 * \sum_{vl} TrCap_{vl} * Nci_{cr_i,cr_j,vl}. \quad (4.20)$$

This formula summarizes the process calculate the capacity between all clustered regions which are direct neighbors. The resulting capacity matrix represents the current system in the base year 2015. In the two other years, 2030 and 2045, the transfer capacity of a connection can be increased by expanding it. To calculate the utilization and potential expansions in the model, the calculation of the transferred capacity additionally requires the length and losses as described in equation (3.6). The definition of this length is the distance between the centers of each regional shape. The losses and cost assumptions for grid expansion, which directly affect the objective function of the optimization problem, are also based on the German grid development plan [203].

An important indicator for evaluating this use case is how the role of a region changes from 2015 to 2045 by the decarbonization process. Therefore, the $Relative\ Regional\ Change_{cr}$ of each clustered region cr is defined by a comparison of energy production $E_{y,te,\mathrm{cr}}$ shares between the years which is defined as follows:

$$Relative\ Regional\ Change_{cr} = \frac{\sum_{te} E_{2045,te,\mathrm{cr}}}{\sum_{te,cr} E_{2045,te,\mathrm{cr}}} - \frac{\sum_{te} E_{2015,te,\mathrm{cr}}}{\sum_{te,cr} E_{2015,te,\mathrm{cr}}}. \quad (4.21)$$

4.3.2. Use case 2: Green Hydrogen Production

Concluding the analysis results, the modeling of green hydrogen production in the developed framework uses the PEM electrolysis and cavern storages. The transport of the produced hydrogen is considered in a post-processing analysis. Furthermore, the modeling of hydrogen globally requires a demand-independent model, which is implemented by a break-even price approach. The general idea and implementation of this approach integrated in the overview of modeled technologies (see Figure 2-3), is visualized in Figure D-14.

The overall model remains equal with the same set of technologies and especially the same decarbonization target of 80%. In addition to the already described option of re-electrifying green hydrogen in a turbine, this use case includes the second option of directly selling the produced hydrogen. The selling process is modeled in break-even price scenarios. As soon as the price in one scenario becomes attractive for green hydrogen production, the model expands wind, PV, and electrolyzer capacities. These three components, potentially even in combination with H_2 storage, can provide green hydrogen to be sold next to the ongoing decarbonization process. The expansion of H_2 production is thereby mainly limited by three factors: the overall decarbonization target, the economic feasibility of expanding the infrastructure for a given price, and the VRES limits for annual expansion and area restrictions in multi-region models. These area restrictions prevent the infrastructure from being built in a region with good potential but without sufficient area to locate the units. Allowing only renewable electricity from wind and PV to power the electrolyzer ensures a carbon-free hydrogen production.

For the presented approach, the modeled H_2 Price scenarios are an important input. The selection of prices must reflect a range of expected future costs down to current H_2 costs by SMR production to

show target prices for competitive green hydrogen production. A literature analysis determines this price range by hydrogen studies until 2030 and 2050 [22], [121], [127]-[129], [204]-[209]. To enable a comparison between different assumptions in these studies and avoid outdated cost assumptions, one dataset scrapes together all available assumptions. For the final evaluation, these values are aligned by the same investment and operation costs of electrolyzers, the same rate of currency conversion, and a CO_2 price of 15 €/t for SMR production. Furthermore, the costs are summarized for three categories: SMR production, electrolysis, and costs at fuel stations. The distribution of costs is shown in Figure 4-4.

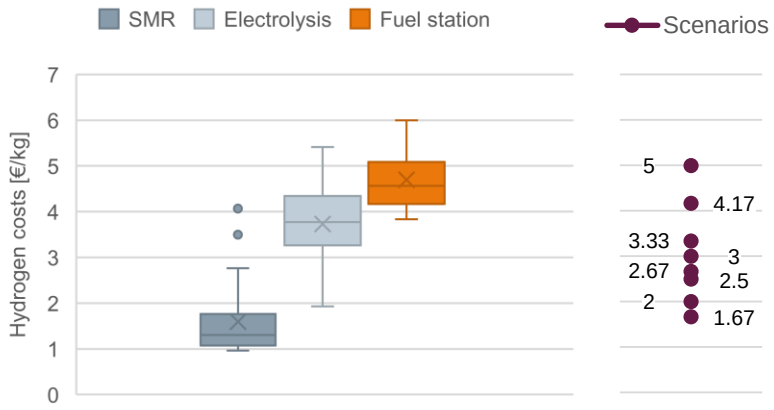

Figure 4-4. Hydrogen costs in €/kg for electrolysis, SMR, and at the fuel station based on a literature analysis (left) to derive different scenarios of break-even prices (right).

The resulting prices demonstrate that SMR is the cheapest technology to produce hydrogen, especially with the applied CO_2 price. These costs represent the lower boundary of price scenarios and define the target costs for green hydrogen production. It is set to 1.67 €/kg, which signifies the average SMR costs. The costs for hydrogen produced by electrolysis vary in a considerable interval between 2 €/kg and 6 €/kg with an accumulation between 3 €/kg and 4.5 €/kg. The upper boundary of evaluated scenarios is set to 5 €/kg to represent this entire interval. However, considering the distribution of costs in the studies and the assumption of falling costs until 2045, fewer scenarios are computed in the upper boundaries and more in the range between 1.67 €/kg and 3.3 €/kg. The costs of fuel stations show that it is essential for a holistic analysis to consider the infrastructure costs addressed by a post-processing calculation. For the defined price scenarios P_{H2}, the green hydrogen break-even price of an archetype at is defined as the lowest price p_{H2} for which hydrogen $E_{H2\,sold,y,at}$ amounting to 10% of the electricity demand $D_{y,at}$ is sold:

$$Break-even\ price_{at} = \min_{P_{H2}} p_{H2} : E_{H2\,sold,y,at} = 0.1 * D_{y,at}. \quad (4.22)$$

In the base scenario, the boundary of 10% ensures to find a comparable basis for all archetypes. The same equation also calculates the break-even price for a country co or a clustered region cr.

Modeling the infrastructure and transportation of hydrogen depends strongly on the transported distance. In the case of the implemented framework, one benefit is the comparison of regional break-even prices to archetype or country break-even prices of another country. This comparison indicates whether it might be economical for countries to import hydrogen from another country rather than producing it themselves. For the calculation, several costs must be considered depending on the type of transportation selected. This type depends on the distance between the countries. According to the *IEA* report *"The future of hydrogen"*, the two long-distance transportation options for hydrogen are pipelines and ships [22]. Trucks are most economical for the local distribution and therefore neglected for long-distance transmission. Pipelines transport gaseous hydrogen and require compressors which

increases costs for longer distances. By contrast, ships transport liquid hydrogen. Therefore, a liquefaction process converts the hydrogen before loading the ship. The overall costs increase with the transported distance since more ships and fuel expenditures are required. Comparing both options, ships become more economical for longer distances as the cost increase per additional kilometer is lower than the increase by additional compressors for pipelines.

The exemplary calculation of transportation costs between two countries requires three steps: (1) selecting transportation options based on the distance, (2) determining all required processes such as storage or potential liquefaction, and (3) calculating the transportation costs for the principal transportation mean. The costs are determined by a literature review of different transportation evaluations. The final distribution costs for the transport from the import/production site to the demand are not considered since they are necessary for both options. The distribution of hydrogen from a harbor or the preferred production location is assumed similar and not part of the analysis.

Overall, essential inputs from the modeling results are the suitable type of transportation, the distance between the two compared countries, and the break-even prices in both countries. Furthermore, OSM data can identify existing infrastructure in the best-suited regions for green hydrogen production, such as harbors or existing pipelines, to validate the calculated transportation route.

4.3.3. Use case 3: Coal Phase-Out

Derived from the analysis, the coal phase-out use case requires evaluating drivers and substituting technologies from a global to a regional level. Furthermore, the existing coal infrastructure needs to be evaluated to identify regions that strongly depend on this commodity.

For the evaluation of drivers, the coal phase-out in the 80% decarbonization scenario is compared across different archetypes currently depending on coal. These results show how existing coal capacities are phased-out in different archetypes. Analyzing countries and later regions deepens this global view and examines the developed hypotheses on a more detailed level.

To enable a regionally resolved evaluation, the existing infrastructure must be analyzed. This analysis identifies coal-dependent regions. The dependency can either come from coal power plants or coal mining. The coal power plants are directly included in the spatial data basis described in chapter 3.2.2. Using this data as an input, the clustering results indicate which regions have a high density of installed coal power plants. The coal mines are detected in two ways. First, the available OSM data can be filtered for the available mines. Therefore, the tags *industrial* = '*mine*', *resource* = '*coal*', and *man_made* = '*mine*' are used. Second, these mines are compared particularly for the selected country researched data. The overlap of both data sets then identifies the clustered regions for which coal mining plays an important role.

Last, the methodological developments included in the first use case, the evaluation of the grid topology, also influence the evaluation of a coal phase-out. The utilizations of connections between clustered regions and the directions of flows indicate the roles of these regions in the country's energy system. The flows and the role of each region can be compared between the base year 2015, which is characterized by significant coal generation, and the two future years 2030 and 2045.

5. Decarbonization Pathways of Archetypes and Use Case Results

The developed framework, depicted in Figure 3-1, is applied to evaluate global challenges in a decarbonization process to reach the COP 21 goals. Figure 5-1 visualizes its application in the following result chapter. After describing the overall scenario framework, the results consist of two steps: first, the 15 archetypes are clustered and their pathways are evaluated in the model. These calculations show general global trends of decarbonization processes. Second, the three use cases, representing trends in a decarbonization process, are analyzed. The use cases apply the entire framework from archetype models down to multi-region clustering and models. Overall, the results have two purposes: they validate the developed framework and the implemented methods while also providing insights about global decarbonization processes from a general global level down to a spatially detailed level.

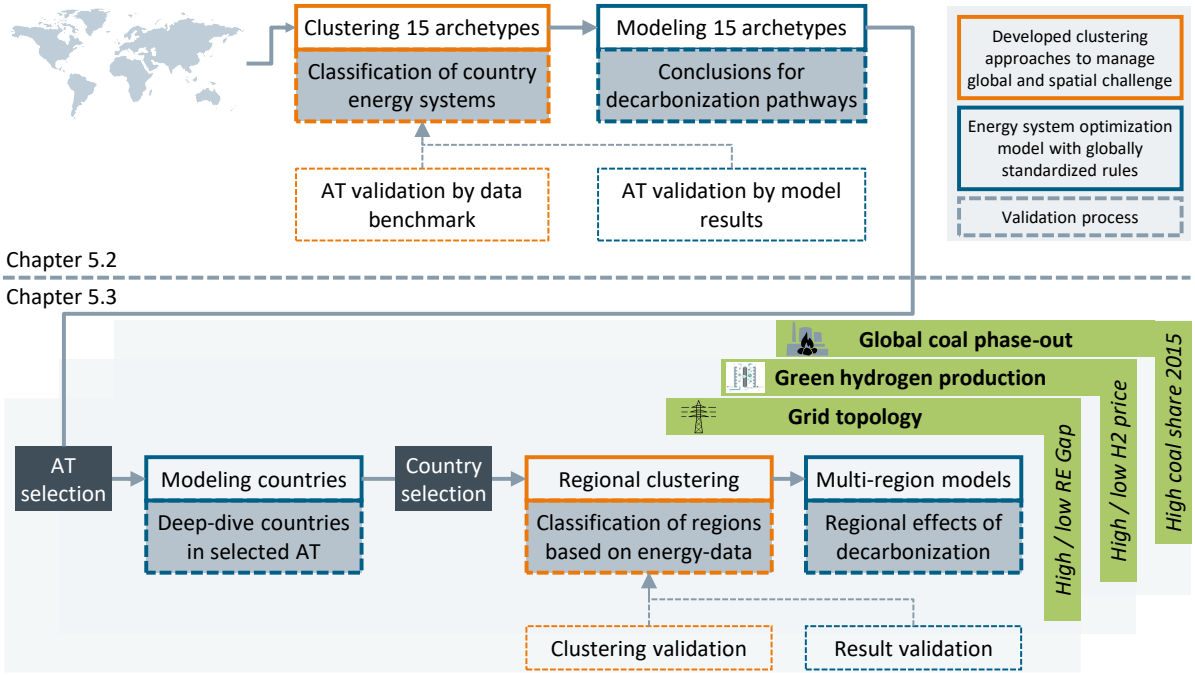

Figure 5-1. Overview of calculated models on different levels in the result chapter.

5.1. General Scenario Framework

Several scenarios evaluate the decarbonization pathways in the following result chapters. To provide an initial overview and explain the context of these scenarios, they are summarized in Table 5-1 by their main characteristics. All scenarios and use cases use the same input parameters for costs, efficiencies, and technical lifetimes. These parameters for resources and technologies are summarized in the appendix in Table B-1 – Table B-3.

Table 5-1. Computed scenarios and their main characteristics.

Scenario name	Base	CO2 Price	Business as usual (BAU)	Grid	H2 Price	H2 – No Cap
Scenario characteristics	80% CO_2 cap until 2045 compared to emissions in 2015 (see equation (3.7))	No Co_2 cap but a CO_2 price of 100 €/t [210]	Cost-optimal energy system until 2045 without any CO_2 limitations	Synthesized grid capacities are reduced by 50%	H_2 prices according to steps defined in chapter 4.3.2	H_2 sales are not capped (see equation (4.22))

The main scenario for all computations is the Base scenario which includes a pathway for 80% decarbonization compared to the computed CO_2 emissions of the electricity sector in 2015. Other scenarios are evaluated in the chronology of the results to contextualize the Base scenario or provide details for the use cases. The CO2 Price scenario represents an alternative way to drive the decarbonization. By contrast, the Business as usual (BAU) scenario shows developments without any emission reduction measures. The other two scenarios refer to the first and second use case. To calculate a sensitivity for the synthesized grid, a Grid scenario is introduced, reducing the determined capacities of the synthesized existing grid $Trp_{2015,elec,cr_i,cr_j}$ by 50%. Furthermore, the hydrogen use case contains several H2 Price scenarios. These scenarios are defined based on the literature research described in Figure 4-4. Additionally, the sensitivity H2 – No Cap evaluates the effect of setting the hydrogen demand to a free optimization limited only by expansion limits or available areas.

5.2. Archetype Results

Following the process in Figure 5-1, the archetype results contain several stages: first, the 15 archetypes resulting from the clustering algorithm described in chapter 4.1 are defined and explained. Second, these archetypes are modeled in the selected energy system model by the defined standardized rules. The results show various global decarbonization pathways since the archetypes represent different types of energy systems. Third, the archetypes and their model results are validated to prove their general applicability, especially for the following use cases.

5.2.1. Archetype Clustering

The archetypes define 15 prototypical energy systems summarizing 141 countries by the data described in Table 3-1. The final result of the clustering process is depicted in Figure 5-2 by visualizing the global distribution of archetypes in a world map.

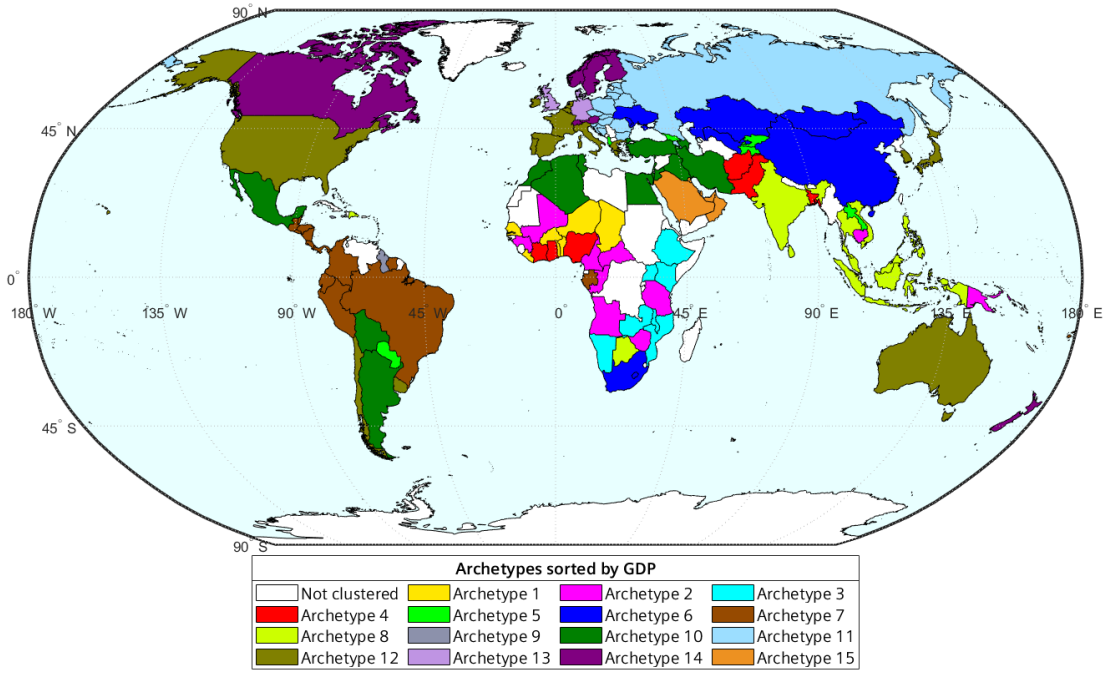

Figure 5-2. Geographic distribution of the 15 archetypes, as published in [177].

At first glance, the distribution of archetypes across the globe directly underlines the idea of this approach. Many of the 15 archetypes contain countries located in different geographic regions, continents, or sub-continents. Examples for these distributions are Archetype (AT) 5, 10, or 14. AT 5 contains countries with a low population density but a high share of electricity generation by hydropower. They are characterized by overproduction leading to large electricity exports. AT 10

summarizes countries from South America, Central America, North Africa, and Europe. Many of these countries are emerging economies that currently have a high share of gas power plants and excellent potential for both VRES technologies. The third example, AT 14, characterizes rather cold countries distributed across North America, Northern Europe, and Australia and Oceania. Similar to AT 5, hydropower is the primary electricity generation source and it has a low PV potential. Even though these archetypes contain countries on different continents, their climate and geographic conditions are still comparable.

Table 5-2. Overview of the 15 archetypes, the countries within each archetype, and the major archetype characteristics, as published in [177].

Archetype	Countries (lead country highlighted)	Major characteristics (compared between archetypes)
Archetype 1	Benin, Burkina Faso, Chad, Comoros, **Gambia**, Liberia, Niger, Sao Tome and Principe, Senegal, Togo, Vanuatu	Lowest GDP/capita and HDI, highest average temperature, Lowest electricity consumption/capita, a high dependency on fossil fuels
Archetype 2	Angola, Cambodia, Cameroon, Central African Republic, Republic of the Congo, Guinea, Mali, Papua New Guinea, **Tanzania**, Zimbabwe	Lowest population density, closest to the equator, diverse energy mix (oil, gas, coal, hydropower)
Archetype 3	**Ethiopia**, Kenya, Malawi, Mozambique, Namibia, Uganda, Zambia	2nd highest population growth, lowest urbanization, a high share of hydropower, good solar conditions
Archetype 4	Afghanistan, Bangladesh, Cote d'Ivoire, Ghana, Nigeria, **Pakistan**	High population density, lowest political stability index, renewables only by hydropower (~30%)
Archetype 5	**Albania**, Georgia, Kyrgyzstan, Laos, Paraguay, Tajikistan	Low population density, Highest share of hydropower, highest share of electricity exports
Archetype 6	China, **Kazakhstan**, Moldova, Mongolia, South Africa, Ukraine, Uzbekistan	A high share of hard coal and lignite, high energy intensity, mixed climate (heating/cooling)
Archetype 7	Belize, **Brazil**, Colombia, Costa Rica, Ecuador, El Salvador, Fiji, Gabon, Guatemala, Honduras, Nicaragua, Panama, Peru, Suriname	High precipitation, high shares of geothermal and biomass, coal exploration, a high share of forests
Archetype 8	Botswana, Dominican Republic, **India**, Indonesia, Malaysia, Philippines, Sri Lanka, Thailand, Vietnam	High dependency on coal, a large increase of CO_2 emissions, low share of renewable generation technologies
Archetype 9	Bahamas, Barbados, Cape Verde, Guyana, Jamaica, **Malta**, Mauritius, Saint Kitts and Nevis, Samoa, Seychelles, Tonga	High population density, high impact of coastline (island states), a high share of oil
Archetype 10	Algeria, Argentina, Azerbaijan, Bolivia, Cyprus, Egypt, Iran, Iraq, Israel, Jordan, Lebanon, **Mexico**, Morocco, Tunisia, Turkey	Low precipitation, a high share of gas power plants, good combination of wind and solar capacity factors
Archetype 11	Armenia, Belarus, Bosnia and Herzegovina, Bulgaria, Croatia, Czech Republic, Estonia, Hungary, Latvia, Lithuania, Poland, **Romania**, Russia, Slovakia, Slovenia	Shrinking population, low temperature, the highest share of lignite, an important role of nuclear
Archetype 12	Australia, Belgium, Chile, France, Greece, Ireland, Italy, Japan, Republic of Korea, Luxembourg, Netherlands, Portugal, **Spain**, United States, Uruguay	High urbanization, high shares of installed renewables, high emission intensity, medium solar and good wind conditions
Archetype 13	Denmark, **Germany**, United Kingdom	Highest HDI, highest shares of installed wind and PV, highest wind and lowest PV capacity factor, emission reduction since 1990
Archetype 14	Austria, Canada, Finland, New Zealand, Norway, **Sweden**, Switzerland	Lowest average temperature, the highest share of electric vehicles, highest electricity consumption/capita, a high share of primary energy from renewables, a high share of hydropower and nuclear
Archetype 15	Kuwait, Oman, Qatar, Saudi Arabia, **United Arab Emirates**	Highest GDP/capita, highest energy consumption/capita, high temperature / low precipitation, the highest share of fossil fuels (~100%), second best solar conditions, the highest emission intensity

Globally, the similar latitude of countries within an archetype confirms the influence of climatic and geographic conditions. For countries with a similar socio-economic development and energy system, archetypes can also be focused on one geographic region. Examples of such archetypes are AT 11 and 15. AT 11 summarizes rather cold countries in Eastern Europe with coal and nuclear power plants as the important generation technologies. AT 15 includes countries in the Middle East with a high share of oil and gas power plants, a high oil and gas production, and a high consumption per capita.

Table 5-2 states a list of countries and a short description of the significant characteristics for each archetype. Next to this summary, Table C-1 provides for non-clustered countries the closest archetype. Thereby, these countries can be associated with challenges or technological developments of an archetype. Furthermore, the archetypes can also be used to set up a simplified model for countries without sufficient data since it only needs to be scaled by the population of the desired country.

In Figure 5-2 and Table 5-2, the archetypes are sorted by their GDP per capita to arrange them in an easily comparable order. Next to this economic criterion, the archetypes are globally compared by differentiating their global population and consumption share, their renewable potentials, or the variance of each cluster according to equation (3.19). These three categories are visualized in Appendix C. The comparison of the global shares, depicted in Figure C-1, shows that the 141 countries and the 15 archetypes cover 93% of the global population and 97% of the global consumption. The relation of these two criteria underlines that archetypes with lower economic development have a lower share of electricity consumption compared to their population share. AT 8 and 12 are examples of this difference. While AT 8 represents 26% of the global population, it only accounts for 8% of the global electricity consumption. By contrast, AT 12 represents 10% of the population with 33% of the global consumption. Besides, the wind and PV potentials across the archetypes, depicted in Figure C-2, vary between favoring either wind or solar. Some archetypes even show good conditions in both. These characteristics are important since VRES play a vital role in the global decarbonization processes. Last, the comparison of the variance for each archetype in Figure C-3 underlines that there are no significant outliers. The interval of variances is well distributed between 0.75 and 1.08. Precisely, AT 3 and 10 show the lowest variance while AT 12 is the most diverse. Next to the description of the characteristics, these three evaluations help to understand the evaluation of model results and prepare the archetype validation in the following chapters.

5.2.2. Archetype Model Results

As described in chapter 3.3, the Base scenario is applied to all 15 archetypes for the three years 2015, 2030, and 2045. The evaluations consist of three parts by comparing the base year 2015, analyzing the pathway over 2030 to 2045, and concluding overall trends from comparing the results of all 15 archetypes. The first results, the energy mix of the archetypes in 2015, are depicted in Figure 5-3.

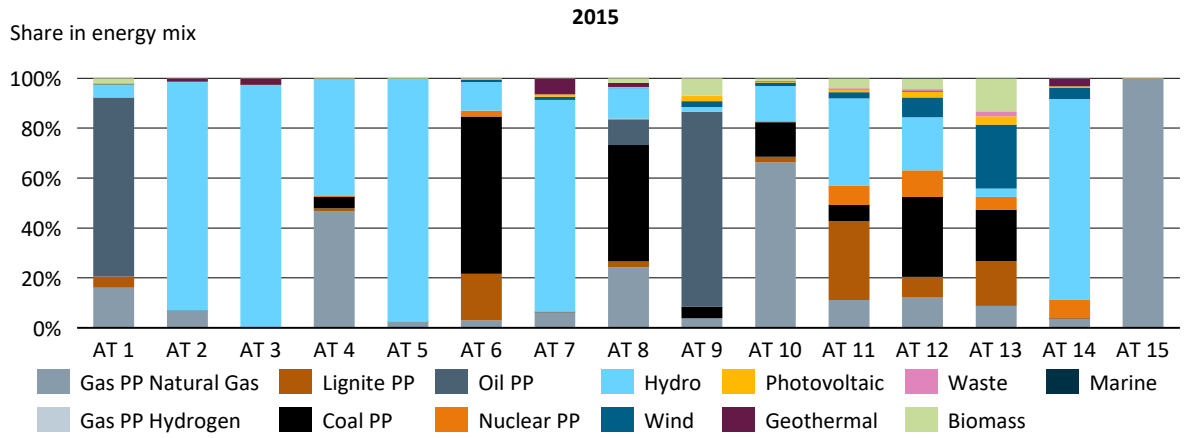

Figure 5-3. Energy mix of the 15 archetypes in 2015.

The computed energy mix confirms the characteristics described in Table 5-2 for all archetypes. For example, AT 2, 3, 4, 5, 7, and 14 are directly visible as archetypes whose electricity system is dominated by hydropower generation. By contrast, AT 10 and 15 are characterized by high shares of gas generation, as described above in the explanation of archetype characteristics. AT 6, 8, 11, 12, and 13 show significant shares of coal generation. Concerning the share of VRES in this early stage, AT 13 has the highest share of wind and solar generation, followed by AT 12. In all other archetypes, these technologies play a minor role in 2015. Overall, the distribution of technologies shows a wide variety and confirms that the energy systems of countries differ in their characteristics. Figure 5-4 visualizes the further developments of all archetypes over 2030 until 2045 in the Base scenario.

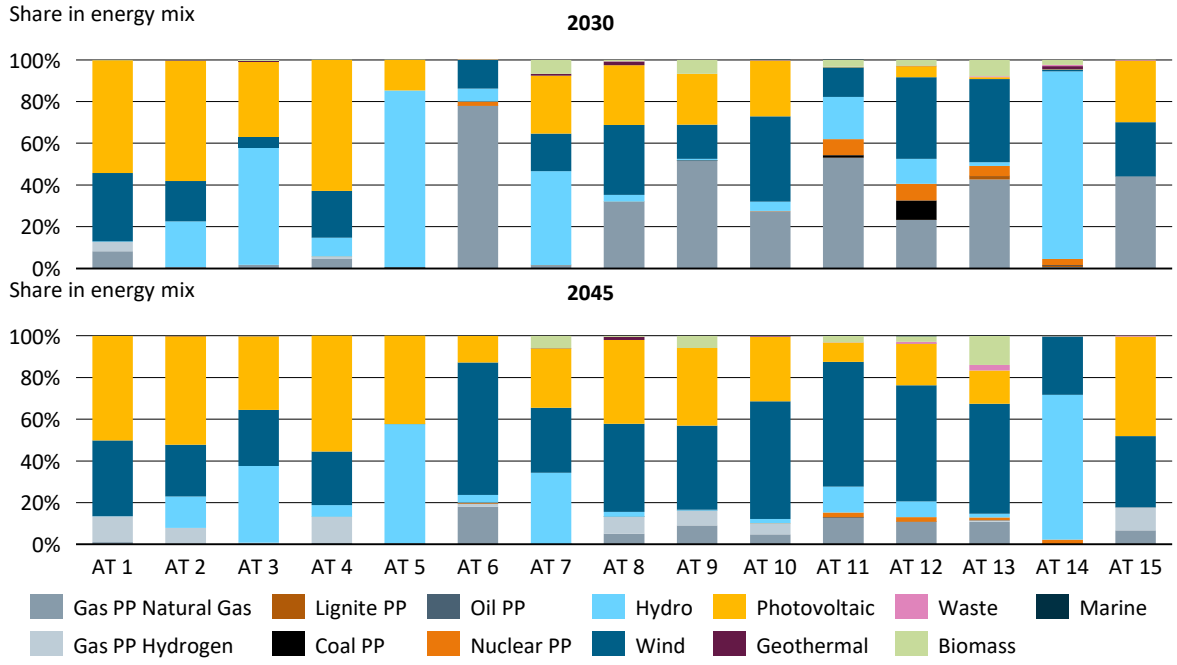

Figure 5-4. Energy mix of 15 archetypes in 2030 and 2045.

In 2030, the technologies within the archetypes show the first changes. Except for AT 12, the four archetypes with high shares of coal generation in 2015 switch to natural gas until 2030. Next to coal and lignite, natural gas also substitutes oil power plants, e.g., in AT 1 and 9. This substitution confirms the described approach of a coal-to-gas shift which can be one solution to reduce emissions in a transition while still keeping flexible generation in the system. In 2045, hydrogen partially supplements natural gas power plants since they can use similar infrastructure and the hydrogen is emission-free. Due to high costs and efficiency losses of electrolyzers, hydrogen becomes economical late and can decarbonize the last percentages. Next to the shift of power plant capacities, all archetypes foresee a substantial increase in VRES generation. Comparing 2030 and 2045, PV becomes more competitive in many archetypes in the second step. In general, all archetypes show a mix of wind and PV generation. The share of wind and PV depends on the archetype characteristics: archetypes with higher PV capacity factors such as AT 2, 4, and 5 favor PV and archetypes with higher wind capacity factors such as AT 11, 13, and 14 wind generation. These correlations are visualized in Figure C-4. In addition to wind and PV, hydropower is still an essential source for emission-free electricity generation in 2045. However, due to rising demands, its share in the energy mix decreases.

Overall, the combination of technologies between the archetypes assimilates during the decarbonization process. While the mix in 2015 shows significant differences between the different archetypes, the development towards an increasing share of just two technologies, wind and PV, leads to very similar systems globally. Even though the shares differentiate and other technologies such as hydropower, gas, or biomass still play a role, VRES are the dominant generation source in 13 out of

the 15 archetypes. The individual developments between the three years for each archetype are also appended in Figure C-5.

Next to these general evaluations of the calculated energy mix, the results are further analyzed to derive conclusions for the role of specific technologies in the global decarbonization process. Based on previous analyses, flexibility plays an essential role in analyzing decarbonized energy systems [177]. Figure 5-5 depicts the shares of technologies providing flexibility compared to the total installed capacity for each archetype.

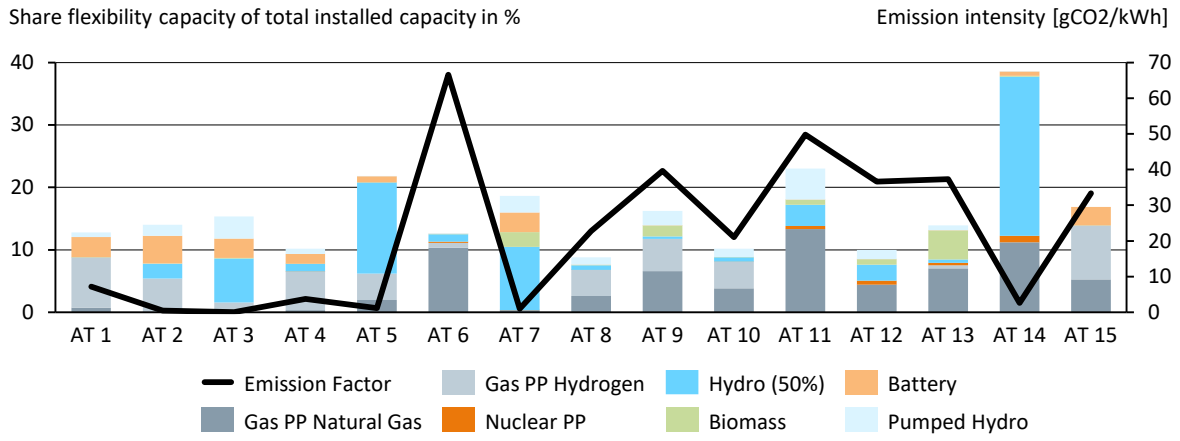

Figure 5-5. Share of flexibility sources compared to total installed capacity in 2045 and the emission intensity in 2015.

The first options for flexibility are gas power plants, nuclear power plants, and the flexible share of hydropower generation. The shares of these technologies are determined by the existing country systems and their emissions in 2015 since these emissions determine the cap for 2045. Therefore, the archetype with the highest emission intensity in 2015, AT 6, can cover almost all its flexibility by gas power plants. By contrast, archetypes with a low emission intensity, such as AT 2 or 3, which also show a high demand growth, require other technologies such as hydrogen. Furthermore, archetypes with high shares of PV generation and lower hydropower or gas shares such as AT 1, 2, 3, 4, 7, and 15 build battery storage to store overcapacities of PV. Due to the physical characteristics, battery storage balances well the day-night cycle of solar generation. An exemplary decarbonization study of a sunbelt region by PV has also shown this relation [211]. Except for AT 8, which is located in tropical regions without seasons and therefore requires less storage [212], all archetypes require a minimum of 10% flexible generation capacities.

Next to the flexibility, the costs of the decarbonization process play an important role. Especially two factors influence the $Specific\ 30-year\ decarbonization\ costs$ of archetypes, described by equation (2.1): the $RE\ Gap$ and the $30-year-Demand\ Growth$ which are defined in equation (2.4) and (2.5). This relation is visualized in Figure 5-6.

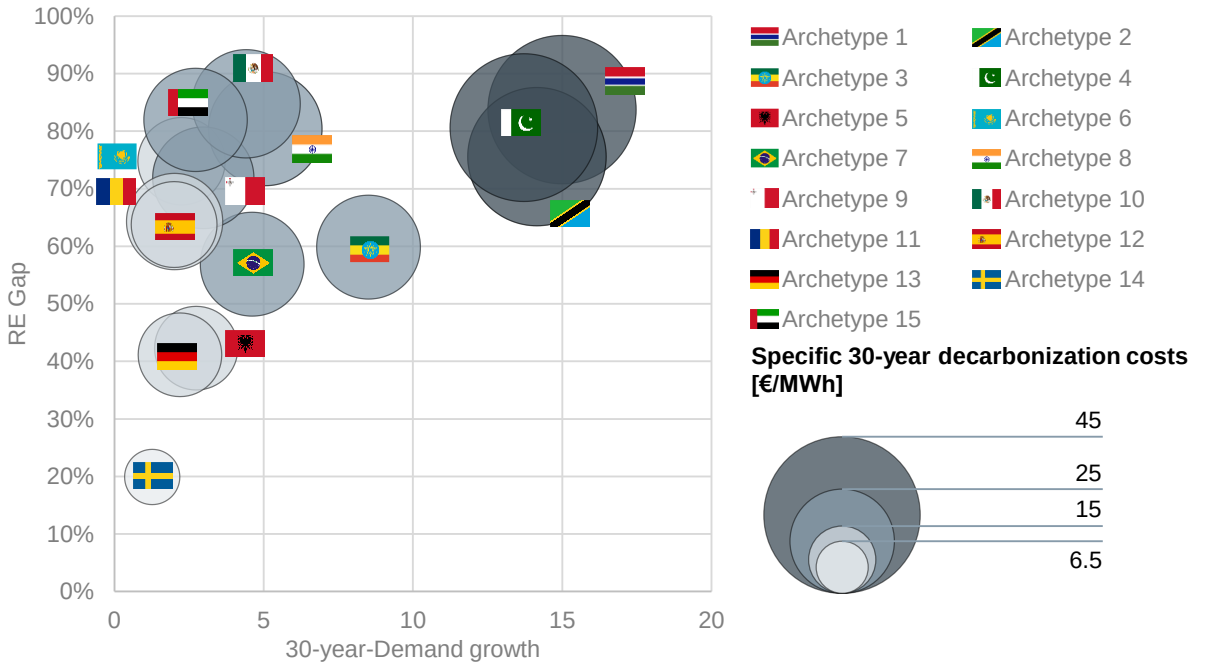

Figure 5-6. *Specific 30 – year decarbonization costs* for the decarbonization pathway of all 15 archetypes concerning their *30 – year – Demand Growth* and their *RE Gap*.

Archetypes with a low ***RE Gap*** and a low ***30 – year – Demand Growth*** show low ***Specific 30 – year decarbonization costs*** for the transformation in an 80% decarbonization scenario. As an example, AT 14 with an ***RE Gap*** of 20% and a demand growth of 25% shows costs of 6.5 €/MWh. By contrast, the demand of AT 1 increases fifteen times from 2015 to 2045 and it has to cover an ***RE Gap*** of 84%. These challenges lead to costs of 46 €/MWh. In general, the 15 archetypes have average ***Specific 30 – year decarbonization costs*** of around 24 €/MWh. AT 10 is very close to this average index with a comparable ***RE Gap*** to AT 1 but a much lower demand growth. The comparison of AT 11 and 12 shows another effect. Both have similar challenges to overcome but differ in their costs since AT 12 shows better VRES conditions and therefore requires fewer investments. Linking the costs and the emission factors, shown in Figure 5-5, countries with low emissions in 2015 often show a high demand increase. They, therefore, need to invest even more in decarbonized and secure electricity generation. The share of investment costs in the ***Specific 30 – year decarbonization costs***, depicted in Figure C-6, proves this effect. The archetypes with a high cost index are characterized by a higher share of CAPEX and lower OPEX. Overall, both figures visualize that a decarbonization process in fast-developing countries is much more cost-intensive than in developed or already decarbonized countries. After these conclusions, the Base scenario is compared in Figure 5-7 to other scenarios described in Table 5-1 to contextualize it.

The Base scenario shows the highest average cost index with 10% higher costs than the CO2 Price and around 40% higher costs than the BAU scenario. As shown in Figure 5-6, the challenges for fast-developing countries, facing a high demand increase, mainly drive these costs. However, the average ***Emission Index***, calculated by equation (2.7), differs strongly between the three scenarios: around four times between Base and CO2 Price and additionally four times between the CO2 Price and BAU scenario. Concluding this context, 40% higher costs of forced decarbonization can significantly reduce the CO_2 emissions of the power sector. A CO_2 price of 100 €/t already leads to a reduction but increases the costs to a similar range as the 80% decarbonization.

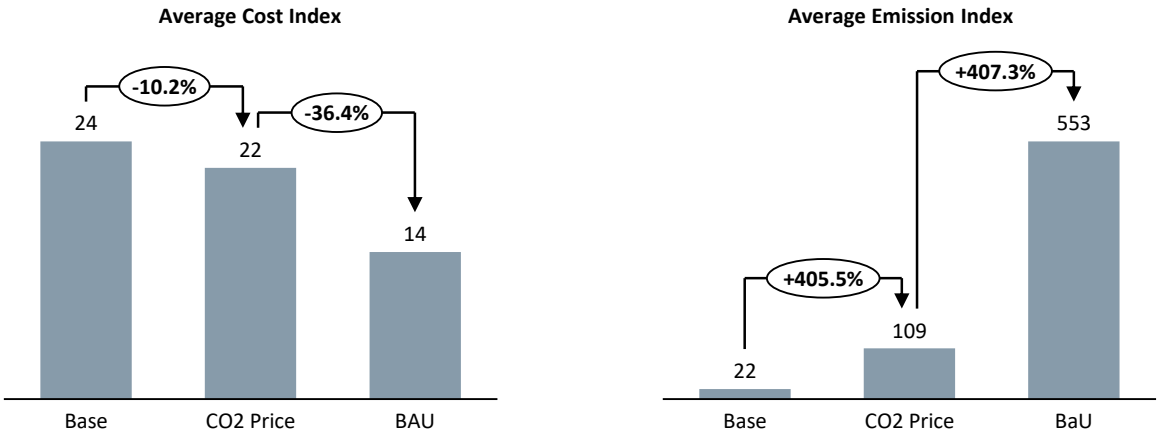

Figure 5-7. Comparison of Base scenario to the CO2 Price and the BAU scenario.

Comparing the archetype results to other global decarbonization studies confirms wind and PV as decisive technologies for the transition. However, the share of these technologies in countries is different based on the selected profiles and cost assumptions. They range from globally strongly wind-dominated systems [42] to strongly solar-dominated systems [43]. The results based on the profiles and price assumptions presented in this thesis include both technologies depending on the country's characteristics, as proven in Figure C-4. The technologies providing flexibility include many frequently mentioned trends such as the coal-to-gas shift, batteries, or hydrogen. Nevertheless, additional sources for flexibility are not considered in the framework, such as demand response, CCUS in combination with more fossil generation, or the flexibility that can be provided by coupling the electricity to other sectors [213].

Furthermore, other studies also highlight the required investments in countries with a lower development status [213]. As mentioned, the Paris Agreement has put in place a clause that these countries receive support from the "advanced economies". Strongly developing countries might leapfrog traditional development steps by new concepts improving and stabilizing the electricity access, e.g., by focusing on small and medium businesses as presented by *Huber et al.* [214]. However, these countries face an additional challenge next to the increasing electricity demand: higher risks in investment policies. These higher risks can lead to more complex financing conditions and to higher costs [213]. Even though not considered in the presented scenario, the model could integrate a country-specific WACC, derived in other studies [79], [80], to quantify these differences.

5.2.3. Archetype Validation

The validation of these archetypes is the last step. Based on the process described in chapter 3.4.1, this validation has two primary goals: first, it verifies that the clustering summarizes countries better than geographic regions. Second, the validation confirms that it is valid in the implemented framework to use the archetype models as a selection filter for the three selected use cases, as shown in Figure 3-1. For these purposes, the validation includes the direct validation of the clustering results and indirectly after the archetype modeling. For all three years, the archetypes are compared to the same number of regions provided by the classification of *UN* subregions, enumerated in Table C-2.

Cluster validation

The direct validation includes the benchmarking of archetypes compared to different geographic classifications. Therefore, the classifications in several global studies are used [38]-[40], [43], [57]. Figure 5-8 compares the variances of these studies to the clustering for the respective number of clusters corresponding to the number of global regions.

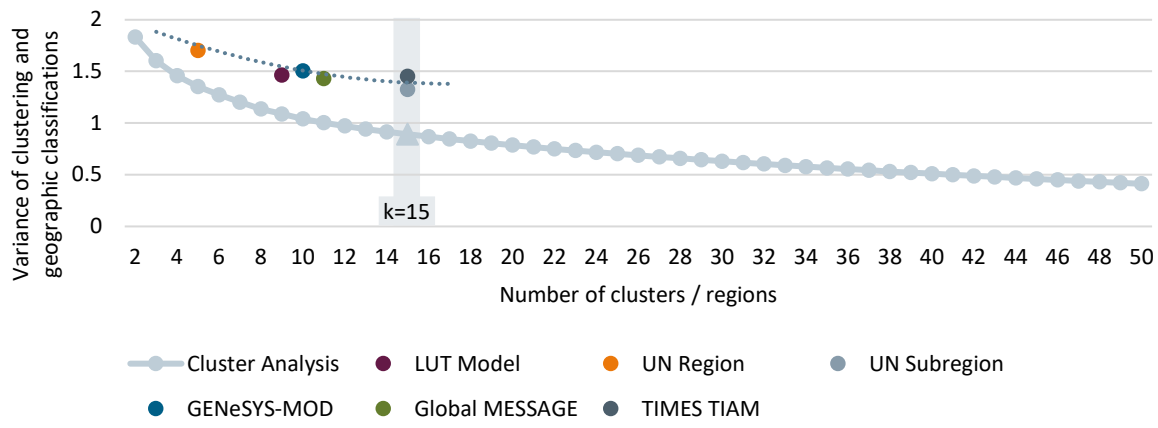

Figure 5-8. Comparison of archetype clustering to other global studies by the using same number of clusters as regions.

The resulting benchmark index, calculated according to equation (3.23), indicates that the clustering is on average 30% better than the global classifications. This benchmark index increases with the number of clusters or regions shown by the increasing gap in Figure 5-8. For the selected number of 15 archetypes, the clustering is 39% better than the TIMES TIAM classification [40] and 33% better than the classification in *UN* subregions [57]. In comparison to the five global *UN* regions, the improvement only amounts to 21%. Overall, this comparison proves that the implemented K-means algorithm classifies countries better for the selected data categories than a classification based on geographic regions.

Result interpretation

The clustering results are interpreted by evaluating the archetypes after the application in the energy system model. For this purpose, all 141 countries are modeled by the standardized rules. The model results are processed by calculating their MAE and RMSE according to Figure 3-12 and equations (3.24)-(3.35). Figure 5-9 compares the errors between all 15 archetypes and 15 subregions, listed in Table 5-2 and Table C-2, for the three evaluated years.

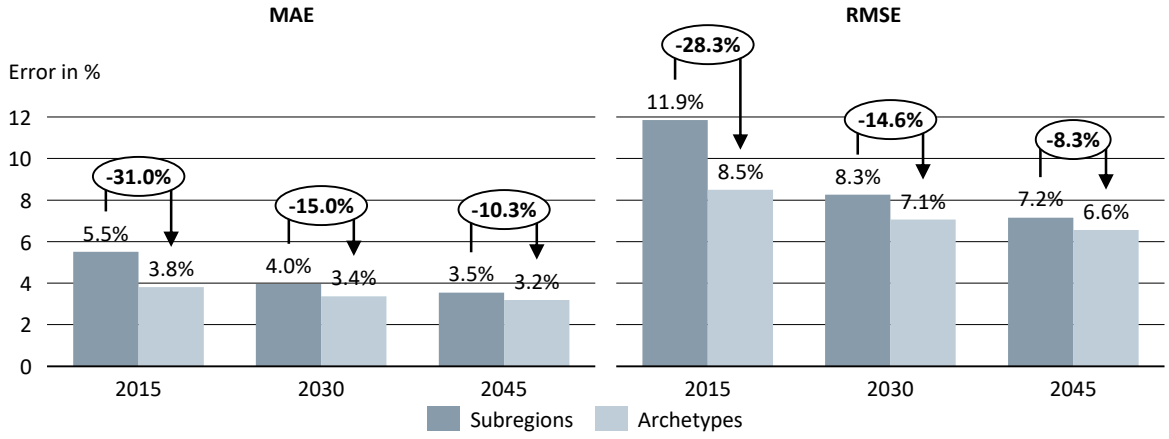

Figure 5-9. Comparison of MAE and RMSE between the geographic classification in 15 subregions and the clustering in 15 archetypes for all three years.

As an overall result of the comparison, for both error types and all three years, the archetypes summarize countries better than a geographic classification even when applying them to an energy system model. Transferring this result to the general idea, energy system archetypes summarize the transformation pathways of countries in an 80% decarbonization scenario better than their representation in geographic regions. After the average Benchmark Index of 30% resulting from the

direct cluster validation in Figure 5-8, this result confirms again the archetypes and justifies their application in an energy system model.

Precisely, the archetype errors are around 30% lower in 2015, around 15% in 2030, and around 10% in 2045. Comparing the MAE and RMSE, these differences are in the same range. The RMSE is by definition higher than the MAE [188]. By squaring the errors, it amplifies outliers in the calculation. The similarity between both types underlines that significant outliers do not affect the errors across all 15 archetypes and subregions. The development of the absolute errors from 2015 until 2045 also confirms the observation derived from Figure 5-4: the systems become more similar by integrating VRES and reducing carbon-intensive technologies. In 2045, the geographic conditions become more important since they strongly influence the wind and PV potential and, thereby, the expansion of VRES. However, this development still does not lead to a preference of geographic regions over the archetypes. Hydropower is exemplary for the better performance of archetypes. It is still essential in 2045, e.g., to provide flexibility, and better considered by archetypes than by geographic regions.

For a detailed analysis, the errors of each region and archetype are evaluated, visualized in Figure C-7 and Figure C-8. In the geographic regions, region 2 shows the highest errors for all three years. It contains four countries with very different systems belonging to AT 5 and 6. Two of these countries are strongly dominated by hydropower generation, while fossil fuels dominate the other two. A relatively high RMSE confirms these outliers. In 2015, other regions with a high error are Sub-Saharan Africa, Western Europe, and Southern Europe, containing many countries or countries with different energy systems. Exemplarily, the countries in Southern Europe belong to four different archetypes. The best performing regions are Northern America and Northern Africa. While Northern America only includes two countries, all countries in Northern Africa are clustered in the same archetype AT 10, which shows their similar energy systems. In 2045, the countries in Australia and Oceania and Southern Asia also become more similar.

Out of the 15 archetypes, AT 5 and 15 are the best performing. As already mentioned in the description of archetypes, AT 5 highlights the advantage of the archetype approach, which is also confirmed by the analysis of region 2 in the geographic regions. In AT 5, globally distributed countries with a high dependency on hydropower, exports of electricity, and a low demand increase are summarized. The second archetype with a low error, AT 15, represents very similar fossil-fuel dependent systems in the base year. They also have similar VRES conditions since they are all located in the same region. By contrast, AT 6, 9, and 11 show higher errors. AT 6 contains coal-dominated countries with different base shares and coal phase-outs. Therefore, it contains outliers shown by the relatively high RMSE compared to the MAE in 2015 and 2030. AT 9 summarizes island states whose systems vary by the type of VRES expanded in 2030 and 2045 since they have different potentials for PV and wind. For AT 11, the difference in the VRES potentials is also significant since, e.g., some countries in southern Europe have good PV potential while other countries in northeast Europe, such as Latvia or Lithuania, have low PV capacity factors.

Overall, the detailed analysis of errors also confirms the archetype approach. For geographic regions with a high error, the archetypes can explain the divergence of energy systems within these regions. An example of this divergence is Central Asia, where two countries are in AT 5 and two in AT 6. Nevertheless, an archetype can still summarize similar energy systems within a geographic region, underlined exemplarily by AT 15. This combination leads to a low overall error since it reflects the status quo energy systems as well as the VRES conditions for future systems. Last, the error results of the archetypes are compared to the variance of the clustering algorithm in Figure C-3. For all 15 archetypes, a slight correlation between these two metrics is observable, e.g., for AT 3 and 4, which show a low variance and a low error. By contrast, AT 6, 9, or 12 have high variances and at the same time a higher MAE. However, this trend is not valid for all archetypes. AT 5 and 15, the best-performing ones in the model, have medium cluster variances. This slight correlation confirms that

the clustering provides a reasonable basis for the energy system model. However, the results are not directly comparable since the model is out of the validity range of the clustering. The clustering is much broader and covers more categories than the ones reflected in the model.

5.3. Application of the Use Cases

According to Figure 5-1, the implemented framework is applied to the three defined use cases by evaluating them from a global level down to spatial details. Therefore, the modeling results are calculated first on the archetype level to identify the relevant archetypes for the individual use case. Afterward, the countries within selected archetypes are analyzed to find relevant countries that are regionally clustered and modeled in multi-region models. The first two models provide a data-driven selection approach to focus on countries without modeling all countries globally. In this chapter, the results for each use case follow the same structure: they are presented by first describing the selection process based on the defined criteria, illustrating the regional characteristics, explaining the multi-region model results, validating the regional clustering, and discussing the overall use case.

5.3.1. Use case 1: Grid Topology

The use case grid topology aims to find countries facing a comparably significant or low challenge of integrating wind and PV. The multi-region model based on the clustered regions provides the basis to identify the respective impact on the grid in two selected countries. Out of the scenarios in Table 5-1, the Base scenario and the Grid scenario are modeled. The Grid scenario, which uses half of the transmission capacities, analyzes whether the results are robust even if capacities are overestimated and amplifies bottlenecks in the existing capacities.

Country selection

For the first step, selecting relevant archetypes, the modeling results in the final year 2045 are evaluated. According to the defined output metrics in the use case description, the *RE Gap*, defined by equation (2.4), is the relevant parameter. Figure 5-10 compares the *RE Gap* of all 15 archetypes.

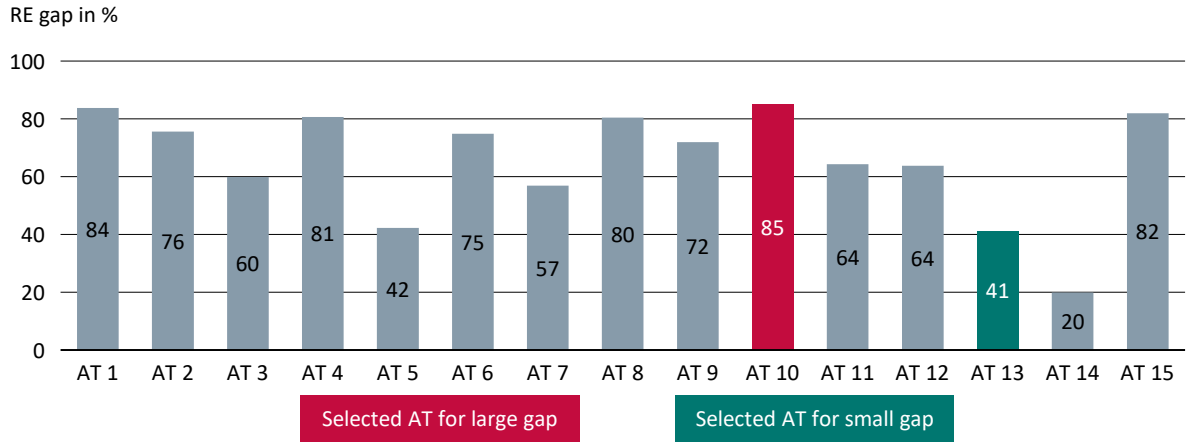

Figure 5-10. Selection of archetypes for the first use case based on their *RE Gap*.

Out of all archetypes, AT 10 shows the largest *RE Gap* with 85%. Besides, AT 10 has good VRES potentials (see Figure C-2). Other archetypes facing a high gap, AT 1, 4, and 8, have worse wind potentials and are therefore not considered. In comparison to AT 15, AT 10 also foresees a stronger demand growth. Considering the described characteristics, AT 10 is selected as the archetype representing a large gap. For the small gap, AT 4, 13, and 14 are analyzed in detail. AT 5 and 14 share their strong dependency on hydropower. Since the use case is especially considering the change evoked by wind and solar, the remaining archetype AT 13 is selected for the small gap.

The next step is the selection of countries within these two archetypes. In AT 10, Morocco faces one of the largest *RE Gap* in comparison to the other countries (see Figure D-7). Two further reasons for the selection of Morocco are its balance between good wind and PV conditions and its ambitious political renewable targets [215]. In AT 13, Denmark has the highest RES share in 2015 and, thereby, the lower *RE Gap* compared to Germany and the UK. In the considered data basis, Denmark also represents the country with the worldwide highest share of RES generation without hydropower [145]. The following two sections present the multi-region model results for these two countries.

Denmark: Multi-region model results

The spatial data basis is aggregated in 99 municipalities which characterize Denmark on the lowest administrative level [75]. In Appendix D, Figure D-5 and Figure D-6 display this aggregation for the considered data categories demand, installed base, and VRES potentials.

The demand structure reflects the distribution of the major cities. Precisely, the household demand is concentrated around Copenhagen, the capital region. The CTSI distribution is more equalized, including other cities with importance for the economy. Especially the cities of Arhus, Odense, and Kolding stand out in the distribution. The latter city is important due to its logistically good location in the country's center where the north-south and east-west connections cross. In contrast to the large demand gap between urban and rural areas, the distribution of the VRES conditions is more balanced. The PV conditions vary little within the country showing just 4% better conditions in the best locations in the northeast and southwest than in the worst locations. In comparison to PV, the wind conditions show a slightly higher variation with 14%. Their best locations are especially along the west coast, decreasing towards the east. Analyzing the potentials in the global context, visualized in Figure 3-4, Denmark shows a very high wind and a relatively low PV potential. Last, most conventional power plants are fueled by coal and located close to the population and industrial centers. Also, onshore and offshore wind farms are already installed without focusing on a particular area.

The smallest administrative regions are in the next step clustered in 13 regions. Even though Denmark's administration currently consists of five major regions, the old classification of 13 "amter" is used. For five regions, the division in four identified islands strongly influences the clustered regions without reflecting the influence of the energy system characteristics. To take advantage of the data-driven classification, it uses the old number of administrative regions in place until 2007. Figure 5-11 visualizes the 13 clusters and their characteristics concerning the different data categories.

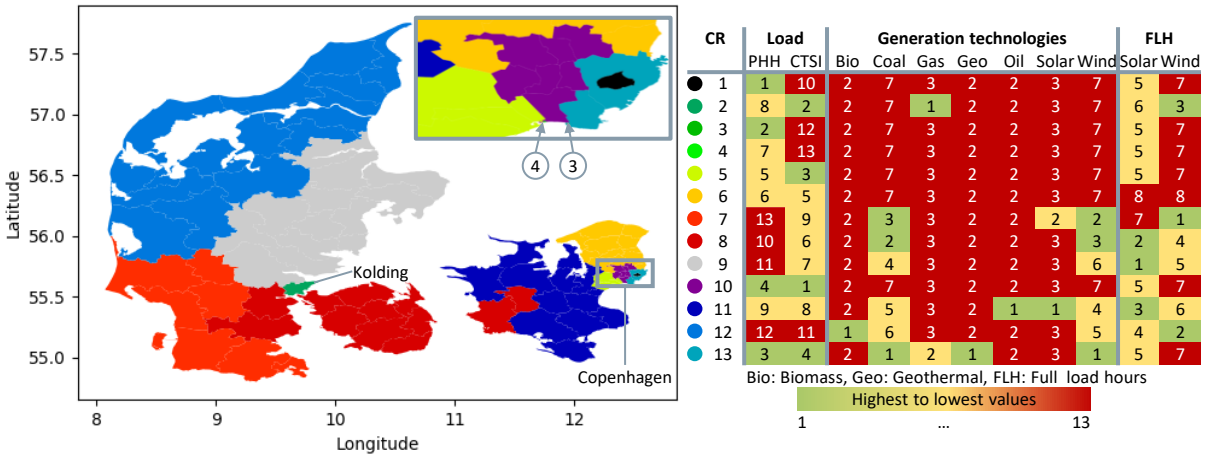

Figure 5-11. Regional clustering results and classification of the cluster characteristics for Denmark by the numbers indicating the highest (1) and lowest (13) values for each category.

The resulting clustered regions (CR) reflect the characteristics of the applied data categories. Six regions are directly close to the Copenhagen area, which all have the same wind and PV conditions.

These regions are CR 1, 3, 4, 5, 10, and 13. CR 1, 3, and 4 are mainly residential areas representing the city center and small areas in the Southern bay of the city. The greater area close to CR 3 and 4 in the southern bay is represented by CR 5, which is rather industrial but without any power plants. CR 10 and 13 are the other two industrial regions around the center. The power plants of the Copenhagen area are located in CR 13, including coal, gas, geothermal, and wind farms. CR 10 shows the highest industrial demand in Denmark. Additionally, CR 6 is north of these areas. It is characterized by the lowest VRES capacity factors, no generation capacities, and medium CTSI and PHH demand. CR 2 includes the region around Kolding, which is already explained in the data description. These mentioned characteristics are confirmed since it has the second highest CTSI demand, including the highest concentration of gas power plants, and a lower PHH demand. The remaining clusters are not concentrated on urban agglomerations and distributed over larger areas. CR 7 and 12 are characterized by low demands but on the other side by the best conditions for wind generation. CR 8 and 9 show lower wind full load hours (FLH) and the best PV potential. The demand and power plants are not outstanding compared to the country with few installed coal and wind capacities and medium or low demands. Figure D-8 compares the resulting clustered regions to Denmark's administrative areas. While the split between the north and south is similar, especially the area around Copenhagen is divided more detailed by the clustering.

The next step of the implemented framework applies these regions in the energy system model according to the schema presented in Figure 3-9. The results of the Base scenario, an 80% decarbonization of the electricity system in Denmark until 2045, are presented in Figure 5-12 for the 13 clustered regions and the three modeled years.

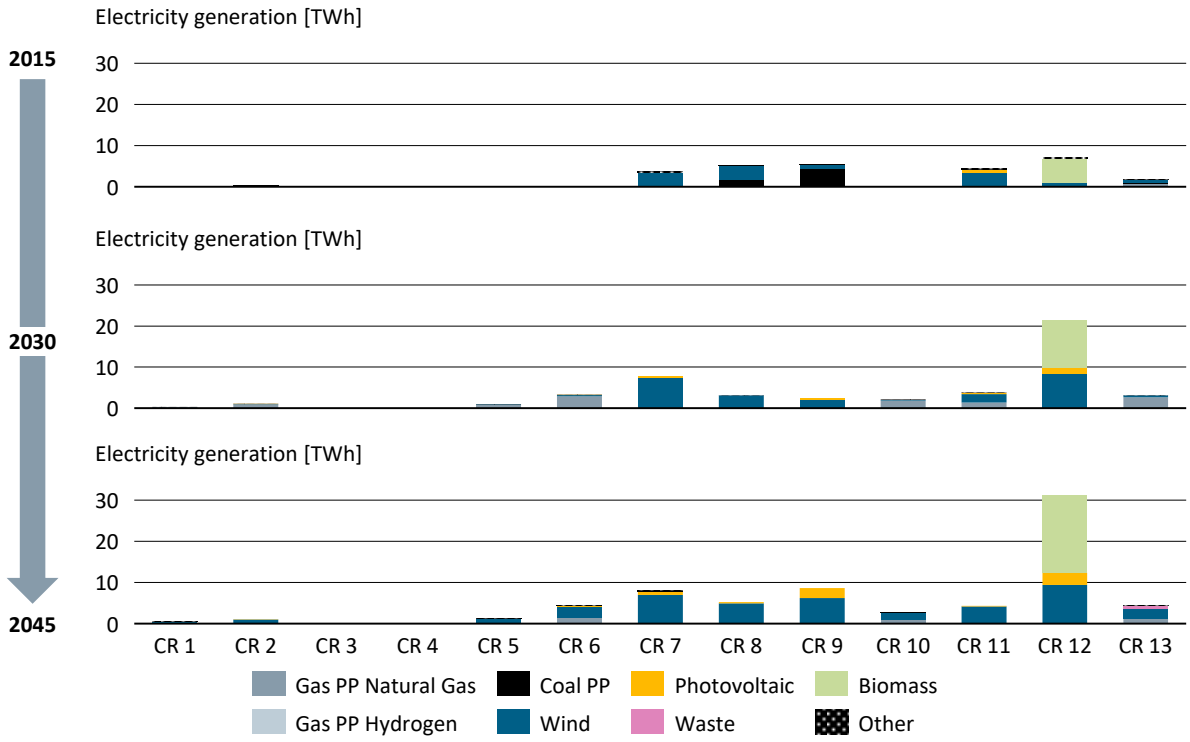

Figure 5-12. Electricity generation of each region in Denmark 2015-2045.

The results of the first year 2015 can be directly linked to the clustering characteristics. CR 8 and 9 are the largest regions and, combined with their high intensity of coal power plants, they show the highest coal generation. The wind generation is distributed to the six regions with existing capacities in Figure 5-11 and CR 13 generates electricity for Copenhagen. The next modeled step, 2030, shows a coal phase-out compensated by gas capacities in CR 6, 10, 11, and 13 and biomass in CR 12. All these regions are close to Copenhagen. Furthermore, wind capacities are expanded, especially in CR 7 and

12, which are the two regions on the west coast with the best wind conditions. In 2045, wind capacities are further expanded in other regions, e.g., CR 8-11. Furthermore, the PV generation supplements the wind generation in CR 7, 9, and 12. For CR 9, the highest FLH reason the PV expansion. CR 7 and 12 have average PV capacity factors, but PV is a suitable addition to the high wind generation. In CR 12, the flexible generation from biomass becomes more significant until 2045. Overall, there are no fundamental shifts and changes for the regions in the transition towards a decarbonized energy system. Even though some regions gain importance, such as CR 7 or 12, regions with a high impact in 2015, e.g., CR 8, 9, 11, and 13, still contribute to the generated electricity in 2045. The change of the regional distribution is further analyzed in Figure 5-13 by evaluating the grid utilization from 2015 until 2045.

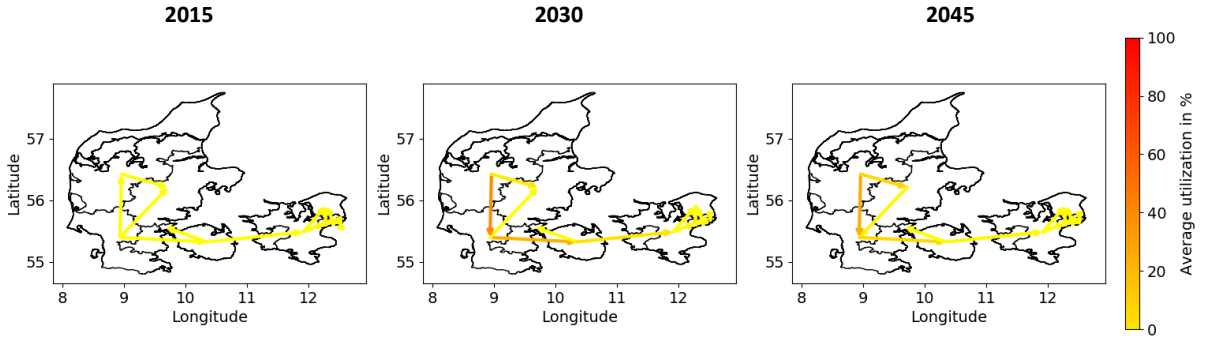

Figure 5-13. Average utilization of grid lines between clustered regions in Denmark for the Base scenario from 2015 until 2045.

For 2015, all lines show a low average grid utilization which confirms the distributed structure of power plants visualized in Figure D-6. The transport pattern shows flow directions from the western to the eastern areas, with the highest demand around Copenhagen. Over the two years 2030 and 2045, only the role of one region, CR 12, changes strongly. Instead of importing electricity from CR 7, it exports electricity to its neighboring regions by increasing the average utilization of the power lines to the range of 50%. Furthermore, these shifts also slightly increase the utilization of east-west lines. The directions of flows do not change in other regions. Overall, the transport patterns in all three years maintain the electricity transmission from the best wind locations in the west to the demand in Copenhagen. To provide further details, the total amounts of transported electricity are depicted in Figure D-9. These total flows confirm the observation of only minor changes in the western regions between 2015 and 2045. To evaluate the robustness of this conclusion, Figure 5-14 compares the results for 2045 to the Grid scenario with reduced grid capacities.

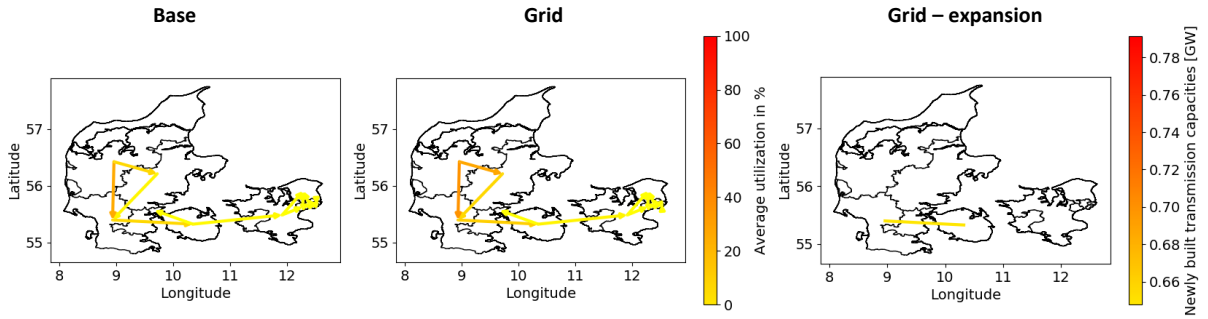

Figure 5-14. Comparison of the Base scenario to the Grid scenario for Denmark in 2045, including grid expansion.

This scenario confirms that even reduced capacities do not lead to a significant change in transport patterns. The only visible effect is the increased utilizations around CR 12. Furthermore, only the capacity of one line requires an expansion of 0.65 GW, which connects the western part of the country with the island around Odense. Summarizing the results of the multi-region model for Denmark, the

decarbonization process changes the energy system topology gradually. It focuses more on the regions with the best wind locations and slightly changes the grid flows around these regions. However, it does not fundamentally change the distributed structure of the country system.

Morocco: Multi-region model results

Morocco contains 399 municipalities on the lowest administrative level. Figure D-10 summarizes the spatial characteristics of these 399 regions for the demand and VRES and Figure D-11 for the power plant distribution. Addressing Morocco's territorial situation, the Western Sahara area is not considered in these evaluations since its official status is not clarified. By analyzing these distributions, the spatial characteristics of the country's energy system can be derived.

The PHH demand distribution reflects the biggest cities in Morocco. The highest demand density is in the area around the three cities Casablanca, Rabat, and Salé, the country's most populated area. Also, Fez, Tangier, Marrakesh, or Agadir are visible by a higher demand density. Similarly, these cities stand out on the CTSI map. The area from Casablanca to Salé shows again the highest demand, followed by Agadir in the southwest. While the first-mentioned area is the most populated one and thereby an important industrial center, the latter area around Agadir is characterized by agriculture and mining activities with an important harbor. Concerning its VRES potentials, Morocco shows a wider variety than Denmark. For PV, regions close to the High Atlas mountain range and the desert southeast of the High Atlas show the highest capacity factors. For wind, the areas at the Atlantic Ocean coastline, in the southwest, and close to the Tunisian border show the best conditions. A lower potential characterizes the central area around the High Atlas. The highest and lowest potentials differ by the factor 4.5, which indicates a large variety. Compared to the global potentials depicted in Figure 3-4, Morocco shows excellent conditions for both VRES technologies. An analysis of the existing power plants indicates that conventional coal, gas, and oil power plants are distributed close to the population and dominant industrial regions, especially in the mentioned area from Casablanca to Salé. Furthermore, in the northwest and northeast of the country, power plants are installed close to the country's borders. Only a few power plants are located in the south, while hydropower plants are primarily inland, close to the mountains. Additionally, first wind farms are installed, especially along the coastline in the west and close to the Strait of Gibraltar.

As the next step, the 399 municipalities are clustered in twelve clustered regions since Morocco is organized in twelve regions on the highest administrative level. The results of this clustering process and the characteristics of each clustered region are summarized in Figure 5-15.

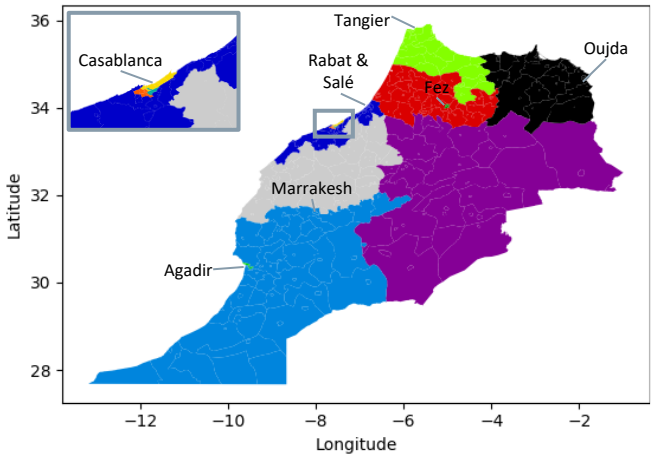

CR	Load		Generation technologies						FLH	
	PHH	CTSI	Coal	Gas	Hyd	Oil	Solar	Wind	Solar	Wind
1	8	7	3	3	6	5	2	4	5	7
2	1	5	4	4	8	5	2	4	6	2
3	2	4	4	4	8	5	2	4	8	5
4	5	2	4	4	8	5	2	4	3	8
5	7	8	4	1	4	4	2	1	10	10
6	4	1	1	4	8	5	2	4	6	2
7	3	3	4	4	8	5	2	4	6	2
8	10	9	4	2	1	1	2	4	9	6
9	11	10	4	4	3	5	2	4	4	1
10	12	12	4	4	2	5	1	3	1	9
11	6	6	2	4	5	2	2	4	7	4
12	9	11	4	4	7	3	2	2	2	3

Hyd: Hydro; FLH: Full load hours

Highest to lowest values

1 ... 12

Figure 5-15. Regional clustering results and classification of the cluster characteristics for Morocco by the numbers indicating the highest (1) and lowest (12) values for each category.

The calculated twelve clusters show an accumulation of four clusters, CR 2, 6, 7, and 11, in the mentioned Casablanca region. CR 11 defines the area around Casablanca and includes Rabat and Salé. It has an average demand, contains some oil power plants, and medium wind and solar conditions. Zooming into the Casablanca region, CR 2, 6, and 7 characterize spatial differences therein. All three show the same VRES conditions with medium PV and high wind FLH. They differentiate by the demand and generation structure: while CR 2 includes more residential areas, CR 7 is more balanced between PHH and CTSI. CR 6 stands out by the countrywide highest CTSI demand and includes coal power plant capacities. Next to the urban area of Casablanca, the clustering detects two other cities as single clusters. The city of Fez defines CR 3 and Agadir CR 4. Fez has a comparably higher PHH demand due to its larger population, while Agadir stands out by its CTSI demand, reflecting the vital role of mining and agriculture. The VRES conditions of the two regions also differ. Fez is characterized by medium wind and low PV capacity factors. Agadir has a high PV potential due to its location in the south but a low wind potential since its bay is covered. Next to these urban clusters, there are six areal clusters. CR 1, 5, and 8 represent the regions located in the north. CR 1 and 5 show a medium demand since they contain cities such as Oujda or Tangier. The neighboring regions CR 5 and 8 have very similar characteristics for the installed capacities since both contain gas, hydropower, and oil power plants. In CR 1, there are coal instead of oil power plants. Due to their location in the north, CR 5 and 8 have low PV and low to medium wind potentials. The PV potential in CR 1 is slightly better being closer to the desert. Last, CR 9, 10, and 12 represent regions in the country's center and south. They are all characterized by comparably low demand and contain hydropower plants. CR 10 includes some installed capacities of PV since it stands out by the countrywide highest PV potential. By contrast, CR 9 and 12 have the highest wind potentials, and, due to their location in the south, also high PV capacity factors. Concluding the twelve clustered regions, they match the observed spatial characteristics and stress out spatial differences. Compared to the administrative regions depicted in Figure D-12, the clustering summarizes aerial areas and highlights demand centers such as Casablanca, Agadir, or Fez.

Consequently, the model determines for Morocco, split into the described clustered regions, the path to an 80% decarbonized system. Figure 5-16 shows the results of each region in this transition.

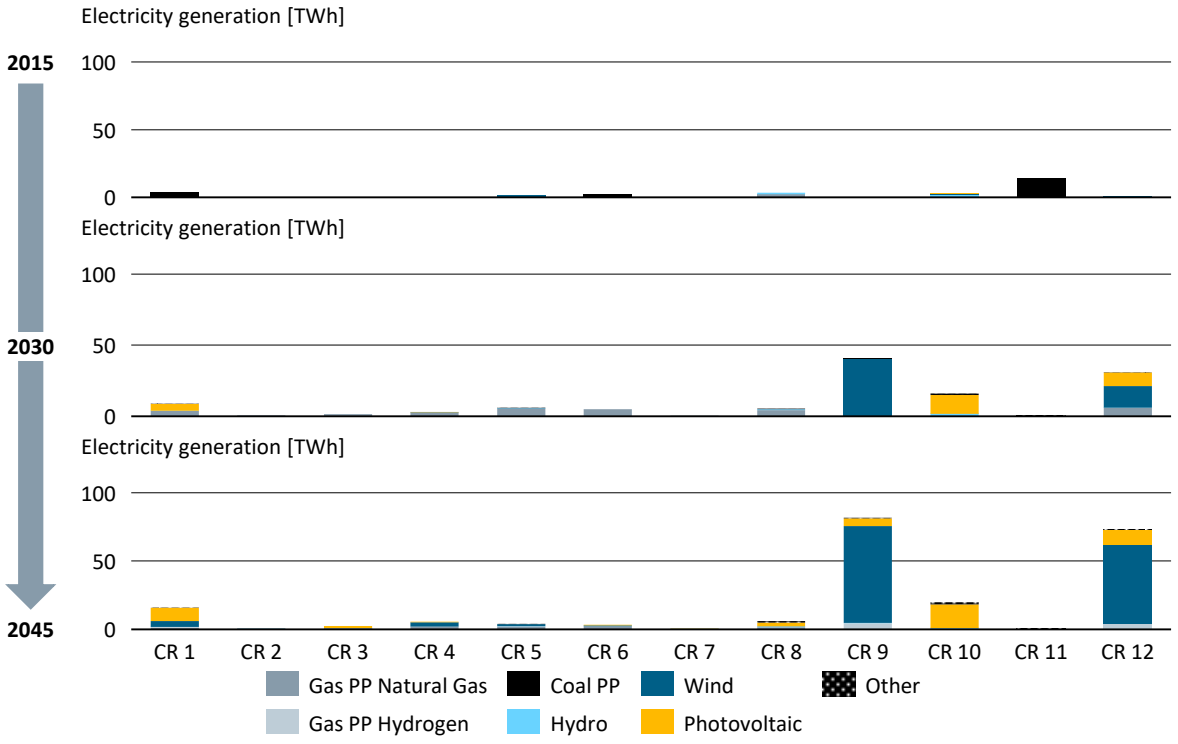

Figure 5-16. Electricity generation of each region in Morocco 2015-2045.

In 2015, electricity generation is mainly dominated by coal and gas power plants. For coal, CR 1, 6, and 11 are the primary regions. CR 11, the region with the highest generation, and CR 6 are close to the demand centers around Casablanca. Besides, CR 8 contributes by gas generation to the electricity mix. The next modeled year step shows several developments: the growing electricity demand increases the overall generation, a coal-to-gas shift substitutes the coal generation by gas power plants to reduce CO_2 emissions, and wind and solar generation become the dominant source. In addition to CR 8, gas power plants are expanded in several regions, such as CR 4, 5, 6, and 11. These regions either have a high electricity demand, a small available area, or medium VRES conditions. CR 1, 10, and 12 show PV generation in 2030. The best potential characterizes CR 10 and 12 while CR 1 uses solar to compensate for the shut-down of coal power plants. Wind generation focuses on two regions with the highest capacity factors, CR 9 and 12. The described developments continue in the target year 2045. Wind and PV are further expanded, particularly in the mentioned regions. As a new technology, hydrogen power plants provide emission-free flexibility. Their installation is focused on regions with high VRES generation, especially with a high share of wind generation, to provide seasonal storage for the variable generation.

Concluding the changes of the twelve regions, the decarbonization pathway leads to a significant shift of different regions. The impact of regions with conventional power plants, especially coal power plants like CR 6 or 11, is lowered until 2045. By contrast, the clustered regions with the best potentials for VRES and large available areas gain importance, such as CR 9, 10, and 12. Figure 5-17 visualizes the impact of these changes on the grid topology and grid flows.

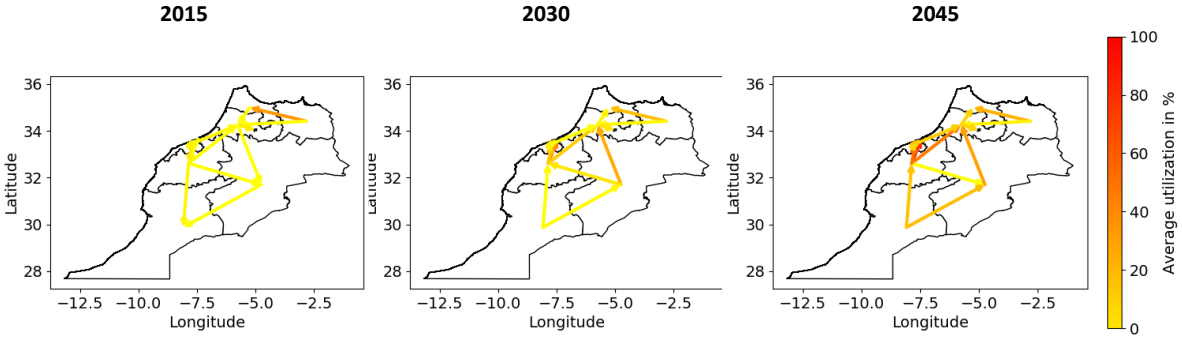

Figure 5-17. Average utilization of grid lines between clustered regions in Morocco for the Base scenario from 2015 until 2045.

The grid utilization in 2015 reflects the structure of power plants concentrated around the demand centers. The electricity flows from the country's center to the regions in the north or south of the country. The only exception is CR 1, which has a high share of generation and transports electricity, e.g., to CR 5. Caused by the regional changes described for the transformation of the power system until 2045, the grid flow and topology also change in this period. Instead of distributing the electricity from the center, it passes from the outer, less populated areas to the center. In this context, especially CR 9, 10, and 12 are important. These regions turn from mainly importing to exporting regions, e.g., towards the Casablanca region. For example, CR 12 changes its role from importing electricity from CR 9 and 10 in 2015 to exporting them with higher utilization of lines in 2030 and 2045. CR 10 also foresees a significant change. In 2015, it imports electricity from the northern and western regions and partially routes it to CR 12. These flows turn around to routing a large amount of wind generation from CR 12 to the north, e.g., around Fez, and even adding electricity generated within the region by high PV installations. These examples underline that many flows turn around by the transformation from demand-dependent located conventional power plants to supply-dependent located VRES. The total flows between the regions, visualized in Figure D-13, support these observations by showing a low amount of transported electricity in the base year and high amounts from the VRES regions in

2045. These changes do not require a grid expansion in the Base scenario, even though some lines around Casablanca show a very high average utilization of around 80%. Modeling the Grid scenario evaluates the sensitivity of these results towards the grid capacities. Figure 5-18 compares its results to the Base scenario.

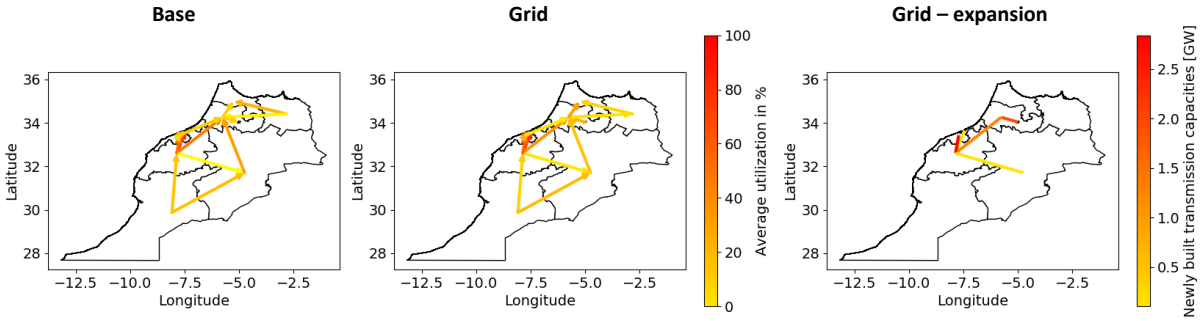

Figure 5-18. Comparison of the Base scenario to the Grid scenario for Morocco in 2045, including grid expansion.

Similarly to Denmark, the reduced capacities do not fundamentally change the grid utilization patterns in Morocco. However, in Morocco, they require expansions of transmission capacities. The lines towards CR 11, which already show a high utilization in the Base scenario, require an expansion of 2.5 GW. Furthermore, two connections for the transmission to the north towards Fez need expansion measures. These expansions underline the fundamental change of regional characteristics in the decarbonization process. Since the generation moves to the best renewable locations, the transported amounts increase and require new lines.

Validation and discussion

The clustering and modeling results need to be validated to classify the quality of the automatically generated models. In general, the clustering approach has one significant advantage: it defines data-driven regions instead of a political, administrative classification for both countries. It thereby stresses out the regional characteristics of the energy system by isolating high demands or summarizing good VRES conditions. Validating the clustering results in detail, both countries show a gap between installed capacities of wind and solar and the capacity factors. In Denmark, the highest wind installations are in CR 13 and in Morocco, in CR 5. In both countries, these clusters have the lowest FLH. For the case of Denmark, this difference results from the proximity to the demand center Copenhagen and a low divergence between the best and worst location within the country. In Morocco, CR 5 is located at the Strait of Gibraltar. A comparison of the clustering results to underlying spatial database confirms the low FLH, while other data sources show an excellent wind potential in this region [216]. In this case, the difference in the data basis is either evoked by the raster size, which combines good locations with less good or the choice of a wind turbine which does not lead to optimal results. Nevertheless, further wind potentials correspond to the external source, e.g., the low FLH in the bay around Agadir [216].

Validating the modeling results as a next step, Figure D-1 compares the model results in the base year 2015 to the actual data for both countries [94]. Overall, the calculated mix of technologies resembles the real values. For both countries, gas generation is under- and coal generation overestimated. The amount of renewable generation matches the accurate results well, indicating sufficient quality of the renewable time series. Besides, the grids are sufficient in 2015 and do not require an expansion, even in the Grid scenario. Analyzing the model results of the grid, the synthetization process of grid capacities seems to overestimate them. Even significant changes and an increasing demand, as observable for Morocco, do not lead to grid expansion in the Base scenario. However, the Grid scenario absorbs the effect of this overestimation. It shows that even lower capacities do not change the model results and indicates which lines are the first ones requiring an expansion. Furthermore, it is essential

to mention in this context that grid expansions might be necessary within the regions since the shift towards VRES mainly requires expansions in lower voltage levels connected to the distribution grid [8]. Additionally, lines with an average utilization of 80%, as observed for Morocco, would probably already be expanded. Operating in this range would require a high share of elements that control the power flow. The interconnections to other countries also play a role without consideration in the scope of these evaluations. These interconnections can affect the placement of generation technologies or transmission capacities. However, the framework itself provides the opportunity to not only focus on one country for a multi-region model but also on several neighboring countries.

The discussion of the use case follows the validation of the clustering and model results. The use case grid topology is based on the hypothesis that countries facing a lower *RE Gap* in their decarbonization process foresee a lower impact on their grid topology. The results of the two selected countries, Denmark and Morocco, confirm this hypothesis. While the flows and roles of regions in Denmark, the example of a low gap, foresee minor changes in the decarbonization process, Morocco's topology changes significantly. Also, Morocco requires a higher expansion of transmission capacity in the Grid scenario. For a detailed evaluation, both countries are compared in Figure 5-19 by the relative changes of each region contributing to the country's electricity generation, defined in equation (4.21).

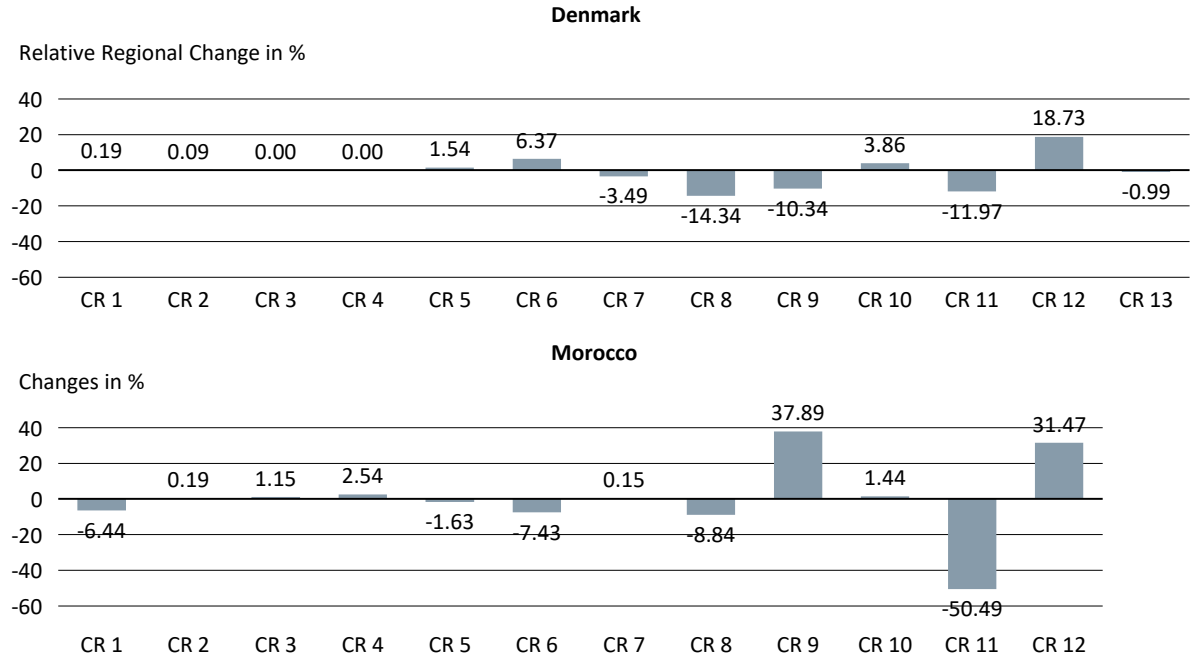

Figure 5-19. Relative changes of the contribution by each region to Denmark's and Morocco's energy mix during the decarbonization process between 2015 and 2045.

The average relative changes of each region account for 5.5% in Denmark and 12.5% in Morocco. These values underline that the roles of regions in Morocco change more than in Denmark. The maximal changes in both countries confirm this result. In Denmark, the maximum changes are in CR 8, 9, 11, and 12, with a relative change between 10% and 20%. In Morocco, CR 9, 11, and 12 show the most extensive changes between 30% and 50%. Overall, six regions in Morocco change more than 5% compared to five in Denmark, even though the number of regions is higher in Denmark.

Concluding the discussion of the general hypothesis, the results are compared to other studies. Concerning the classifications of prototypical countries and their decarbonization challenges by *De Vivero et al.* [61], Denmark is comparable to Germany or Ireland and Morocco to Argentina or Turkey. For Ireland and Germany, the primary challenges are expanding the existing grid or ensuring the technical feasibility in the operation with high VRES shares. By contrast, for Argentina and Turkey,

the grid requires fundamental expansions or completely new capacities to transport the electricity from the best locations to the demand. These results first confirm the classification of archetypes since Denmark is in the same or a similar archetype as Germany and Ireland and Morocco in the same as Argentina and Turkey. It secondly also confirms the *RE Gap* as a decisive selection criterion. Ultimately, it confirms the hypothesis that countries with a large *RE Gap* face bigger challenges with their grid than countries with a small gap.

The effect of grid expansion as a preferred measure to overcome bottlenecks resulting from the additional Grid scenario is also confirmed in other energy system optimization studies. Precisely, two studies that evaluate future scenarios in Germany and Europe show this effect even in a sector-coupled scenario [96], [217]. However, other options such as battery storage could become an attractive alternative in the distribution grid, which is out of scope for the presented models. The role of grid expansion within the clustered regions could be evaluated more in detail by increasing the number of regions to the second administrative level around 50 regions with a lower temporal resolution. Furthermore, the defined model and its results can provide a basis for more detailed grid-related evaluations, such as calculating the distributed flexibility to cope with grid failures as developed by *Kolster et al.* [174] .

5.3.2. Use case 2: Green Hydrogen Production

The second use case analyzes global conditions for green hydrogen production. As described in chapter 4.3.2, a break-even price determines the potential in different energy systems. Comparable to the first use case evaluations, one country with a globally low and one country with a high break-even price is selected, evaluated, and compared in multi-region models. A post-processing step calculates an example for hydrogen transportation opportunities by using different break-even prices. Out of the presented scenarios in Table 5-1, the H2 Price and the H2 – No Cap scenarios are relevant for the following evaluations.

Country selection

For the country selection, all 15 archetypes are modeled for the scenarios defined in Figure 4-4, which offer an H_2 price between 1.67 and 5€/kg. The archetypes are then compared by their break-even prices, as defined in equation (4.22). Since 2045 is the target year of the evaluations, the following result discussion focuses on this year. In Figure 5-20, the break-even prices of all archetypes are compared. In the appendix, Figure D-15 also visualizes these prices on a map to compare these prices globally with other studies and reference the archetype map in Figure 5-2.

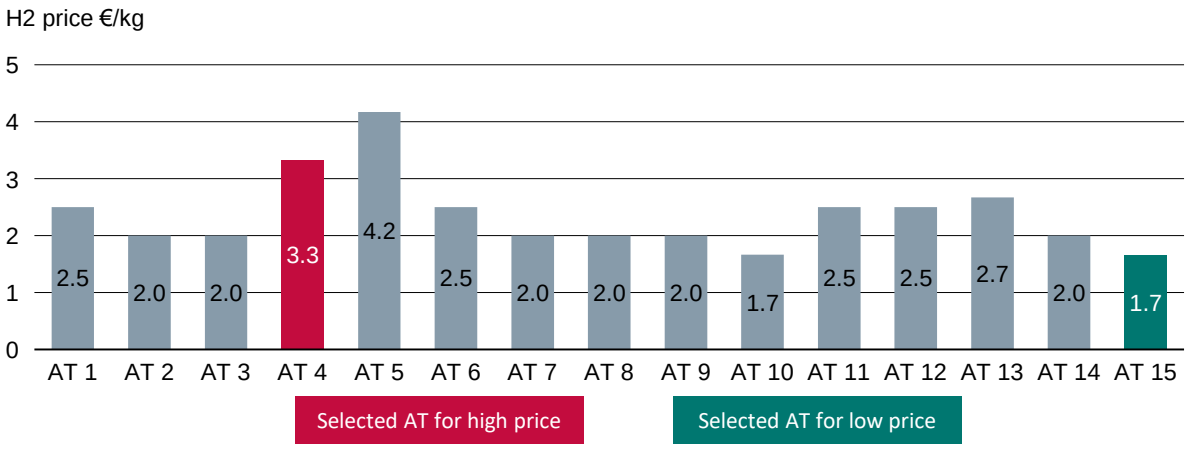

Figure 5-20. Break-even prices of green hydrogen production for all archetypes in 2045.

The results show the highest prices for AT 4 and 5, which are, according to Figure C-2, the two archetypes with the lowest wind and medium PV capacity factors. Comparing these two archetypes, AT 4 is chosen as the example for a high price since AT 5 is dominated by hydropower and therefore does not require a substantial expansion of wind and solar (see Figure 5-6 and Figure C-5). The lowest break-even prices and, thereby, the best conditions for green hydrogen production are in AT 10 and 15. Both archetypes show a combination of good wind and PV conditions. In the context of the use case, AT 15 is selected. It summarizes countries that currently strongly depend on fossil fuels. Therefore, green hydrogen production offers an attractive alternative to use existing knowledge and infrastructures for an emission-free fuel. Furthermore, AT 10 is already evaluated for the first use case in chapter 5.3.1. As the next step, the countries of both selected archetypes are modeled. Figure 5-21 provides the resulting H_2 break-even prices.

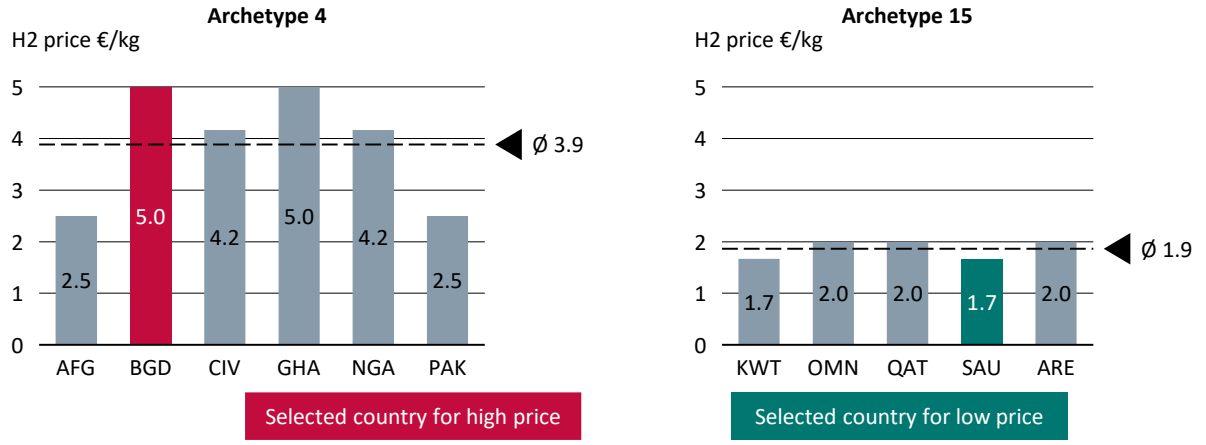

Figure 5-21. Break-even prices of green hydrogen production for all countries in Archetype 4 and 15, indicated by their ISO 3166-1 abbreviation, in 2045.

In general, the comparison of the countries within the two archetypes confirms the trend of the archetype modeling. The average break-even price in AT 4 is much higher than in AT 15. Both average values are slightly higher than the archetype values. Additionally, no country within AT 4 has a lower break-even price than a country within AT 15.

Analyzing the results of AT 4, Afghanistan and Pakistan show the lowest values since they have better wind and PV conditions as well as hydropower supporting the decarbonization process. By contrast, Bangladesh and Ghana have the highest break-even prices. Bangladesh is selected for a detailed evaluation to choose countries on different continents by including an Asian country. In AT 15, the break-even prices show fewer variations. Out of the five countries, the lowest prices are computed for Kuwait and Saudi Arabia. Consequently, Saudi Arabia is selected as it is by far the larger country and economy. Therefore, it has more space, regional differences, and economic power to produce large amounts of green hydrogen. The clustering and multi-region modeling results of the two selected countries, Saudi Arabia and Bangladesh, are explained in the following sections.

Saudi Arabia: Multi-region model results

Saudi Arabia, the country selected as an example for a low break-even price, is divided into 142 municipalities as the lowest administrative area. The spatial characteristics of demand, generation, and VRES potentials are visualized in Figure D-16 and Figure D-17.

Several regions show a high concentration of PHH electricity demand: the highest demand is located around Dammam at the country's east coast, the second-highest opposite at the west coast close to Jeddah and Mecca, and the third-highest around the capital Riyadh in the center of the country. Furthermore, the areas close to the cities Buraydah, northwest of Riyadh, and Jazan, in the country's

far southwest, stand out by their demand. Another important agglomeration within the country, Medina, has a lower demand density since it is part of a larger region on the municipality level. The CTSI demand is distributed similarly to the PHH demand, with the highest demand around Dammam. Another area, North of Dammam, includes Ras Tanura. Both locations are important for Saudi Arabia's oil industry. The map indicates other major demand centers in Riyadh and Jeddah. The PV conditions vary between 1650 and 1850 FLH. The best conditions are located north- and southwest, while the worst are in the east and southeast of the country. This distribution predominantly complements the potentials for wind generation. Their best locations are in the midwest and east, while the worst locations are north and south, especially along the west coast. The FLH range between 500 and 2250 hours per year. According to the global map (see Figure 3-4), the potentials for both technologies are good, for PV within the entire country and wind at the best locations. The power plants are primarily located close to the coastlines, with an accumulation of oil power plants at the west coast close to many refineries and gas power plants at the east coast. In Riyadh, there are capacities of both technologies installed. Oil and gas represent the two technologies covering the vast share of all currently installed power plants in the country.

These 142 regions are in the next step clustered in 13 regions. The number of regions is equal to the 13 political regions which divide Saudi Arabia [75]. The clustering results and characteristics of each cluster are summarized in Figure 5-22.

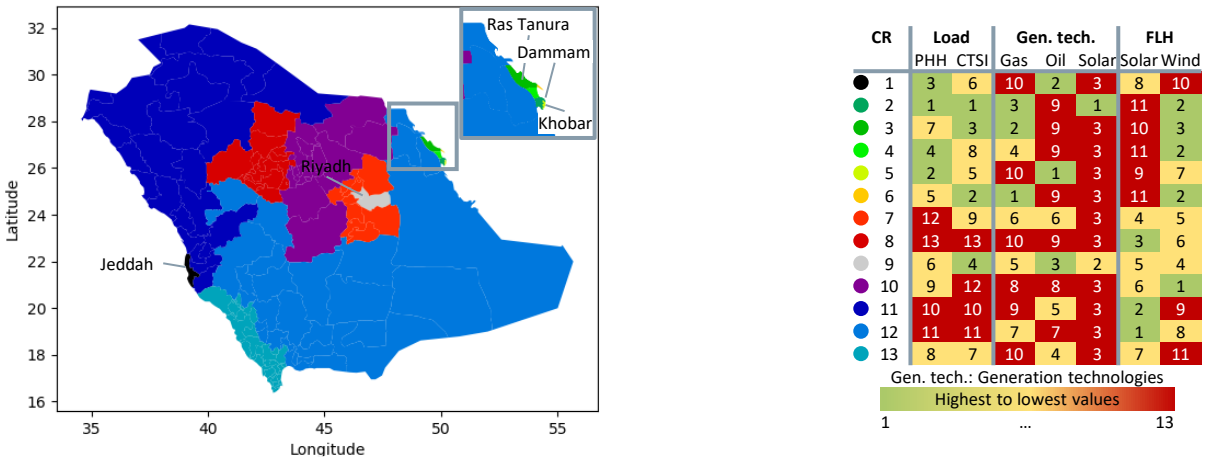

CR	Load		Gen. tech.			FLH	
	PHH	CTSI	Gas	Oil	Solar	Solar	Wind
1	3	6	10	2	3	8	10
2	1	1	3	9	1	11	2
3	7	3	2	9	3	10	3
4	4	8	4	9	3	11	2
5	2	5	10	1	3	9	7
6	5	2	1	9	3	11	2
7	12	9	6	6	3	4	5
8	13	13	10	9	3	3	6
9	6	4	5	3	2	5	4
10	9	12	8	8	3	6	1
11	10	10	9	5	3	2	9
12	11	11	7	7	3	1	8
13	8	7	10	4	3	7	11

Gen. tech.: Generation technologies
Highest to lowest values
1 ... 13

Figure 5-22. Regional clustering results and classification of the cluster characteristics for Saudi Arabia by the numbers indicating the highest (1) and lowest (13) values for each category.

CR 1 represents the region around Jeddah with a high PHH and CTSI demand, e.g., by refineries, oil power plants to serve the demand, medium PV conditions, and low wind FLH. CR 2-6 represent the area around Dammam and Ras Tanura and are also characterized by high demand. Within these clusters, CR 2 is the city of Dammam and CR 3 and 6 are around Ras Tanura. These three clusters show relatively higher CTSI demands signifying their industrial character. Additionally, Dammam has the highest PHH demand. By contrast, CR 2 and 4 represent regions between the two industrial cities with relatively higher PHH demands. The last region in this area, CR 5, represents the city Khobar which includes beach areas. All these clustered regions contain a high concentration of gas capacities except for CR 5, where oil is the dominant fuel. They are characterized by high wind and low PV capacity factors. The third set of urban areas, located around Riyadh, is represented by CR 7 and 9. CR 9 includes the city's demand and CR 7 the surrounding areas with rather industrial demands. Both regions contain oil and gas power plants. Their PV and wind conditions are ranked medium compared to the other regions. CR 8, 10, and 11 represent rural areas north of the country without significant load and generation. CR 11 is an exception containing some oil power plants of remote cities. These regions cover large areas of the country and differ in their VRES conditions: while CR 11 shows good PV and CR 10 the best wind potentials, CR 8 has good potentials for both technologies.

Last, CR 12 and 13 represent the other part of aerial clustered regions located in the south. CR 12 covers a large area without significant load, with few gas power plants, but with the best PV potential. CR 13 represents the coastline in the southwest with medium demand, oil power plants, medium PV FLH, and the worst wind conditions. Compared to the 13 administrative regions, shown in Figure D-18, the clustered regions cover larger areas and highlight demand centers while the administrative regions are distributed more equally.

For the second use case, the next step is to model Saudi Arabia's pathway of 80% decarbonization by resolving the country in the 13 clustered regions. Figure 5-23 compares the electricity mix and contribution of each region for the three years.

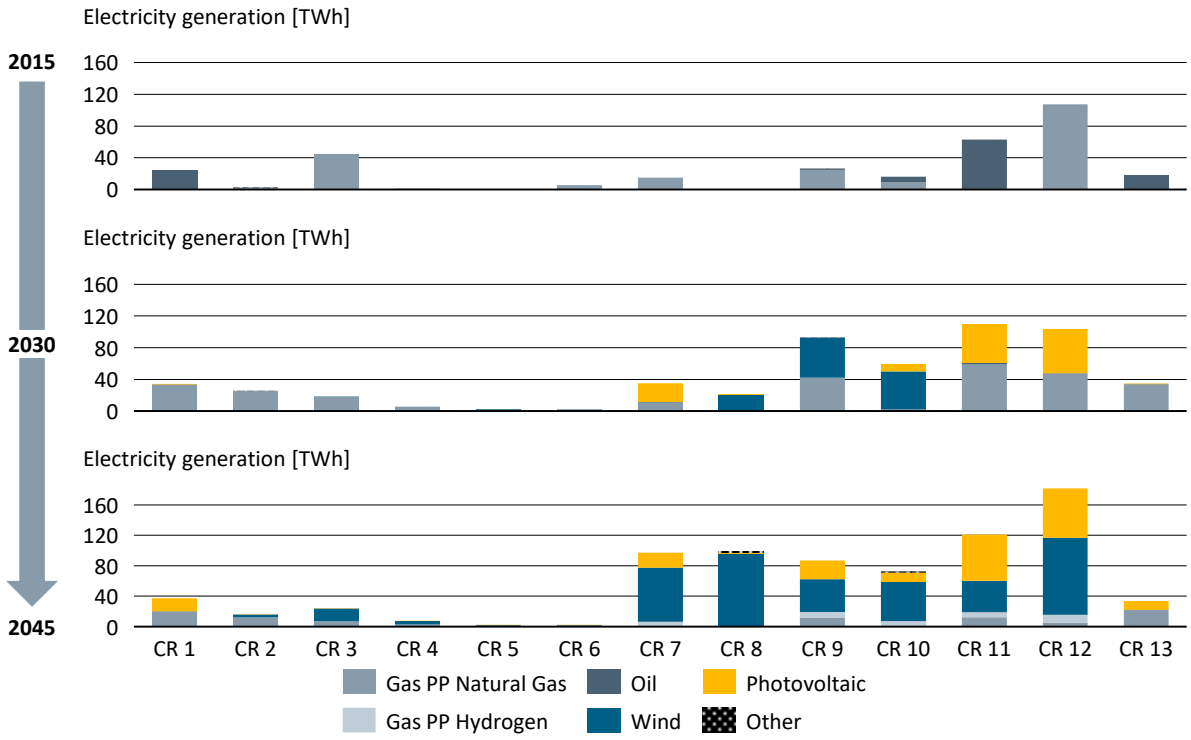

Figure 5-23. Electricity generation of each region in Saudi Arabia 2015-2045.

In 2015, the regions CR 3, 7, 9, and 12 are the major regions generating electricity by gas power plants and CR 1, 11, and 13 the major regions for oil power plants. This distribution represents the split between the east and west, mentioned in the description of the spatial details. CR 11 and 12 have a high amount of generated electricity since they cover a vast share of the country's area. In 2030 and 2045, the generation shifts towards wind and PV. CR 11 and 12 are the dominating regions for both technologies. In the Base scenario, CR 9, 11, and 12 also produce hydrogen to provide flexibility to the electricity system. In CR 1-6 and CR 13, the model expands almost no capacities since these regions have low capacity factors and less available space for VRES expansions. These results reflect the characteristics of the clusters by building VRES in the aerial regions and considering the potentials such as high PV FLH in CR 7, 11, or 12 and high wind FLH in CR 10, 9, 7, or 8.

For validation purposes, the electricity mix and the break-even price are calculated for the multi-region model and compared to the results of Saudi Arabia resolved in one single node. Figure D-19 visualizes these two indicators. Both models calculate the same break-even prices and similar electricity mixes, even for the VRES technologies. This result validates the link between the second selection level, the country modeling, and the multi-region model. Based on this validation, the results for each region are evaluated in detail. Therefore, Figure 5-24 shows the respective break-even price in each clustered region and the share of sold hydrogen of each region compared to the entire country.

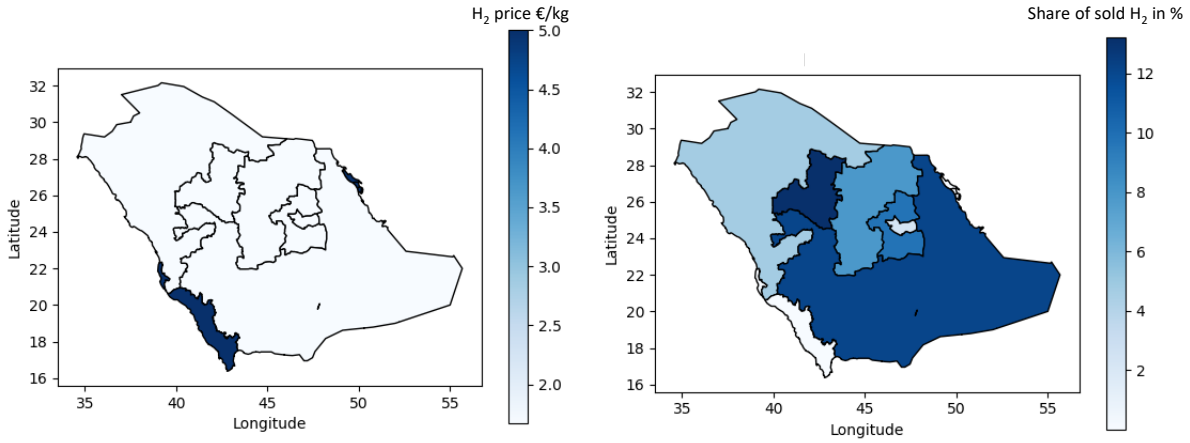

Figure 5-24. Regional break-even prices for green hydrogen production and shares of sold hydrogen in Saudi Arabia.

Overall, the distribution of break-even prices confirms the suitable conditions for H_2 production. In the six regions, CR 7-12, hydrogen is attractive for the lowest scenario of 1.67 €/kg. Most of these regions are aerial regions. However, even in the Riyadh region, CR 9, a low share of the produced hydrogen is sold. CR 13 is not attractive since its VRES potential is among the lowest in the country. CR 1-6 show only good potentials for one of the technologies and have only limited areas available since they all represent very dense urban areas. The results are comparable to the generation mix in 2045, depicted in Figure 5-23, in which the electricity generation also stands out in CR 7-12. The second map, which contains the produced shares, visualizes that CR 7, 8, and 12 produce the most considerable amounts of hydrogen. CR 7 and 8 are smaller but characterized by a good combination of wind and PV FLH. CR 12 has the best PV conditions and much available space. The contribution of the second extensive region, CR 11, is much lower because of lower wind capacity factors.

All these results assume that the sellable amount of hydrogen is capped to 10% of the electricity demand in 2045, accounting for 2.1 Mt H_2 in Saudi Arabia. Furthermore, the available prices are limited to the globally comparable range defined in Figure 4-4. To determine the lowest possible break-even price and the producible hydrogen for each price, the H2 – No Cap scenario lifts this cap. The results in Figure 5-25 compare the produced H_2 amount for different prices.

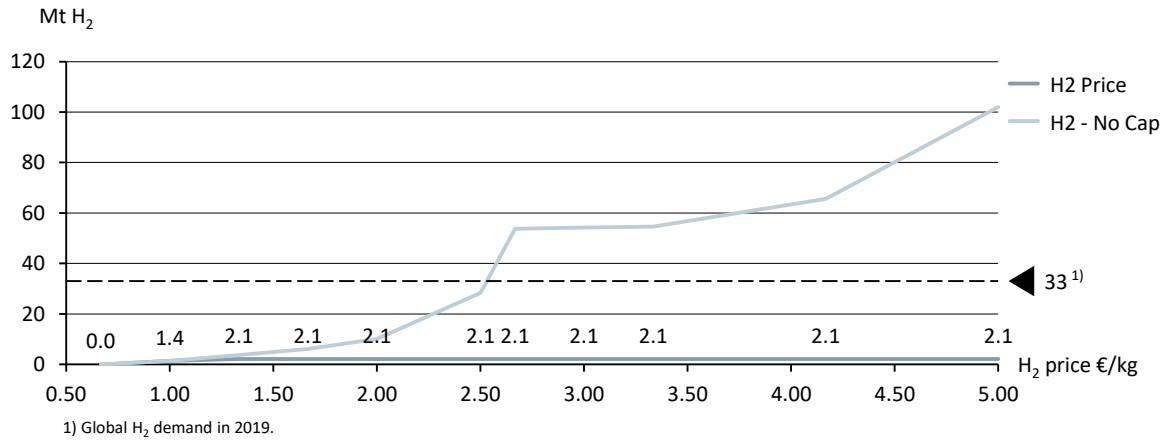

Figure 5-25. Comparison of produced hydrogen in the H2 Price and H2 – No Cap scenario for different break-even prices, including the global hydrogen demand of 33 Mt in 2019 from [218].

The produced amount over different H_2 prices visualizes the cap, reached from 1.33 €/kg onwards. In both scenarios, the production is attractive starting from 1 €/kg, which underlines that the actual break-even price is below the lowest considered price in the H2 Price scenarios. In the H2 – No Cap scenario, the price of 2.67 €/kg marks the transition where the hydrogen production would exceed the

current global demand [218]. In this chapter, these results for Saudi Arabia are further used below to calculate the transportation costs in a hydrogen export case.

Bangladesh: Multi-region model results

Bangladesh is evaluated in detail as an exemplary country for a high break-even price. It consists of 545 municipalities on the lowest administrative level, which provide the basis for the analysis of spatial characteristics [75]. The distributions of demand, FLH, and power plants are visualized in Figure D-20 and Figure D-21.

In Bangladesh, the PHH demand is concentrated clearly around the capital Dhaka. The second biggest city located in the southeast, Chittagong, is also visible with higher demand. Both cities are identified as demand centers in the distribution of the CTSI demand. While Dhaka is an important center for the financial, commercial, and textile industries, Chittagong has a significant harbor and industrial role. Additionally, Khulna represents a third area combining characteristics of the other two cities by being important for trade by its harbor and important for the textile industry [219]. The PV FLH vary between the country's center, which has around 1300-1400 FLH, and the northwest and southeast with 1400-1500 FLH. The wind conditions vary more, showing the best conditions in the south and the worst towards the north and the southeast area close to Myanmar. In a global comparison, the PV capacity factors are medium and the wind capacity factors relatively low. Partially, the wind FLH are even lower than PV. Bangladesh's larger power plants, which are predominantly oil and gas power plants, are distributed close to major demand centers, especially the Dhaka region. Some smaller power plants are in cities across the country. The only coal power plant in the northwest of the country is close to the Barapukuria coal mine [220].

For a comparable basis to the eight divisions in Bangladesh, all smallest administrative regions are clustered in eight regions. The results of the clustering algorithm and the characteristics of each region are shown in Figure 5-26.

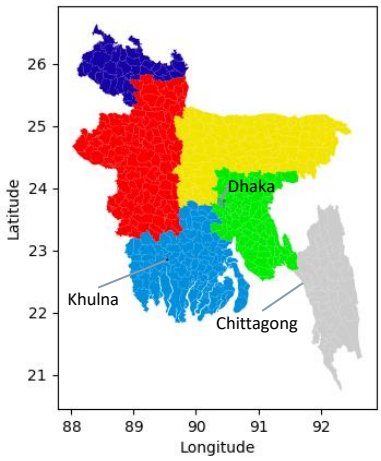

CR	Load		Gen. tech.				FLH	
	PHH	CTSI	Coal	Gas	Hyd	Oil	Solar	Wind
1	2	1	2	1	2	7	7	3
2	8	5	1	7	2	5	1	7
3	6	3	2	6	2	6	6	4
4	1	2	2	7	2	7	8	1
5	4	4	2	2	2	3	5	2
6	7	7	2	3	2	4	4	6
7	5	8	2	4	2	2	3	5
8	3	6	2	5	1	1	2	8

Hyd.: Hydro, Gen. tech.: Generation technologies

Highest to lowest values

1 ... 8

Figure 5-26. Regional clustering results and classification of the cluster characteristics for Bangladesh by the numbers indicating the highest (1) and lowest (8) values for each category.

The eight clusters form six aerial and two dense areas, which are CR 1 and 4. CR 1 is the city of Khulna with a comparably higher CTSI than PHH demand representing its economic importance. Gas power plants ensure electricity generation. In comparison to CR 1, Dhaka in CR 4 has a higher PHH and the second highest CTSI demand density but does not contain any power plants. For both regions, the solar potential is relatively low and the wind potential good. CR 3, 5, and 8 are other regions with high demands next to these urban clusters. CR 3 shows a relatively higher CTSI demand due to its location close to the sea, while CR 8, which includes Chittagong, is characterized by household demand. Both regions contain oil and gas power plants. The third region, CR 5, is located around Dhaka, leading to

a relatively high PHH and CTSI demand. It primarily includes significant installations of oil and gas power plants to ensure the electricity generation for the city center. Regarding their VRES potentials, all three regions differ. CR 3 has medium FLH for both technologies, CR 5 a high wind capacity factor, and CR 8 a high solar capacity factor. Last, CR 2, 6, and 7 define the three northern areas. CR 2 has an industrial character, influenced by the coal mining area, which is confirmed by containing the only coal power plant in the country. In comparison to CR 2, CR 7 is more residential, containing a few cities close to the Indian border. CR 6 shows a low demand and a few distributed power plants. Concerning the VRES conditions, CR 2 has the best potential of all regions while CR 6 and 7 have preferable PV conditions. Comparing these clusters to the divisions in Bangladesh, the detection of the two demand centers, which are usually located in larger regions, is a clear difference. Furthermore, some divisions are split or partially merged with other divisions in another compass direction. Figure D-22 visualizes these differences between the political organization and the data-driven clustering.

The eight defined clustered regions of Bangladesh are modeled until 2045 for the Base scenario. Figure 5-27 presents the modeling results by the generation in each region for each year.

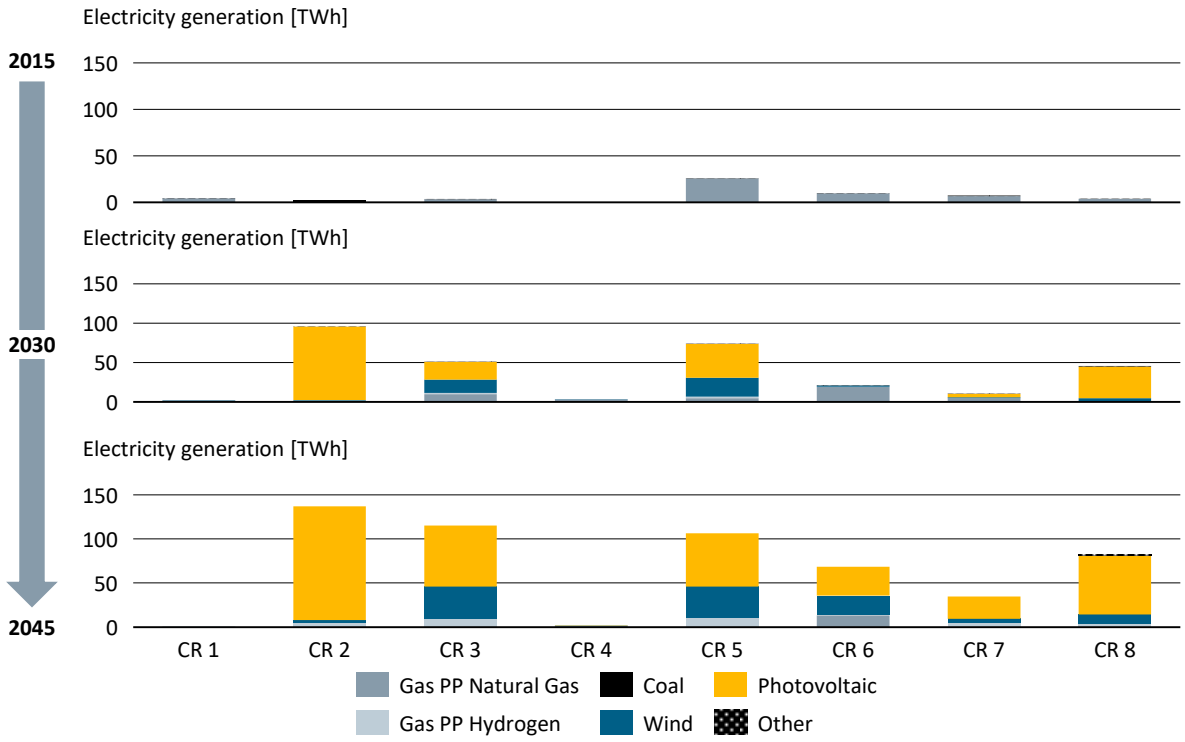

Figure 5-27. Electricity generation of each region in Bangladesh 2015-2045.

In 2015, CR 5, which is the region around Dhaka, provides the primary electricity generation. Overall, the system predominantly dispatches gas power plants. They are more economical in the model than oil power plants installed, e.g., in CR 8. In the two years 2030 and 2045, high capacities of VRES are installed to fulfill the decarbonization goal while facing a substantial increase in demand. For these expansions, CR 2, 3, 5, and 8 are the preferred regions. CR 2 and 8, the clusters with the highest FLH, prefer PV installations. CR 3 and 5 show a mix of wind and PV since they are the two aerial regions with the best wind conditions regardless of the two urban regions CR 1 and 4. These two regions and CR 2, the region with the highest total capacities, install H_2 power plants in 2045 to provide a flexible source for electricity generation.

After understanding Bangladesh's energy system and its transition towards a decarbonized system, the break-even prices in the hydrogen scenarios are evaluated. For this purpose, a comparison to the country model first validates the multi-region model in Figure D-23. Comparing the electricity mix

shows that resolving the country in regions leads to a system that favors PV more than wind. This effect follows the evaluation that two of the best wind locations, CR 1 and 4, cannot be used since there is no space available in these urban areas. However, the systems do not show completely different technologies. Concerning the break-even prices, both models calculate the same break-even price of 5 €/kg, which is the highest available price of all scenarios and higher than the archetype price.

Concluding the hydrogen evaluations of Bangladesh, the regional differences in the country are analyzed in detail. Therefore, Figure 5-28 depicts the break-even prices of each region and the installed electrolyzer capacities.

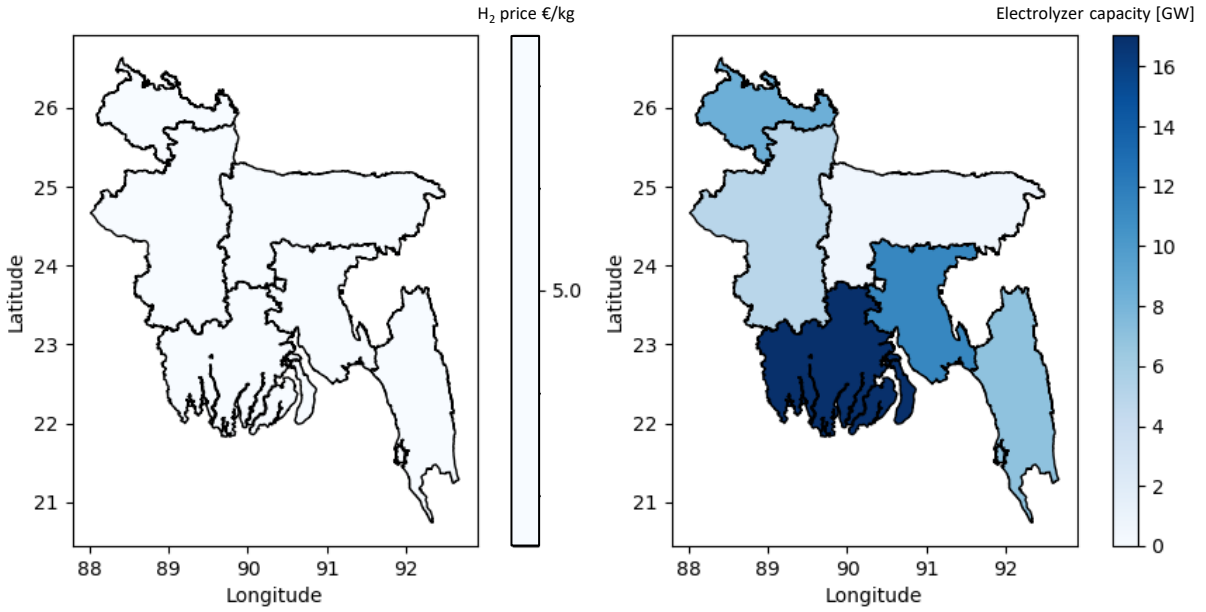

Figure 5-28. Regional break-even prices for green hydrogen production and shares of sold hydrogen in Bangladesh.

The detailed evaluation of regions confirms the break-even price of 5 €/kg. None of the eight clustered regions is attractive for green hydrogen production for a lower price. However, as explained in Figure 5-27, hydrogen still plays a role in Bangladesh's decarbonized energy system. Many regions install electrolyzer capacities for green hydrogen production. This hydrogen is required to provide flexible electricity generation since it can balance seasonal volatilities once stored. The installation of electrolyzers follows areas with high PV and wind installations and close to high electricity demands. CR 2 and 5 are examples of such regions ensuring the electricity generation for the urban areas CR 1 and 4. Due to the low attractiveness of hydrogen production, the H2 – No Cap scenario is not evaluated for Bangladesh.

Overall, the example of Bangladesh shows that economic green hydrogen production is much more challenging in a country with a high $30 - year - Demand\ Growth$ and $RE\ Gap$. This result confirms the relations indicated in Figure 5-6. In this context, producing and selling green hydrogen might compete with the required resources to reach the decarbonization goal. This challenge is even more complex if the country has low PV and wind capacity factors as identified for Bangladesh.

Post-processing by evaluating transportation costs

The use case results confirm the selection of Saudi Arabia as an interesting country for green H_2 production. Based on the modeling results, the evaluation of an exemplary hydrogen export case for Saudi Arabia highlights the strength of the implemented standardized modeling approach. For this purpose, Germany is selected to import the produced green hydrogen since it is an industrial country

with a relatively high break-even price, according to Figure 5-20. Also, Germany has already published a national hydrogen strategy that underlines the intention to integrate it into their economy [221].

The calculation uses Saudi Arabia's lowest available break-even price. According to Figure 5-25, this price is 1 €/kg. Following the three steps defined in chapter 4.3.2, first, the transportation option must be selected. For the distance between Saudi Arabia and Germany, transportation by ship is the preferred option based on the evaluations of the *IEA* [22]. The costs for pipelines, which are the alternative option, increase enormously with the distance. Second, all preparation steps to ship the green hydrogen must be considered. According to the literature, these steps are the inland pipeline in Saudi Arabia, the liquefaction and export process, the shipping, and the import infrastructure. Since the shipping depends on the concrete use case and the distance between the two countries, it is calculated precisely in the third step. All other costs are summarized based on a benchmarking process by using costs from other studies. This process includes inland transport since the distance is uncertain based on the large areas of potential production sites visualized in Figure 5-24. Figure D-24 shows the estimation of the mentioned cost factors in several studies assessing the costs of hydrogen shipment and its associated infrastructure [22], [121], [222]-[224]. Summarizing the different results, a value of 1.2 €/kg is selected for the exemplary calculation. This value is slightly higher than the average, but none of the five studies has considered all defined cost factors. The third step includes a detailed calculation of the shipment. Therefore, the calculation approach and cost assumptions of *Heuser et al.* are reproduced for their use case of transporting hydrogen from Patagonia to Japan [121] and then applied to the shipment route between Saudi Arabia and Germany. For the calculated distance of 4,935 nautical miles [225], equivalent to 9,140 kilometers, the shipment costs amount to 0.51 €/kg. Concluding the calculation, Figure 5-29 provides the results of the cost calculation and its comparison to Germany's break-even prices.

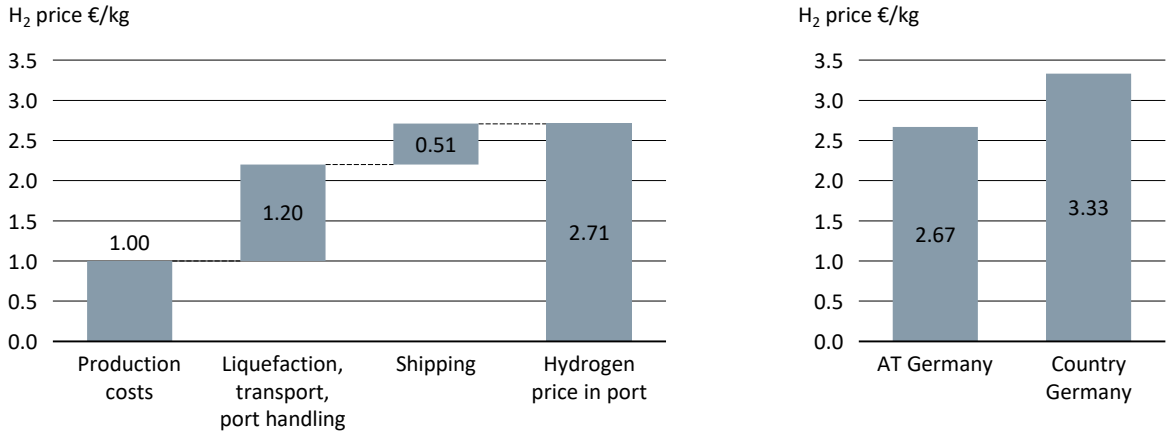

Figure 5-29. Cost breakdown for the transportation calculation of green hydrogen between Saudi Arabia and Germany, including Germany's break-even prices.

The total costs import at the harbor in Germany accumulate to 2.71 €/kg. Compared to the break-even price of AT 13, Germany's archetype, these costs are already in a competitive range. For the country-specific break-even price of Germany, the costs are even 0.62 €/kg lower. This calculation shows that a shipment of green hydrogen from Saudi Arabia to Germany can be economical in the medium- to long-term future.

Validation and discussion

Validating the second use case, first, the clustering results are analyzed. In Saudi Arabia, the clustering algorithm shows similar behavior to Demark and Morocco: it separates the most demand-intensive region very detailed. By contrast, in Bangladesh, the share between urban and extensive aerial regions is identified well, with only two demand centers and six other regions. Since VRES currently do not

play a role in both countries, their distribution cannot be compared to the FLH. The clustering of power plants especially shows an effect in the modeling results of Saudi Arabia in 2015 since regions with gas and with oil generation are separated.

Validating the model results more detailed, the actual values in 2015 show an overestimation of gas for both countries. Since oil power plants are primarily distributed to remote cities (see Figure D-17 and Figure D-21), their operation might be not only for economic reasons. They can provide a secure, local energy supply or be preferred by an existing oil infrastructure. The expansion of PV and wind in the regions during the decarbonization process shows that the regions reflect the respective potentials, e.g., CR 7, 11, and 12 in Saudi Arabia. The analysis of urban areas in both models shows the validity of the implemented area restrictions. There is almost no capacity built in these regions, such as CR 1 and 4 in Bangladesh.

For hydrogen use, the break-even price modeling approach also needs to be validated. Therefore, the Sankey diagrams in Figure 5-30 visualize Saudi Arabia's energy flows in 2045 for the Base scenario and an exemplary H2 Price scenario.

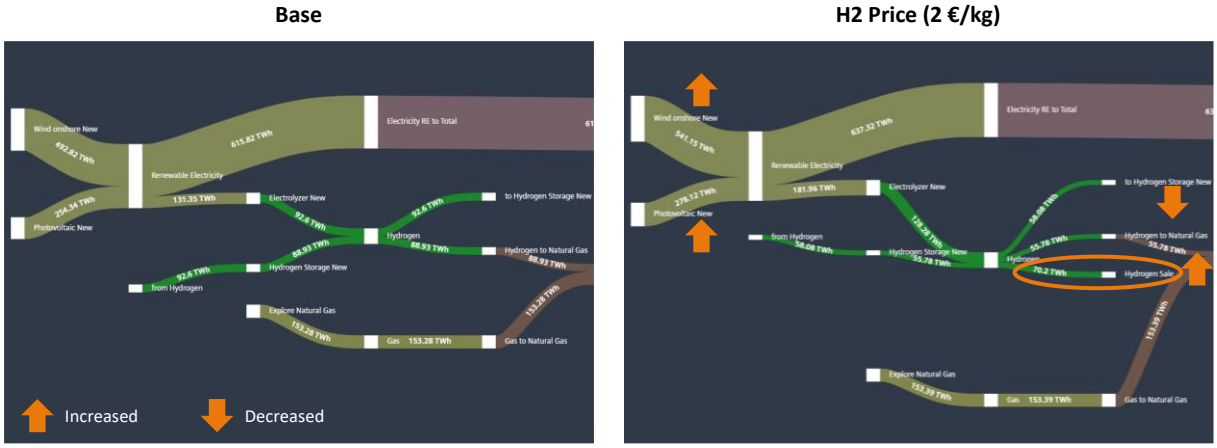

Figure 5-30. Validation of the H_2 break-even price implementation by comparing the energy flows in 2045 between the Base and the H_2 Price 2 €/kg scenario for Saudi Arabia.

In both scenarios, H_2 is added to the turbines to generate emission-free electricity by a flexible source. However, the amount is reduced from 88.9 TWh_{th} in the Base scenario to 55.8 TWh_{th} in the H2 Price scenario. Additionally, 70.2 TWh_{th} hydrogen are sold, which is equivalent to the 2.1 Mt in Figure 5-25. This green hydrogen production, which requires VRES and electrolyzer capacities, leads to an expansion of wind and PV. Predominantly, additional wind power plants supply the increase of around 80 TWh_{el}. These expansions partially substitute the reduced electricity generation from hydrogen compared to the Base scenario to reach the country decarbonization target. The other part is fed into the electrolyzer to produce more hydrogen. The possibility of selling hydrogen reduces the storage amount by 38%, which increases efficiency by reducing storage losses. These observations validate the approach of a break-even price that aims to increase renewable capacities and produce more hydrogen if the price is attractive.

Additionally, the similar break-even prices of multi-region, country and archetype models further validate the implemented modeling approach. Since each archetype includes outliers, the prices are not equal. However, the selected archetypes confirm trends, such as the significant difference between AT 4, 13, and 15. Furthermore, the attractive regions for green hydrogen production match the VRES conditions of the clustered regions underlining the advantage of using data-driven regions for a regional evaluation.

Overall, the hydrogen use case shows that the implemented framework is well suited to determine the attractiveness from a global down to a regional level. The data-driven classification amplifies the regional characteristics in the energy system model and thereby distinguishes the suitability of each region for green hydrogen production. The exemplary calculation of a transportation use case between Saudi Arabia and Germany shows another strength of the approach: the attractiveness between two countries can easily be compared based on the same model assumptions.

The calculated global break-even prices and the costs for the transportation use case are benchmarked to other studies. Global evaluations of the *IEA* [22] and the *Hydrogen Council* [222] provide a basis to contextualize the break-even prices. For the transportation costs, values are extracted from the *Hydrogen Council* [222] and a study to calculate the import of hydrogen in Germany and Japan [224]. Both studies include Saudi Arabia so that they support the validation of the break-even price.

Comparing the map in Figure D-15 to the similar map with an equal color code in the *IEA* report [22], Central America, parts of Africa, the Middle East, Europe, or Australia show similar patterns. These results confirm that the archetype is a suitable proxy for a simplified evaluation of the green hydrogen potential. Furthermore, the price range is almost equal, which validates the resulting break-even prices. However, three effects lead to differences in specific areas: the higher resolution of the *IEA* map, which resolves differences within a country, the variety of countries within an archetype in this thesis, and the consideration of the energy system for decarbonization. An example for the first effect is Argentina which has low production costs in the South corresponding to good wind conditions in Patagonia and higher costs in the northeast. The second effect is shown, for example, in South-East Asia, where India is characterized by low costs and Indonesia or Malaysia by higher costs. All these countries belong to the same archetype, which is closer to India, and it indicates good conditions for all of them. The countries from AT 14 are an example for the last effect. They face low costs for the decarbonization (see Figure 5-6) and, therefore, lower break-even prices for the hydrogen production than in a mere VRES evaluation.

The *Hydrogen Council* classification, which is partially based on the *IEA* evaluation, leads to similar observations. Also, their map includes information on low-carbon resources. In this study, Australia, Chile, the US, and the Middle East are classified as good locations, while the EU and Japan/Korea represent potential importers. Chile, Australia, and the US are good examples of two of the before-mentioned effect: they are in an archetype with many countries and have a large area in which some regions favor hydrogen while others are not well suited.

Overall, the comparison of break-even prices indicates that the archetypes are a good indicator for general attractiveness. The resulting prices are in a reasonable range. Furthermore, the framework addresses the drawbacks of the spatial resolution and the divergence of countries within an archetype. As shown in this use case, the model can be applied to the country and multi-region level based on the same assumptions increasing the level of detail in every step. This evaluation underlines the advantage of covering all levels from global to regional in the framework.

The results of the transportation case are close to the two selected studies. *Brändle et al.* calculate for Saudi Arabia an LCOH of 1.6 $/kg for an amount of 3.1 Mt in 2050 [224]. These results are in the range of the cost-supply curve in Figure 5-25. The hydrogen council calculates 3.4 $/kg for the shipping from Saudi Arabia to Germany in 2030 [222]. Higher production costs are the reason for the difference to the calculated 2.7 €/kg in this thesis, resulting from higher investment costs for PV, wind, and electrolyzers in 2030. Both studies validate the production costs and potentials for green hydrogen production in Saudi Arabia, as well as the transportation costs for the export to Germany.

5.3.3. Use case 3: Coal Phase-Out

The third use case evaluates coal phase-outs from a global view down to regional effects. Therefore, an archetype and a country with a currently high share of coal power generation are selected. For this country, the effects of a coal phase-out are then analyzed in a regional resolution by its clustered regions. For this use case, important output parameters are the relative change of regions, and the grid flows as described for the first use case. Furthermore, a GIS analysis can identify mining areas.

Country selection

The energy mix in 2015, compared for all archetypes in Figure 5-3, clearly identifies AT 6 with the highest coal share. Only one country is selected for the third use case since an opposite country without coal generation does not face any coal phase-out. Next, Figure 5-31 compares the seven countries within this archetype by their lignite and coal generation share.

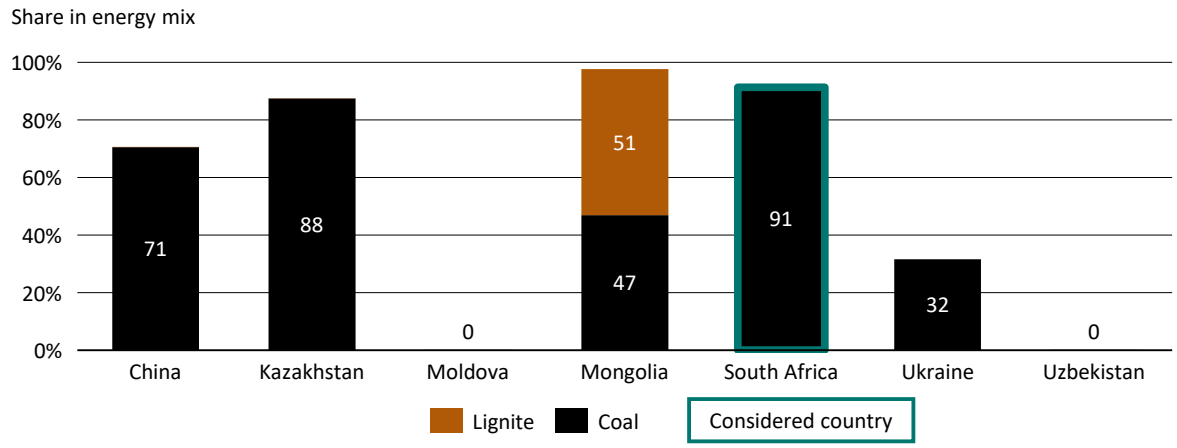

Figure 5-31. Selection of considered country in AT 6 based on shares of coal power plants.

Two of the seven countries, Moldova and Uzbekistan, do not have any coal generation in 2015. These outliers lead to the high RMSE of AT 6, explained in chapter 5.2.3 and depicted in Figure C-8. By contrast, Kazakhstan, Mongolia, and South Africa show the highest shares of coal generation. Mongolia and Kazakhstan have much smaller energy systems with a lower demand than South Africa, which is therefore chosen. Furthermore, South Africa is the fifth biggest coal exporter worldwide [226], highlighting its importance for the global coal industry. It also has good wind and PV conditions (see Figure 3-4). For these reasons, South Africa provides a well-suited country to evaluate the transformation of its electricity system on a regional level and project an outlook on how the decarbonization process copes with the critical economic factor of coal. A previous publication has already described a similar evaluation for South Africa [144]. However, the clustering methodology and some model assumptions have been further developed, leading to different results in the framework of this thesis.

South Africa: Multi-region model results

South Africa is classified in 234 municipalities on the lowest administrative level [75]. These regions are the basis to explain the spatial characteristics, visualized in Figure D-25 and Figure D-26.

The PHH demand shows the highest demand in the region around the biggest city Johannesburg. Next to Johannesburg, other agglomerations with a large population such as Cape Town, Durban, and Port Elizabeth stand out. These centers also show high CTSI demand. Additionally, two rural zones in the center and south of Johannesburg are striking in the CTSI distribution. They indicate industrial mining areas, which this use case focuses on during the evaluation. The PV conditions follow a clear pattern showing the best conditions in the northwest and the worst in the southeast. For wind, the

highest FLH are located along the coastline and in the central areas. As already mentioned in the context of the country selection, South Africa has excellent potential for both technologies globally. The area around Johannesburg locates the vast majority of coal power plants. Besides, gas and nuclear power plants are installed around Cape Town and smaller oil, waste, and hydropower plants close to other cities. South Africa also shows some VRES installations. They follow the indicated FLH distributions with PV installations focused in central areas and wind along the coastlines.

After analyzing the data basis, South Africa is clustered in nine regions, reflecting the number of its provinces [75]. By showing the map and a table of the spatial data characteristics, Figure 5-32 visualizes the results and their interpretation.

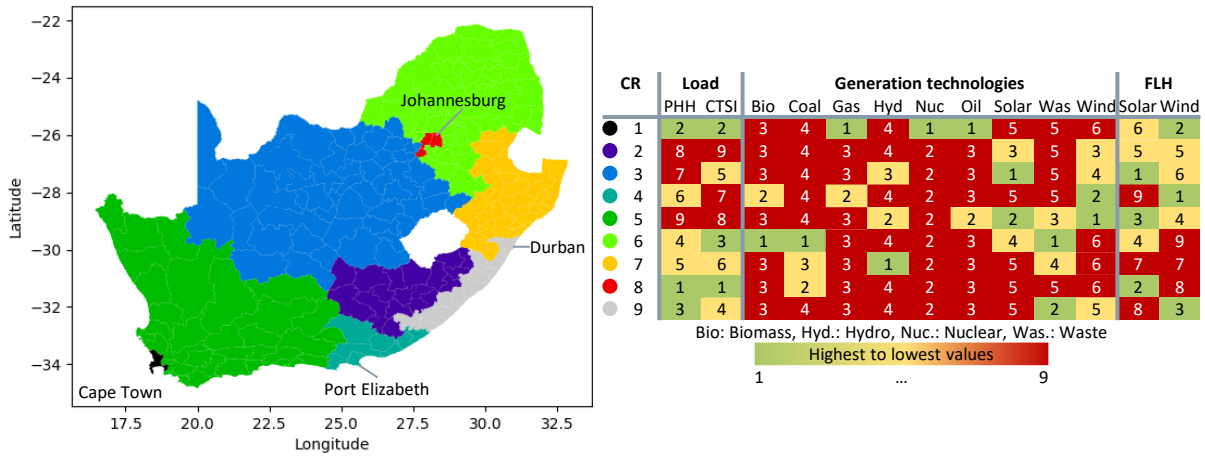

CR	Load		Generation technologies									FLH	
	PHH	CTSI	Bio	Coal	Gas	Hyd	Nuc	Oil	Solar	Was	Wind	Solar	Wind
1	2	2	3	4	1	4	1	1	5	5	6	6	2
2	8	9	3	4	3	4	2	3	3	5	3	5	5
3	7	5	3	4	3	3	2	3	1	5	4	1	6
4	6	7	2	4	2	4	2	3	5	5	2	9	1
5	9	8	3	4	3	2	2	2	2	3	1	3	4
6	4	3	1	1	3	4	2	3	4	1	6	4	9
7	5	6	3	3	3	1	2	3	5	4	6	7	7
8	1	1	3	2	3	4	2	3	5	5	6	2	8
9	3	4	3	4	3	4	2	3	5	2	5	8	3

Bio: Biomass, Hyd.: Hydro, Nuc.: Nuclear, Was.: Waste

Highest to lowest values

1 ... 9

Figure 5-32. Regional clustering results and evaluation of the cluster characteristics for South Africa by the numbers indicating the highest (1) and lowest (9) values for each category.

Comparable to the clustering results in the other four presented countries, South Africa's clustering also shows a combination of urban and aerial regions. The two largest cities, Johannesburg and Cape Town, are identified as CR 8 and 1. CR 8, Johannesburg, has the highest demand, the second-highest density of coal power plants, good solar, and poor wind conditions due to its location in the northeast and far from the coast. Having direct access to the coast, Cape Town (CR 1) has good wind but poor PV conditions. It shows the second-highest PHH and CTSI demand as well as gas, nuclear, and oil power plant capacities, confirming the described distribution of power plants. CR 2, 3, and 5 are three regions with a low demand but good wind and PV conditions. The existing capacities of both technologies reflect these conditions. Only CR 3 shows a relatively higher CTSI demand which reflects mining activities. Similarly, CR 6 shows a higher CTSI demand. Together with CR 7, it describes regions close to Johannesburg with high installations of coal power plants. The renewable potentials of both regions, except for PV in CR 6, are among the lowest in the country. The remaining two regions, CR 4 and 9, are located along the coastline in the south. Therefore, they show the best wind and the worst PV conditions. Existing installed wind farms confirm the good wind conditions. The two regions differ in their demand structure. Except for Port Elizabeth, CR 4 includes rural areas with medium or low demand while CR 9 comprises more cities along the coastline, e.g., Durban. Compared to the administrative provinces (see Figure D-27), the most significant difference is the detection of the two cities by the clustering. Other regions, e.g., close to the coast, are re-arranged to represent their renewable potentials better. Concluding the clustering results regarding the topic of the use case, CR 6, 7, and 8 locates all coal power plants. Therefore, the following evaluations focus primarily on these regions.

Consequently, the nine explained clustered regions are modeled in the energy system model to calculate the transformation pathway in the Base scenario. The resulting electricity generation in each region and the relative regional changes between 2015 and 2045 are depicted in Figure 5-33.

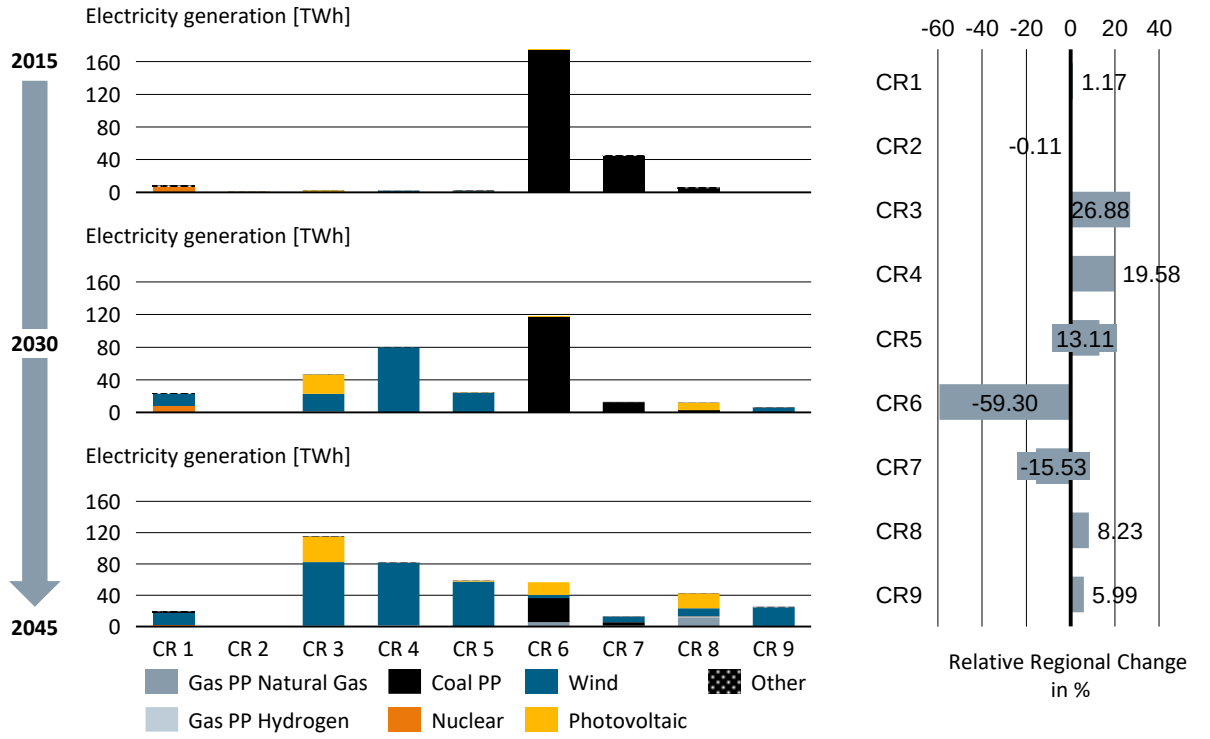

Figure 5-33. Electricity generation of each region in South Africa 2015-2045 and the relative changes of contribution to the country electricity generation.

The first modeled year, 2015, clearly confirms the coal-dominated system in South Africa. Especially CR 6, 7, and 8, the regions identified by the clustering to focus on in this use case, generate by far the largest part of South Africa's electricity. CR 1 is the only visible further generation cluster, representing the power plants around Cape Town. The transformation process over 2030 to 2045 significantly reduces coal generation. An expansion of solar and especially wind capacities aims at compensating for this reduction. The wind installations are first focused on CR 4 and 5 and then expanded to CR 3 and 9. The wind expansion of CR 5 and 9 shows the advantage of integrating the grid and available areas in the optimization. They both have comparably good conditions. However, CR 5 is preferred to CR 9 since more area is available, and the region is well connected by the high grid capacities connecting Johannesburg and Cape Town [144]. PV expansion is focused first on CR 3 and 8, the clusters with the best conditions. In 2045, it is also expanded in CR 6 to compensate for the shut-down of the large coal capacities. To ensure some flexibility in former coal-dominated regions and close to the high demand in the Johannesburg region, gas power plants are built in CR 6 and 8. However, South Africa does not foresee a general coal-to-gas shift as the archetype model of AT 6.

Analyzing the change of each region's role from 2015 to 2045, the coal-dominated regions CR 6 and 7 lose their importance for the national energy system. CR 6, which has the highest generation in 2015, loses 60% and CR 7 15% of its contribution to South Africa's electricity generation. Regions with good wind and PV conditions, such as CR 3, 4, and 5, compensate this generation. These regions have lower demand and low capacities in the current system but good VRES potentials and available areas to power the country in a decarbonized system. The significant changes of regions' contributions to the national system require analyzing the impact on grid flows for the coal use case. Figure 5-34 visualizes the development of the absolute flows between the clustered regions.

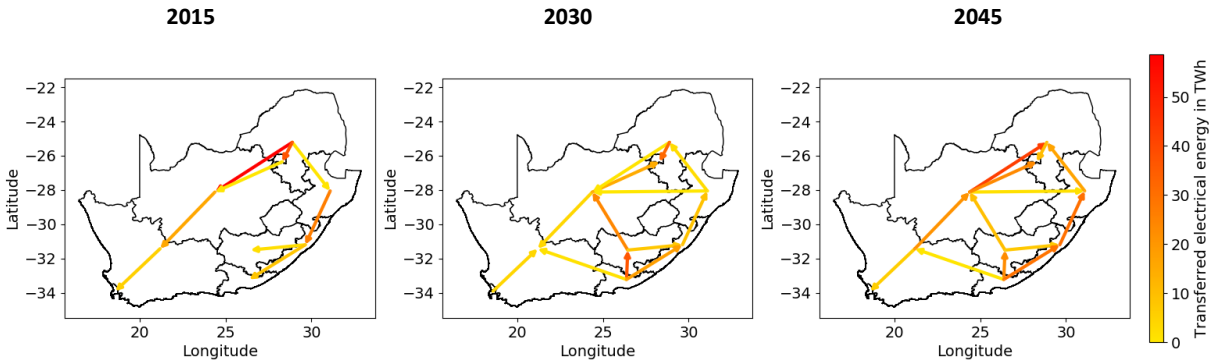

Figure 5-34. The transferred electricity on grid lines between the clustered regions in South Africa for the Base scenario from 2015 until 2045.

The grid flows confirm the importance and transformation of the coal-dominated regions CR 6, 7 and 8. In 2015, especially CR 6 is essential since it is the center for electricity transmission in South Africa. However, these flow patterns are almost all turned around over 2030 until 2045. CR 6 and 7 import electricity from regions with high wind and solar capacities, such as CR 3, 4, and 5. This development leads to the fact that CR 6 imports in 2045 almost the same amount of electricity from CR 3 as it exports in 2015. The last step to understand the role of coal regions is to identify the regions in which coal mining plays an important role. Therefore, Figure 5-35 compares the OSM evaluation of mines in the clustered regions to an official classification by the *Minerals Council* [227].

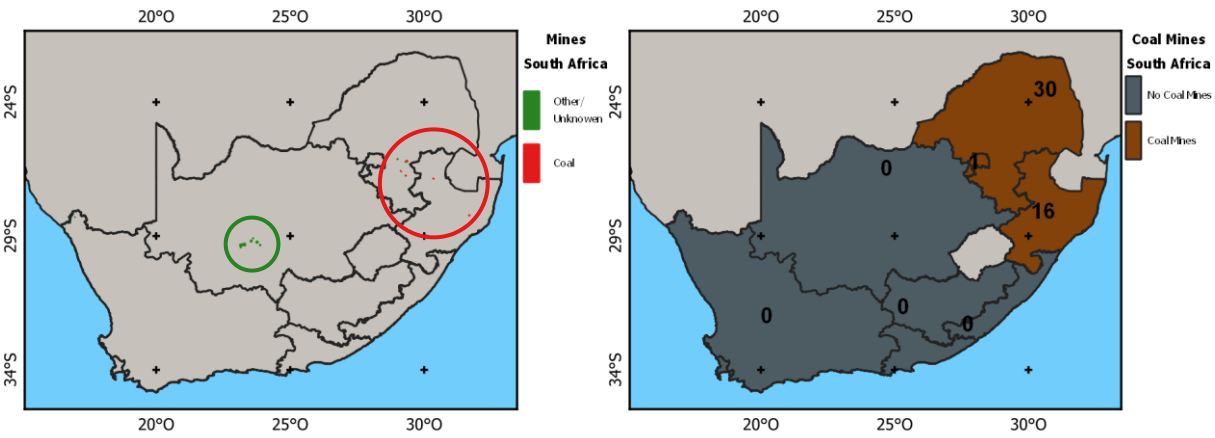

Figure 5-35. Distribution of mines in South Africa identified by OSM [116] and the *Minerals Council South Africa* [227].

First, the OSM map shows mining activities in the central area. The spatial data analysis already identifies this area by its high CTSI demand. Therein, other resources, e.g., precious metals, are exploited. All coal mines are in CR 6 and 7, which also contain the power plant capacities. The distribution stated by the *Minerals Council* confirms this observation. The mines are distributed precisely to the three clustered regions, which the evaluation of the modeling results analyzes in detail. Therefore, the localization of mines only confirms the selection of coal-dominated regions and does not identify additional essential regions.

Validation and discussion

The third use case, analyzing the coal phase-out, also shows the advantages of the implemented framework. The archetypes can reduce the number of analyzed countries by filtering coal-dependent archetypes. South Africa represents a particularly relevant country. The data-driven approach stresses out coal-dependent regions since it is an input factor of the clustering process.

In general, the clustering results for South Africa seem reasonable. They highlight clusters with high demands such as the Johannesburg and Cape Town regions, clusters with high power plant capacities, e.g., CR 6 and 7, and clusters with good VRES conditions such as CR 3, 4, and 5. In this case, the installations of existing VRES also correspond well to the potentials in the database.

The model results show a good match between the actual generation in 2015 and the dispatch of the automated model, as indicated in Figure D-1. The generated electricity by coal power plants, the dominant generation technology, fits the actual values. Also, the grid flows in 2015 represent the system structure. Starting from the locations of power plants, electricity is transmitted to all regions in the country, including a high grid capacity between the two demand centers Johannesburg and Cape Town. For the phase-out until 2045, the modeling results do not force a complete coal-to-gas shift. Due to the high dependency on coal as a source for electricity and export to other countries, this result is reasonable even though the archetype foresees a coal-to-gas shift. Besides, South Africa has excellent wind and PV potentials, leading to the high integration of VRES already in 2030.

Overall, the exemplary application of the use case underlines that regions within coal-dependent countries face a significant transformation, especially if their VRES conditions are not outstanding within the country. Thereby, a coal phase-out substantially changes the role of regions within a country's energy system. The use case also shows similarities to the first use case since countries with a coal phase-out also face a high *RE Gap* and their grid topology might drastically change. In South Africa, for example, with an *RE Gap* of 76%, almost all flow directions turn around during the transformation from a demand-oriented to a VRES supply-oriented energy system.

Transferring these results to South Africa's economy, renewables might offer considerable potential for two reasons. First, the country shows outstanding potentials for both VRES technologies, wind and solar, which help to decarbonize the country's energy system. Second, the global analysis of all archetypes shows that most countries tend towards a coal-to-gas shift which affects the South African coal export. Since more than 90,000 people are currently employed in the coal mining industry, it is essential for the country [227]. The good renewable potential and the urgency to act are supported by comparing the BAU and CO2 Price scenarios to the Base scenario in Figure D-28. In the BAU, the *Decarbonization Index* shows that emissions are already reduced by 16% even though the demand is rising. Also, the cost difference between the Base and the BAU scenario is only 9.2%. Last, a CO_2 price of 100 €/t leads to higher costs and a decarbonization index of 93%.

These results, especially the good VRES conditions, are confirmed by other studies. Even without policies, they can already be competitive with coal in South Africa. In a cost-optimal power system evaluation by *Merven et al.*, the system reduces coal capacities, leading to a RES share of around 65% in the electricity mix. This shift reduces emissions by 65%. Regarding the choice of RES technologies, this study favors wind generation [228]. A second study calculates a 100% RES system in South Africa, including a regional resolution. This study expects more PV expansion due to the model assumptions with comparably low PV costs. However, the regional distribution shows high wind installations in regions identified as promising wind regions in this thesis [51]. Even though the choice of technologies varies between the results, the regional distribution is therefore validated. Overall, the studies confirm that South Africa is attractive for wind and PV expansion. It depends on the cost developments and the regulatory framework which technology is preferred.

5.3.4. Discussion of the Use Cases and the Regional Clustering Approach

All three use cases apply the entire framework, which identifies countries by archetype modeling for a detailed evaluation in multi-region models. Based on defined indicators for each use case, the first two levels provide the basis to decide for relevant countries. As shown in Figure D-1, the standardized modeling rules lead to valid results for the base year 2015.

Evaluating the regional clustering in detail, the use cases prove the purpose to highlight differences in demand, power plants, and VRES conditions. Furthermore, the clustering characteristics help to analyze and interpret the modeling results. Compared to existing approaches, the combination of point data and time series in spatial clustering is another improvement. To quantify the improvement of the regional clustering and thereby validate the approach, the results are compared to the same number of administrative regions for the five countries. As a second comparison, the high dimensional clustering without the dimension reduction by DTW and PCA, indicated as an option in Figure 4-2, is also included. The exact values of the SI score and the Euclidean distance for the entire dataset of the demand, generation, and the complete time series in Figure 5-36 compare the three approaches.

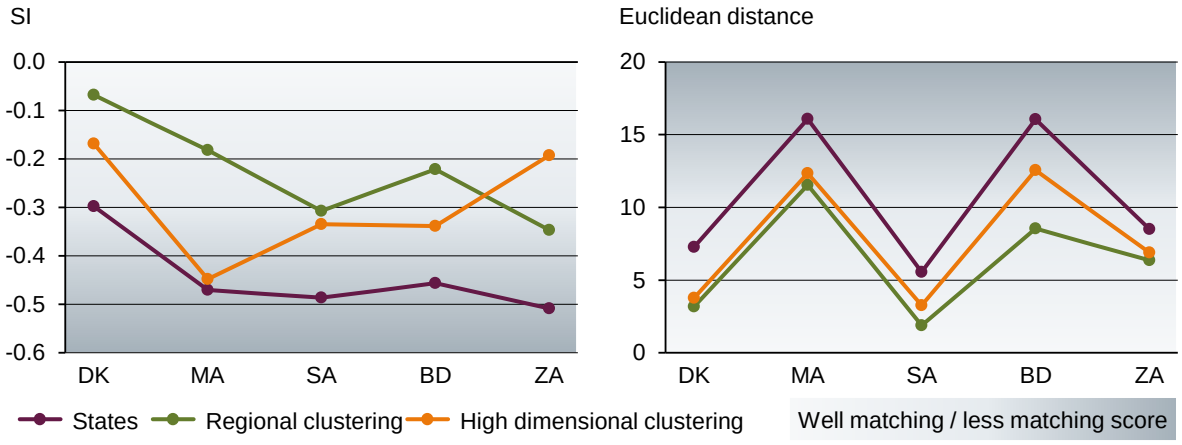

Figure 5-36. Analysis of the different classification approaches by SI score and Euclidean distance for the evaluated five countries and applied to the complete data set, including the hourly renewable time series.

For both metrics and all countries, the clustering outperforms the classification in administrative regions on level 1. Additionally, the metrics of the regional clustering are in nine out of ten cases better than the high dimensional clustering. Only in South Africa, the high dimensional clustering shows a better SI score. The application of low dimensional clustering is validated by combining the better classification with a significantly lower runtime due to the reduced complexity. Two further considerations underline this advantage: comparing the three approaches based on the reduced dataset and introducing a country with a higher number of smallest administrative regions.

The comparison for the dataset with reduced time series, which is the data input for the developed regional clustering, confirms the benefit of the regional clustering with SI scores between 0.2 and 0.35 (see Figure D-2). Except for South Africa, the Euclidean distance confirms this dominance again. Applying the comparison to a more complicated country further increases the advantages: Being divided in more than 4,000 smallest regions on the lowest level [75], the cluster calculation for Germany is computationally intensive. As shown in Figure D-3 in the appendix, the high dimensional clustering cannot cope with the renewable time series due to the curse of dimensionality. The clusters represent mainly demand and generation centers leaving two aerial regions with very different VRES conditions. By contrast, the dimension reduction leads to distributed clusters with similar sizes. It identifies three primary demand and generation centers: the Rhein-Ruhr area around Cologne, Dusseldorf, and Essen, the Rhein-Main area around Frankfurt, and Munich. The almost rectangular cluster shapes follow the small number of administrative regions and the raster resolution of wind and PV. The algorithm calculates this improved result in just 2% of the high dimensional clustering computation time. Overall, these comparisons validate the implementations of the regional clustering algorithm by the SI scores, the Euclidean distances, and the evaluation of Germany as another exemplary country.

However, applying the clustering to the use cases also shows opportunities to improve the methodology. Using the smallest administrative regions and normalizing the data, the input data for

the clustering depends on the area of the administrative region. These areas differ globally in their size (see Figure 3-7). Thereby, dense areas are preferably identified than larger areas with potentially higher demand or installed capacity. Alternatively, using a constant raster with the same size as *Siala and Mahfouz* can split cities or large agglomerations [72]. A mixed approach might be helpful for further developments using similar sizes of areas but still considering the administrative area to reflect city borders. Furthermore, geography affects the results since especially the variances of the VRES conditions are usually higher in large countries. This framework includes an implementation of determining an optimal cluster number based on the SI score, visualized in Figure 4-2, to include this effect in the clustering.

6. Conclusion and Outlook

This thesis implements a globally applicable approach to calculate decarbonization paths for energy systems using an energy system optimization model. It uses data-driven clustering to improve and simplify the global applicability and the spatial resolution for projections on a regional level. Two new clustering methods, which are directly applied within these models, represent the novelty of this approach by introducing archetypes and regional clustering. Another improvement is the extension of the dimension to include hourly renewable time series in the regional clustering. Next to the advancements of the two methods, the hierarchical combination of both in one framework allows for an integrated data-driven analysis of use cases. These use cases address three significant future challenges of energy systems: the transformation of power grids due to increasing renewable sources, the production of green hydrogen, and the coal phase-out. Thereby, it provides support to analyze worldwide decarbonization pathways of countries to reach the COP21 goals, evaluate the role of specific technologies in future markets or specifically defined locations, and simplify the setup of energy system models worldwide.

Three sub-questions are derived from the central question of implementing an integrated analysis: they cover a globally transferable setup of country energy system models, an adaptive resolution of modeling based on appropriate clustering techniques and evaluation criteria, and an appropriate integration of the use cases. The primary requirement for the first sub-question is the balance between global data categories and categories that need to be included or derived for countries or regions individually. Furthermore, the model needs to integrate a global data basis, including country data and spatially highly resolved data. For the clustering techniques, the characteristics of clustering algorithms, especially for the application to geospatial data, need to be considered. Challenges are especially the number of clusters, finding an optimal result, and avoiding the curse of dimensionality for spatio-temporal clustering. The three applied use cases require several specific requirements, such as synthesizing a transmission grid based on OSM data, finding a demand-independent approach to model green hydrogen production, and zooming into coal-dependent regions from a global view.

The application of the two clustering algorithms in a common framework to the three use cases shows several advantages and further development steps, summarized in Figure 6-1. The use cases underline the applicability of the overall framework to global decarbonization challenges, confirming the central research question. For most cases, the results are consistent between the different levels. The archetypes provide a suitable selection mechanism to reduce the complexity while the regional clustering incorporates spatial details. By including the two clustering algorithms, such evaluations can be executed fast and in a globally comparable way. Furthermore, the data-driven approach improves the understanding of each step by providing a link between the data-driven model input and the model results. Overall, the hypotheses of all three selected use cases are confirmed. The respective sub-chapters contain a detailed discussion of all developed methodologies and this final discussion shortly highlights the main aspects.

The definition of a global data basis and standardized modeling rules provides the opportunity to model all countries from their archetypes to a detailed multi-region model with the same set of assumptions. Thereby, models can easily compare the effects of specific technologies or regulations, and the modeler can focus on evaluating models. Results for the starting year 2015 validate the method. However, for detailed country studies, specific values such as gas prices or particular regulatory aspects still must be researched. Furthermore, the data basis and rules focus on the electricity sector and must be extended to consider the full potential of flexibilities in a decarbonized energy system. Another technology that requires a more detailed analysis is hydropower. Since the hydro potential strongly depends on geological and weather conditions, the modeling includes other dimensions of research that could be addressed in further research globally.

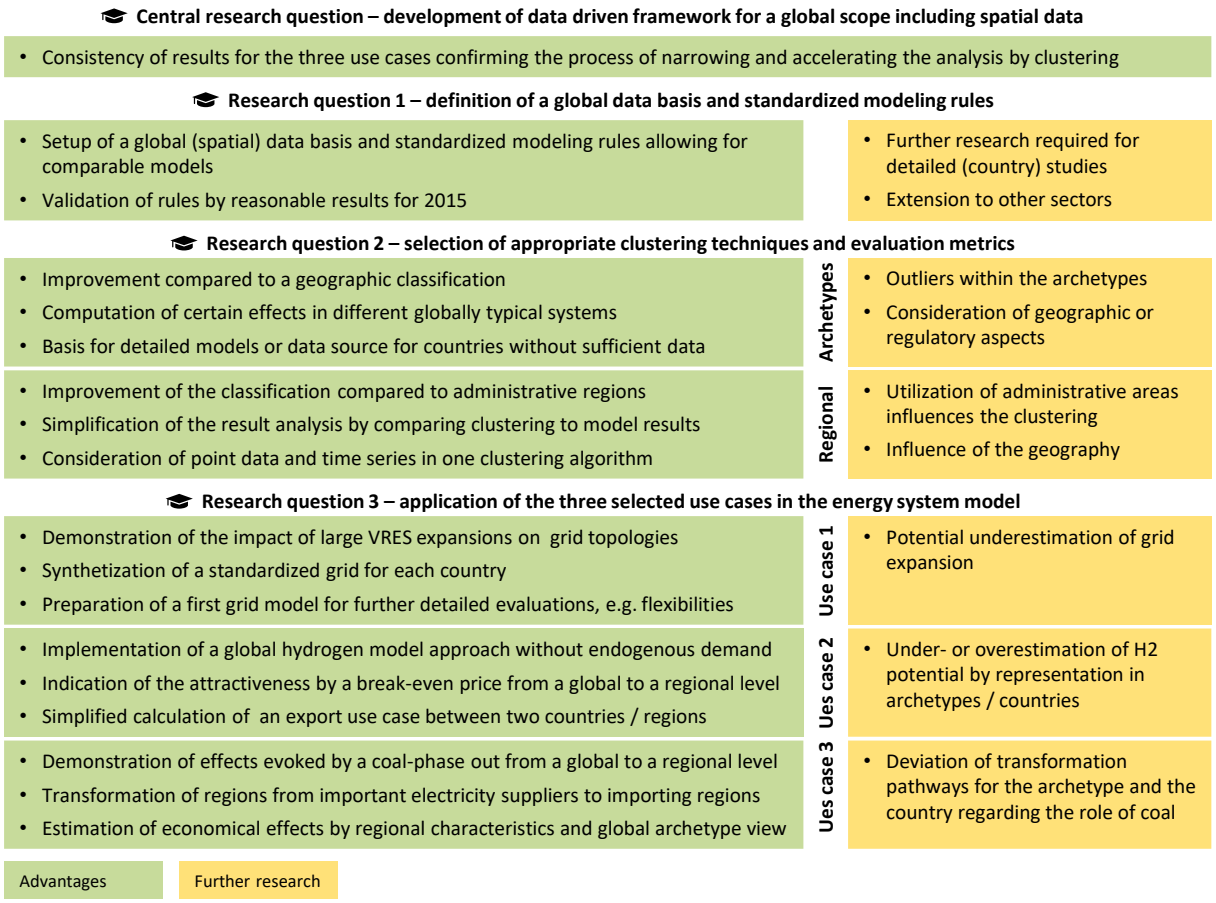

Figure 6-1. Advantages and further research potential for each research question.

Both clustering techniques confirm their applicability by a validation process compared to the state-of-the-art of using administrative classifications. They also both highlight characteristics of the energy system directly linked to the model results. In particular, the archetypes define a novel approach of modeling energy transitions by synthetic global countries. They guide to compare countries worldwide and even to reconstruct data. Even though they classify countries better than continents or sub-continents, the archetypes also show outliers. Further research could potentially incorporate geographic or regulatory aspects such as continental interconnected systems or not quantifiable policy measures. For the regional clustering, extending the spatial dimension to the time dimension by including hourly renewable time series is the main contribution. In the validation process, reducing the time dimension by Dynamic Time Warping and Principal Component Analysis shows better results than applying the hourly time series. However, the results are influenced by the definition of the smallest administrative regions, leading, e.g., to a strong influence of cities in certain countries.

Last, the three use cases are summarized to answer the third research sub-question. As mentioned before, the framework successfully evaluates all use cases, and the results confirm the initial hypotheses. In detail, the grid topology demonstrates the effect of different VRES expansion scenarios on the spatial distribution of generation capacities. Methodologically, it synthesizes the transmission grid based on OSM data. According to the results, this globally applicable process risks an underestimation of required grid expansion. Nevertheless, the method developed here provides a first grid model for further improvements and more detailed evaluations. The second use case evaluates the attractiveness of green hydrogen production while decarbonizing the energy system by a break-even price to sell hydrogen. The transferable character of the framework enables a straightforward assessment of an export calculation between two countries as a post-processing step. Exemplarily, Germany and Saudi Arabia are evaluated in the result chapter. Further research can better include

detailed regional hydrogen characteristics within countries since the potentials might be under- or overestimated by the archetypes or countries. The last use case stresses that coal-dependent countries and even regions face fundamental changes by a coal phase-out by the example of South Africa. Combining the regional results with the archetype view allows for including the global context, e.g. by estimating economic perspectives for the world market.

Overall, the major strengths of the framework are the acceleration of the modeling process, the globally transferable approach and data basis, and the reduction of complexity which helps to understand input data and results better. Thereby, the developed methods can support the quality or economic efficiency of modeling future energy systems. Better models support policymaking, technology companies and research institutions to tackle the global challenge of transforming the energy systems. For this transformation, the comprehension of essential technologies and pathways is the basis for profound decisions leading to the development of new technologies or effective policies. Both approaches are required to substantially reduce CO_2 emissions, which is fundamental to limit the observable impacts on our planet.

Appendix A. Model Description

The energy system development plan (ESDP) is an energy system optimization model minimizing the total system costs. A very brief description of the model is also provided by *Müller et al.* [114]. In general, the model can be used to calculate the energy mix in target years or for transition pathways. The regional resolution can cover single node as well as multi-region models. This description only states the equations of a linear optimization problem which is used in the thesis. However, the model also includes equations of Mixed Integer Linear Programming. To represent various technologies and sectors in a flexible way, the model uses conversion processes and sub-processes. They convert certain commodities with a given efficiency.

The overall objective function aims at minimizing the total costs C^{TOTEX} which is the sum of the capital expenditures C^{CAPEX} and the operational expenditures C^{OPEX}:

$$\min\ C^{CAPEX} + C^{OPEX}. \tag{A.1}$$

Cost Calculations

First, the capital costs C^{CAPEX} are calculated by summing the capacity expansions $Ca^{new}_{y,cp,reg}$ in all regions reg multiplied by the specifc costs $Cs_{y,cp}$ for each conversion process cp and the discount factor F^{disc}_{y} for all modeled years y:

$$C^{CAPEX} = \sum_{y} F^{disc}_{y} * \sum_{cp} Cs_{y,cp} \sum_{reg} Ca^{new}_{y,cp,reg}. \tag{A.2}$$

Second, the operational costs use a similar approach but consider different cost terms of operation and maintenance (O&M) costs: the operational costs per installed capacity $Cs^{O\&M,Ca}_{y,cp}$ and per produced unit of energy $Cs^{O\&M,E}_{y,cp}$. Furthermore, the calculation includes the fuel costs $Cs^{Fuel}_{y,te}$ of the input commodity processed in the conversion process and, if defined, the CO_2 price $COPR_y$. These factors are multiplied either to the total capacity $Ca^{tot}_{y,cp,reg}$ or the total energy $E^{tot}_{y,cp,reg}$ as follows:

$$\begin{aligned} C^{OPEX} = \sum_{y} F^{disc}_{y} * \sum_{cp} (& Cs^{O\&M,Ca}_{y,cp} * \sum_{reg} Ca^{tot}_{y,cp,reg} \\ & + Cs^{O\&M,E}_{y,cp} * \sum_{reg} E^{tot}_{y,cp,reg} \\ & + Cs^{Fuel}_{y,cp} * \sum_{reg} E^{tot}_{y,cp,reg} \\ & + EF_{cp} * COPR_{y} * \sum_{reg} E^{tot}_{y,cp,reg}). \end{aligned} \tag{A.3}$$

Installed Capacities

The installed capacities in each modeled year step along a pathway are based on the residual capacities $Ca^{residual}_{y,cp,reg}$ from the year step before. Additionally, the early retired capacities $Ca^{early\ retired}_{y,cp,reg}$ and the new capacity expansions $Ca^{new}_{y,cp,reg}$ between the current and the last modeled year are considered as follows:

$$Ca_{y,cp,reg} = Ca^{residual}_{y,cp,reg} - Ca^{early\ retired}_{y,cp,reg} + Ca^{new}_{y,cp,reg}. \tag{A.4}$$

The residual capacity between two year steps considers also retirements of installed capacities that reach the end of their technical lifetime LT_{te}. In the first modeled year, they represent the existing capacities in the energy system. Early retired capacities are not economical anymore and have the

option to be phased out before the end of their lifetime. For the new capacity expansions, the user can also define a constant maximum of expansions per year or define lower $Ca^{min}_{y,cp}$ and upper expansion limits $Ca^{max}_{y,cp}$ for each modeled year step.

For a multi-region model, the regional allocation of capacities is influenced by two factors: the regional distribution $\mathrm{RD}^{Ca}_{cp,reg}$ and the regional availability $\mathrm{RA}_{cp,reg}$ which are multiplied to the total capacity in all regions $\mathrm{Ca}^{tot}_{y,cp}$ as stated in the following two equations:

$$Ca_{y,cp,reg} = \mathrm{RD}^{Ca}_{cp,reg} * \mathrm{Ca}^{tot}_{y,cp}, \tag{A.5}$$

$$Ca_{y,cp,reg} \leq \mathrm{RA}_{cp,reg} * \mathrm{Ca}^{tot}_{y,cp}. \tag{A.6}$$

Equation (A.5) can consider regionally fixed distributions of technologies, e.g., the distribution of existing power plants in the current system. The regional availability factor in equation (A.6) mainly aims at limiting technologies in certain regions. An exemplary application is to prevent the expansion of wind offshore capacities in regions without a coastline.

Power outputs

In general, the power output $\mathrm{P}^{out}_{y,te,reg,t}$ of each modeled time step t is computed by multiplying the input power $\mathrm{P}^{in}_{y,te,reg,t}$ with the efficiency $\mathrm{TEF}_{y,te}$ of the technology te:

$$\mathrm{P}^{out}_{y,te,reg,t} = \mathrm{TEF}_{y,te} * \mathrm{P}^{in}_{y,te,reg,t}. \tag{A.7}$$

For the integration of outages or planned maintenances, the output of a technology can be limited by an average technical availability factor $\mathrm{AvgTe}_{y,te}$ to

$$\mathrm{P}^{out}_{y,te,reg,t} \leq \mathrm{AvgTe}_{y,te} * \mathrm{Ca}_{y,te,reg}. \tag{A.8}$$

If the user assigns a time profile for a certain technology, the time step with the maximum power output is limited.

The energy input $E^{in}_{y,te,reg}$ and output $E^{out}_{y,te,reg}$ of each technology can then be calculated as the sum of the respective power over all time steps within a modeled year:

$$E^{out}_{y,te,reg} = \sum_{t} \mathrm{P}^{out}_{y,te,reg,t}, \tag{A.9}$$

$$E^{in}_{y,te,reg} = \sum_{t} \mathrm{P}^{in}_{y,te,reg,t}. \tag{A.10}$$

If not all hourly time steps of one year are explicitly modeled, the energy is scaled by a weighting factor. The total output energy can be limited by minimum and maximum full load hours as upper or lower boundaries as follows:

$$FLH^{min}_{y,te} * \mathrm{Ca}^{tot}_{y,te} \leq E^{out}_{y,te} \leq FLH^{max}_{y,te} * \mathrm{Ca}^{tot}_{y,te}. \tag{A.11}$$

For the power and energy output of technologies, further constraints can be added by the user. The output can be fixed by providing a time series for a technology or in multi-region models a separate time profile for each region. These time profiles also consider must run requirements and the model calculates curtailments if allowed for certain technologies.

Additionally, the model can link two technologies $te1$ and $te2$ by a fixed output factor $TLINK^{out}_{y,te1,te2}$ or capacity factor $TLINK^{Ca}_{y,te1,te2}$. If a certain technology generates an output or its capacity is increased, the linked technology follows accordingly adjusted by the value of the factor. The respective equations are defined as follows:

$$P^{out}_{y,te1,reg,t} = TLINK^{out}_{y,te1,te2} * P^{out}_{y,te2,reg,t}, \tag{A.12}$$

$$Ca_{y,te1,reg} = TLINK^{Ca}_{y,te1,te2} * Ca_{y,te2,reg}. \tag{A.13}$$

Energy Storage

Storage technologies are also implemented by the concept of conversion processes and commodities. To model the storage level $E_{y,st,reg,t}$ and its change between different modeled time steps Δt, the energy calculation of conversion processes flagged as energy storage deviate from other technologies. The equation considers the self-discharge by the self-discharge rate $SDR_{y,st}$, the storage efficiency $TEF_{y,st}$ to store the input power $P^{in}_{y,st,reg,t}$, and the time-dependent efficiency $TEF^{timedep}_{y,st,t}$ to deliver the output power $P^{out}_{y,st,reg,t}$ as follows:

$$\begin{aligned} E_{y,st,reg,t} = E_{y,st,reg,t-1} * \left(1 - SDR_{y,st} * \Delta t\right) \\ + TEF_{y,st} * P^{in}_{y,st,reg,t} * \Delta t \\ - \frac{P^{out}_{y,st,reg,t} * \Delta t}{TEF^{timedep}_{y,st,t}} \end{aligned} . \tag{A.14}$$

Storage processes also consider average availabilities $\mathrm{AvgTe}_{y,st}$. Furthermore, the user can dimension the storage by using the ratio between input power capacity $Ca_{y,st,reg}$ and storable energy $Ca^{storage}_{y,st,reg}$ (C-Rate). The minimum $CRATE^{min}_{y,st}$ and maximum $CRATE^{max}_{y,st}$ C-Rate influence the dimensioning by the following equation:

$$Ca^{storage}_{y,st,reg} * CRATE^{min}_{y,st} \leq Ca_{y,st,reg} \leq Ca^{storage}_{y,st,reg} * CRATE^{max}_{y,st} . \tag{A.15}$$

Transport Equations

The model includes several transport equations to consider the exchange of commodities between different regions in a multi-region model. They can be used to model grids such as the electricity grid or the gas grid. In general, the total transport capacity is calculated by summing all transport links between two regions and multiply them by 0.5 in case of unsymmetrical lines. In case the user defines symmetric lines, the capacity $Trp_{y,com,reg1,reg2}$ of a transported commodity com between two regions $reg1$ and $reg2$ does not depend on the direction:

$$Trp_{y,com,reg1,reg2} = Trp_{y,com,reg2,reg1}. \tag{A.16}$$

The output power of a transport line $P^{out,trans}_{y,com,reg1,reg2,t}$ depends on its input power $P^{in,trans}_{y,com,reg1,reg2,t}$, the line length LE, and the specific losses $LL_{y,com}$

$$P^{out,trans}_{y,com,reg1,reg2,t} = P^{in,trans}_{y,com,reg1,reg2,t} * (1 - LE * LL_{y,com}), \tag{A.17}$$

while the input power must be lower than the line capacity at every time step

$$P^{in,trans}_{y,com,reg1,reg2,t} \leq Trp_{y,com,reg1,reg2}. \tag{A.18}$$

The total transport balance per time step for a region $reg0$ is then calculated by considering the import from all neighboring regions $reg1$ and the export to all neighboring regions $reg2$:

$$Trp^{tot}_{y,com,reg0,t} = \sum_{reg1} P^{in,trans}_{y,com,reg0,reg1,t} - \sum_{reg2} P^{out,trans}_{y,com,reg2,reg0,t}. \quad (A.19)$$

For statistical regions, the transported energy of each region or in total for all regions is determined by summing the power over all time steps, similar to equation (A.9).

Global Constraints

Last, the model includes some overarching constraints that consider the emissions and the power balance.

The calculation of annual emissions Em_y, e.g. CO_2 emissions, requires the output energy of a conversion process $E^{out}_{cp,y}$ and its specific emission factor $EF_{y,cp}$:

$$Em_y = \sum_{cp} \left(E^{out}_{y,cp} * EF_{y,cp}\right). \quad (A.20)$$

To limit these emissions, the user can choose between the definition of annual emission limits EL_y and a total budget for the entire pathway EL:

$$Em_y \leq EL_y. \quad (A.21)$$

$$\sum_{y} Em_y \leq EL. \quad (A.22)$$

For the operation of an energy system, demand and generation must be balanced at any time. This important constraint is considered in the power balance equation. In this equation, optional slack variables $P^{in,slack}_{y,com,reg,t}$ and $P^{out,slack}_{y,com,reg,t}$ can avoid infeasibility of models:

$$\sum_{cp} P^{in}_{y,cp,reg,t} + P^{in,slack}_{y,com,reg,t} + Trp^{tot}_{y,com,reg,t} = \sum_{cp} P^{out}_{y,cp,reg,t} + P^{out,slack}_{y,com,reg,t}. \quad (A.23)$$

Appendix B. Model Assumptions

Table B-1. Exploration and import prices for the modeled resources and their specific emissions.

Energy resource	Exploration €/MWh		Import €/MWh		Emissions kg CO_2/kWh	Sources
	2015	2050	2015	2050		
Natural gas	9.90	17.46	19.80	34.92	0.2	[229][230][203]
Crude oil	22.14	42.52	29.52	56.70	0.28	[229][230][203]
Hard coal	7.37	8.20	11.16	12.42	0.34	[229][230][203]
Lignite	3.10	5.80			0.4	[229][230][203]
Uranium	8	8				[231]
Biomass	42	7				[231]

Table B-2. Efficiency, lifetime, and price assumptions for the modeled technologies for the year 2015, based on [232].

Technology	Efficiency %	Lifetime a	CAPEX €/kW	O&M Fix % CAPEX	O&M Var €/MWh	Storage €/kWh
Gas	48.5	30	700	2.25	7	
Hard coal	45	40	1600	2.5	3.6	
Lignite	42	40	2000	2.5	4.5	
Oil	44	40	850	2.1	1.5	
Nuclear	33	40	4500	2.1	8	
Hydropower	100	60	3850	1.375	4.5	
Wind onshore	100	20	1200	2.7	0	
Wind offshore	100	20	3080	3.7	0	
Photovoltaic	100	25	1000	1.7	0	
Geothermal	15.6	30	8366.7	1.77	0	
Waste	27	25	6080	3	6.9	
Biomass	35	23.75	3635	2.575	4.65	
Marine	100	20	10006	3.23	0	
Battery	86	10	390	1.4	2.6	752
Pumped hydro	80	60	2500	1.5	0	

Table B-3. Projections of efficiency, lifetime, and price assumptions of the modeled technologies for the years 2030 and 2045, based on [232].

Technology	Efficiency %		Lifetime a	CAPEX €/kW		O&M Fix % CAPEX		O&M Var €/MWh	Storage €/kWh	
Gas combined cycle	62	62.5	30	850		2.5		2		
Gas single cycle	43	44.5	30	550		3		11		
Hard coal	48		40	1600		2.5		3.6		
Lignite	47		40	2000		2.5		4.5		
Oil	44		40	850		2.1		1.5		
Hydropower	100		60	3922.5		1.375		4.5		
Wind onshore	116	140	25	1000	850	2.2	1.8	0		
Wind offshore	109	118	30	2280	1940	3	2.55	0		
Photovoltaic	123	130	25	520	445	1.7		0		
Geothermal	16.6	17.4	30	6570	5968	2	2.2	0		
Waste	34	39.5	25	5240	4705	3		6.9		
Biomass	39	41.9	23.75	2650	2276	2.575		4.65		
Marine	100		20	3646	2156	3.48	4.11	0		
Battery	86	96	10	110		1.4		2.6	250	247
Pumped hydro	85	89	60	2500		1.5		0		
Electrolyzer	65.5	70.5	20	943	482	2		0		
Hydrogen storage	98		20	256		4		0	0.24	

Appendix C. Clustering Results and Geographic Regions

Table C-1. Assigned archetypes for not clustered countries.

Country	Archetype	Country	Archetype
Antigua and Barbuda	Archetype 12	Micronesia	Archetype 9
Bahrain	Archetype 15	Montenegro	Archetype 5
Bhutan	Archetype 5	Myanmar	Archetype 2
Brunei	Archetype 15	Nauru	Archetype 9
Burundi	Archetype 3	Nepal	Archetype 5
Cuba	Archetype 9	Rwanda	Archetype 3
Democratic People's Republic of Korea	Archetype 6	Saint Lucia	Archetype 9
Democratic Republic of the Congo	Archetype 3	Saint Vincent and Grenadines	Archetype 9
Djibouti	Archetype 1	Serbia	Archetype 11
Dominica	Archetype 9	Sierra Leone	Archetype 2
Equatorial Guinea	Archetype 8	Singapore	Archetype 9
Eritrea	Archetype 1	Solomon Islands	Archetype 1
Grenada	Archetype 9	Somalia	Archetype 1
Guinea-Bissau	Archetype 1	South Sudan	Archetype 4
Haiti	Archetype 1	Sudan	Archetype 3
Iceland	Archetype 14	Swaziland	Archetype 4
Kiribati	Archetype 9	Syria	Archetype 10
Lesotho	Archetype 3	Timor-Leste	Archetype 2
Libya	Archetype 10	Trinidad and Tobago	Archetype 15
Macedonia	Archetype 11	Turkmenistan	Archetype 6
Madagascar	Archetype 2	Tuvalu	Archetype 7
Maldives	Archetype 9	Venezuela	Archetype 7
Mauritania	Archetype 1	Yemen	Archetype 4

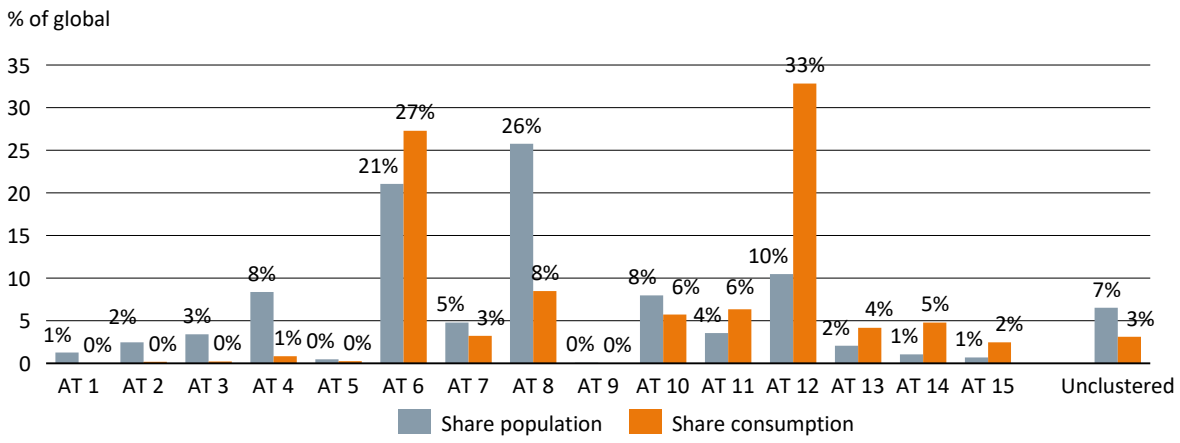

Figure C-1. Global share of population and electricity consumption for each archetype and the non-clustered countries.

Table C-2. *UN* subregion classification for clustered countries [57].

***UN* subregion**	**Countries**
Reg 1: Australia and New Zealand	Australia, New Zealand
Reg 2: Central Asia	Kazakhstan, Kyrgyzstan, Tajikistan, Uzbekistan
Reg 3: Eastern Asia	China, Japan, Republic of Korea, Mongolia
Reg 4: Eastern Europe	Belarus, Bulgaria, Czech Republic, Hungary, Moldova, Poland, Romania, Russia, Slovakia, Ukraine
Reg 5: Latin America and the Caribbean	Argentina, Bahamas, The, Barbados, Belize, Bolivia, Brazil, Chile, Colombia, Costa Rica, Dominican Republic, Ecuador, El Salvador, Guatemala, Guyana, Honduras, Jamaica, Mexico, Nicaragua, Panama, Paraguay, Peru, Saint Kitts and Nevis, Suriname, Uruguay
Reg 6: Melanesia and Polynesia	Fiji, Papua New Guinea, Vanuatu, Samoa, Tonga
Reg 7: Northern Africa	Algeria, Egypt, Morocco, Tunisia
Reg 8: Northern America	Canada, United States
Reg 9: Northern Europe	Denmark, Estonia, Finland, Ireland, Latvia, Lithuania, Norway, Sweden, United Kingdom
Reg 10: South-eastern Asia	Cambodia, Indonesia, Laos, Malaysia, Philippines, Thailand, Vietnam
Reg 11: Southern Asia	Afghanistan, Bangladesh, India, Iran, Pakistan, Sri Lanka
Reg 12: Southern Europe	Albania, Bosnia and Herzegovina, Croatia, Greece Italy, Malta, Portugal, Slovenia, Spain
Reg 13: Sub-Saharan Africa	Angola, Benin, Botswana, Burkina Faso, Cameroon, Cape Verde, Central African Republic, Chad, Comoros, Congo (Brazzaville), Cote d'Ivoire (Ivory Coast), Ethiopia, Gabon, Gambia, The, Ghana, Guinea, Kenya, Liberia, Malawi, Mali, Mauritius, Mozambique, Namibia, Niger, Nigeria, Sao Tome and Principe, Senegal, Seychelles, South Africa, Tanzania, Togo, Uganda, Zambia, Zimbabwe
Reg 14: Western Asia	Armenia, Azerbaijan, Cyprus, Georgia, Iraq, Israel, Jordan, Kuwait, Lebanon, Oman, Qatar, Saudi Arabia, Turkey, United Arab Emirates
Reg 15: Western Europe	Austria, Belgium, France, Germany, Luxembourg, Netherlands, Switzerland

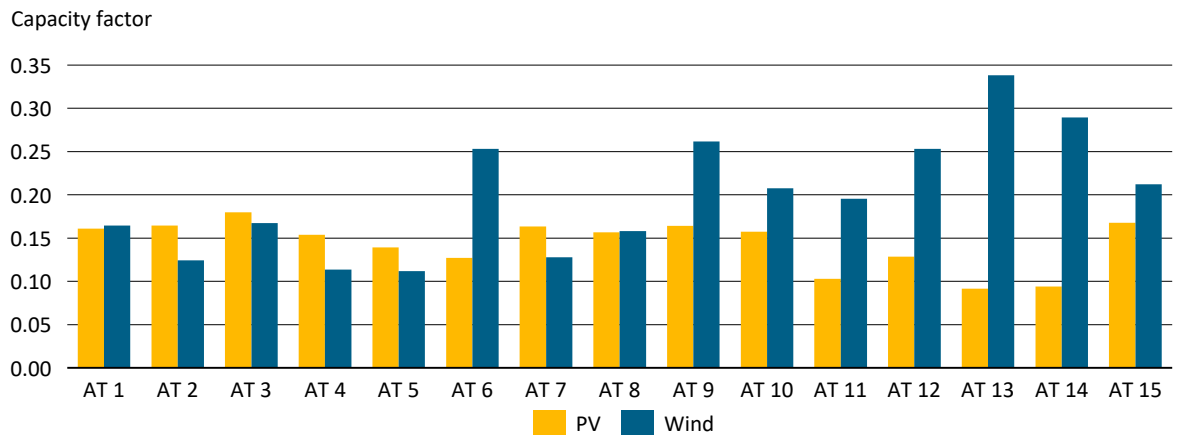

Figure C-2. Wind and PV capacity factors of each archetype.

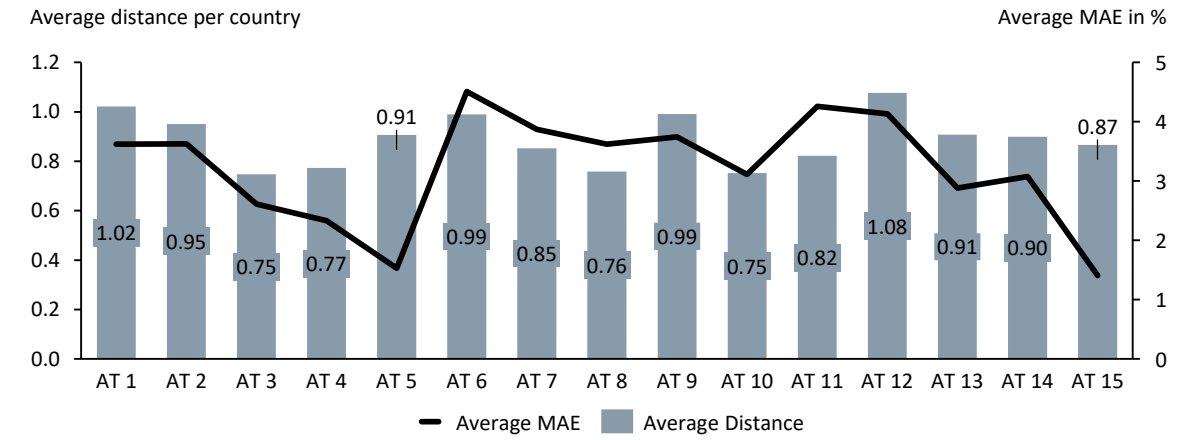

Figure C-3. Average distance calculated by the K-means algorithm for each archetype per country compared to the average MAE calculated after modeling.

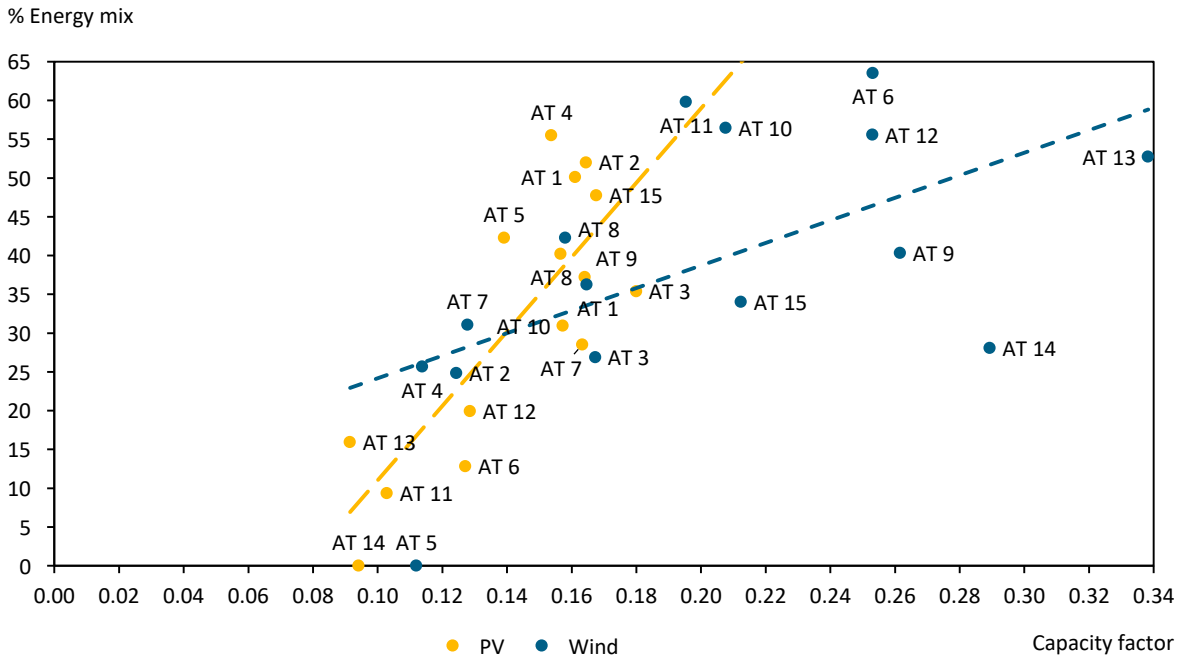

Figure C-4. Capacity factor and share in the energy mix for PV and wind.

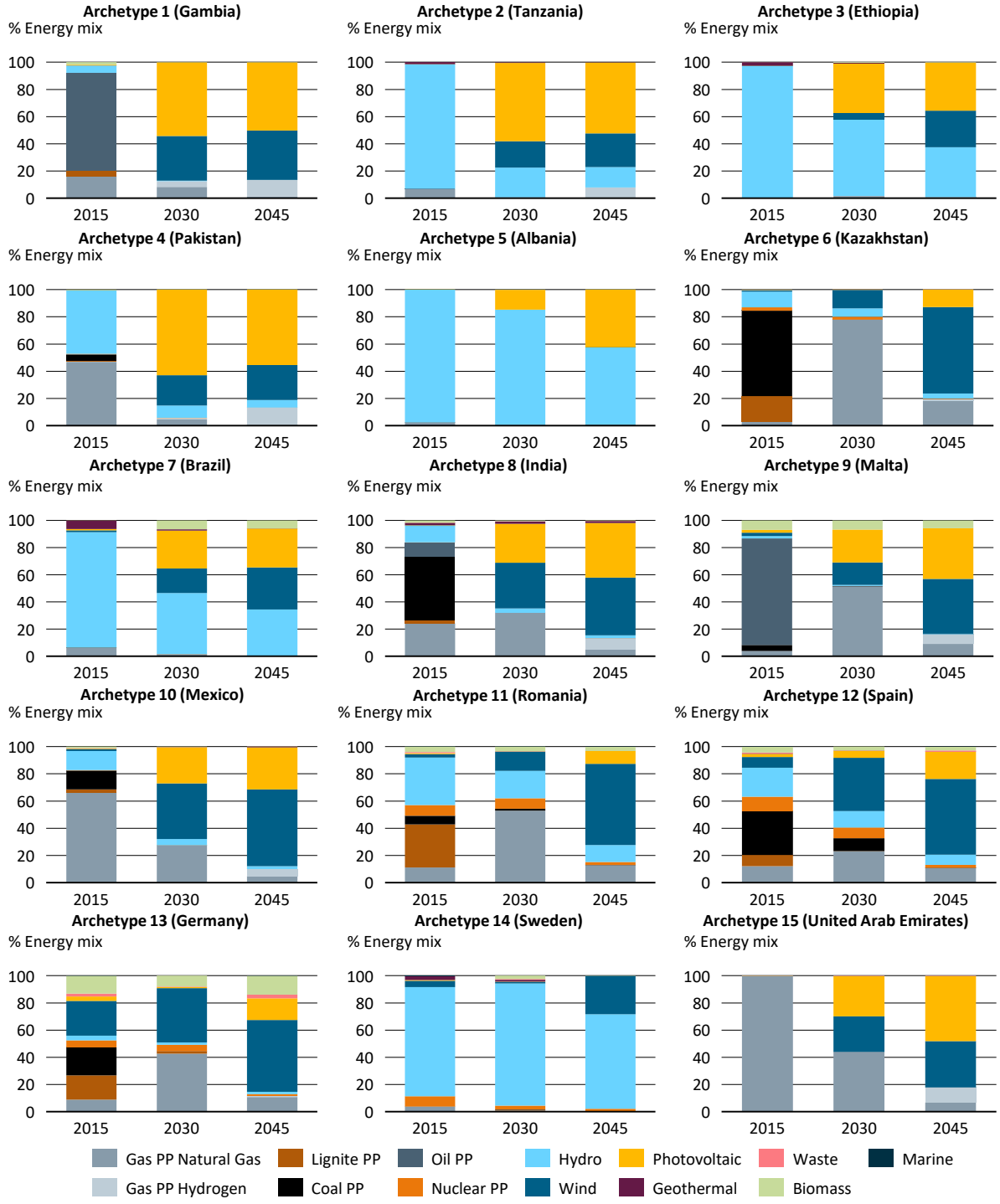

Figure C-5. The energy mix of all 15 archetypes in the Base scenario for the three modeled years.

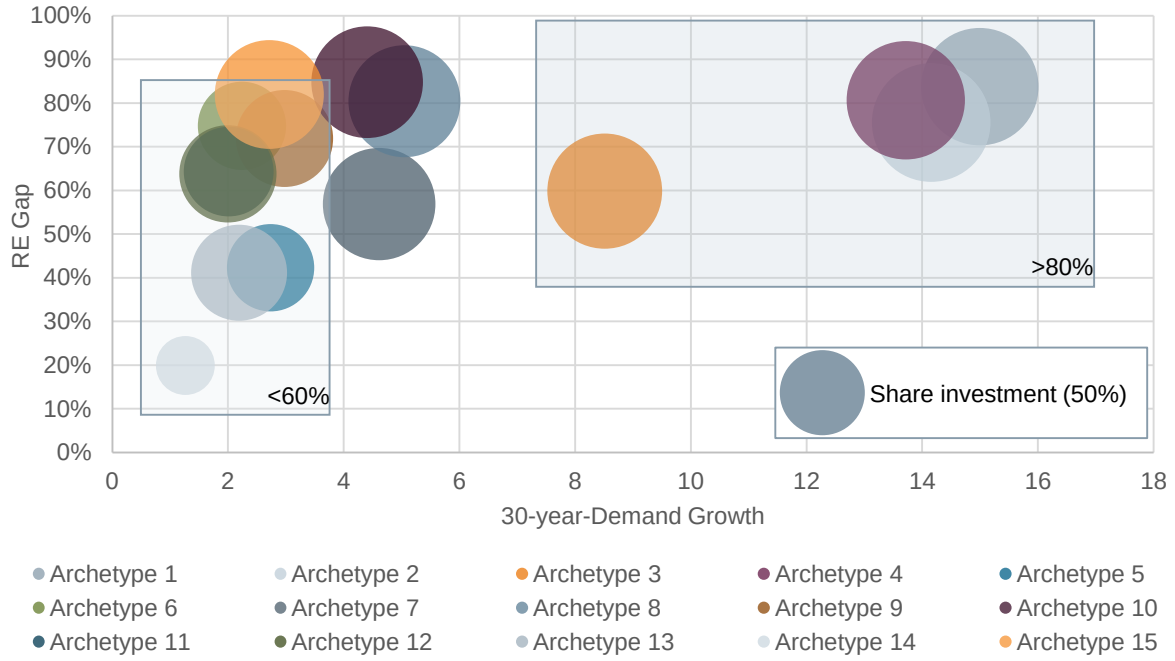

Figure C-6. Share of investment costs (CAPEX) compared to total costs (TOTEX).

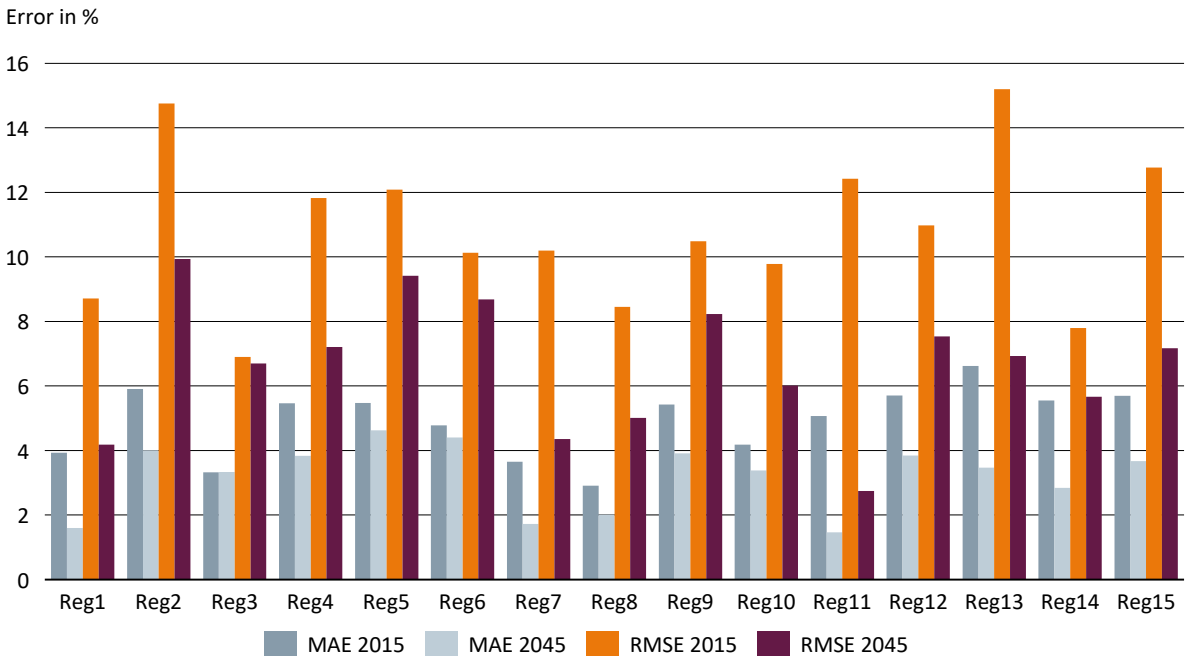

Figure C-7. MAE and RMSE for the 15 geographic subregions in 2015 and 2045.

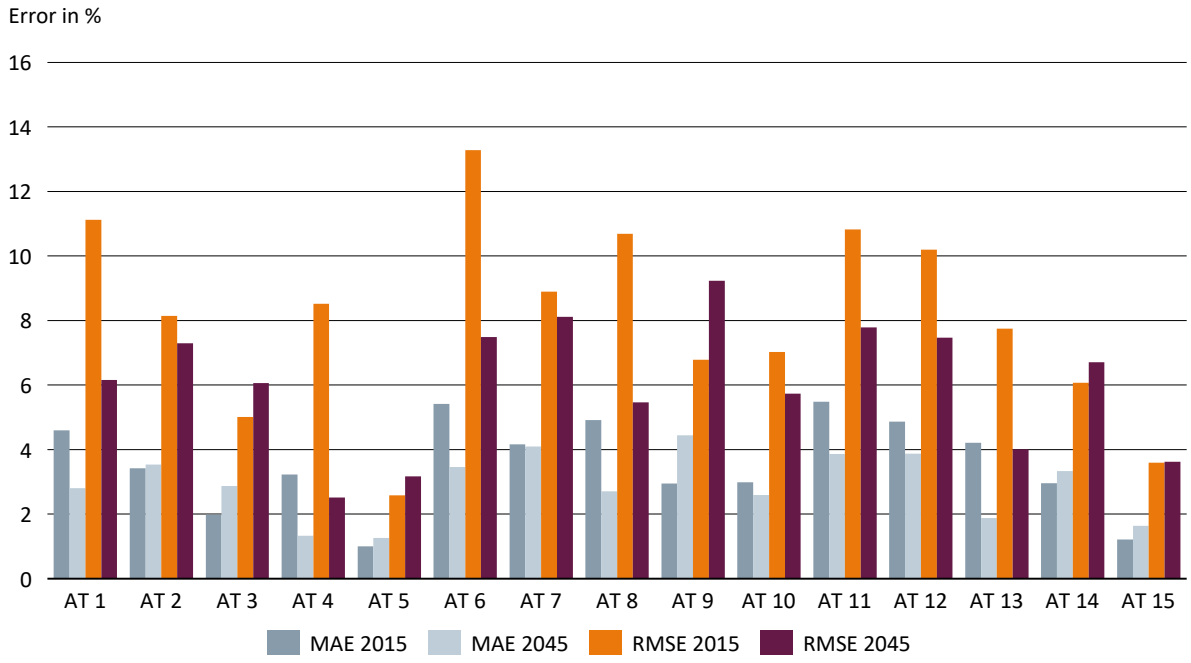

Figure C-8. MAE and RMSE for the 15 archetypes in 2015 and 2045.

Appendix D. Additional Results Evaluating the Use Cases and the Regional Clustering

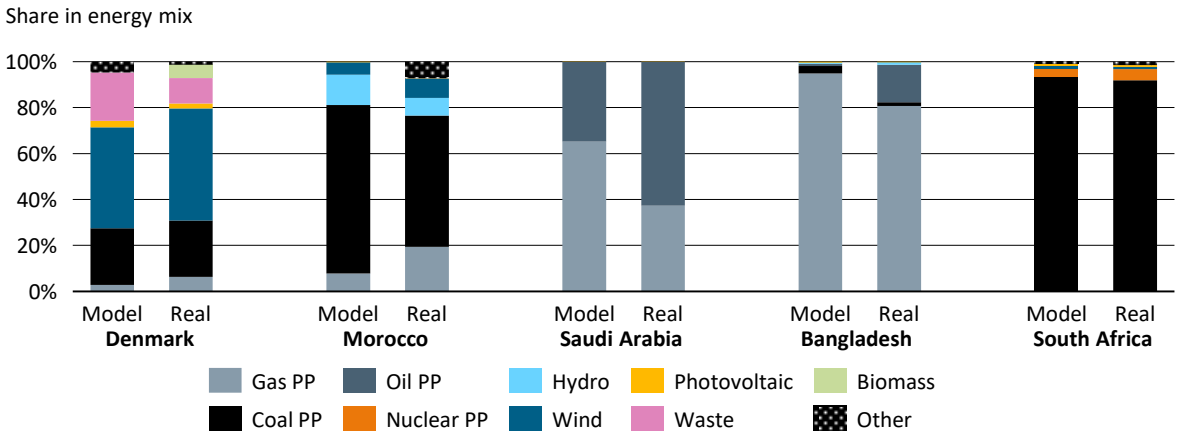

Figure D-1. Validation of the year 2015 for all three use cases and the five modeled countries with real data from [94].

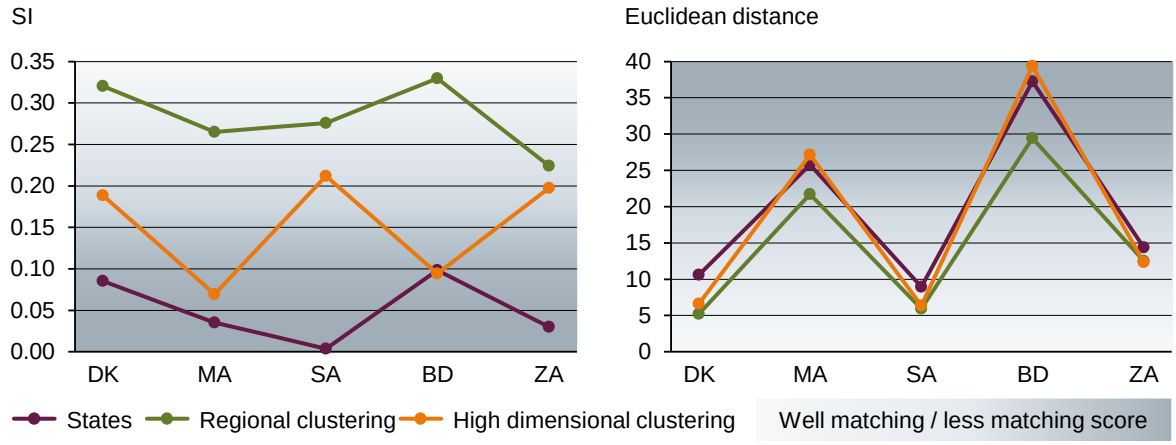

Figure D-2. Analysis of the different classification approaches by SI score and Euclidean distance for the evaluated five countries and applied to the data set with a reduced time dimension.

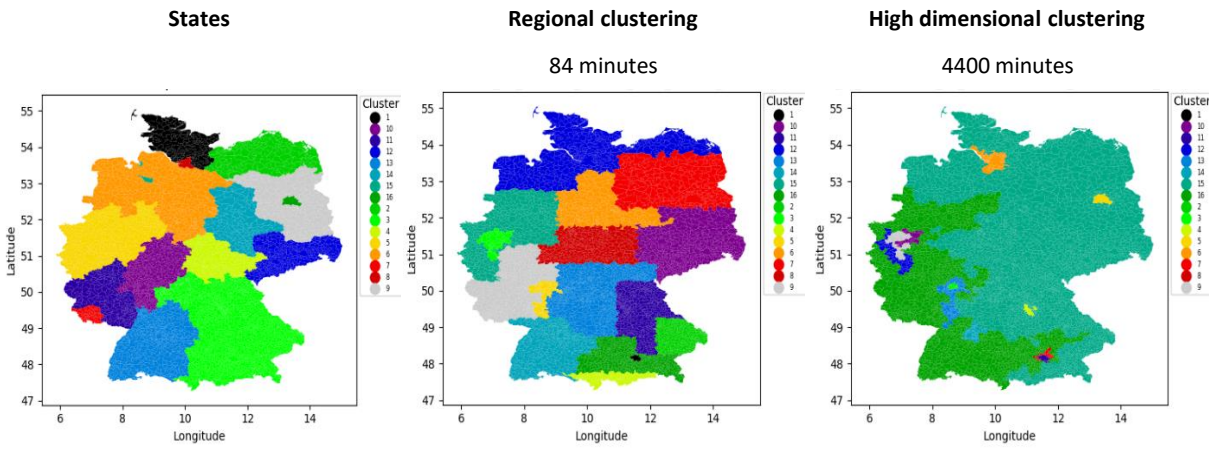

Figure D-3. Comparison of the three classifications for the example of Germany including exemplary computation times of the regional clustering algorithm.

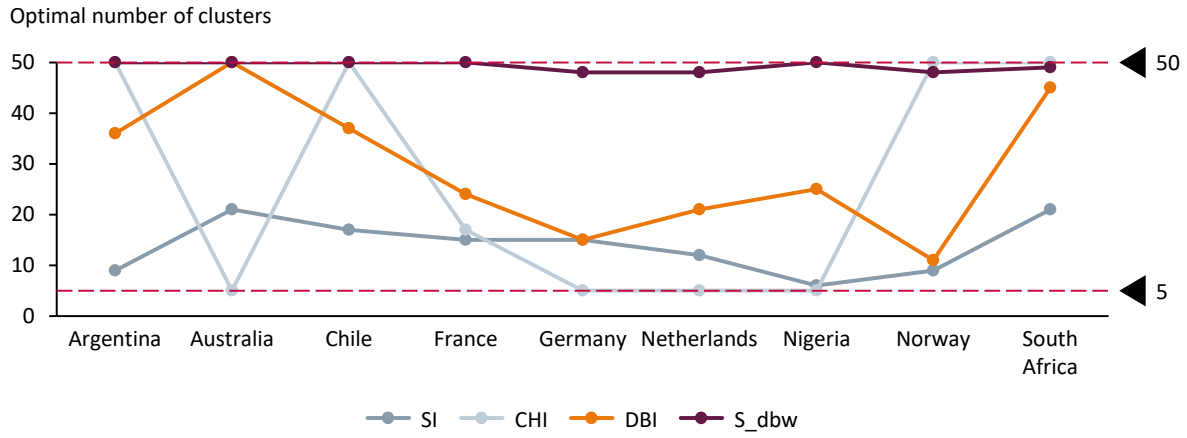

Figure D-4. The optimal number of clusters for four CVI in different exemplary countries evaluated for the interval between 5 and 50.

D.1. Use case 1: Grid Topology

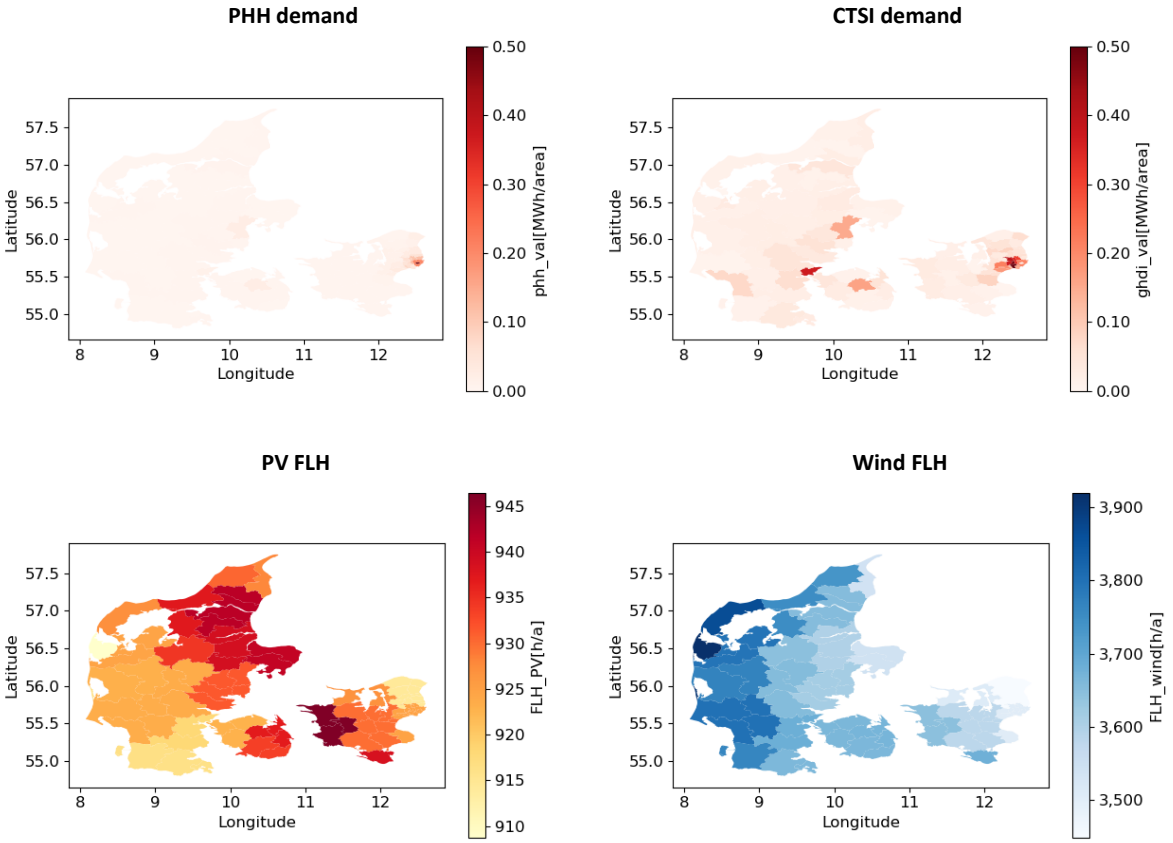

Figure D-5. Spatial data basis for Denmark: normalized PHH and CTSI demand and FLH of wind and PV.

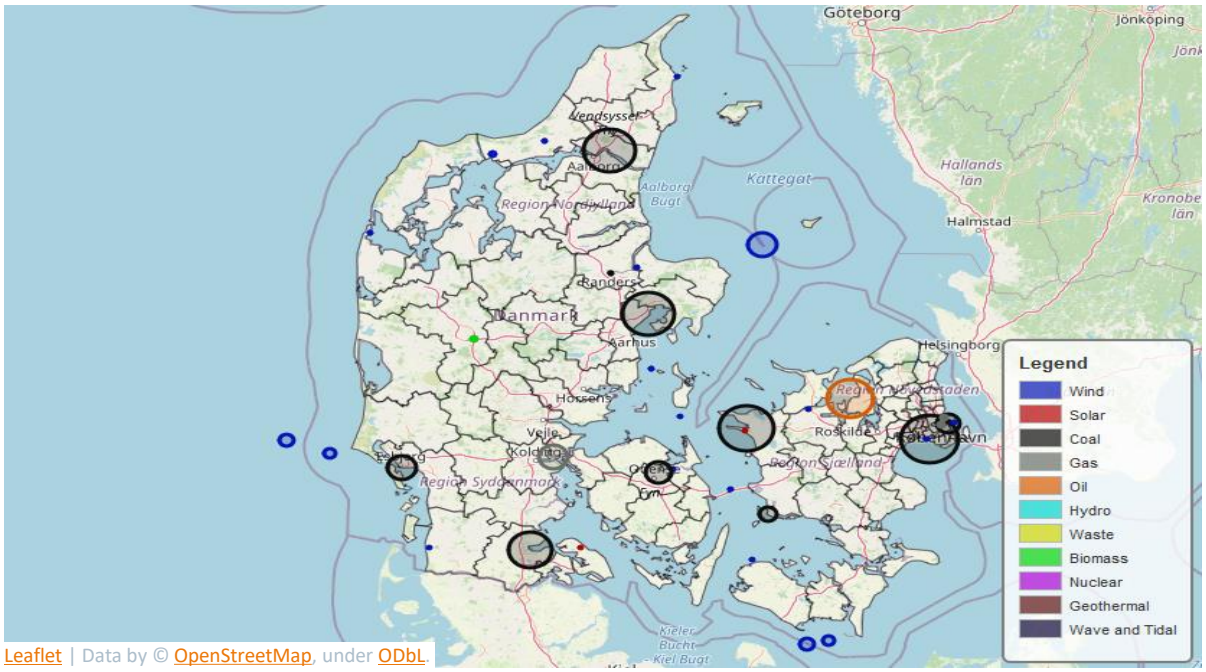

Figure D-6. Spatial data basis for Denmark: distribution and types of power plants based on [156].

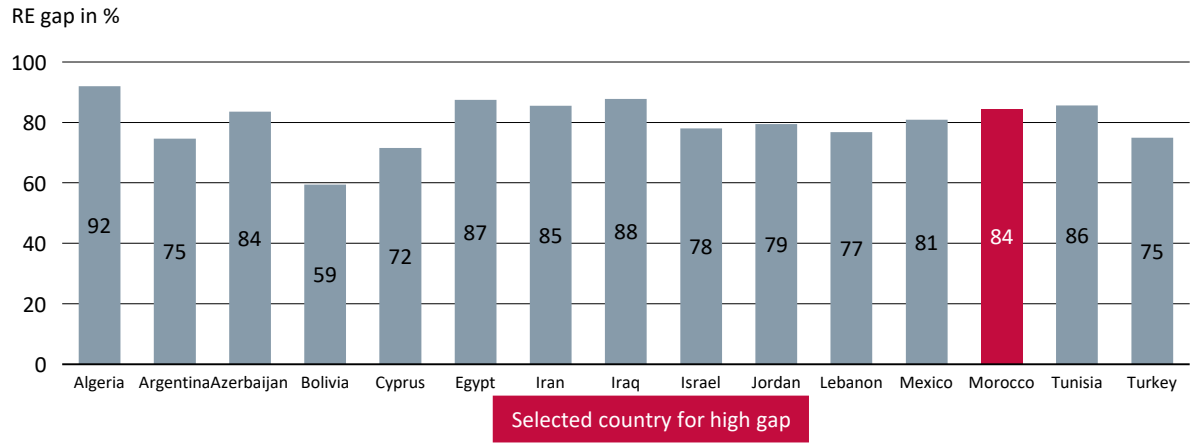

Figure D-7. $RE\ Gap$ of all countries in AT 10.

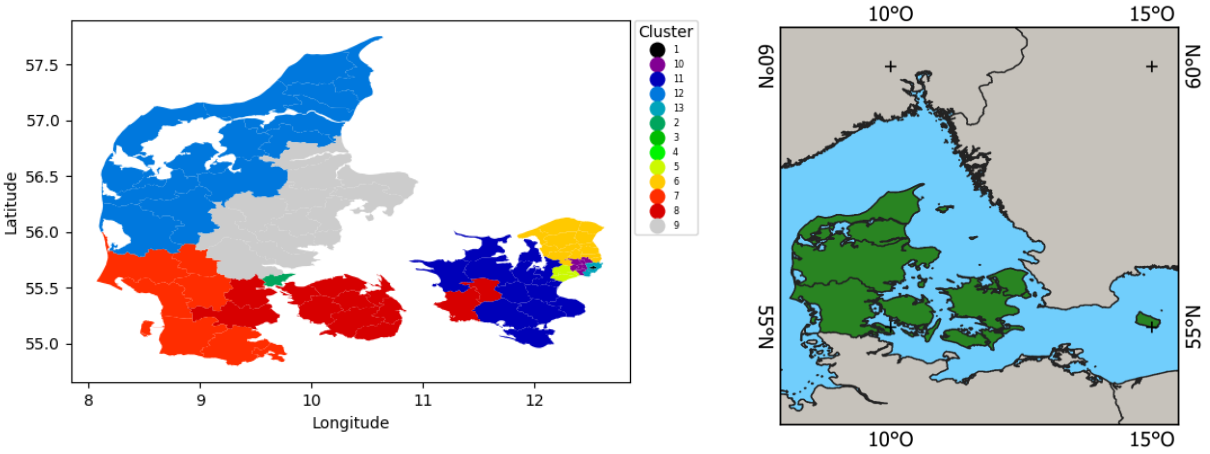

Figure D-8. Comparison of clustering results and administrative regions on level 1 in Denmark.

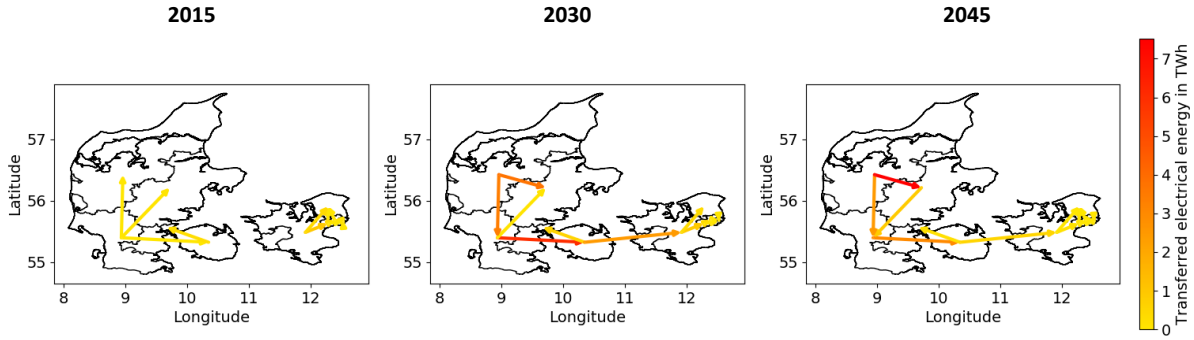

Figure D-9. Transported electricity on grid lines between clustered regions in Denmark for the Base scenario from 2015 until 2045

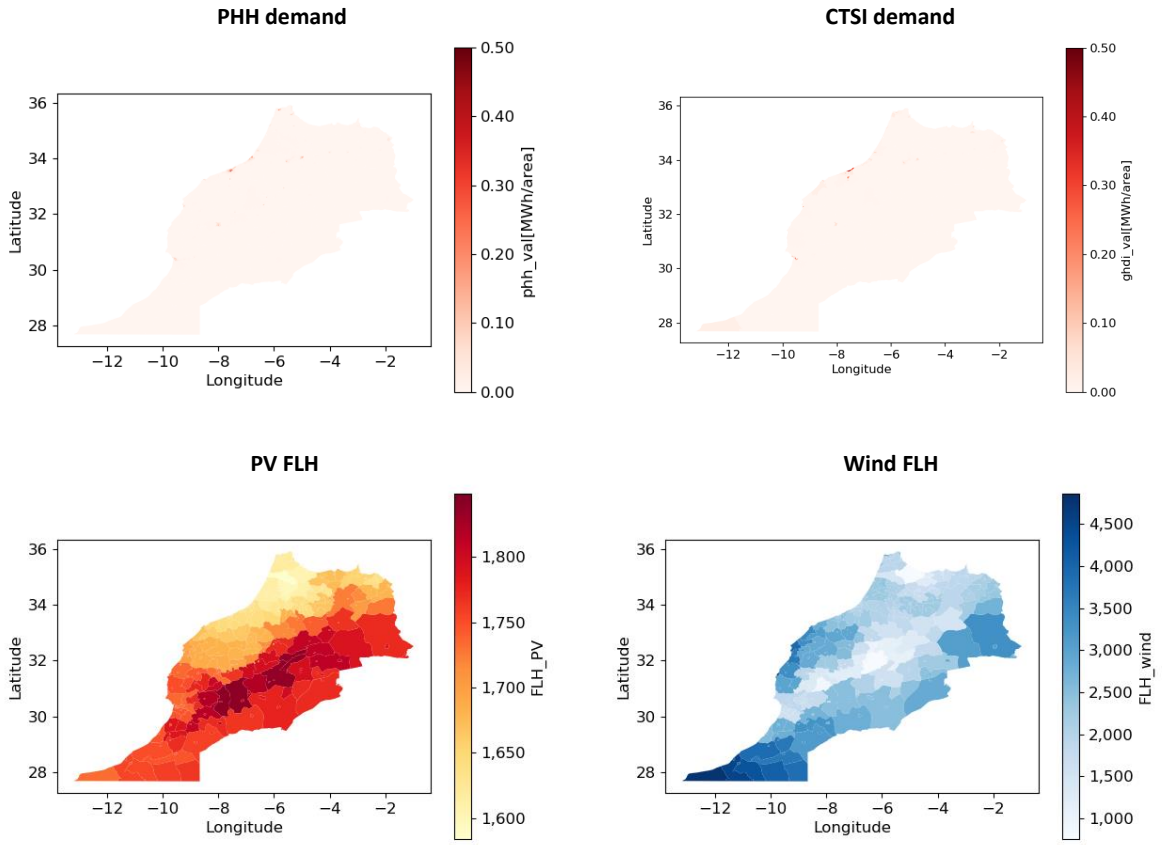

Figure D-10. Spatial data basis for Morocco: normalized PHH and CTSI demand and FLH of wind and PV.

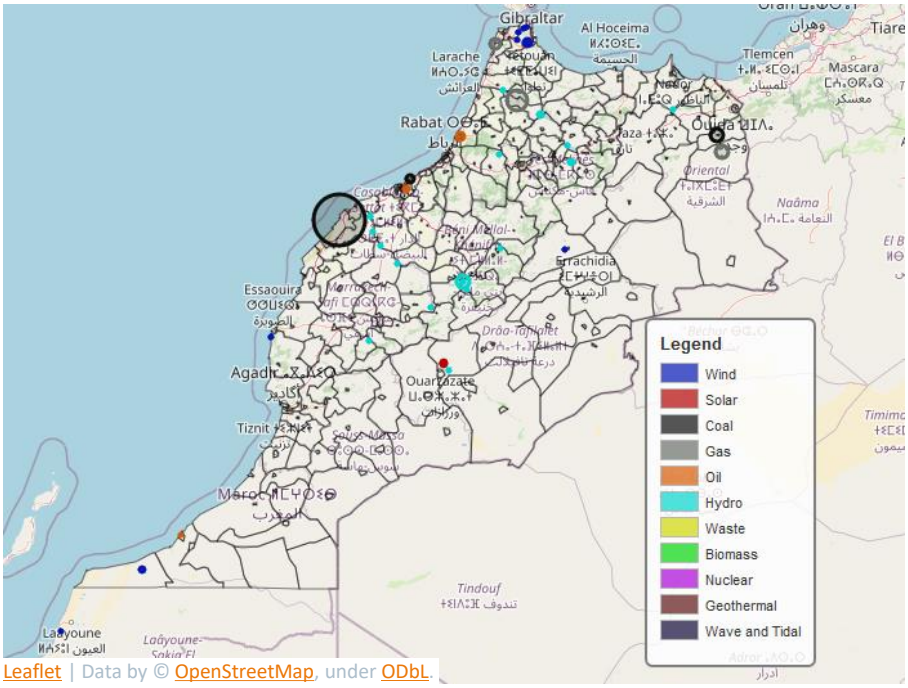

Figure D-11. Spatial data basis for Morocco: distribution and types of power plants based on [156].

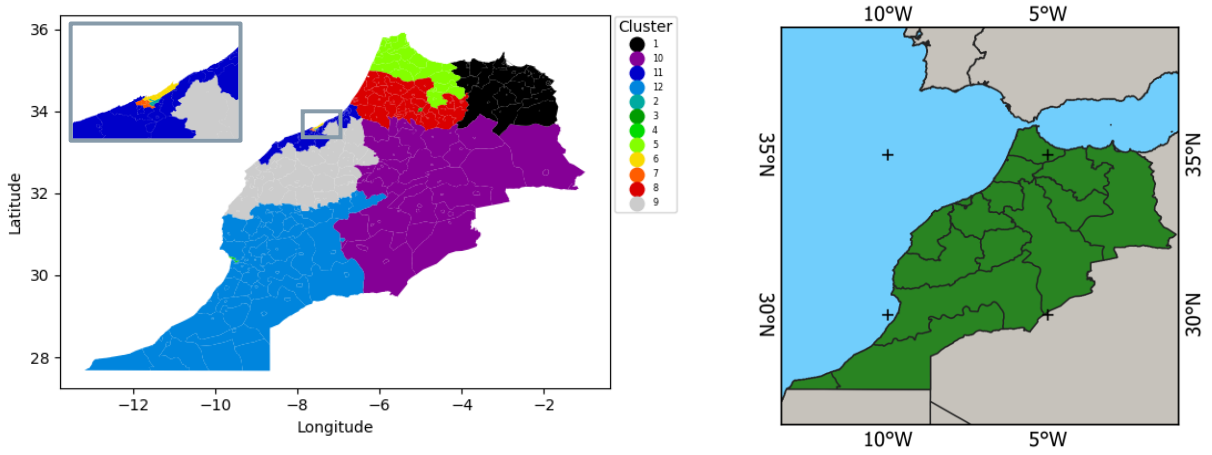

Figure D-12. Comparison of clustering results and administrative regions on level 1 in Morocco.

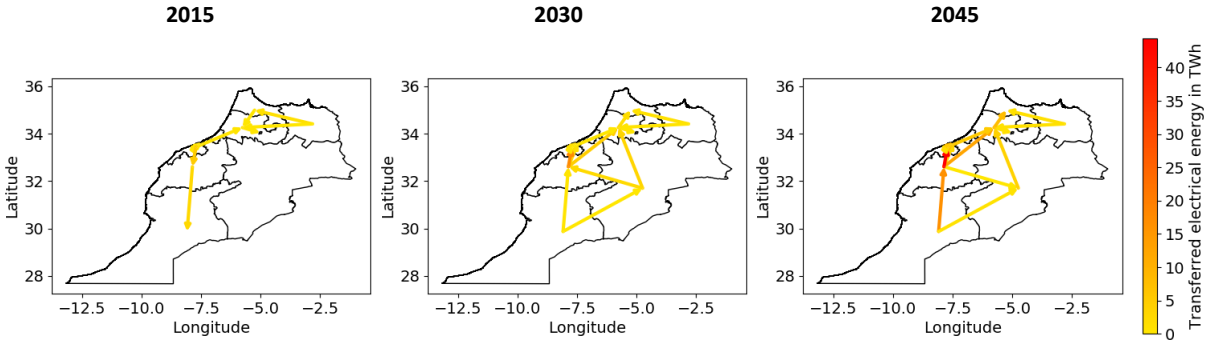

Figure D-13. Transported electricity on grid lines between clustered regions in Morocco for the Base scenario from 2015 until 2045.

D.2. Use Case 2: Green Hydrogen Production

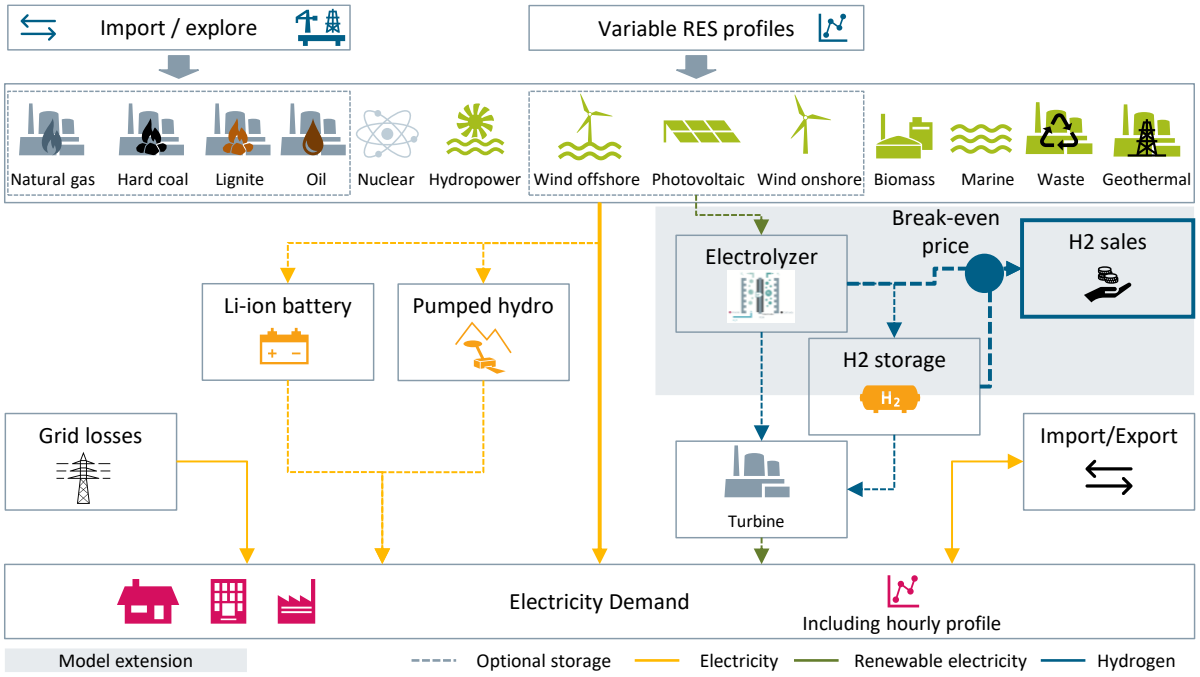

Figure D-14. Implementation of H_2 break-even price approach in the overall model framework.

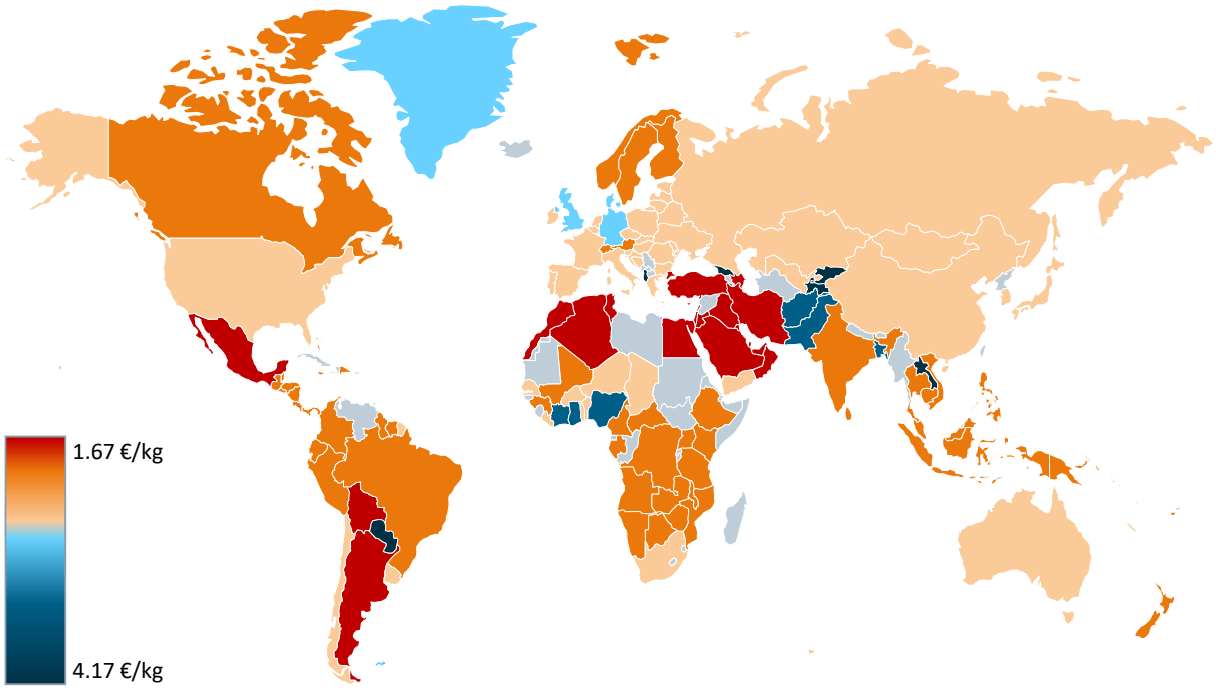

Figure D-15. Global distribution of break-even prices for the 15 archetypes.

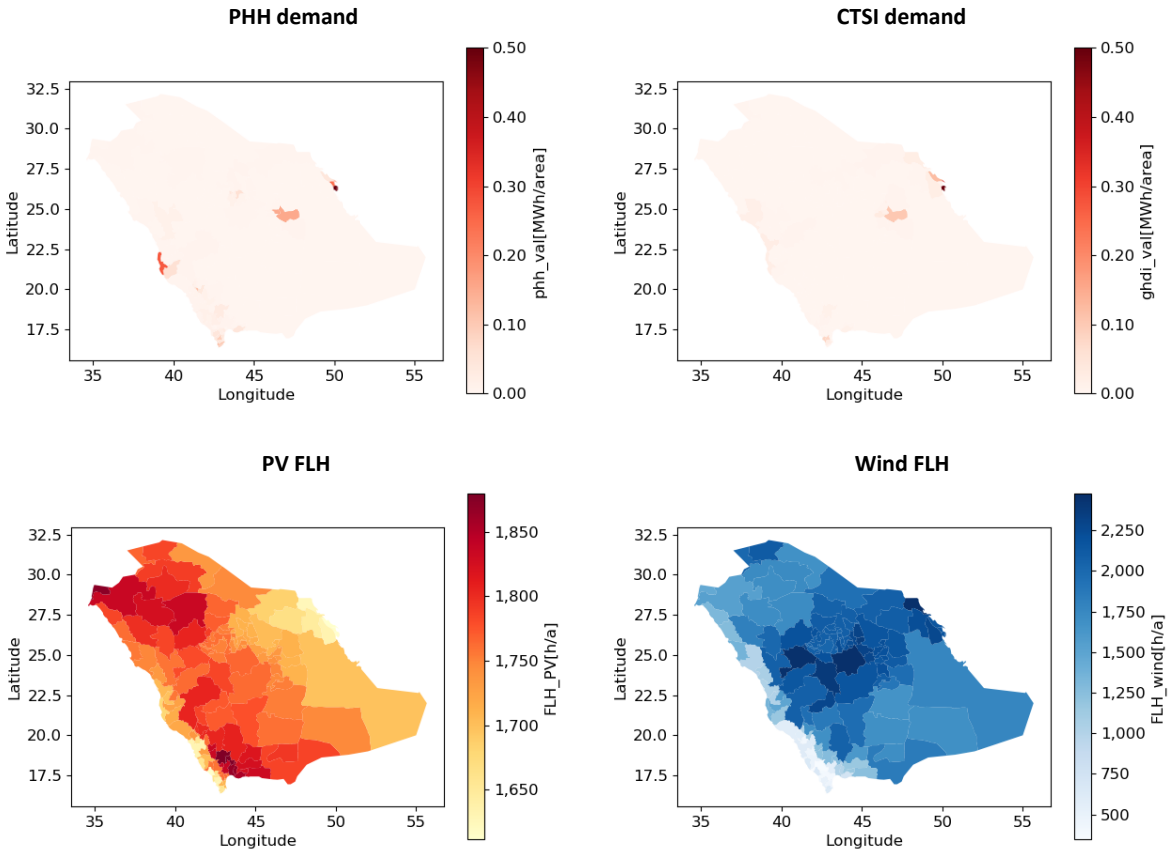

Figure D-16. Spatial data basis for Saudi Arabia: normalized PHH and CTSI demand and FLH of wind and PV

.

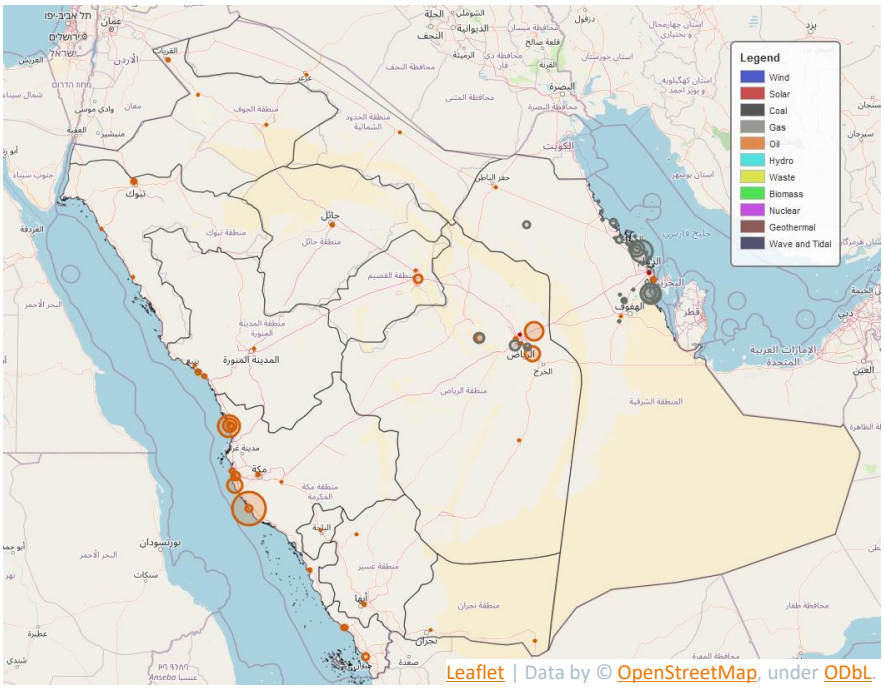

Figure D-17. Spatial data basis for Saudi Arabia: distribution and types of power plants based on [156].

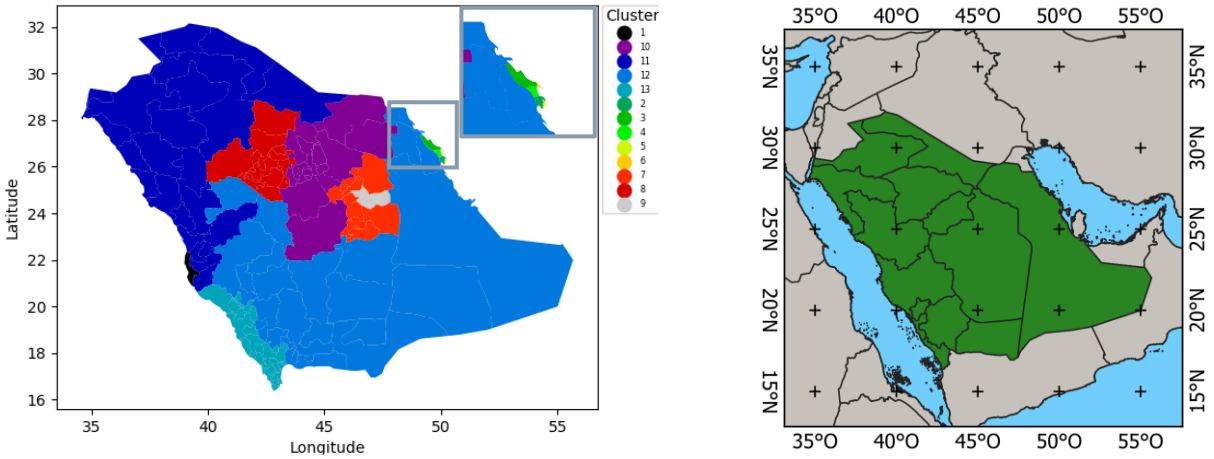

Figure D-18. Comparison of clustering results and administrative regions on level 1 in Saudi Arabia.

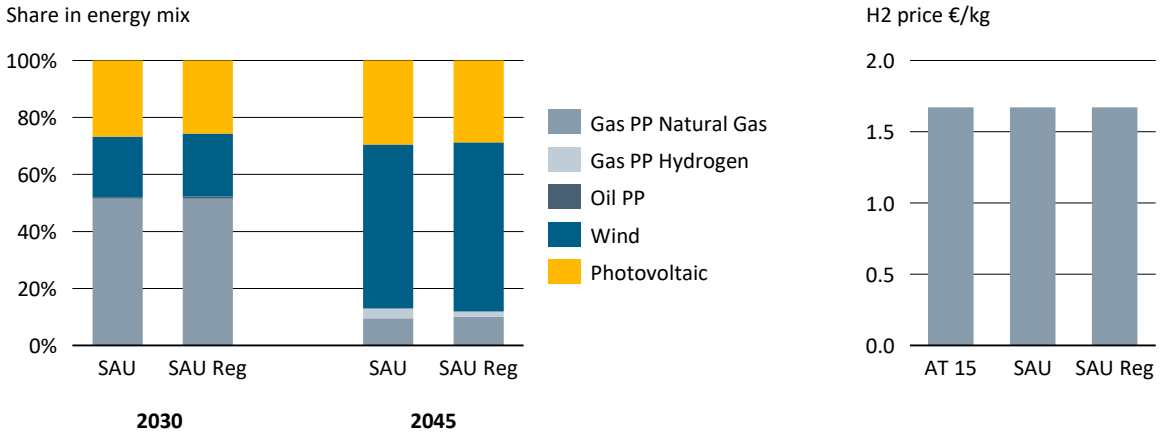

Figure D-19. Validation of the modeling approach for Saudi Arabia by comparing the energy mix and the break-even prices of the archetype (AT 15), country (SAU), and multi-region results (SAU Reg).

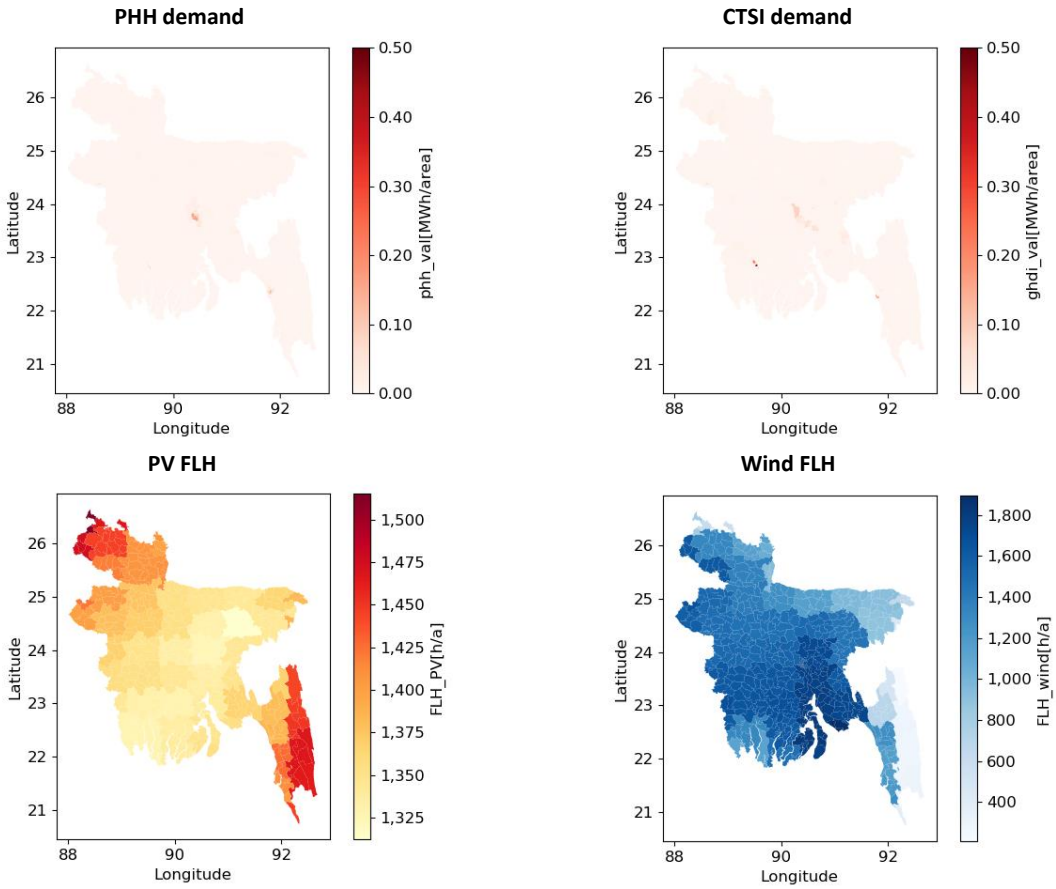

Figure D-20. Spatial data basis for Bangladesh: normalized PHH and CTSI demand and FLH of wind and PV.

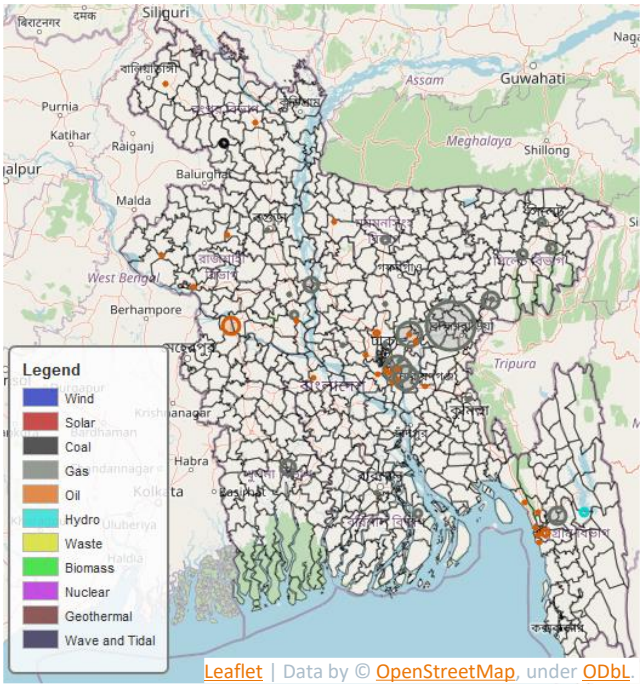

Figure D-21. Spatial data basis for Bangladesh: distribution and types of power plants based on [156].

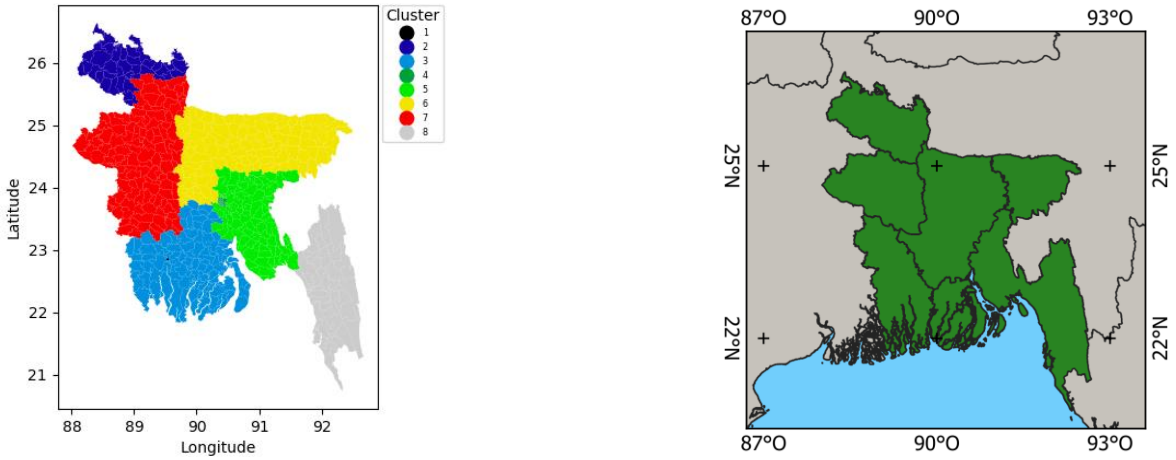

Figure D-22. Comparison of clustering results and administrative regions on level 1 in Bangladesh.

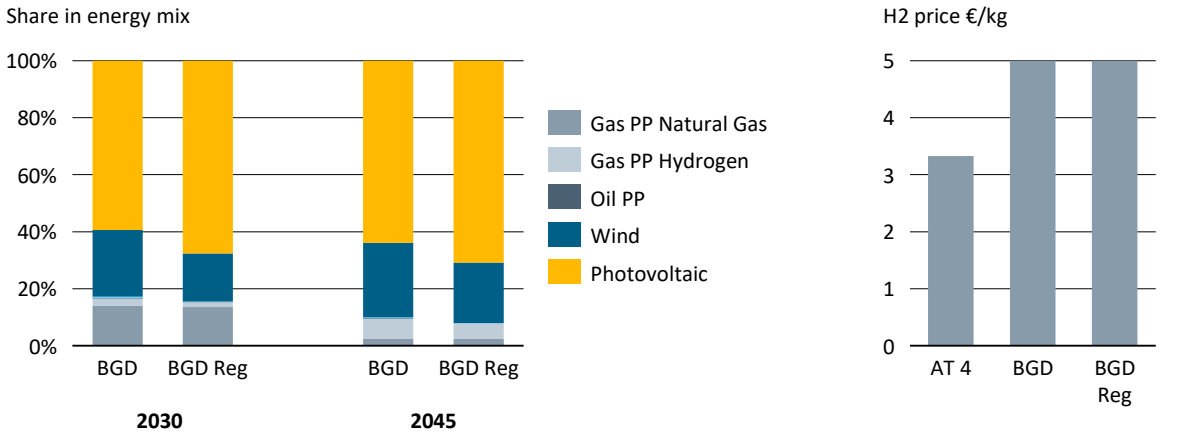

Figure D-23. Validation of the modeling approach for Bangladesh by comparing the energy mix and the break-even prices of the archetype (AT 4), country (BGD), and multi-region results (BGD Reg).

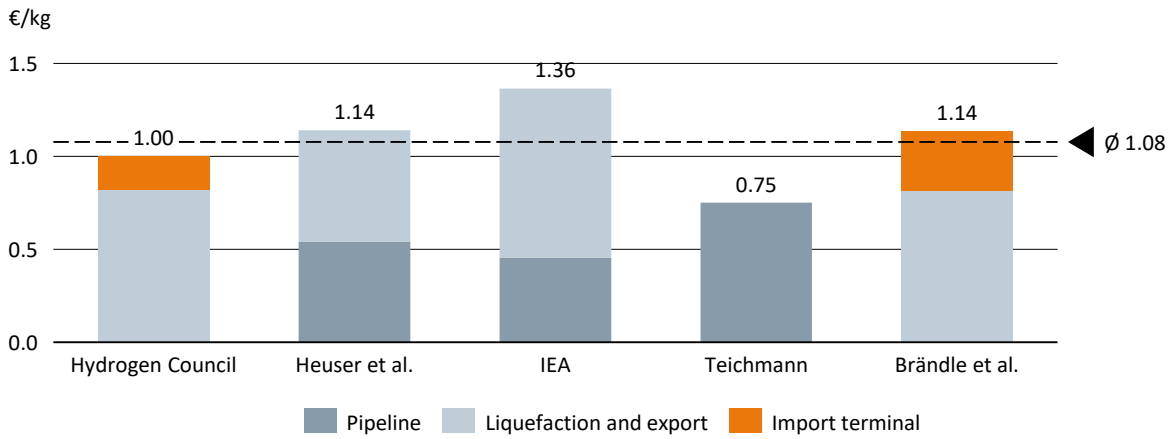

Figure D-24. Benchmark of five studies providing costs in the value chain of green hydrogen transportation by ship [22], [121], [222]-[224].

D.3. Use Case 3: Coal Phase-Out

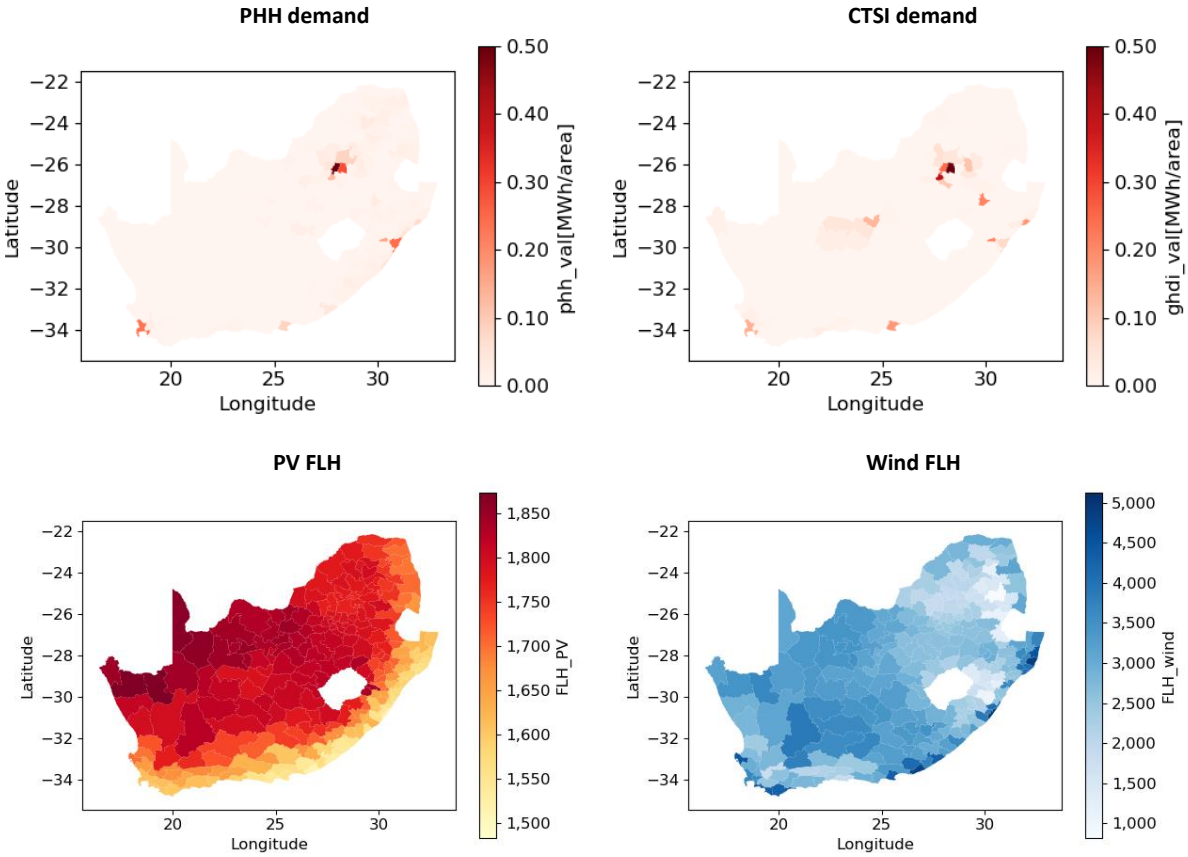

Figure D-25. Spatial data basis for South Africa: normalized PHH and CTSI demand and FLH of wind and PV.

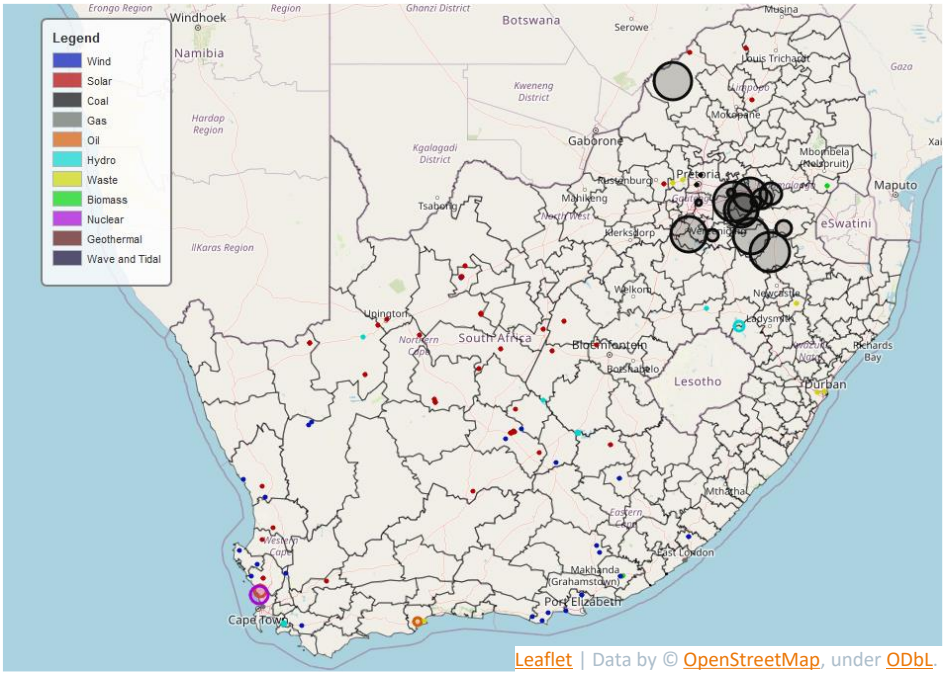

Figure D-26. Spatial data basis for South Africa: distribution and types of power plants based on [156].

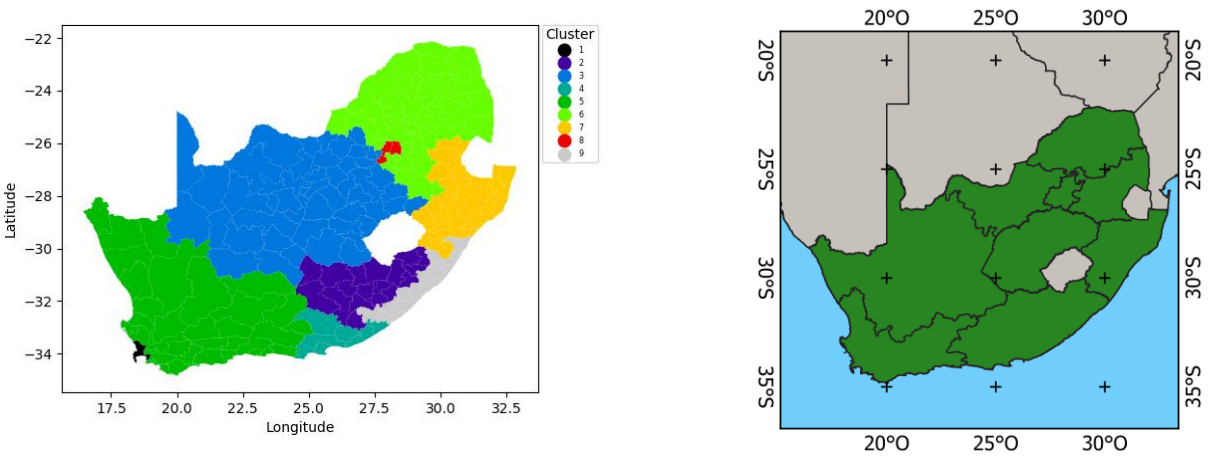

Figure D-27. Comparison of clustering results and administrative regions on level 1 in South Africa.

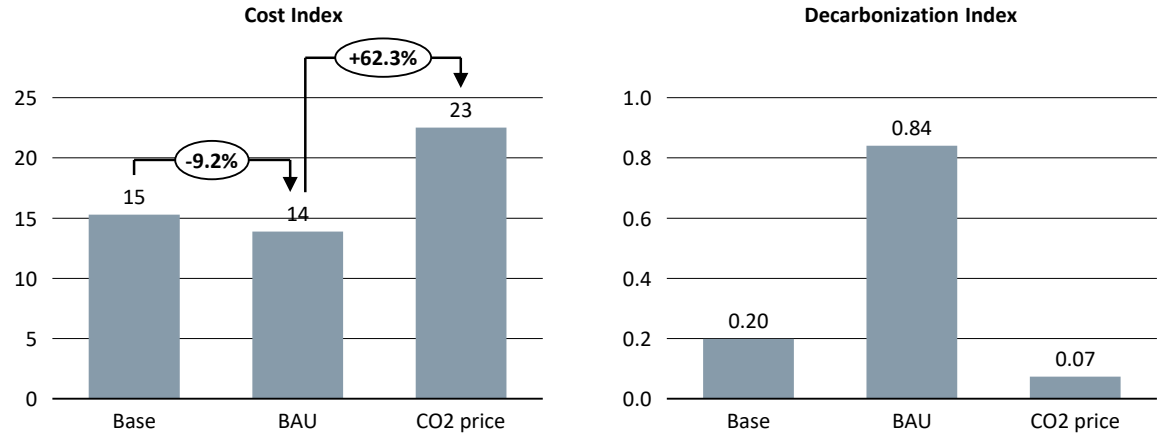

Figure D-28. Comparison of the Base scenario for South Africa to the BAU and CO2 Price scenarios.

Erklärungen laut Promotionsordnung

§ 8 Abs. 1 lit. c PromO

Ich versichere hiermit, dass die elektronische Version meiner Dissertation mit der schriftlichen Version übereinstimmt.

§ 8 Abs. 1 lit. d PromO

Ich versichere hiermit, dass zu einem vorherigen Zeitpunkt noch keine Promotion versucht wurde. In diesem Fall sind nähere Angaben über Zeitpunkt, Hochschule, Dissertationsthema und Ergebnis dieses Versuchs mitzuteilen.

§ 9 Abs. 1 PromO

Ich versichere hiermit, dass die vorliegende Dissertation selbstständig und nur unter Verwendung der angegebenen Quellen verfasst wurde.

§ 9 Abs. 2 PromO

Die Arbeit hat bisher noch nicht zu Prüfungszwecken gedient.

Martin Küppers, 29.06.2021, Paris

Curriculum Vitae

Martin Küppers, born in Grevenbroich, Germany

EDUCATION

DOCTORATE IN ELECTRICAL ENGINEERING, TU DARMSTADT | 01/2018 – 10/2021

Industrial doctoral studies supervised by Prof. Dr. Stefan Niessen MBA, Technology and Economics of Multimodal Energy Systems lab, Department of Electrical Engineering and Information Technology, TU Darmstadt

M.SC. ELECTRICAL ENGINEERING, RWTH AACHEN UNIVERSITY | 10/2014 – 09/2017

Major in power engineering with majority of courses in power system planning and operations, graduated with honors, topic of the master thesis: "Development of a Method for the Implementation of Two Grid-Oriented Operational Strategies within the Scheduling Process of Topological Power Plants"

ERASMUS+ EXCHANGE SEMESTER, INSA LYON | 08/2016 – 02/2017

Courses about the French / European energy system and environmental impacts in the energy and environment department

B.SC. ELECTRICAL ENGINEERING, RWTH AACHEN UNIVERSITY | 10/2011 – 09/2014

Courses in electrical engineering, higher mathematics and informatics, major in power engineering, topic of the bachelor thesis: "Parameterization and Validation of a Method for Determining the Optimal Network Expansion in Low-Voltage"

PROFESSIONAL EXPERIENCE

JUNIOR ENERGY MODELER, INTERNATIONAL ENERGY AGENCY, PARIS | SINCE 05/2021

Contributing to modeling and drafting the industry sector in the World Energy Outlook (WEO) and driving several projects improving the geospatial data usage especially for electrification planning in Sub-Saharan Africa.

RESEARCH ENGINEER AND PHD CANDIDATE, SIEMENS AG, MUNICH | 01/2018 – 05/2021

Involved in a team working on energy system modelling in Siemens' central R&D department planning, executing and managing customer projects about energy systems in different scales and scopes such as the German coal phase out, electrification strategies in Africa, or identifying key technologies in different decarbonized energy systems.

TEMPORARY STRATEGY CONSULTANT, SIEMENS MANAGEMENT CONSULTING, MUNICH | 05/2016 – 08/2016

Conducted consultant activities in two projects (for a Siemens Joint Venture on digital grid solutions and in the field of grid control systems) in the internal strategy consultancy of Siemens (now Siemens Advanta).

TECHNICAL SALES INTERN, SIEMENS PTE LTD, SINGAPORE | 10/2014 – 04/2015

Successfully prepared offers and finalized negotiations with customers to sell electrical drives, supported the development of a business plan to extend the activities in a specific business, and developed an approach to improve the customer access for sales activities by using tablets and available apps.

Nomenclature

Indices / sets

Index	Set	Description
ar	AR	Administrative regions
at	AT	Defined 15 Archetypes
cap		Per capita
cl	CL	Clustering results for a specified number of clusters k
co	CO	Considered 141 countries
co_ncl	CO_NCL	Non-clustered countries
com	COM	Modeled commodities
cp	CP	Modelled conversion processes
cr	CR	Clustered regions
df	DF	Considered 62 data features for clustering
geo	GEO	Classification in geographic zones
iter	ITER	Number of iterations for K-means
k	K	Number of clusters
n	N	Observations in the clustered dataset
pp	PP	Power plant technologies
reg	REG	Modeled regions in an energy system model
sdf	SDF	Spatial data features
st	ST	Modeled storage technologies
t	T	Modeled timesteps
te	TE	Modeled technologies
ts	TS	Time series data input
y	Y	Modeled years

Variables

Variable	Description
C	Costs
Ca	Capacity
CAPEX	CAPEX
Cs	Specific costs
D	Demand
E	Energy

Em	Emissions
EM	Energy Mix
J	Variance of K-means algorithm
MAE	Medium Average Error
OPEX	OPEX
P	Power
RMSE	Root Mean Square Error
SM	Storage Mix
TOTEX	TOTEX
Trp	Transport capacity between regions
Var	Clustering Variance

Parameters

Parameter	Description
AvgTe	Averagte technical availability of a technology
CRATE	C-Rate of storage technologies [1/h]
COPR	CO2 price [€/t]
EF	Specific emission factor [t CO_2/kWh]
EL	Limit of CO2 emissions [t CO_2]
F^{disc}	Discount factor
FLH	Full load hours per year
LE	Length of transmission line [km]
LL	Line losses per km [1/km]
LT	Technical lifetime of technologies [years]
SDR	Self discharge rate [1/h]
SRPC	Shares resources production/consumption
TEF	Technical efficiency
TLINK	Linking factor between two technologies

Acronyms

Acronym	Description
AC	Alternating current
CAPEX	Capital expenditures
CCUS	Carbon capture utilization and storage
CHI	Calinski-Harabasz Index
CO_2	Carbon dioxide
COP21	21st Conference of the Parties
CR	Clustered region
CTSI	Commercial, trade, service, and industrial
CVI	Clustering validity indicators
DBI	Davies-Bouldin Index
DC	Direct current
DTW	Dynamic Time Warping
EBC	Elbow criterion
ESDP	Energy System Development Plan
GDP	Gross domestic product
GH_2	Gaseous hydrogen
GUI	Graphical User Interface
H_2	Hydrogen
LCOE	Levelized costs of electricity
LH_2	Liquified hydrogen
LOHC	Liquid Organic Hydrogen Carrier
MAE	Mean Absolute Error
MAPE	Mean Average Percentage Error
MILP	Mixed-integer linear programming
MSE	Mean Square Error
NDC	National Determined Contributions
OPEX	Operational expenditures
OSM	OpenStreetMap
O&M	Operation and Maintenance
PCA	Principal Component Analysis
PEM	Polymer Electrolyte Membrane
PHH	Private household
PV	Photovoltaic

RES	Renewable energy sources
RMSE	Root Mean Square Error
SI	Silhouette Index
SMR	Steam Methane Reforming
SOC	State of charge
SOEC	Solid Oxide Electrolyzer Cells
TOTEX	Total expenditures
VRES	Variable renewable energy sources
WACC	Weighted Average Cost of Capital

Institution	**Description**
ENTSO-E	European Network of Transmission System Operators for Electricity
GADM	Database of Global Administrative Areas
IEA	International Energy Agency
IRENA	International Renewable Energy Agency
MERRA-2	Modern-Era Retrospective analysis for Research and Applications, Version 2
UN	United Nations

Bibliography

[1] B. Obama, "Remarks by the President at U.N. Climate Change Summit," United Nations Headquarters, New York, New York, Sep. 23, 2014.

[2] "GLOBAL Station Temperature Index." https://data.giss.nasa.gov/gistemp/tabledata_v3/GLB.Ts.txt (accessed May 29, 2020).

[3] J. Hansen, R. Ruedy, M. Sato, M. Imhoff, W. Lawrence, D. Easterling, T. Peterson, and T. Karl, "A closer look at United States and global surface temperature change," *J. Geophys. Res.*, vol. 106, no. D20, pp. 23947–23963, Oct. 2001, doi: 10.1029/2001JD000354.

[4] IPCC, "Intergovernmental Panel on Climate Change (IPCC) Observed Climate Change Impacts Database Version 2.01," Socioeconomic Data and Applications Center (SEDAC), Columbia University, Palisades, NY, 2017. Accessed: May 29, 2020. [Online]. Available: http://sedac.ipcc-data.org/ddc/observed_ar5/.

[5] IPCC, "Climate Change 2014: Mitigation of Climate Change," Contribution of Working Group III to the Fifth Assessment Report of the Intergovernmental Panel on Climate Change, Cambridge, United Kingdom and New York, NY, USA, 2014.

[6] World Resources Institute, "CAIT Climate Data Explorer." http://cait.wri.org/ (accessed Nov. 01, 2018).

[7] Based on IEA data from IEA, "Global CO2 emissions in 2019," International Energy Agency, Paris, Feb. 2020. Accessed: May 26, 2020. [Online]. Available: https://www.iea.org/articles/global-co2-emissions-in-2019. All rights reserved; as modified by M. Kueppers.

[8] IEA, "World Energy Outlook 2020," International Energy Agency, Paris, Oct. 2020. Accessed: Nov. 12, 2020. [Online]. Available: https://www.iea.org/reports/world-energy-outlook-2020. All rights reserved.

[9] United Nations, "Paris Agreement." 2015.

[10] European Commission, "A European Green Deal - Striving to be the first climate-neutral continent." https://ec.europa.eu/info/strategy/priorities-2019-2024/european-green-deal_en (accessed Jun. 05, 2020).

[11] United Nations Environment Programme, "Emissions Gap Report 2019," UNEP, Nairobi, 2019.

[12] IEA, "Energy Transition Indicators," International Energy Agency, Paris, Dec. 2019. Accessed: Apr. 24, 2020. [Online]. Available: https://www.iea.org/articles/energy-transitions-indicators. All rights reserved.

[13] Based on IEA data from IEA, "Global Energy & CO2 Status Report 2019," International Energy Agency, Paris, Mar. 2019. Accessed: Jun. 05, 2020. [Online]. Available: https://www.iea.org/reports/global-energy-co2-status-report-2019/emissions. All rights reserved; as modified by M. Kueppers.

[14] J. Després, N. Hadjsaid, P. Criqui, and I. Noirot, "Modelling the impacts of variable renewable sources on the power sector: Reconsidering the typology of energy modelling tools," *Energy*, vol. 80, pp. 486–495, Feb. 2015, doi: 10.1016/j.energy.2014.12.005.

[15] IRENA, "Renewable power generation costs in 2018," International Renewable Energy Agency, Abu Dhabi, 2019.

[16] IRENA, "Electrification with renewables: Driving the transformation of energy services," International Renewable Energy Agency, Abu Dhabi, 2019.

[17] S. Pfenninger, A. Hawkes, and J. Keirstead, "Energy systems modeling for twenty-first century energy challenges," *Renewable and Sustainable Energy Reviews*, vol. 33, pp. 74–86, May 2014, doi: 10.1016/j.rser.2014.02.003.

[18] Cambridge Dictionary, "Model – Definition in the Cambridge English Dictionary." https://dictionary.cambridge.org/us/dictionary/english/model (accessed Jun. 15, 2020).

[19] IRENA, *REthinking Energy 2017: accelerating the global energy transformation*. Abu Dhabi: International Renewable Energy Agency (IRENA), 2017.

[20] World Energy Council 2019 in partnership with OLIVER WYMAN, "World Energy Trilemma Index 2019," World Energy Council 2019 in partnership with OLIVER WYMAN, Sep. 2019.

[21] S. Pfenninger, L. Hirth, I. Schlecht, E. Schmid, F. Wiese, T. Brown, C. Davis, M. Gidden, H. Heinrichs, C. Heuberger, S. Hilpert, U. Krien, C. Matke, A. Nebel, R. Morrison, B. Müller, G. Pleßmann, M. Reeg, J. C. Richstein, A. Shivakumar, I. Staffell, T. Tröndle, and C. Wingenbach, "Opening the black box of energy modelling: Strategies and lessons learned," *Energy Strategy Reviews*, vol. 19, pp. 63–71, Jan. 2018, doi: 10.1016/j.esr.2017.12.002.

[22] IEA, "The Future of Hydrogen," International Energy Agency, Paris, 2019. [Online]. Available: https://www.iea.org/reports/the-future-of-hydrogen. All rights reserved.

[23] B. Lapillonne and C. Sebi, "Coal phase-out: Towards a Major Shift?," Enerdata Executive Brief, Mar. 2020.

[24] C. Stoll, "Fuel Switching and Deep Decarbonization," *MIT Center for Energy and Environmental Policy Research Working Paper Series*, vol. CEEPR WP 2019-005, Mar. 2019.

[25] V. Quaschning, "Specific Carbon Dioxide Emissions of Various Fuels," Jun. 2015. https://www.volker-quaschning.de/datserv/CO2-spez/index_e.php (accessed Jun. 15, 2020).

[26] H.-K. Ringkjøb, P. M. Haugan, and I. M. Solbrekke, "A review of modelling tools for energy and electricity systems with large shares of variable renewables," *Renewable and Sustainable Energy Reviews*, vol. 96, pp. 440–459, Nov. 2018, doi: 10.1016/j.rser.2018.08.002.

[27] S. Collins, J. P. Deane, K. Poncelet, E. Panos, R. C. Pietzcker, E. Delarue, and B. Pádraig Ó Gallachóir, "Integrating short term variations of the power system into integrated energy system models: A methodological review," *Renewable and Sustainable Energy Reviews*, vol. 76, pp. 839–856, Sep. 2017, doi: 10.1016/j.rser.2017.03.090.

[28] P. Crespo del Granado, R. H. van Nieuwkoop, E. G. Kardakos, and C. Schaffner, "Modelling the energy transition: A nexus of energy system and economic models," *Energy Strategy Reviews*, vol. 20, pp. 229–235, Apr. 2018, doi: 10.1016/j.esr.2018.03.004.

[29] N. Neshat, M. R. Amin-Naseri, and F. Danesh, "Energy models: Methods and characteristics," Journal of Energy in Southern Africa, vol. 25, no. 4, Nov. 2014.

[30] S. C. Bhattacharyya and G. R. Timilsina, "A review of energy system models," *International Journal of Energy Sector Management*, vol. 4, pp. 494–518, Nov. 2010, doi: 10.1108/17506221011092742.

[31] P. Lopion, P. Markewitz, M. Robinius, and D. Stolten, "A review of current challenges and trends in energy systems modeling," *Renewable and Sustainable Energy Reviews*, vol. 96, pp. 156–166, Nov. 2018, doi: 10.1016/j.rser.2018.07.045.

[32] P. Mancarella, G. Andersson, J. A. Pecas-Lopes, and K. R. W. Bell, "Modelling of integrated multi-energy systems: Drivers, requirements, and opportunities," Genoa, Italy, Jun. 2016, pp. 1–22, doi: 10.1109/PSCC.2016.7541031.

[33] M. Child, O. Koskinen, L. Linnanen, and C. Breyer, "Sustainability guardrails for energy scenarios of the global energy transition," *Renewable and Sustainable Energy Reviews*, vol. 91, pp. 321–334, Aug. 2018, doi: 10.1016/j.rser.2018.03.079.

[34] S. Pfenninger, J. DeCarolis, L. Hirth, S. Quoilin, and I. Staffell, "The importance of open data and software: Is energy research lagging behind?," *Energy Policy*, vol. 101, pp. 211–215, Feb. 2017, doi: 10.1016/j.enpol.2016.11.046.

[35] H. Teichgraeber and A. R. Brandt, "Clustering methods to find representative periods for the optimization of energy systems: An initial framework and comparison," *Applied Energy*, vol. 239, pp. 1283–1293, Apr. 2019, doi: 10.1016/j.apenergy.2019.02.012.

[36] L. Kotzur, P. Markewitz, M. Robinius, and D. Stolten, "Impact of different time series aggregation methods on optimal energy system design," *Renewable Energy*, vol. 117, pp. 474–487, Mar. 2018, doi: 10.1016/j.renene.2017.10.017.

[37] W. Short, "Regions in Energy Market Models," National Renewable Energy Laboratory (NREL), Golden, CO., US, Feb. 2007. doi: 10.2172/899298.

[38] H. Rogner, "IIASA's Integrated Assessment Framework," presented at the Pathways to Sustainable Energy Workshop, Geneva, 20 Apr. 2016.

[39] K. Löffler, K. Hainsch, T. Burandt, P.-Y. Oei, C. Kemfert, and C. von Hirschhausen, "Designing a model for the global energy system—GENeSYS-MOD: An Application of the Open-Source Energy Modeling System (OSeMOSYS)," *Energies*, vol. 10, p. 1468, Sep. 2017, doi: 10.3390/en10101468.

[40] K. Vaillancourt, M. Labriet, R. Loulou, and J.-P. Waaub, "The role of nuclear energy in long-term climate scenarios: An analysis with the World-TIMES model," *Energy Policy*, vol. 36, pp. 2296–2307, Jul. 2008, doi: 10.1016/j.enpol.2008.01.015.

[41] S. Chatzivasileiadis, D. Ernst, and G. Andersson, "The Global Grid," *Renewable Energy*, vol. 57, pp. 372–383, Sep. 2013, doi: 10.1016/j.renene.2013.01.032.

[42] T. Aboumahboub, "Modeling and Optimization of the Global Electricity Generation System with High Shares of Fluctuating Renewable Energy Sources," PhD, Technische Universität München, München, 2012.

[43] M. Ram, D. Bogdanov, A. Aghahosseini, A. Gulagi, A.S. Oyewo, M. Child, U. Caldera, K. Sadovskaia, J. Farfan, LSNS. Barbosa, M. Fasihi, S. Khalili, B. Dalheimer, G. Gruber, T. Traber, F. De Caluwe, H.-J. Fell, and C. Breyer, "Global Energy System Based On 100% Renewable Energy - Power, Heat, Transport and Desalination Sectors," Lappeenranta, Berlin, Mar. 2019.

[44] D. Bogdanov, J. Farfan, K. Sadovskaia, A. Aghahosseini, M. Child, A. Gulagi, A. S. Oyewo, LSNS. Barbosa, and C. Breyer, "Radical transformation pathway towards sustainable electricity via evolutionary steps," *Nat Commun*, vol. 10, no. 1, p. 1077, Dec. 2019, doi: 10.1038/s41467-019-08855-1.

[45] K. Schaber, F. Steinke, and T. Hamacher, "Transmission grid extensions for the integration of variable renewable energies in Europe: Who benefits where?," *Energy Policy*, vol. 43, pp. 123–135, Apr. 2012, doi: 10.1016/j.enpol.2011.12.040.

[46] M. Huber, A. Roger, and T. Hamacher, "Optimizing long-term investments for a sustainable development of the ASEAN power system," *Energy*, vol. 88, pp. 180–193, Aug. 2015, doi: 10.1016/j.energy.2015.04.065.

[47] U. Caldera, D. Bogdanov, S. Afanasyeva, and C. Breyer, "Role of Seawater Desalination in the Management of an Integrated Water and 100% Renewable Energy Based Power Sector in Saudi Arabia," *Water*, vol. 10, no. 1, p. 3, Dec. 2017, doi: 10.3390/w10010003.

[48] H. Lund and B. V. Mathiesen, "Energy system analysis of 100% renewable energy systems—The case of Denmark in years 2030 and 2050," *Energy*, vol. 34, no. 5, pp. 524–531, May 2009, doi: 10.1016/j.energy.2008.04.003.

[49] D. Connolly, H. Lund, B. V. Mathiesen, and M. Leahy, "The first step towards a 100% renewable energy-system for Ireland," *Applied Energy*, vol. 88, no. 2, pp. 502–507, Feb. 2011, doi: 10.1016/j.apenergy.2010.03.006.

[50] S. Samsatli, I. Staffell, and N. J. Samsatli, "Optimal design and operation of integrated wind-hydrogen-electricity networks for decarbonising the domestic transport sector in Great Britain," *International Journal of Hydrogen Energy*, vol. 41, no. 1, pp. 447–475, Jan. 2016, doi: 10.1016/j.ijhydene.2015.10.032.

[51] A. S. Oyewo, A. Aghahosseini, M. Ram, A. Lohrmann, and C. Breyer, "Pathway towards achieving 100% renewable electricity by 2050 for South Africa," *Solar Energy*, vol. 191, pp. 549–565, Oct. 2019, doi: 10.1016/j.solener.2019.09.039.

[52] G. He, A.-P. Avrin, J. H. Nelson, J. Johnston, A. Mileva, J. Tian, and D. M. Kammen, "SWITCH-China: A Systems Approach to Decarbonizing China's Power System," *Environmental Science & Technology*, vol. 50, pp. 5467–5473, May 2016, doi: 10.1021/acs.est.6b01345.

[53] A. Mileva, J. Johnston, J. H. Nelson, and D. M. Kammen, "Power system balancing for deep decarbonization of the electricity sector," *Applied Energy*, vol. 162, pp. 1001–1009, Jan. 2016, doi: 10.1016/j.apenergy.2015.10.180.

[54] D. P. Kaundinya, P. Balachandra, N. H. Ravindranath, and V. Ashok, "A GIS (geographical information system)-based spatial data mining approach for optimal location and capacity planning of distributed biomass power generation facilities: A case study of Tumkur district, India," *Energy*, vol. 52, pp. 77–88, Apr. 2013, doi: 10.1016/j.energy.2013.02.011.

[55] J. Gawlick, P. Kuhn, and T. Hamacher, "Szenarien für die bayerische Stromversorgung bis 2040.pdf," IHK für München und Oberbayern, München, ifo-Studie im Auftrag der IHK für München und Oberbayern, Mar. 2020.

[56] M. Brinkerink, B. Ó. Gallachóir, and P. Deane, "Building and Calibrating a Country-Level Detailed Global Electricity Model Based on Public Data," *Energy Strategy Reviews*, vol. 33, p. 100592, Jan. 2021, doi: 10.1016/j.esr.2020.100592.

[57] United Nations, "Geographic Regions." https://unstats.un.org/unsd/methodology/m49/ (accessed Jul. 01, 2019).

[58] T. Atallah and P. Bean, "Determinants of energy productivity: A comparison of 39 countries," *KAPSARC Discussion Paper*, no. KS-1518-DP012A, May 2015.

[59] Z. Csereklyei, P. W. Thurner, J. Langer, and H. Küchenhoff, "Energy paths in the European Union: A model-based clustering approach," *CCEP Working Paper 1701*, Jan. 2017.

[60] P. Stuckenberger, H. Wildemann, C. Blomberg, T. Engelmeier, C. Hellmann, and M. A. Offizier, "Connecting Possibilities - Scenarios for Optimizing Energy Systems," Siemens Energy Sector, Erlangen, 2013.

[61] G. De Vivero, K. Burges, M.-J. Kurdziel, and M. Hagemann, "Transition towards a decarbonised electricity sector - A framework of analysis for power system transformation," NewClimate Institute, 2019.

[62] T. Zipperle and C. Orthofer, "Same Same but Different? - Machine Learning Algorithmen zur Indikatoren basierten Regionenbildung," in *11. Internationale Energiewirtschaftstagung an der TU Wien*, 2019, pp. 1–18.

[63] K.-K. Cao, K. von Krbek, M. Wetzel, F. Cebulla, and S. Schreck, "Classification and Evaluation of Concepts for Improving the Performance of Applied Energy System Optimization Models," *Energies*, vol. 12, no. 24, p. 4656, Dec. 2019, doi: 10.3390/en12244656.

[64] D. Stetter, "Enhancement of the REMix energy system model: global renewable energy potentials, optimized power plant siting and scenario validation," Universität Stuttgart, 2014.

[65] M. Biberacher, "Modelling and optimisation of future energy systems using spatial and temporal methods," PhD, University of Augsburg, 2004.

[66] R. M. Assunção, M. C. Neves, G. Câmara, and C. Da Costa Freitas, "Efficient regionalization techniques for socio-economic geographical units using minimum spanning trees," *International Journal of Geographical Information Science*, vol. 20, no. 7, pp. 797–811, Aug. 2006, doi: 10.1080/13658810600665111.

[67] D. Guo, "Regionalization with dynamically constrained agglomerative clustering and partitioning (REDCAP)," *International Journal of Geographical Information Science*, vol. 22, no. 7, pp. 801–823, Jul. 2008, doi: 10.1080/13658810701674970.

[68] K.-K. Cao, J. Metzdorf, and S. Birbalta, "Incorporating Power Transmission Bottlenecks into Aggregated Energy System Models," *Sustainability*, vol. 10, no. 6, p. 1916, Jun. 2018, doi: 10.3390/su10061916.

[69] J. Hörsch and T. Brown, "The role of spatial scale in joint optimisations of generation and transmission for European highly renewable scenarios," Piscataway, NJ, 2017, Accessed: May 11, 2018. [Online]. Available: http://ieeexplore.ieee.org/servlet/opac?punumber=7970794.

[70] T. Anderski, "e-HIGHWAY 2050 - Modular Development Plan of the Pan-European Transmission System 2050: European cluster model of the Pan-European transmission grid," Deliverable public funded project, Jul. 2015.

[71] J. M. Weinand, R. McKenna, and W. Fichtner, "Developing a municipality typology for modelling decentralised energy systems," *Utilities Policy*, vol. 57, pp. 75–96, Apr. 2019, doi: 10.1016/j.jup.2019.02.003.

[72] K. Siala and M. Y. Mahfouz, "Impact of the choice of regions on energy system models," *Energy Strategy Reviews*, vol. 25, pp. 75–85, Aug. 2019, doi: 10.1016/j.esr.2019.100362.

[73] C. E. Fleischer, "Minimising the effects of spatial scale reduction on power system models," *Energy Strategy Reviews*, p. 12, 2020.

[74] T. Hastie, R. Tibshirani, and J. Friedman, "Unsupervised Learning," in *The Elements of Statistical Learning*, New York, NY: Springer New York, 2009, pp. 485–585.

[75] GADM, "GADM maps and data," 2018. https://gadm.org/index.html (accessed Jul. 11, 2019).

[76] T. Zipperle and C. L. Orthofer, "d2ix: A Model Input-Data Management and Analysis Tool for MESSAGEix," *Energies*, vol. 12, no. 8, p. 1483, Apr. 2019, doi: 10.3390/en12081483.

[77] D. Keles, P. Jochem, R. McKenna, M. Ruppert, and W. Fichtner, "Meeting the Modeling Needs of Future Energy Systems," *Energy Technol.*, vol. 5, no. 7, pp. 1007–1025, Jul. 2017, doi: 10.1002/ente.201600607.

[78] M. Howells, H. Rogner, N. Strachan, C. Heaps, H. Huntington, S. Kypreos, A. Hughes, S. Silveira, J. DeCarolis, M. Bazillian, and A. Roehrl, "OSeMOSYS: The Open Source Energy Modeling System," *Energy Policy*, vol. 39, pp. 5850–5870, Oct. 2011, doi: 10.1016/j.enpol.2011.06.033.

[79] B. Steffen, "Estimating the Cost of Capital for Renewable Energy Projects," *SSRN Journal*, 2019, doi: 10.2139/ssrn.3373905.

[80] J. Ondraczek, N. Komendantova, and A. Patt, "WACC the dog: The effect of financing costs on the levelized cost of solar PV power," *Renewable Energy*, vol. 75, pp. 888–898, Mar. 2015, doi: 10.1016/j.renene.2014.10.053.

[81] D. Bogdanov, M. Child, and C. Breyer, "Reply to 'Bias in energy system models with uniform cost of capital assumption,'" *Nat Commun*, vol. 10, no. 1, p. 4587, Dec. 2019, doi: 10.1038/s41467-019-12469-y.

[82] C. Egenhofer, A. Marcu, V. Rizos, A. Behrens, J. Núñez-Ferrer, A. Hassel, and M. Elkerbout, "Towards an effective EU framework for road transport and GHG emissions," Jul. 2016.

[83] M. Z. Jacobson, M. A. Delucchi, Z. A.F. Bauer, S. C. Goodman, W. E. Chapman, M. A. Cameron, C. Bozonnat, L. Chobadi, H. A. Clonts, P. Enevoldsen, J. R. Erwin, S. N. Fobi, O. K. Goldstrom, E. M. Hennessy, J. Liu, J. Lo, C. B. Meyer, S. B. Morris, K. R. Moy, P. L. O'Neill, I. Petkov, S. Redfern, R. Schucker, M. A. Sontag, J. Wang, E. Weiner, and A. S. Yachanin, "100% Clean and Renewable Wind, Water, and Sunlight All-Sector Energy Roadmaps for 139 Countries of the World," *Joule*, vol. 1, pp. 108–121, Sep. 2017, doi: 10.1016/j.joule.2017.07.005.

[84] C. Kuster, Y. Rezgui, and M. Mourshed, "Electrical load forecasting models: A critical systematic review," *Sustainable Cities and Society*, vol. 35, pp. 257–270, Nov. 2017, doi: 10.1016/j.scs.2017.08.009.

[85] A. Toktarova, L. Gruber, M. Hlusiak, D. Bogdanov, and C. Breyer, "Long term load projection in high resolution for all countries globally," *International Journal of Electrical Power & Energy Systems*, vol. 111, pp. 160–181, Oct. 2019, doi: 10.1016/j.ijepes.2019.03.055.

[86] WSJ News Graphics, "Barrel Breakdown," *The Wall Street Journal*, Apr. 15, 2016. http://graphics.wsj.com/oil-barrel-breakdown/ (accessed Jul. 24, 2020).

[87] F. Roar Aune, K. Einar Rosendahl, and E. Lund Sagen, "Globalisation of Natural Gas Markets - Effects on Prices and Trade Patterns," *EJ*, vol. 30, no. 01, Sep. 2009, doi: 10.5547/ISSN0195-6574-EJ-Vol30-NoSI-4.

[88] IEA, "Nuclear Power in a Clean Energy System," International Energy Agency, Paris, May 2019. All rights reserved.

[89] B. K. Sovacool, A. Gilbert, and D. Nugent, "Risk, innovation, electricity infrastructure and construction cost overruns: Testing six hypotheses," *Energy*, vol. 74, pp. 906–917, Sep. 2014, doi: 10.1016/j.energy.2014.07.070.

[90] B. Stoll, J. Andrade, S. Cohen, G. Brinkman, and C. Brancucci Martinez-Anido, "Hydropower Modeling Challenges," NREL/TP--5D00-68231, 1353003, Apr. 2017. doi: 10.2172/1353003.

[91] I. Kougias, G. Aggidis, F. Avellan, S. Deniz, U. Lundin, A. Moro, S. Muntean, D. Novara, J. I. Pérez-Díaz, E. Quaranta, P. Schild, and N. Theodossiou, "Analysis of emerging technologies in the hydropower sector," *Renewable and Sustainable Energy Reviews*, vol. 113, p. 109257, Oct. 2019, doi: 10.1016/j.rser.2019.109257.

[92] L. Igual and S. Seguí, *Introduction to Data Science*. Cham: Springer International Publishing, 2017.

[93] F. Ueckerdt, L. Hirth, G. Luderer, and O. Edenhofer, "System LCOE: What are the costs of variable renewables?," *Energy*, vol. 63, pp. 61–75, Dec. 2013, doi: 10.1016/j.energy.2013.10.072.

[94] IEA, "Electricity statistics," Apr. 30, 2020. https://www.iea.org/subscribe-to-data-services/electricity-statistics (accessed Aug. 07, 2020). All rights reserved.

[95] IEA, "Tracking the decoupling of electricity demand and associated CO2 emissions," Mar. 08, 2019. https://www.iea.org/commentaries/tracking-the-decoupling-of-electricity-demand-and-associated-co2-emissions (accessed Aug. 07, 2020). All rights reserved.

[96] K. Schaber, "Integration of Variable Renewable Energies in the European power system: a model-based analysis of transmission grid extensions and energy sector coupling," PhD, Technische Universität München, München, 2013.

[97] R. Xu and D. C. Wunsch, *Clustering*. Hoboken, N.J. : Piscataway, NJ: Wiley ; IEEE Press, 2009.

[98] M. Bramer, *Principles of Data Mining*. London: Springer London, 2016.

[99] A. K. Jain, "Data clustering: 50 years beyond K-means," *Pattern Recognition Letters*, vol. 31, pp. 651–666, Jun. 2010, doi: 10.1016/j.patrec.2009.09.011.

[100] J. C. Duque, R. Ramos, and J. Suriñach, "Supervised Regionalization Methods: A Survey," *International Regional Science Review*, vol. 30, no. 3, pp. 195–220, Jul. 2007, doi: 10.1177/0160017607301605.

[101] P. Berkhin, "Survey Of Clustering Data Mining Techniques," *A Survey of Clustering Data Mining Techniques. Grouping Multidimensional Data: Recent Advances in Clustering.*, vol. 10, 2002, doi: 10.1007/3-540-28349-8_2.

[102] T. S. Madhulatha, "An Overview On Clustering Methods," *IOSRJEN*, vol. 02, no. 04, pp. 719–725, Apr. 2012, doi: 10.9790/3021-0204719725.

[103] J. Han, M. Kamber, and A. K. Tung, "Spatial clustering methods in data mining," *Geographic data mining and knowledge discovery*, pp. 188–217, 2001.

[104] T. M. Kodinariya and P. R. Makwana, "Review on determining number of Cluster in K-means Clustering," *International Journal of Advance Research in Computer Science and Management Studies*, vol. 1, no. 6, p. 6, 2013.

[105] J. C. Duque, L. Anselin, and S. J. Rey, "The max-P-regions problem," *Journal of Regional Science*, vol. 52, no. 3, pp. 397–419, Aug. 2012, doi: 10.1111/j.1467-9787.2011.00743.x.

[106] S. Kisilevich, F. Mansmann, M. Nanni, and S. Rinzivillo, "Spatio-temporal clustering," in *Data Mining and Knowledge Discovery Handbook*, O. Maimon and L. Rokach, Eds. Boston, MA: Springer US, 2009, pp. 855–874.

[107] M. Verleysen and D. François, "The Curse of Dimensionality in Data Mining and Time Series Prediction," in *Computational Intelligence and Bioinspired Systems*, vol. 3512, J. Cabestany, A. Prieto, and F. Sandoval, Eds. Berlin, Heidelberg: Springer Berlin Heidelberg, 2005, pp. 758–770.

[108] O. Arbelaitz, I. Gurrutxaga, J. Muguerza, J. M. Pérez, and I. Perona, "An extensive comparative study of cluster validity indices," *Pattern Recognition*, vol. 46, no. 1, pp. 243–256, Jan. 2013, doi: 10.1016/j.patcog.2012.07.021.

[109] P. J. Rousseeuw, "Silhouettes: A graphical aid to the interpretation and validation of cluster analysis," *Journal of Computational and Applied Mathematics*, vol. 20, pp. 53–65, Nov. 1987, doi: 10.1016/0377-0427(87)90125-7.

[110] D. L. Davies and D. W. Bouldin, "A Cluster Separation Measure," *IEEE Trans. Pattern Anal. Mach. Intell.*, vol. PAMI-1, no. 2, pp. 224–227, Apr. 1979, doi: 10.1109/TPAMI.1979.4766909

[111] T. Calinski and J. Harabasz, "A dendrite method for cluster analysis," *Comm. in Stats. - Theory & Methods*, vol. 3, no. 1, pp. 1–27, 1974, doi: 10.1080/03610927408827101.

[112] M. Halkidi and M. Vazirgiannis, "Clustering validity assessment: finding the optimal partitioning of a data set," in *Proceedings 2001 IEEE International Conference on Data Mining*, San Jose, CA, USA, 2001, pp. 187–194, doi: 10.1109/ICDM.2001.989517.

[113] A. Botchkarev, "A New Typology Design of Performance Metrics to Measure Errors in Machine Learning Regression Algorithms," *IJIKM*, vol. 14, pp. 045–076, 2019, doi: 10.28945/4184.

[114] C. Müller, A. Hoffrichter, L. Wyrwoll, C. Schmitt, M. Trageser, T. Kulms, D. Beulertz, M. Metzger, M. Duckheim, M. Huber, M. Küppers, D. Most, S. Paulus, H. J. Heger, and A. Schnettler, "Modeling framework for planning and operation of multi-modal energy systems in the case of Germany," *Applied Energy*, vol. 250, pp. 1132–1146, Sep. 2019, doi: 10.1016/j.apenergy.2019.05.094.

[115] W. Medjroubi, U. P. Müller, M. Scharf, C. Matke, and D. Kleinhans, "Open Data in Power Grid Modelling: New Approaches Towards Transparent Grid Models," *Energy Reports*, vol. 3, pp. 14–21, Nov. 2017, doi: 10.1016/j.egyr.2016.12.001.

[116] OpenStreetMap (OSM) - OpenStreetMap and contributors, OpenStreetMap Foundation, Cambridge, edited: 2019 2004. Accessed: Feb. 07, 2019. [Online]. Available: http://www.openstreetmap.org/.

[117] W. Heitkoetter, W. Medjroubi, T. Vogt, and C. Agert, "Comparison of Open Source Power Grid Models—Combining a Mathematical, Visual and Electrical Analysis in an Open Source Tool," *Energies*, vol. 12, no. 24, p. 4728, Dec. 2019, doi: 10.3390/en12244728.

[118] S. Raths, S. Koopmann, C. Mueller, A. Meinerzhagen, T. Falke, M. Cramer, T. Kulms, D. Beulertz, H. Barrios, A. Schnettler, M. Tackenberg, F. Steinke, P. Wolfrum, M. Metzger, B. Schlageter, W. Kusian, and A. Schmidt, "The Energy System Development Plan (ESDP)," Bonn, 2015, p. 8.

[119] ENTSO-E, "Grid Map," 2019. https://www.entsoe.eu/data/map/ (accessed Aug. 14, 2020).

[120] M. E. Reuß, "Techno-ökonomische Analyse alternativer Wasserstoffinfrastruktur," PhD, RWTH Aachen University, Aachen, 2019.

[121] P.-M. Heuser, D. S. Ryberg, T. Grube, M. Robinius, and D. Stolten, "Techno-economic analysis of a potential energy trading link between Patagonia and Japan based on CO2 free hydrogen," *International Journal of Hydrogen Energy*, vol. 44, no. 25, pp. 12733–12747, May 2019, doi: 10.1016/j.ijhydene.2018.12.156.

[122] R. Ramachandran, "An overview of industrial uses of hydrogen," *International Journal of Hydrogen Energy*, vol. 23, no. 7, pp. 593–598, Jul. 1998, doi: 10.1016/S0360-3199(97)00112-2.

[123] A. Sgobbi, W. Nijs, R. De Miglio, A. Chiodi, M. Gargiulo, and C. Thiel, "How far away is hydrogen? Its role in the medium and long-term decarbonisation of the European energy system," *International Journal of Hydrogen Energy*, vol. 41, no. 1, pp. 19–35, Jan. 2016, doi: 10.1016/j.ijhydene.2015.09.004.

[124] S. Yeh, A. Farrell, R. Plevin, A. Sanstad, and J. Weyant, "Optimizing U.S. Mitigation Strategies for the Light-Duty Transportation Sector: What We Learn from a Bottom-Up Model," *Environ. Sci. Technol.*, vol. 42, no. 22, pp. 8202–8210, Nov. 2008, doi: 10.1021/es8005805.

[125] K. Karlsson and P. Meibom, "Optimal investment paths for future renewable based energy systems—Using the optimisation model Balmorel," *International Journal of Hydrogen Energy*, vol. 33, no. 7, pp. 1777–1787, Apr. 2008, doi: 10.1016/j.ijhydene.2008.01.031.

[126] P. Agnolucci and W. McDowall, "Designing future hydrogen infrastructure: Insights from analysis at different spatial scales," *International Journal of Hydrogen Energy*, vol. 38, no. 13, pp. 5181–5191, May 2013, doi: 10.1016/j.ijhydene.2013.02.042.

[127] J. Eichman, A. Townsend, and M. Melaina, "Economic Assessment of Hydrogen Technologies Participating in California Electricity Markets," NREL/TP--5400-65856, 1239543, Feb. 2016. doi: 10.2172/1239543.

[128] J. Michaelis, F. Genoese, and M. Wietschel, "Evaluation of Large-Scale Hydrogen Storage Systems in the German Energy Sector," *Fuel Cells*, vol. 14, no. 3, pp. 517–524, Jun. 2014, doi: 10.1002/fuce.201300213.

[129] G. Glenk and S. Reichelstein, "Economics of converting renewable power to hydrogen," *Nat Energy*, vol. 4, no. 3, pp. 216–222, Mar. 2019, doi: 10.1038/s41560-019-0326-1.

[130] U.S. Department of Energy, "DOE H2A Analysis." https://www.hydrogen.energy.gov/h2a_analysis.html (accessed Aug. 21, 2020).

[131] V. Papadopoulos, J. Desmet, J. Knockaert, and C. Develder, "Improving the utilization factor of a PEM electrolyzer powered by a 15 MW PV park by combining wind power and battery storage – Feasibility study," *International Journal of Hydrogen Energy*, vol. 43, no. 34, pp. 16468–16478, Aug. 2018, doi: 10.1016/j.ijhydene.2018.07.069.

[132] S. H. Siyal, D. Mentis, and M. Howells, "Economic analysis of standalone wind-powered hydrogen refueling stations for road transport at selected sites in Sweden," *International Journal of Hydrogen Energy*, vol. 40, no. 32, pp. 9855–9865, Aug. 2015, doi: 10.1016/j.ijhydene.2015.05.021.

[133] P. A. Yanguas Parra, G. Ganti, R. Brecha, B. Hare, M. Schaeffer, and U. Fuentes, "Global and regional coal phase-out requirements of the Paris Agreement: Insights from the IPCC Special Report on 1.5°C," Climate Analytics, Sep. 2019.

[134] McKinsey, "Global Energy Perspective 2019: Reference Case," McKinsey, Jan. 2019.

[135] CarbonBrief, "Mapped: The world's coal power plants," Mar. 26, 2020. https://www.carbonbrief.org/mapped-worlds-coal-power-plants (accessed Aug. 15, 2020).

[136] M. Kittel, L. Goeke, C. Kemfert, P.-Y. Oei, and C. von Hirschhausen, "Scenarios for Coal-Exit in Germany—A Model-Based Analysis and Implications in the European Context," *Energies*, vol. 13, no. 8, p. 2041, Apr. 2020, doi: 10.3390/en13082041.

[137] M. Metzger, M. Duckheim, M. Franken, H. J. Heger, M. Huber, M. Knittel,T. Kolster, M. Kueppers, C. Meier, D. Most, S. Paulus, L. Wyrwoll, A. Moser, and S. Niessen, "Pathways toward a Decarbonized Future—Impact on Security of Supply and System Stability in a Sustainable German Energy System," *Energies*, vol. 14, no. 3, p. 560, Jan. 2021, doi: 10.3390/en14030560.

[138] E. Künle, P. Theile, and C. Wagner, "Entwicklung der Momentanreserve und Abschätzung des Bedarfes an Fast Frequency Response im Europäischen Verbundsystem," Energiewirtschaftliches Institut an der Universität zu Köln gGmbH (EWI), Köln, Mar. 2020.

[139] R. Figueiredo, P. Nunes, M. Meireles, M. Madaleno, and M. C. Brito, "Replacing coal-fired power plants by photovoltaics in the Portuguese electricity system," *Journal of Cleaner Production*, vol. 222, pp. 129–142, Jun. 2019, doi: 10.1016/j.jclepro.2019.02.217.

[140] T. Burandt, B. Xiong, K. Löffler, and P.-Y. Oei, "Decarbonizing China's energy system – Modeling the transformation of the electricity, transportation, heat, and industrial sectors," *Applied Energy*, vol. 255, p. 113820, Dec. 2019, doi: 10.1016/j.apenergy.2019.113820.

[141] W. M. Harris, M. Beck, and I. Gerasimchuk, "The End of Coal: Ontario's coal phase-out," International Institute for Sustainable Development, Winnipeg, Jun. 2015.

[142] P.-Y. Oei and R. Mendelevitch, "Prospects for steam coal exporters in the era of climate policies: a case study of Colombia," *Climate Policy*, vol. 19, no. 1, pp. 73–91, Jan. 2019, doi: 10.1080/14693062.2018.1449094.

[143] M. Küppers, M. Metzger, M. Huber, and S. Paulus, "Archetypes of Country Energy Systems," in *2019 IEEE Milan PowerTech*, Milan, Italy, Jun. 2019, pp. 1–6, doi: 10.1109/PTC.2019.8810765.

[144] M. Kueppers, C. Perau, M. Franken, H. J. Heger, M. Huber, M. Metzger, and S. Niessen, "Data-Driven Regionalization of Decarbonized Energy Systems for Reflecting Their Changing Topologies in Planning and Optimization," *Energies*, vol. 13, no. 16, p. 4076, Aug. 2020, doi: 10.3390/en13164076.

[145] U.S. Energy Information Administration, "International Energy Statistics." https://www.eia.gov/beta/international/data/browser (accessed Nov. 01, 2018).

[146] United Nations Development Programm, "Human Development Reports." http://hdr.undp.org/en/data (accessed Nov. 01, 2018).

[147] The World Bank, "World Development Indicators." https://databank.worldbank.org/source/world-development-indicators (accessed Nov. 01, 2018).

[148] wattEV2Buy, "Global EV Sales." https://wattev2buy.com/global-ev-sales/ (accessed Nov. 01, 2018).

[149] United Nations Department of Economic and Social Affairs, "World Population Prospects 2019." https://population.un.org/wpp/ (accessed Mar. 01, 2019).

[150] IRENA, "Installed Renewable Power Capacity." http://dashboard.irena.org/ (accessed Mar. 01, 2019).

[151] Gscociology, "International data sets." http://gsociology.icaap.org/dataupload.html (accessed Nov. 01, 2018).

[152] Dataset Publishing Language, "Countries.csv." https://developers.google.com/public-data/docs/canonical/countries_csv (accessed Nov. 01, 2018).

[153] World Bank Group, "Climate Change Knowledge Portal." https://climateknowledgeportal.worldbank.org/ (accessed Nov. 01, 2018).

[154] K. Baumert and M. Selman, "Heating and Cooling Degree Days," 2003. https://www.scribd.com/document/34318847/Dagree-Days (accessed Nov. 01, 2018).

[155] S. Pfenninger and I. Staffell, "Renewables ninja." https://www.renewables.ninja/ (accessed Mar. 01, 2019).

[156] World Resources Institute, "Global Power Plant Database." http://datasets.wri.org/dataset/globalpowerplantdatabase (accessed Jul. 01, 2019).

[157] Office of Electricity Delivery & Energy Reliability, "DOE Global Energy Storage Database." https://www.energystorageexchange.org/projects (accessed Nov. 01, 2018).

[158] S. Pfenninger and I. Staffell, "Long-term patterns of European PV output using 30 years of validated hourly reanalysis and satellite data," *Energy*, vol. 114, pp. 1251–1265, Nov. 2016, doi: 10.1016/j.energy.2016.08.060.

[159] I. Staffell and S. Pfenninger, "Using bias-corrected reanalysis to simulate current and future wind power output," *Energy*, vol. 114, pp. 1224–1239, Nov. 2016, doi: 10.1016/j.energy.2016.08.068.

[160] FfE - Forschungsstelle für Energiewirtschaft e.V., "Siemens Global Energy Demand - Modellierung des weltweiten Stromverbrauchs." https://www.ffe.de/themen-und-methoden/erzeugung-und-markt/911-siemens-global-energy-demand-modellierung-des-weltweiten-stromverbrauchs (accessed Jun. 11, 2020).

[161] European Commission, Joint Research Centre and Columbia University, Center for International Earth Science Information Network, "GHS-POP R2015A - GHS population grid, derived from GPW4, multitemporal (1975, 1990, 2000, 2015)," European Commission, Joint Research Centre (JRC), Dataset, 2015. [Online]. Available: http://data.europa.eu/89h/jrc-ghsl-ghs_pop_gpw4_globe_r2015a.

[162] IEA, "Electricity Information 2018," International Energy Agency, Paris, 2018. All rights reserved.

[163] Global Energy Observatory, Google, KTH Royal Institute of Technology in Stockholm, Enipedia, World Resources Institute, "A Global Database of Power Plants," Published on Resource Watch and Google Earth Engine, 2018. [Online]. Available: http://resourcewatch.org/, https://earthengine.google.com/.

[164] MERRA-2 tavg1_2d_slv_Nx: 2d, 1-Hourly, Time-Averaged,Single-Level, Assimilation, Single-Level Diagnostics V5.12.4; Global Modeling and Assimilation Office (GMAO), Goddard Earth Sciences Data and Information Services Center (GES DISC): Greenbelt, MD, USA, 2015.

[165] MERRA-2 tavg1_2d_lnd_Nx: 2d, 1-Hourly, Time-Averaged,Single-Level, Assimilation, Land Surface Diagnostics V5.12.4; Global Modeling and Assimilation Office (GMAO), Goddard Earth Sciences Data and Information Services Center (GES DISC): Greenbelt, MD, USA, 2015.

[166] MERRA-2 tavg1_2d_flx_Nx: 2d, 1-Hourly, Time-Averaged,Single-Level, Assimilation, Surface Flux Diagnostics V5.12.4; Global Modeling and Assimilation Office (GMAO), Goddard Earth Sciences Data and Information Services Center (GES DISC): Greenbelt, MD, USA, 2015.

[167] MERRA-2 tavg1_2d_rad_Nx: 2d, 1-Hourly, Time-Averaged,Single-Level, Assimilation, Radiation Diagnostics V5.12.4; Global Modeling and Assimilation Office (GMAO), Goddard Earth Sciences Data and Information Services Center (GES DISC): Greenbelt, MD, USA, 2015.

[168] MERRA-2 const_2d_asm_Nx: 2d, constants V5.12.4; Global Modeling and Assimilation Office (GMAO), Goddard Earth Sciences Data and Information Services Center (GES DISC): Greenbelt, MD, USA, 2015.

[169] P. Albrecht, "Development of a Tool for the Analysis of the Global Solar and Wind Energy Potential," Master Thesis, Technische Universität München, München, 2016.

[170] European Environment Agency, "Natura 2000 data - the European network of protected sites," 2011. https://www.eea.europa.eu/data-and-maps/data/natura-1 (accessed Dec. 01, 2019).

[171] European Environment Agency, "Nationally designated areas (CDDA)," 2017. https://www.eea.europa.eu/data-and-maps/data/nationally-designated-areas-national-cdda-12 (accessed Dec. 01, 2019).

[172] Japan Aerospace Exploration Agency, "ALOS Global Digital Surface Model 'ALOS World 3D - 30m (AW3D30)'" 2015. https://www.eorc.jaxa.jp/ALOS/en/aw3d30/index.htm (accessed Dec. 01, 2019).

[173] Siemens AG, "Siemens' Position on Decarbonization and Energy Transition in Germany," Siemens AG, 2017.

[174] T. Kolster, R. Krebs, S. Niessen, and M. Duckheim, "The contribution of distributed flexibility potentials to corrective transmission system operation for strongly renewable energy systems," *Applied Energy*, vol. 279, p. 115870, Dec. 2020, doi: 10.1016/j.apenergy.2020.115870.

[175] D. Beulertz, S. Charousset, D. Most, S. Giannelos, and I. Yueksel-Erguen, "Development of a Modular Framework for Future Energy System Analysis," in *2019 54th International Universities Power Engineering Conference (UPEC)*, Bucharest, Romania, Sep. 2019, pp. 1–6, doi: 10.1109/UPEC.2019.8893472.

[176] S. N. Paredes Pineda, "Development and Evaluation of a Simplified Approach for Modeling Country Energy Systems," Master Thesis, Technische Universität München, München, 2019.

[177] M. Kueppers, S. N. Paredes Pineda, M. Metzger, M. Huber, S. Paulus, H. J. Heger, and S. Niessen, "Decarbonization pathways of worldwide energy systems – Definition and modeling of archetypes," *Applied Energy*, vol. 285, p. 116438, Mar. 2021, doi: 10.1016/j.apenergy.2021.116438.

[178] ENTSO-E, "ENTSO-E Transparency Platform," 2019. https://transparency.entsoe.eu/dashboard/show.

[179] Gobierno De Mexico, "Estimación de la Demanda Real del Sistema," 2019. https://www.cenace.gob.mx/SIM/VISTA/REPORTES/DemandaRealSist.aspx.

[180] Electricity Market Information New Zealand, "Wholesale reports," 2019. https://www.emi.ea.govt.nz/Wholesale/Reports.

[181] Fraunhofer ISE, "Net installed electricity generation capacity in Germany." https://energy-charts.info/charts/installed_power/chart.htm?l=en&c=DE&stacking=sorted&expansion=installed_power&sum=0&partsum=0 (accessed Oct. 10, 2020).

[182] Office of Energy Efficiency & Renewable Energy, "Advantages and Challenges of Wind Energy." https://www.energy.gov/eere/wind/advantages-and-challenges-wind-energy (accessed Apr. 13, 2021).

[183] S. Ong, C. Campbell, P. Denholm, R. Margolis, and G. Heath, "Land-Use Requirements for Solar Power Plants in the United States," NREL/TP-6A20-56290, 1086349, Jun. 2013. doi: 10.2172/1086349.

[184] P. Denholm, M. Hand, M. Jackson, and S. Ong, "Land Use Requirements of Modern Wind Power Plants in the United States," NREL/TP-6A2-45834, 964608, Aug. 2009. doi: 10.2172/964608.

[185] K. Eisenack, S. Villamayor-Tomas, G. Epstein, C. Kimmich, N. R. Magliocca, C. Oberlack, M. Roggero, and D. Sietz, "Design and quality criteria for archetype analysis," *E&S*, vol. 24, no. 3, p. art6, 2019, doi: 10.5751/ES-10855-240306.

[186] V. R. Patel and R. G. Mehta, "Impact of outlier removal and normalization approach in modified K-means clustering algorithm," *IJCSI International Journal of Computer Science Issues*, vol. 8, no. 5, Sep. 2011.

[187] D. Arthur and S. Vassilvitskii, "K-means++: The Advantages of Careful Seeding," in *Proceedings of the eighteenth annual ACM-SIAM symposium on Discrete algorithms*, 2007, pp. 1027–1035.

[188] T. Chai and R. R. Draxler, "Root mean square error (RMSE) or mean absolute error (MAE)? – Arguments against avoiding RMSE in the literature," *Geosci. Model Dev.*, vol. 7, no. 3, pp. 1247–1250, Jun. 2014, doi: 10.5194/gmd-7-1247-2014.

[189] R. J. Kate, "Using dynamic time warping distances as features for improved time series classification," *Data Min Knowl Disc*, vol. 30, no. 2, pp. 283–312, Mar. 2016, doi: 10.1007/s10618-015-0418-x.

[190] MathWorks, *Statistics and Machine Learning Toolbox*.

[191] The PostGIS Development Group, "PostGIS 3.1.2dev Manual." Apr. 11, 2021, Accessed: Apr. 15, 2021. [Online]. Available: https://postgis.net/docs/manual-3.1/.

[192] F. Pedregosa, G. Varoquaux, A. Gramfort, V. Michel, B. Thirion, O. Grisel, M. Blondel, P. Prettenhofer, R. Weiss, V. Dubourg, J. Vanderplas, A. Passos, D. Cournapeau, M. Brucher, M. Perrot, and E. Duchesnay, "Scikit-learn: Machine Learning in Python," *Journal of Machine Learning Research*, vol. 12, pp. 2825–2830, 2011.

[193] marineregions.org, "Maritime Boundaries." https://www.marineregions.org/eezsearch.php (accessed Feb. 13, 2021).

[194] D. J. Berndt and J. Clifford, "Using Dynamic Time Warping to Find Patterns in Time Series," in *Knowledge discovery in databases: papers from the 1994 AAAI Workshop, August 2, Seattle, Washington*, U. M. Fayyad, R. Uthurusamy, and Workshop on Knowledge Discovery in Databases, Eds. Menlo Park, Calif: AAAI, 1994, pp. 359–370.

[195] L. J. P. van der Maaten, E. O. Postma, and H. J. van den Herik, "Dimensionality Reduction: A Comparative Review," 2008.

[196] I. T. Jolliffe and J. Cadima, "Principal component analysis: a review and recent developments," *Phil. Trans. R. Soc. A.*, vol. 374, no. 2065, p. 20150202, Apr. 2016, doi: 10.1098/rsta.2015.0202.

[197] D. Guo, "Greedy Optimization for Contiguity-Constrained Hierarchical Clustering," in *2009 IEEE International Conference on Data Mining Workshops*, Miami, FL, USA, Dec. 2009, pp. 591–596, doi: 10.1109/ICDMW.2009.75.

[198] OpenStreetMap Wiki contributors, "Map features," Nov. 29, 2020. https://wiki.openstreetmap.org/w/index.php?title=Map_features&oldid=2066570 (accessed Dec. 30, 2020).

[199] Next Kraftwerke, "What does utility frequency mean?" https://www.next-kraftwerke.com/knowledge/utility-frequency (accessed Dec. 30, 2020).

[200] D. Oeding and B. R. Oswald, *Elektrische Kraftwerke und Netze*. Springer-Verlag Berlin Heidelberg, 2016.

[201] R. Puffer, "Optimierungspotenziale bei Freileitungen - Was ist machbar?," presented at the BNetzA Technikdialog, Apr. 17, 2012, Accessed: Jun. 11, 2020. [Online]. Available: https://docplayer.org/33699070-Optimierungspotenziale-bei-freileitungen-was-ist-machbar.html.

[202] Bundesnetzagentur, "Bedarfsermittlung 2017–2030 Bestätigung Netzentwicklungsplan Strom," Bundesnetzagentur, Bonn, Germany, 2017.

[203] Bundesnetzagentur, "Kostenschaetzungen NEP 2030." https://www.netzentwicklungsplan.de/de/kostenschaetzungen-zu-kapitel-42-2 (accessed Jun. 03, 2020).

[204] Deutsche Energie-Agentur GmbH (dena), Forschungszentrum Karlsruhe GmbH, Fraunhofer-Institut für System- und Innovationsforschung (ISI), Ludwig-Bölkow-Systemtechnik GmbH, and Wuppertal Institut für Klima, Umwelt, Energie GmbH, "GermanHy: Studie zur Frage 'Woher kommt der Wasserstoff in Deutschland bis 2050?,'" Berlin, Aug. 2009.

[205] M. Ruth and T. Ramsden, "Current (2009) State-of-the-Art Hydrogen Production Cost Estimate Using Water Electrolysis," National Renewable Energy Laboratory (NREL), Golden, CO., NREL/BK-6A1-46676, Sep. 2009.

[206] F. Muellerlanger, E. Tzimas, M. Kaltschmitt, and S. Peteves, "Techno-economic assessment of hydrogen production processes for the hydrogen economy for the short and medium term," *International Journal of Hydrogen Energy*, vol. 32, no. 16, pp. 3797–3810, Nov. 2007, doi: 10.1016/j.ijhydene.2007.05.027.

[207] B. D. James, D. A. DeSantis, and G. Saur, "Final Report: Hydrogen Production Pathways Cost Analysis (2013 –2016)," Strategic Analysis, Arlington VA, DOE-StrategicAnalysis-6231-1, Sep. 2016.

[208] R. G. Lemus and J. M. Martínez Duart, "Updated hydrogen production costs and parities for conventional and renewable technologies," *International Journal of Hydrogen Energy*, vol. 35, no. 9, pp. 3929–3936, May 2010, doi: 10.1016/j.ijhydene.2010.02.034.

[209] M. Mulder, P. L. Perey, and J. L. Moraga, "Outlook for a Dutch hydrogen market: economic conditions and scenarois," Centre for Energy Economics Research, University of Groningen, 5, 2019.

[210] High-Level Commission on Carbon Prices, "Report of the High-Level Commission on Carbon Prices," World Bank, Washington, DC, 2017. [Online]. Available: https://www.carbonpricingleadership.org/report-of-the-highlevel-commission-on-carbon-prices.

[211] O. Walter, M. Huber, M. Kueppers, A. Tremel, and S. Becker, "Energy system design for deep decarbonization of a sunbelt city by using a hybrid storage approach," presented at the Proceedings of the 13th International Renewable Energy Storage Conference 2019 (IRES 2019), Düsseldorf, Germany, 2019, doi: 10.2991/ires-19.2019.23.

[212] O. D. Doleski, T. Kaiser, M. Metzger, S. Niessen, and S. Thiem, *Digitale Dekarbonisierung Technologieoffen Die Klimaziele Erreichen*. Wiesbaden: Springer Fachmedien Wiesbaden GmbH, 2021.

[213] E. Papadis and G. Tsatsaronis, "Challenges in the decarbonization of the energy sector," *Energy*, vol. 205, p. 118025, Aug. 2020, doi: 10.1016/j.energy.2020.118025.

[214] M. Huber, N. Namockel, R. Rezgui, M. Kueppers, and H. J. Heger, "Electrification seeds – A flexible approach for decentralized electricity supply in developing countries", *Energy for Sustainable Development*, vol. 62, pp. 176 – 185, Jun. 2021, doi: 10.1016/j.esd.2021.04.001.

[215] Africa Energy Portal, "Morocco on course to meet renewable energy targets for 2030," Jul. 2019. https://africa-energy-portal.org/news/morocco-course-meet-renewable-energy-targets-2030 (accessed Jan. 10, 2021).

[216] DTU, "Global Wind Atlas," 2019. https://globalwindatlas.info/ (accessed Jan. 24, 2020).

[217] M. Huber, "Flexibility in Power Systems - Requirements, Modeling and Evaluation," PhD, Technische Universität München, München, 2017.

[218] IEA, "Global hydrogen demand by sector in the Sustainable Development Scenario, 2019-2070," International Energy Agency, Paris, Sep. 2020. Accessed: Jan. 14, 2021. [Online]. Available: https://www.iea.org/data-and-statistics/charts/global-hydrogen-demand-by-sector-in-the-sustainable-development-scenario-2019-2070. All rights reserved.

[219] Wikipedia, "Khulna." https://en.wikipedia.org/wiki/Khulna (accessed Jan. 26, 2020).

[220] Wikipedia, "Barapukuria coal mine." https://en.wikipedia.org/wiki/Barapukuria_coal_mine (accessed Jan. 26, 2020).

[221] Federal Ministry for Economic Affairs and Energy, "The National Hydrogen Strategy," Berlin, Jun. 2020. Accessed: Jan. 26, 2020. [Online]. Available: https://www.bmwi.de/Redaktion/EN/Publikationen/Energie/the-national-hydrogen-strategy.html.

[222] Hydrogen Council, "Path to hydrogen competitiveness - A cost perspective," Hydrogen Council, Brussels, Jan. 2020. Accessed: Nov. 30, 2020. [Online]. Available: https://hydrogencouncil.com/en/path-to-hydrogen-competitiveness-a-cost-perspective/.

[223] D. Teichmann, W. Arlt, and P. Wasserscheid, "Liquid Organic Hydrogen Carriers as an efficient vector for the transport and storage of renewable energy," *International Journal of Hydrogen Energy*, vol. 37, no. 23, pp. 18118–18132, Dec. 2012, doi: 10.1016/j.ijhydene.2012.08.066.

[224] G. Brändle, M. Schönfisch, and S. Schulte, "Estimating Long-Term Global Supply Costs for Low-Carbon Hydrogen," *EWI Working Paper*, vol. 20/04, p. 72, Nov. 2020.

[225] Ports.com, "Sea route & distance." http://ports.com/sea-route/jeddah-islamic-port,saudi-arabia/port-of-hamburg,germany/ (accessed Jan. 26, 2020).

[226] IEA, "Coal Information: Overview," International Energy Agency, Paris, Jul. 2020. Accessed: Jan. 14, 2021. [Online]. Available: https://www.iea.org/reports/coal-information-overview. All rights reserved.

[227] Minerals Council South Africa, "Coal." https://www.mineralscouncil.org.za/sa-mining/coal (accessed Jan. 16, 2020).

[228] B. Merven, G. Ireland, F. Hartley, C. Arndt, A. Hughes, F. Ahjum, B. McCall, and T. Caetano, "Quantifying the Macro- and Socio- Economic Benefits of a Transition to Renewable Energy in South Africa," *SA-TIED Working Paper*, no. 19, p. 16, Jun. 2018.

[229] Bundesministeriums für Umwelt, Naturschutz und nukleare Sicherheit, "Projektionsbericht 2019 für Deutschland." May 15, 2019.

[230] IHS Markit, "IHS long-term planning and energy scenarios – IHS Energy Rivalry," 2018.

[231] European Climate Foundation, "Roadmap 2050: a practical guide to a prosperous, low-carbon Europe," European Climate Foundation, Apr. 2010.

[232] J. Carlsson, "ETRI 2014 - Energy Technology Reference Indicator projections for 2010-2050," EUR - Scientific and Technical Research Reports JRC92496. [Online]. Available: 10.2790/057687.